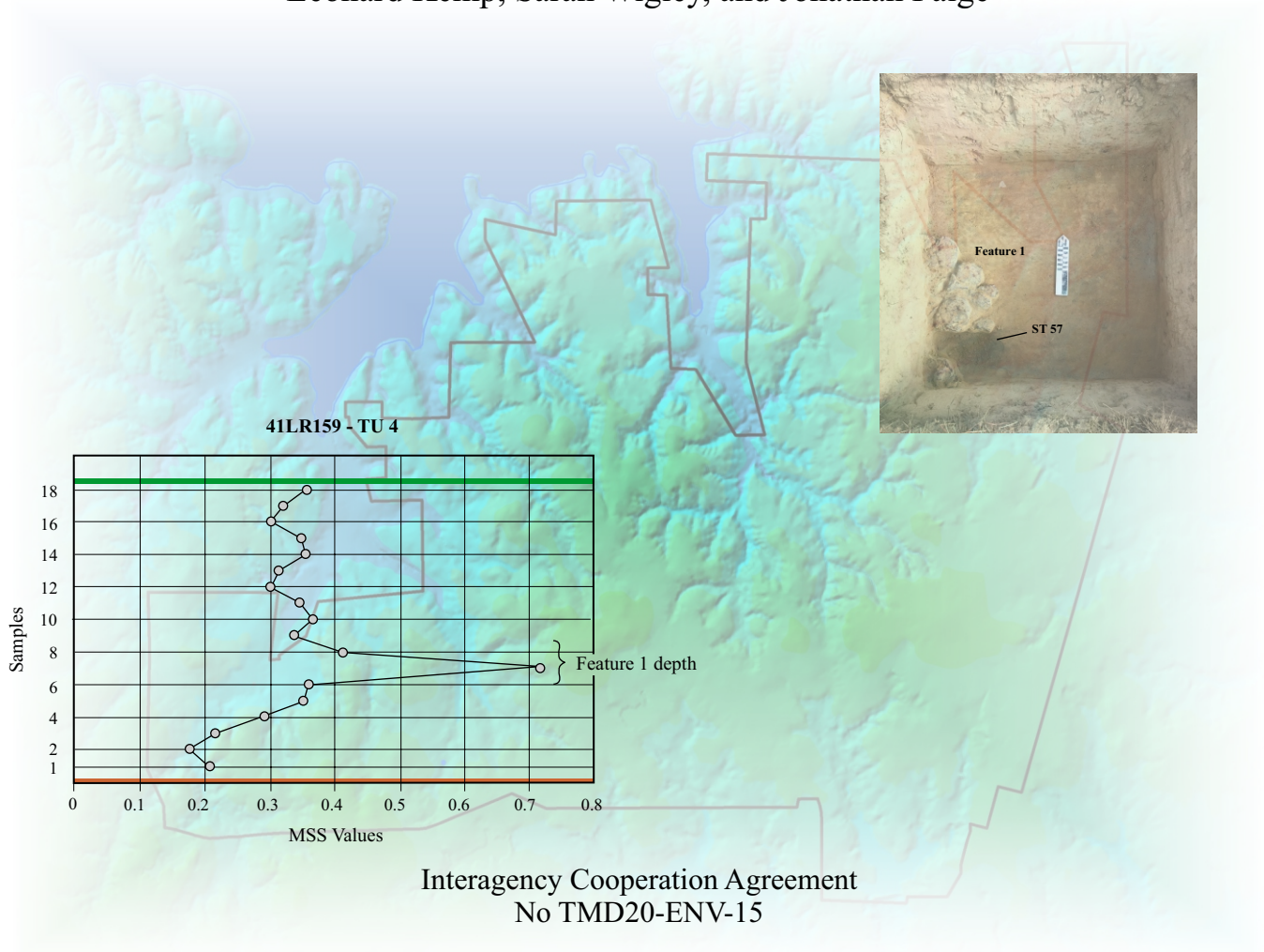


National Register Eligibility Testing of Ten Sites on Camp Maxey, Lamar County, Texas

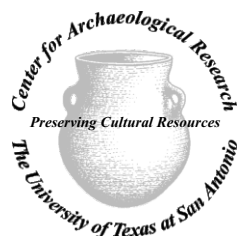
by
Leonard Kemp, Sarah Wigley, and Jonathan Paige



REDACTED

Principal Investigator
Raymond Mauldin

Prepared for:
Texas Military Department
P.O. Box 5218
Austin, Texas 78763



Prepared by:
Center for Archaeological Research
The University of Texas at San Antonio
One UTSA Circle
San Antonio, Texas 78249-1644
Archaeological Report, No. 499

© CAR May 2023

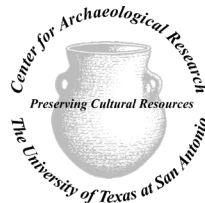
**National Register Eligibility Testing
of Ten Sites on Camp Maxey,
Lamar County, Texas**

by
Leonard Kemp, Sarah Wigley, and Jonathan Paige

Interagency Cooperation Agreement
No TMD20-ENV-15

REDACTED

Principal Investigator
Raymond Mauldin



Prepared for:
Texas Military Department
P.O. Box 5218
Austin, Texas 78763

Prepared by:
Center for Archaeological Research
The University of Texas at San Antonio
One UTSA Circle
San Antonio, Texas 78249
Archaeological Report, No. 499

Abstract:

The Center for Archaeological Research (CAR) at The University of Texas at San Antonio (UTSA) conducted National Register of Historic Places (NRHP) eligibility testing of ten archaeological sites located on Camp Maxey, a facility operated by the Texas Military Department (TMD) in Lamar County, Texas. While the project was not conducted under a Texas Antiquities Permit, it was conducted in a manner consistent with the requirements of the Antiquities Code of Texas. The testing was performed under Interagency Cooperation Agreement TMD20-ENV-15, with Dr. Raymond Mauldin serving as Principal Investigator and Leonard Kemp serving as Project Archaeologist.

Prior to testing, CAR performed reconnaissance of 12 archaeological sites having NRHP undetermined eligibility. These sites are 41LR154, 41LR159, 41LR161, 41LR162, 41LR165, 41LR175, 41LR177, 41LR184, 41LR203, 41LR213, 41LR226, and 41LR238. Shovel tests were excavated on seven of these sites to refine the placement of test units for the current project and any future projects. CAR excavated 93 shovel tests on 41LR154, 41LR159, 41LR161, 41LR162, 41LR165, 41LR213, and 41LR226. Ten of the 12 sites were selected and tested under Section 106 of the National Historic Preservation Act (NHPA) of 1966, as amended. These ten sites are 41LR154, 41LR159, 41LR161, 41LR162, 41LR165, 41LR175, 41LR177, 41LR203, 41LR226, and 41LR238. Work was conducted in the summer of 2021 and late spring of 2022. CAR excavated 23 1-x-1 m test units and screened approximately 10.1 m³ of deposits.

CAR recovered four bifaces, a uniface, two cores, two edge modified flakes, six native ceramic fragments (four of which refitted), 165 pieces of debitage, 2.45 kg of non-feature burned rock, burned faunal bone, and a quartzite crystal, as well as historic artifacts, including a 1903 U.S. penny, glass fragments, and a bullet. CAR identified two burned rock features, one at 41LR159 and another at 41LR161.

CAR used three interrelated research domains to determine NRHP eligibility of the ten sites. These criteria are the chronological potential of a site, the integrity of a site, and the content of a site. Based on this research, CAR recommends that site 41LR159 is eligible for listing on the NRHP. Sites 41LR154, 41LR161, 41LR162, 41LR165, 41LR175, 41LR177, 41LR203, 41LR226, and 41LR238 are recommended as not eligible for NRHP listing. In addition, CAR redefined the boundaries of four sites, 41LR154, 41LR159, 41LR161, and 41LR162 reflecting findings from the current investigation.

Following analyses and quantification, artifacts associated with this project possessing little scientific value were discarded pursuant to Chapter 26.27(g)(2) of the Antiquities Code of Texas and in consultation with the TMD. All cultural materials and records obtained and/or generated during the project were prepared in accordance with federal regulation 36 CFR part 79 and THC requirements for State Held-in-Trust collections and placed in Accession file number 2603.

This page intentionally left blank.

Table of Contents:

Abstract	iii
List of Figures	ix
List of Tables.....	xi
Acknowledgements	xiii
Chapter 1: Introduction and Project Description	1
Measures of Eligibility Determination	3
Report Organization	3
Chapter 2: Project Environment and Setting	5
Climate	5
Geology and Soils.....	6
The Sandy Mantle.....	6
Regional and Project Setting	8
Flora and Fauna	9
Flora	9
Fauna	10
Chapter 3: Cultural History of Northeast Texas and Past Archaeological Investigations of the Camp Maxey Region	11
North Texas Cultural Chronology	11
Paleoindian Period	11
Archaic Period.....	11
Caddo Prehistory	12
Historic Period.....	14
Past Archaeological Investigations.....	15
Chapter 4: Archaeological Patterns at Camp Maxey	17
Regional Radiocarbon Dates and Camp Maxey Temporal Patterns.....	17
Intensity of Site Use	20
Debitage Density	20
Maximum Level Density.....	21
Debitage Characteristics.....	23
Lithic Tools and Ceramics	26
Tool Distribution	28
Tool Material	28
Summary.....	29
Chapter 5: Field and Laboratory Methods	31
Field Methods	31
Pre-Field and Reconnaissance.....	31
Shovel Testing	31
NRHP Eligibility Testing.....	31
Laboratory Methods	32
Lithic Analysis	32
Magnetic Soil Susceptibility Analysis	33
Flotation	33
Radiocarbon Dating	33
Curation	33
Chapter 6: Site Descriptions, Work Accomplished, and Material Recovered	35
41LR154.....	35
Background	36
Current Investigation.....	36
41LR159.....	38
Background	38
Current Investigation.....	38

41LR161	43
Background	43
Current Investigation.....	43
41LR162	47
Background	47
Current Investigation.....	47
41LR165	50
Background	50
Current Investigation.....	50
41LR175	52
Background	52
Current Investigation.....	52
41LR177	54
Background	54
Current Investigation.....	54
41LR203	55
Background	55
Current Investigation.....	56
41LR226	58
Background	58
Current Investigation.....	58
41LR238	61
Background	61
Current Investigation.....	61
Preliminary Investigation of 41LR184 and 41LR213	63
41LR184 Background and Current Investigation	63
41LR213 Background and Current Investigation	65
Summary.....	67
Chapter 7: Chronological Potential.....	69
Temporal Diagnostics	69
Radiocarbon Dates and Potential Radiocarbon Samples.....	69
Summary.....	71
Chapter 8: Site Content.....	73
Overview	73
The Maxey Lithic Assemblage.....	73
41LR159.....	75
41LR161.....	76
Measuring reduction intensity at 41LR159 using the Cortex Ratio Method.....	78
Results	79
Discussion.....	80
Summary.....	81
Chapter 9: Site Integrity.....	83
Natural and Human Impacts to Sites	83
Artifact Distribution	84
Artifact Distribution Summary	87
Magnetic Soil Susceptibility.....	87
41LR154.....	88
41LR159.....	88
41LR161.....	90
41LR177.....	90
41LR203.....	91
41LR226.....	91
MSS Summary	91
Conclusions	91

Chapter 10: Summary and Recommendations.....	95
Recommendations	95
References Cited.....	97
Appendix A: Radiocarbon Dates	105
Appendix B: MSS Sampling Information.....	109
Appendix C: Debitage Attribute Data.....	115
Appendix D: Measuring Cortex Ratios at 41LR159.....	129
Introduction	129
Measuring the Amount of Surface Area Covered by Cortex in the Assemblage	129
Measuring the Total Volume of Chert and Quartzite in the Assemblage	129
Estimating Volume and Surface Area of Nodules Reduced at 41LR159	129
Estimating the Number of Nodules Reduced to Produce the 41LR159 Assemblage	130
Measuring the Expected Amount of Cortex.....	130
Measuring the Cortex Ratio (Expected/Observed)	130
Appendix E: R Code for Monte Carlo Simulation.....	131

This page intentionally left blank.

List of Figures:

Figure 1-1. The location of Camp Maxey in Lamar County, Texas	1
Figure 1-2. The locations of the 12 archaeological sites investigated during this project REDACTED IMAGE	2
Figure 2-1. The average maximum (red) and minimum (blue) monthly temperature at Paris, Texas based on data from 1991 to 2020 (NOAA 2021)	5
Figure 2-2. The average monthly rainfall at Paris, Texas based on data from 1991-2020. Peak rainfall occurs in May with a secondary peak in October (NOAA 2022).....	6
Figure 2-3. Profile and floor of a unit excavated in the Sandy Mantle with a sandy, potentially artifact bearing horizon over an artifact-sterile clay terminal level	7
Figure 2-4. Models of pedogenic and geomorphic formation process for the Sandy Mantle (Ahr et al. 2012).....	8
Figure 2-5. Physiographic regions and features surrounding Camp Maxey.....	9
Figure 2-6. A raster map showing elevations and drainages of Camp Maxey.....	10
Figure 3-1. The Southern and Northern Caddo Areas as shown in Perttula (2012: Figure 1) with the Middle Red River Valley cultural area as defined by Bruseth in the red box (1998)	13
Figure 4-1. The summed probability distribution of 87 radiocarbon dates from the Middle Red River counties.....	18
Figure 4-2. The temporal distribution of all previous analyzed radiocarbon dates from Camp Maxey.....	18
Figure 4-3. Density of debitage recovered by cubic meter for each site reviewed.....	20
Figure 4-4. Debitage density by cubic meter plotted against site MLD average. Blue circles indicate high-density grouping, white circles indicate medium-density grouping, and gray indicate low-density grouping.....	22
Figure 4-5. Percentage of non-cortical debitage by site	23
Figure 4-6. Number of material types by total debitage count	26
Figure 4-7. Number of tools recorded at each site plotted against number of tool types	28
Figure 6-1. Locations of the twelve Camp Maxey sites (Lyle et al. 2001: Figure 8-1; Nickels et al. 1998: Figure 7-1 REDACTED IMAGE	35
Figure 6-2. View to the south of 41LR154 from the current investigation.....	36
Figure 6-3. Site map of 41LR154 showing previous work by CAR as depicted in Nickels et al. (1998: Figure 8- 9).....	37
Figure 6-4. New site boundary of 41LR154 with shovel tests and unit excavated by CAR during this investigation	38
Figure 6-5. View to the northeast of 41LR159	39
Figure 6-6. Site map of 41LR159 showing previous work by CAR as depicted in Nickels et al. (1998: Figure 8-14).....	39
Figure 6-7. New site boundary of 41LR159 with shovel tests and units excavated by CAR during this investigation.....	40
Figure 6-8. Plan and profiles views of Feature 1 on 41LR159	42
Figure 6-9. View to the north of 41LR161 in the footprint of a two-track road.....	43
Figure 6-10. Site map of 41LR161 showing previous work by CAR as depicted in Nickels et al. (1998: Figure 8-16).....	44
Figure 6-11. New site boundary of 41LR161 with shovel tests and units excavated by CAR during this investigation.....	45
Figure 6-12. Plan views of Feature 1 on 41LR161	46
Figure 6-13. View to the south of the dense vegetation found on 41LR162	48
Figure 6-14. Site map of 41LR162 showing previous work by CAR as depicted in Nickels et al. (1998: Figure 8-17).....	48
Figure 6-15. New site boundary of 41LR162 with shovel tests and units excavated by CAR during this investigation.....	49
Figure 6-16. View of Visor Creek that borders the south and east portions of 41LR165.....	50
Figure 6-17. Site map of 41LR165 showing previous work by CAR as depicted in Nickels et al. (1998: Figure 8-20).....	51
Figure 6-18. Locations of shovel test and units excavated to determine the location of 41LR165.....	51
Figure 6-19. View from Test Unit 1 excavated on 41LR175.....	52
Figure 6-20. Site map of 41LR175 showing previous work by CAR as depicted in Nickels et al. (1998: Figure 8-24).....	53
Figure 6-21. The current site map of 41LR175 showing the location of the test unit and identifying landmarks	53
Figure 6-22. View to the north of 41LR177 from the excavated test unit	54
Figure 6-23. Site map of 41LR177 showing previous work by CAR as depicted in Nickels et al. (1998: Figure 8-26).....	54
Figure 6-24. Location of the test unit excavated on 41LR177	55
Figure 6-25. View to the north of 41LR 203 to the base boundary in the background	55
Figure 6-26. Site map of 41LR203 showing previous work by CAR (Lyle et al. 2001: Figure 8-6).....	56
Figure 6-27. The location of test units excavated on 41LR203. The site boundary shown here is from the TMD geodatabase and different from the one in Figure 6-26	57

Figure 6-28. View to the north of 41LR226 towards the base boundary.....	58
Figure 6-29. Site map of 41LR226 showing previous work by CAR (Lyle et al. 2001: Figure 8-14). Shovel test A-28 is identified REDACTED IMAGE	59
Figure 6-30. The locations of shovel tests and test units excavated by CAR during the current investigation REDACTED IMAGE	60
Figure 6-31. View to the northwest of 41LR238 and towards to Unit 1.....	61
Figure 6-32. Site map of 41LR238 showing previous work by CAR (Lyle et al. 2001: Figure 8-16).....	62
Figure 6-33. Location of two test units excavated on 41LR238.....	62
Figure 6-34. View to the north from 41LR184 in the vicinity of positive shovel tests excavated by Lyle et al. (2001).....	63
Figure 6-35. Site map of 41LR184 showing previous work by CAR (Lyle et al. 2001: Figure 8-2).....	64
Figure 6-36. View to the northeast from the southern portion of 41LR213	65
Figure 6-37. Site map of 41LR213 showing previous work by CAR (Lyle et al. 2001: Figure 8-11)	66
Figure 6-38. Site map of 41LR213 showing shovel test excavated during the current investigation	66
Figure 7-1. The calibrated radiocarbon sample from Feature 1 of 41LR159	70
Figure 7-2. The calibrated radiocarbon sample from Feature 1 of 41LR161	70
Figure 8-1. Left: Amount of debitage elements per raw material type, and by site. Right: weight of raw material by raw material, and by site	74
Figure 8-2. Left: number of chipped stone debris elements per raw material across the seven sites sampled. Right: total weight of chipped stone debris by raw material	75
Figure 8-3. Density of debitage recovered by cubic meter for 41LR159 and 36 previously tested sites on Camp Maxey (see Chapter 4). 41LR159 is highlighted in red.....	76
Figure 8-4. Dimensions of complete flakes recovered from 41LR159 differentiated by amount of cortex	77
Figure 8-5. Top: FS 87, a biface on a fine-grained brown chert. Note relict cortex on both faces, despite the piece being only 8 mm in thickness. Bottom: FS 86. A similar small and relatively thick biface manufactured on a banded fine grained brown chert	77
Figure 8-6. Dimensions of complete flakes recovered from 41LR161 separated by cortex cover.....	78
Figure 8-7. Test distribution generated by pooling all artifacts at 41LR159, and randomly sampling new pairs of assemblages and their respective cortex ratio differences 10,000 times. The dashed vertical line highlights the observed difference in cortex ratio between chert and quartzite assemblages. The area in blue represents values more extreme than 95% of cortex ratio differences generated through resampling the pooled data. The difference between quartzite and chert cortex ratios are unlikely to be statistically significant (p-value=0.57)	80
Figure 9-1. Image on the right show roots of various sizes throughout the unit profile of TU 1 on 41LR154. Image on the left shows active rodent borrowing in the upper levels of TU 3 on 41LR159.....	84
Figure 9-2. Two scenarios of debitage distribution by site. In blue, artifacts cluster at the bottom of the units near the clay floor suggesting that these artifacts are in secondary contexts and have low integrity. The other pattern in red indicates some degree of integrity where two peaks are represented suggesting two occupations	84
Figure 9-3. Vertical distributions of chipped stone and or burned rock from test units on 41LR159	86
Figure 9-4. Vertical distribution of burned rock recovered from TU 2 on 41LR161	87
Figure 9-5. Four hypothetical patterns of MSS values (Mauldin et al. 2018: Figure 7-12)	88
Figure 9-6. MSS values of test unit sampled at 41LR154. Green bar represents surface. Orange bar represents terminal depth	88
Figure 9-7. MSS values of test units sampled at 41LR159. Green bar represents surface. Orange bar represents terminal depth	89
Figure 9-8. MSS values of test units sampled at 41LR161. Green bar represents surface. Orange bar represents terminal depth	90
Figure 9-9. MSS values of test unit sampled at 41LR177. Green bar represents surface. Orange bar represents terminal depth	91
Figure 9-10. MSS values of test units sampled at 41LR203. Green bar represents surface. Orange bar represents terminal depth	91
Figure 9-11. MSS values of test unit sampled at 41LR226. Green bar represents surface. Orange bar represents terminal depth	92

List of Tables:

Table 2-1. Soils Specific to the 12 Sites.....	7
Table 3-1. A Generalized Chronology of Northeast Texas (Kenmotsu and Perttula 1993:Table 2.1.2).....	11
Table 3-2. The Caddo Chronology of Middle Red River Region (Bruseh 1998:Figure 3-4).....	14
Table 4-1. Temporal Diagnostics found on Camp Maxey	19
Table 4-2. Site MLD average from highest to lowest.....	21
Table 4-3. Mean Thickness to Length Ratios (Mahoney 2001, Mahoney et al. 2002).....	24
Table 4-4. Summary of Debitage Material Type.....	25
Table 4-5. Summary of Lithics and Prehistoric Ceramics Recovered from Sites Reviewed at Camp Maxey	27
Table 5-1. Summary of Shovel Tests on Seven Maxey Sites.....	31
Table 5-2. Summary of Tests Units on Ten Maxey Sites	32
Table 5-3. Flotation Samples Collected During the Present Project.....	33
Table 6-1. Summary of Positive Shovel Tests at 41LR154	38
Table 6-2. Summary of Positive Shovel Tests at 41LR159	41
Table 6-3. Summary of Test Units Excavations at 41LR159.....	41
Table 6-4. Summary of Artifacts by Unit and Level from 41LR159.....	43
Table 6-5. Summary of Positive Shovel Tests at 41LR161	45
Table 6-6. Summary of Test Units Excavations at 41LR161.....	46
Table 6-7. Summary of Artifacts by Unit and Level from 41LR161.....	47
Table 6-8. Summary of Positive Shovel Tests at 41LR162	49
Table 6-9. Summary of Test Units Excavations at 41LR162.....	49
Table 6-10. Summary of Test Units Excavations at 41LR165.....	52
Table 6-11. Summary of Test Units Excavations at 41LR203.....	57
Table 6-12. Summary of Artifacts by Unit and Level from 41LR203	57
Table 6-13. Summary of Test Units Excavations at 41LR226.....	60
Table 6-14. Summary of Artifacts by Unit and Level from 41LR226.....	60
Table 6-15. Summary of Test Units Excavations at 41LR238.....	63
Table 6-16. Summary of the Previous and Current Investigations	67
Table 7-1. Presence of Charcoal by Site and Units at and below Level 4	69
Table 7-2. Radiocarbon Results from 41LR159 and 41LR161	69
Table 7-3. Chronological Potential of the Ten Tested Maxey Sites.....	71
Table 8-1. Summary of Chipped Stone Across Sites Separated by Raw Material.....	74
Table 8-2. Assemblage volume and surface area, compared to the amount of cortical area represented across artifacts grouped by raw material. The observed cortical area is compared to a modelled cortical area we would expect if the entirety of core reduction happened on site.	79
Table 8-3. Summary of Site-Level Content Analysis	81
Table 9-1. Site- Level Observations of Natural and Human Impacts	83
Table 9-2. Test Unit-Level Observations of Bioturbation.....	83
Table 9-3. Summary of Excavated Test Units from the Maxey Project.....	85
Table 9-4. Summary of Test Unit Integrity Determination Based on Chipped Stone and Burned Rock Distribution	87
Table 9-5. Summary of Test Unit Integrity Determination Based on MSS Analysis	92
Table 9-6. Chipped Stone and Burned Rock Site Summary Data from Unit Profiles	92
Table 9-7. MSS Site Summary Data from Unit Profiles.....	92
Table 10-1. Summary of the Ten Archaeological Sites Tested for NRHP Eligibility	95
Table A-1. Radiocarbon Dates Used to Create the Middle Red River SPD	105
Table B-1. MSS Sampling Information	109
Table C-1. Debitage Attribute Data.....	115

This page intentionally left blank.

Acknowledgements:

The Maxey project involved the relocation of twelve sites recorded some 20 to 25 years ago, the shovel testing of seven of those sites, and the testing of ten of those twelve sites. A project of this magnitude involved more than just the three authors, but the combined talents and energies of multiple CAR personnel. The authors would like to thank the primary field crew, Michelle Carpenter and Jason Perez who performed with dedication and professionalism despite the swarms of mosquitoes, ticks, poison ivy, bull nettle, thorny brush, and the intense humidity and heat of Camp Maxey. A second crew consisting of David Burns and Brooke Salzman returned to Maxey and experienced a somewhat diminished experience and performed admirably. The processing of artifacts was undertaken by CAR's lab staff, Mikaela Razo under the guidance of the Lab director, Cindy Munoz. Ms. Munoz participated in the initial site relocation and attempted to keep the lead author out of harm's way. Sarah Wigley (Chapter 4) and Dr. Jonathan Paige (chapter 8) provided understanding to this archaeological effort at Camp Maxey by placing into context the past work undertaken by CAR. We hope these chapters will add to our knowledge of the prehistory of the region. Report production was undertaken by Peggy Wall who edited the final version of the report, created and finalized figures, and created the layout for the final document. We have very deep gratitude for the pain you endured during that process. Dr. Raymond Mauldin, the Principal Investigator and Dr. Mary Whisenhunt also edited the report. And finally, the crew and authors would like to acknowledge our deep gratitude to Dr. Mauldin for his insights, wisdom, and good sense of humor.

We also would like to thank Richard Martinez, the director of the Texas Military Department's Environmental Branch, who brought the project to a conclusion and Kristen Mt. Joy, formerly head of cultural resources of TMD, who initiated and supported the Maxey National Registry project. The lead author also acknowledges and thanks officials and delegates of the Choctaw Nation of Oklahoma, the Kickapoo Tribe of Oklahoma, and the Mescalero Apache Tribe for visiting and providing comments during the excavation of 41LR159. And finally, we thank the staff of Camp Maxey for keeping us out of harm's way during the reconnaissance, survey, and testing phases of this project.

This page intentionally left blank.

Chapter 1: Introduction and Project Description

Leonard Kemp

The Center for Archaeological Research (CAR) at The University of Texas at San Antonio conducted National Register of Historic Places (NRHP) eligibility testing of ten archaeological sites located on Camp Maxey, a facility operated by the Texas Military Department (TMD) in Lamar County, Texas. Prior to testing, CAR performed an exploratory survey of 12 archaeological sites having undetermined eligibility. Shovel tests were excavated on seven of these sites to refine the placement of test units. Ultimately, ten sites were selected and tested under Section 106 of the National Historic Preservation Act (NHPA) of 1966, as amended. These ten sites are 41LR154, 41LR159, 41LR161, 41LR162, 41LR165, 41LR175, 41LR177, 41LR203, 41LR226, and

41LR238. While the project was not conducted under a Texas Antiquities Permit, it was conducted in a manner consistent with the requirements of the Antiquities Code of Texas. The testing was performed under Interagency Cooperation Agreement TMD20-ENV-15, with Dr. Raymond Mauldin serving as Principal Investigator and Leonard Kemp serving as Project Archaeologist.

Camp Maxey is a 2570-hectares military training facility located approximately 15 km north of the City of Paris, the county seat of Lamar County and just west of Powderly, an unincorporated community along US Highway 271 (Figure 1-1). The facility is located on the Pat Mayse Lake East USGS

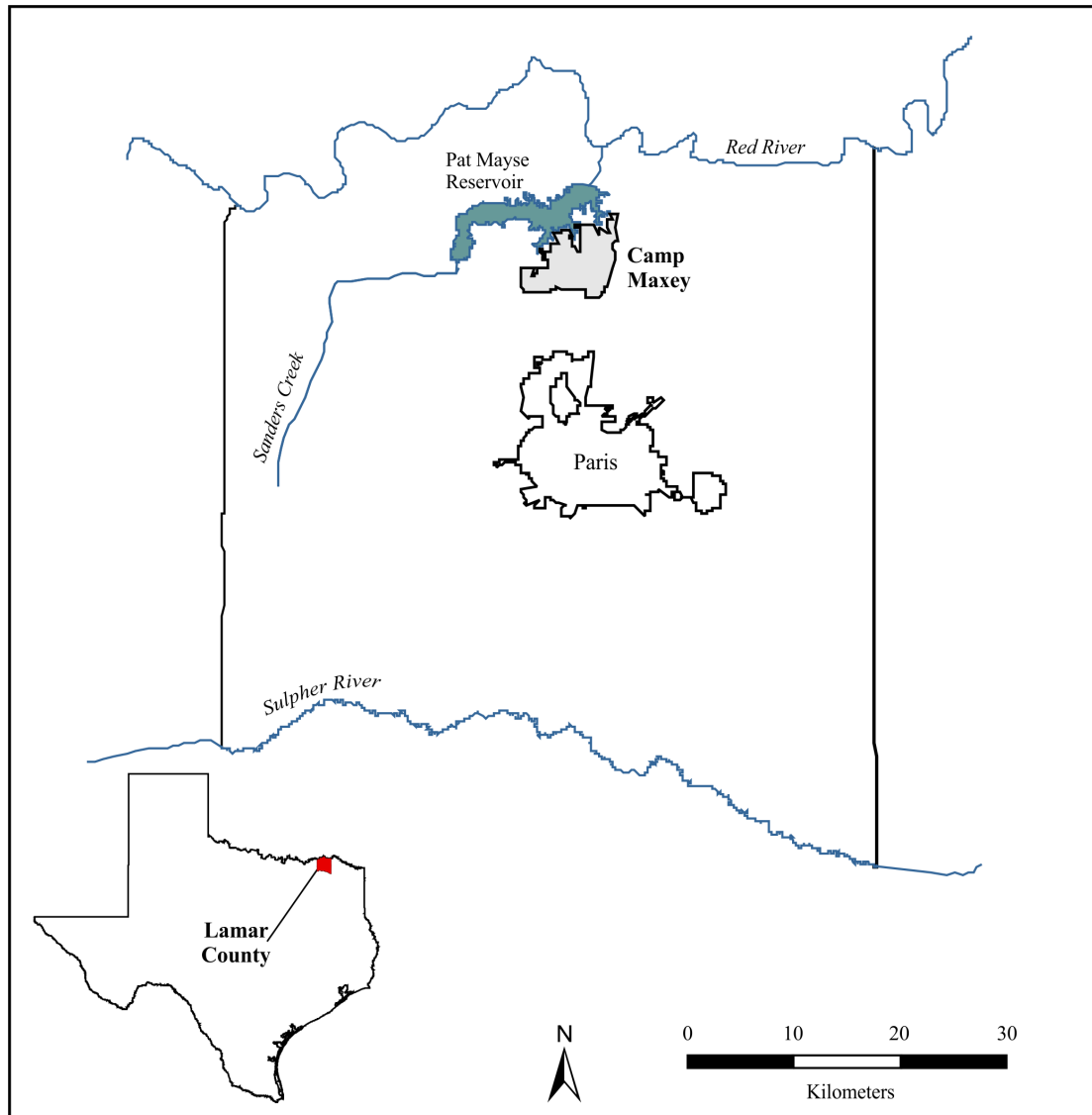


Figure 1-1. The location of Camp Maxey in Lamar County, Texas.

7.5-minute quadrangle maps. Camp Maxey was created in 1942 to train infantry combat troops during World War II. By 1943, the base had grown to 28,328 hectares with over 2,000 buildings and could house approximately 30,000 soldiers. It would eventually train almost 194,000 troops and employ 10,000 civilians. The base was placed on inactive status in October of 1945. Since 1949, the facility has been the training ground for the TMD, generally for troops stationed in the northeast portion of the state (Leffler 2001:13). The northern portion of the facility was inundated by Pat Mayse Lake, a reservoir constructed in 1965-1967 under the direction of the U.S. Army Corps of Engineers.

There are 139 archaeological sites recorded on Camp Maxey with 12 of those sites having undetermined NRHP eligibility (Figure 1-2). The initial Maxey survey (Nickels et al: 1998) was the first CAR project to use a GPS to record datums and boundaries of archaeological sites. Unfortunately, multiple

issues including a lack of precision and the learning curve to operate the GPS contributed to conflicting site locations and boundaries. CAR utilized multiple map sources from including the overall sites maps and individual site maps which in some cases had different boundaries. The archaeological testing of 10 of these sites to determine eligibility was conducted in the summer of 2021 and late spring of 2022. CAR excavated 93 shovel tests, 23 1-x-1 m and screened approximately 10.1 m³ of test unit deposits. From both shovel tests and test units, CAR recovered four bifaces, a uniface, two cores, two edge-modified flakes, six native ceramic fragments (4 of which refitted), 165 pieces of debitage, 2.45 kg of non-feature burned rock, burned faunal bone, and a quartzite crystal, as well as historic artifacts, including a 1903 U.S. penny, glass fragments, and bullets. CAR identified two burned rock features, one at 41LR159 and another at 41LR161. Ultimately, CAR recommends that site 41LR159 is eligible for listing on the NRHP. Sites 41LR154,



Redacted Image

Figure 1-2. The locations of the 12 archaeological sites investigated during this project.

41LR161, 41LR162, 41LR165, 41LR175, 41LR177, 41LR203, 41LR226, and 41LR238 are recommended as not eligible for NRHP listing. In addition, CAR redefined the boundaries of four sites, 41LR154, 41LR159, 41LR161, and 41LR162 reflecting findings from the current investigation.

Following laboratory processing and analysis, and in consultation with the TMD, selected items that had no remaining scientific value were discarded. Discarded artifacts included non-feature burned rock, heat spalls, and soil samples. This discard conformed to THC guidelines. All remaining archaeological samples, associated artifacts, documents, notes, and photographs were prepared for curation according to THC guidelines and are permanently curated at CAR at UTSA.

Measures of Eligibility Determination

The current project involves NRHP testing of ten sites to determine their eligibility status for inclusion to the National Register. The National Register is maintained by the National Parks Service (NPS) with the criteria for eligibility determination identified in Title 36, Code of Federal Regulations (CFR) 60.4 (NPS 2016). There are four criteria, A-D, that were developed to assess “the quality of significance” in a variety of areas, including archaeology (NPS 2016). Generally, Criterion D is the most relevant to archaeological sites as it states sites that possess integrity and that “have yielded, or may be likely to yield, information important in prehistory or history” or data are eligible for inclusion on the NRHP (NPS 2016).

CAR used three measures to address the question of whether an archaeological site is eligible to the National Register. These measures are site chronology, the content of a site, and site integrity with each one of these measures related to the other. This three-part approach has been previously employed in Mauldin et al. (2018) with relative success in accessing a site’s overall contribution or potential contribution to add important information in prehistory.

The first measure focuses on the chronological context or possibility of placing in time a set of data using temporally diagnostic artifacts and/or radiocarbon dating. The second

and third measures, which focus on data and integrity, are specifically stated in Criterion D. Considerations of site content assume that a site with a limited variety of data can only address a limited number of questions, while a site that has a more robust data set can address a greater number of research questions. The final measure is that of integrity such that if a site’s generated data is not in context, it has little scientific validity to address a suite of research questions.

Report Organization

This report contains ten chapters and four appendices. Following this introduction, Chapter 2 provides an overview of the modern and paleoenvironment of Camp Maxey. Chapter 3 presents the cultural history of northeast Texas and previous archaeology investigations of Camp Maxey. Chapter 4 explores regional radiocarbon trends of the Red River Basin and synthesizes Camp Maxey archaeological data based on previous testing by CAR (Greaves 2003; Lyle et al. 2001; Mahoney et al. 2001; Mahoney et al. 2002). This 4th chapter provides context for the current investigation and summarizes archaeological patterns found at sites on Camp Maxey. Chapter 5 describes the field and laboratory methods used on the project. Chapter 6 provides a detailed account of each site, including information on the work accomplished and a summary of the materials recovered. Chapter 7 reports on the chronological potential of each site. Chapter 8 presents information on site content, specifically data on the lithic assemblage. It also summarizes the potential of each of the ten tested sites to contribute to our understanding of the past. Unfortunately, the majority of the site had none or few lithics. This small sample size essentially eliminates them from in-depth analysis. One site, 41LR159 had a sufficient quantity of lithic which permitted a more in-depth analysis of the assemblage. Chapter 9 assesses site integrity of the ten tested sites. Chapter 10 provides a summary of the project, including recommendations for the NRHP eligibility of the ten sites. Five appendices are included in this volume. Appendix A presents details on the radiocarbon dates. The magnetic susceptibility data is presented in Appendix B. Appendix C provides details on the chipped stone assemblage. Appendix D describes the process for the cortex ratio methods used to analyze the lithic assemblage at 41LR159. Appendix E provides the computer code, in R, used in the analysis.

This page intentionally left blank.

Chapter 2: Project Environment and Setting

Leonard Kemp

Camp Maxey is in the northern portion of Lamar County in northeast Texas. The first section of this chapter describes the modern climate followed by a description of the geology and soils found on Camp Maxey. The following section of this chapter describes the regional environment. The chapter concludes with a summary of plants and animals found in the region.

Climate

Lamar County has a humid subtropical climate with warm summers and dry winters (Ressel 1979). Ressel (1979:1) states the region is also subject to extreme temperatures from both polar fronts and heat waves. Figure 2-1 shows the average monthly maximum and minimum temperatures

from 1991 to 2020 for Paris, Texas (National Oceanic and Atmospheric Association [NOAA] 2021). The hottest months of the year are June, July, and August with an average maximum temperature ranging from 32.8°C to 36°C. January is the coldest month of the year with an average minimum temperature of -0.1°C followed by December at 1.0°C.

Ressel (1979) characterizes the region's rainfall as abundant and evenly distributed throughout the year. Rainfall, as characterized by data from the Paris weather station, averaged 124.1 cm per year from 1991 to 2020 (NOAA 2022). The month of May has the highest rainfall amount with an average of 14.3 cm followed by October with 11.73 cm (Figure 2-2). The driest month is August with 7.4 cm followed by January with 7.8 cm.

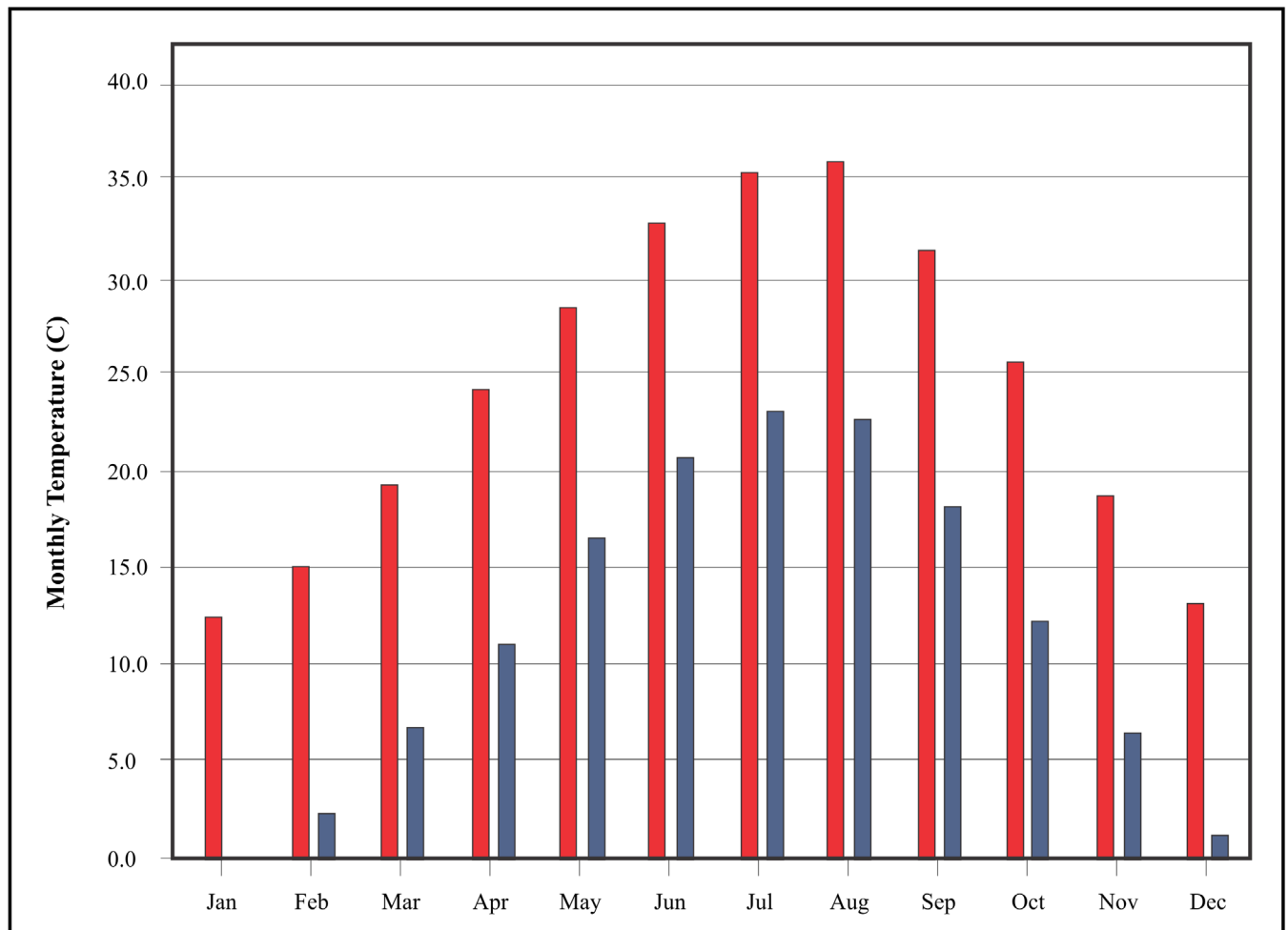


Figure 2-1. The average maximum (red) and minimum (blue) monthly temperature at Paris, Texas based on data from 1991 to 2020 (NOAA 2021).

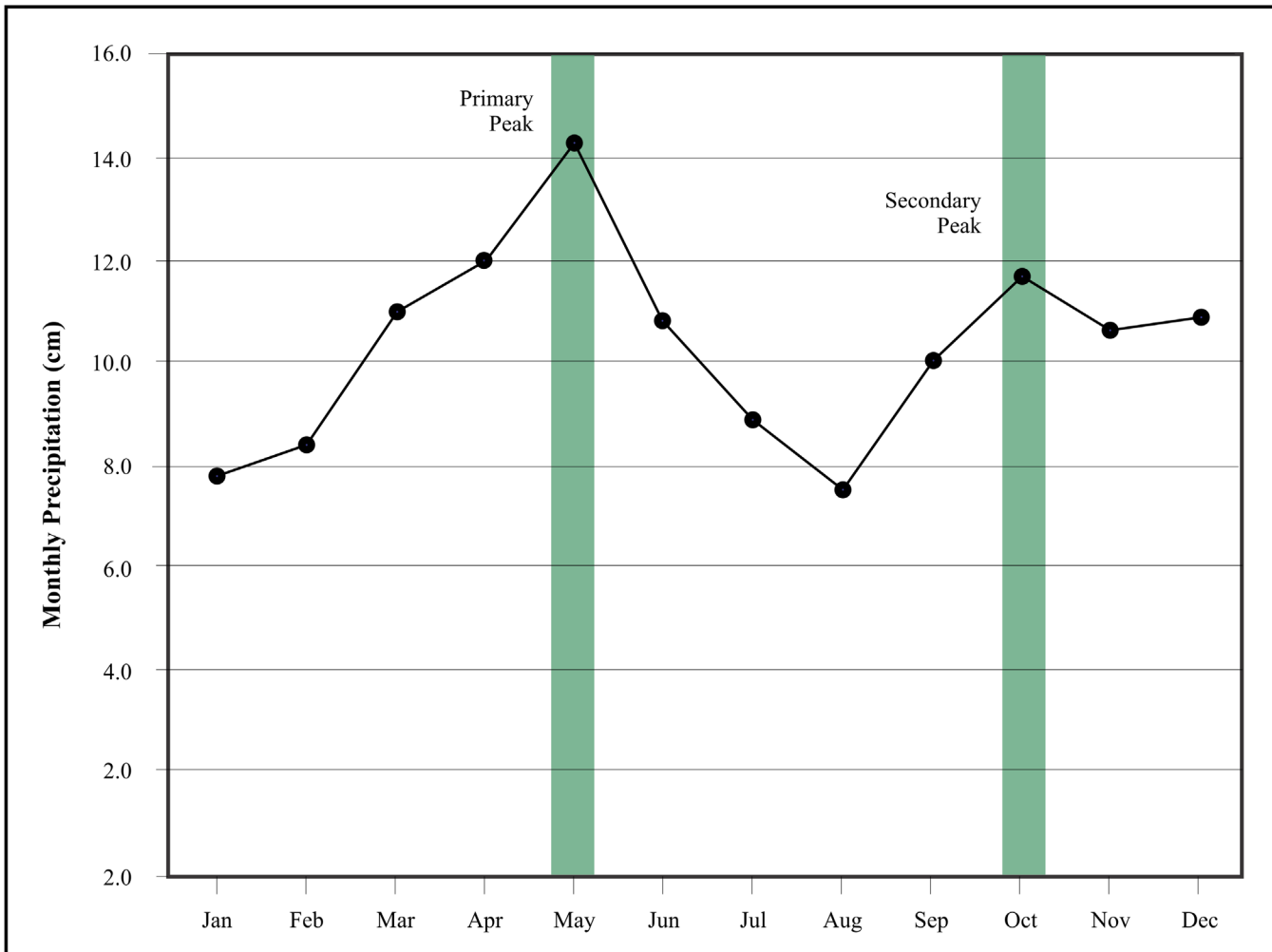


Figure 2-2. The average monthly rainfall at Paris, Texas based on data from 1991-2020. Peak rainfall occurs in May with a secondary peak in October (NOAA 2022).

Geology and Soils

The Cretaceous Eagle Ford and Bonham formations underlie Camp Maxey (Fisher et al. 1996). The Eagle Ford Formation is composed of thin sandstone sandy limestone grading to fine to coarse quartz sand at the Lamar and Red River County line (USGS 2022). The Bonham Formation is less prominent and found in the southeast portion of the base. It is composed of marl and clay becoming sandier towards the east (USGS 2022).

The majority of the base falls within the Freestone-Hicota soil complex found in the flats and uplands of the base. The complex is characterized by 40-80 cm of sandy loam over a clay loam to clay Ct horizon. Five sites or portions thereof fall within this soil series. Soils found along stream drainages are Woodtell loam, Whakana fine sandy loam, and Annona loam. These soils are typically very deep loam with gradually increasing clay to depth. Eight sites or portions of

those sites fall within these soil classes. Table 2-1 lists the specific soil(s) associated with each site.

The Sandy Mantle

Pertinent to this discussion of soils, Camp Maxey is within the Sandy Mantle of Texas. Alfisols within the Texas Gulf Coast Plain commonly exhibit textural contrasts between sandy, artifact-bearing A-E horizons (i.e., sandy mantle), and artifact-sterile clay-rich Bt (argillic) horizons as shown in Figure 2-3. This has invoked debate about the origins of the Sandy Mantle which has implications for the integrity of buried archaeological sites.

At present there are two models of the development of the Sandy Mantle, the pedogenic and the geomorphic, with the former suggesting that Sandy Mantle sites have low integrity and the latter suggesting that sites may have varying degrees of integrity (Figure 2-4). The pedogenic model (see Bruseth and Martin

Table 2-1. Soils Specific to the 12 Sites

Site	Soils	Site	Soils
41LR154	Freestone-Hicota complex, 0-3% slopes	41LR177	Whakana fine sandy loam 1-5% slopes
41LR159	Woodtell loam, 5-12% slopes and Freestone-Hicota complex, 0-3% slopes	41LR184	Woodtell loam soil, 5-12% slopes
41LR161	Woodtell loam, 5-12% slopes and Freestone-Hicota complex, 0-3% slopes.	41LR203	Freestone-Hicota, 0-3% slopes
41LR162	Woodtell loam, 5-12% slopes and the Annona loam, 1-4% slopes.	41LR213	Freestone-Hicota complex, 0-3% slopes and Woodtell loam soil, 5-12% slopes
41LR165	Lassiter silt loam 0-1% slopes	41LR226	Whakana fine sandy loam, 1-5% slopes and Woodtell loam, 5-12% slopes
41LR175	Freestone-Hicota 0-3% slopes	41LR238	Whakana fine sandy loam, 1-5% slopes and Woodtell loam, 5-12% slopes



Figure 2-3. Profile and floor of a unit excavated in the Sandy Mantle with a sandy, potentially artifact bearing horizon over an artifact-sterile clay terminal level.

2001) suggests that the Sandy Mantle and the argillic horizons are derived in situ from weathering Tertiary bedrock. Based on this model, the landscape is pre-Holocene in origin with artifacts moving downwards via bioturbation. Archaeologically, this

viewpoint assumes that artifacts are in secondary contexts with limited to no research or preservation value. The geomorphic model (Bousman and Fields 1991; Frederick and Bateman 2001) proposes that the Sandy Mantle is Holocene-age eolian

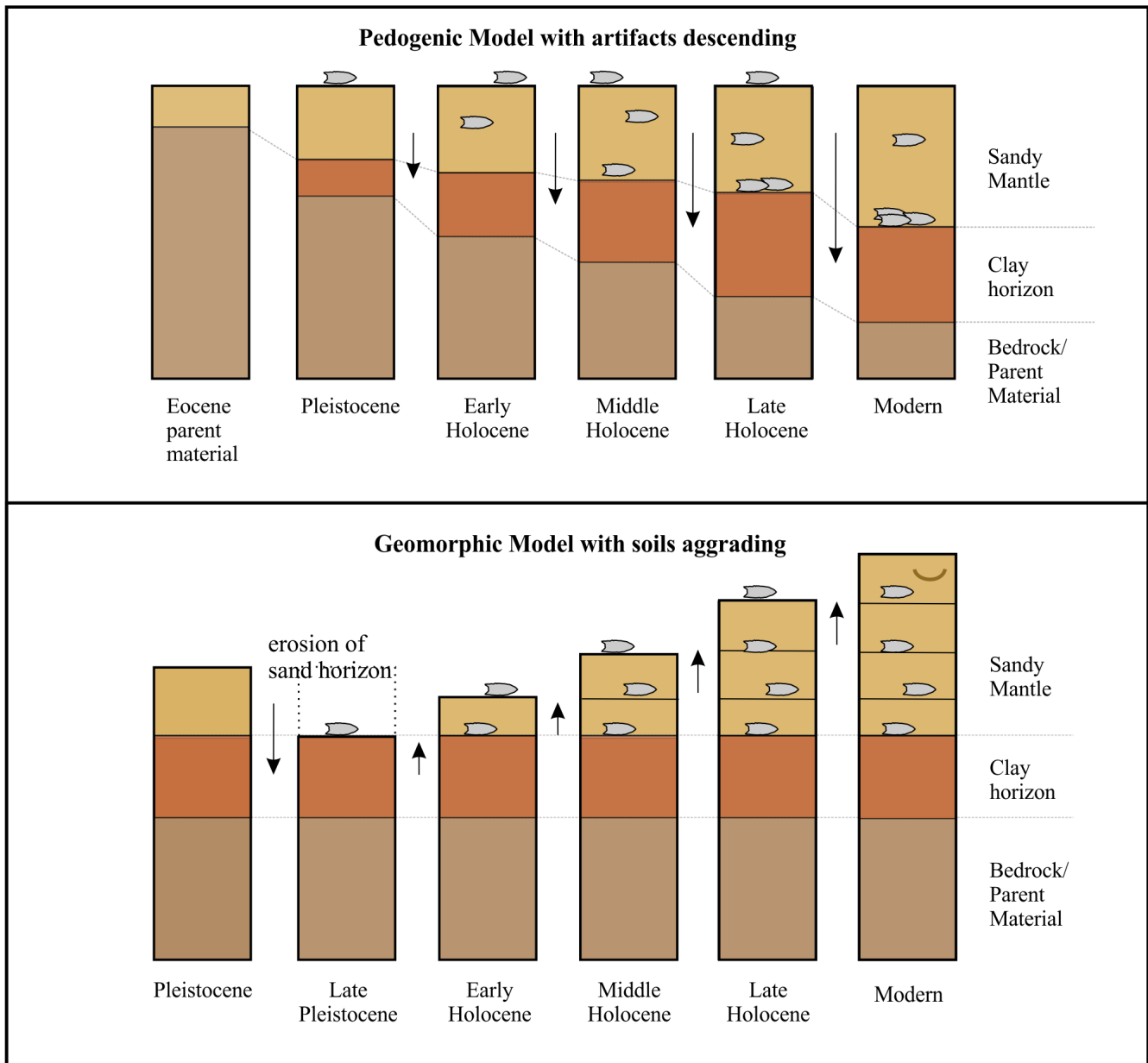


Figure 2-4. Models of pedogenic and geomorphic formation process for the Sandy Mantle (Ahr et al. 2012).

and colluvial deposits overlaying the developed argillic horizon. If this scenario is accurate, archaeological deposits have the potential to be in a stratified context (Bousman and Fields 1991; Frederick and Bateman 2001).

Ahr et al. (2012) suggest the geomorphology of the Sandy Mantle region is complex with multiple formation processes (alluvial, colluvial, and eolian) likely working at several different scales. These processes could potentially preserve aspects of the archaeological record in some cases. Past archaeological testing on sites within the Sandy Mantle suggest that they fit within the pedogenic model (Nickels 2008; Mauldin et al. 2018; Kemp et al. 2019; Kemp et al. 2023). That is, in some cases, the majority of large artifacts are found lying on the

clay floor of test units. Conversely, these past investigations have also found sites, or portions of sites, that have integrity with discrete and distinct horizon and artifact sequences that are internally consistent and supported by chronometric dates suggesting some integrity. As such, excavation of a site in the Sandy Mantle should use multiple means of analysis to determine if a unit within a site has integrity.

Regional and Project Setting

Camp Maxey is located in the Red River Basin that creates the Texas/Oklahoma of northeast Texas. Camp Maxey is in the post oak and hickory woodlands and savannahs of the East

Central Texas Plains (Griffith et al. 2007). This sub region is described as level to rolling plains and moderately dissected by drainages (Griffith et al. 2007). As shown in Figure 2-5, the Red River, a major west to east drainage bisects the region and serves as a boundary between Oklahoma and Texas. Four major creeks drain into the Red River from the Texas side. These are the Bois d'Arc, Sanders, Pine, and Big Pine creeks. On the Oklahoma side of the border three drainages flow into the Red River, the Kiamichi River, the Blue River, and Boggy Mud Creek (Figure 2-5). To the north of this region in Oklahoma are the Ouachita Mountains, an east to west trending, low mountain range and its drainage, the Little River. To the south of Camp Maxey is the tall grass prairie of the Blackland Prairie (Griffith et al. 2007). The Sulphur rivers flow west to east through the Blackland Prairie (Figure 2-5).

The geomorphic landforms of Camp Maxey are varied with floodplains, fluvial terraces, slopes, and ridge crests (Lyle et al. 2001:6). A subtle east-west ridge runs through Lamar County and is partially located on the southern portion of the base. This ridge creates drainages that flow either to the north or to the south (Figure 2-6; Pertulla and Tomka 2001:5).

Drainages on Camp Maxey flow north to Sanders Creek, a tributary of the Red River located 11 km to the north. The principal drainage on Camp Maxey is the intermittent Visor Creek, a tributary to Sanders Creek. Sanders Creek is the main source of Pat Mayse Lake, a reservoir created in the late 1960s. In addition, there are several wetlands, numerous ponds, and lakes within the facility (Gravett et al. 1999).

Flora and Fauna

Flora

There is high diversity of plants at Camp Maxey with over 590 species (Natural Resources Environmental Branch [NREB] 2020:16). Approximately 65% of Camp Maxey is woodland comprised of post oak (*Quercus stellata*), black hickory (*Carya texana*), southern red oak (*Q. falcata*), and blackjack oak (*Q. marilandica* [Ford and Hampton 2005:361]). The understory of this woodland includes dogwood (*Cornus florida*), yaupon (*Ilex vomitoria*), and farkleberry (*Vaccinium arboreum* [Ford and Hampton

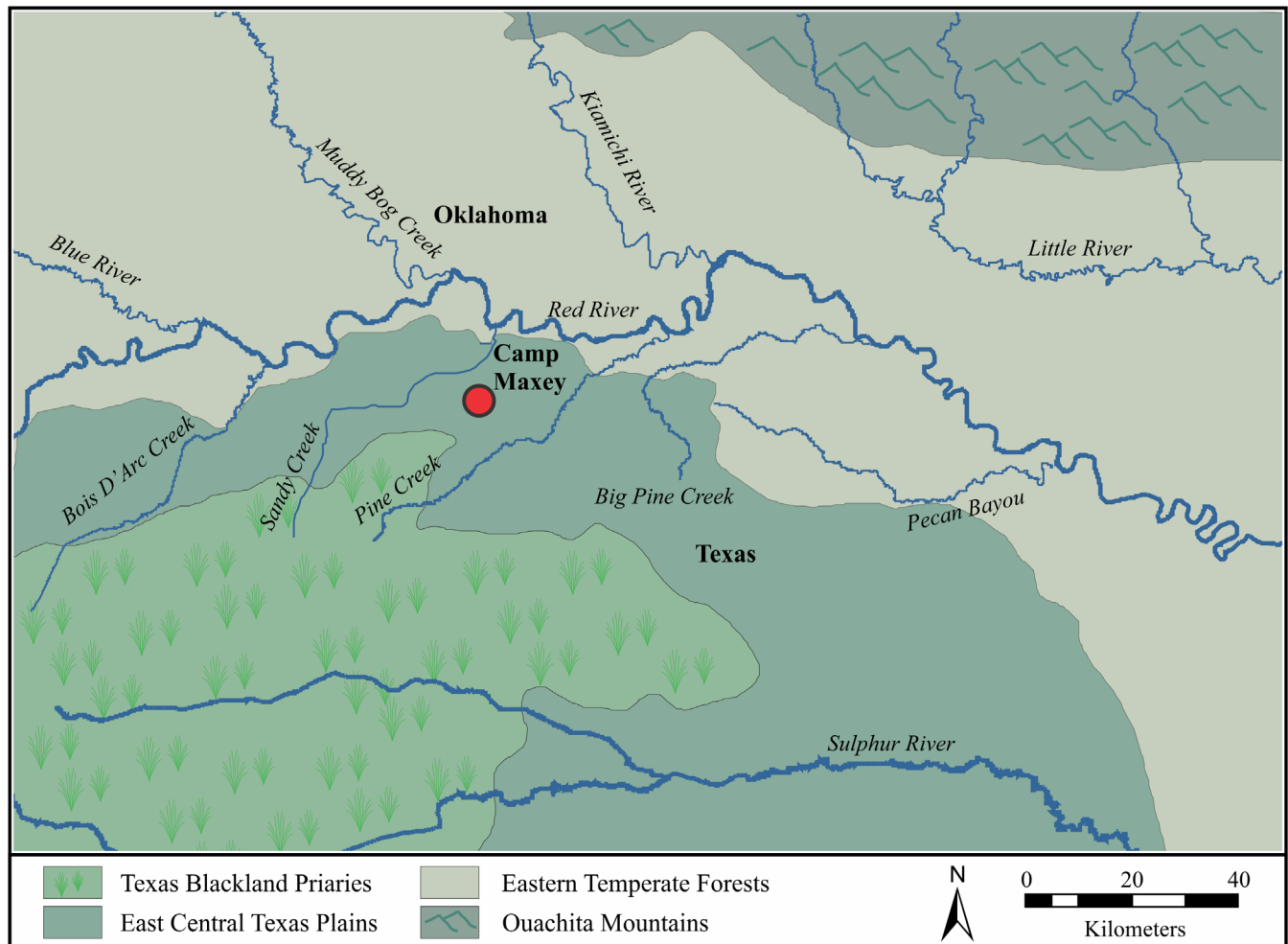


Figure 2-5. Physiographic regions and features surrounding Camp Maxey.

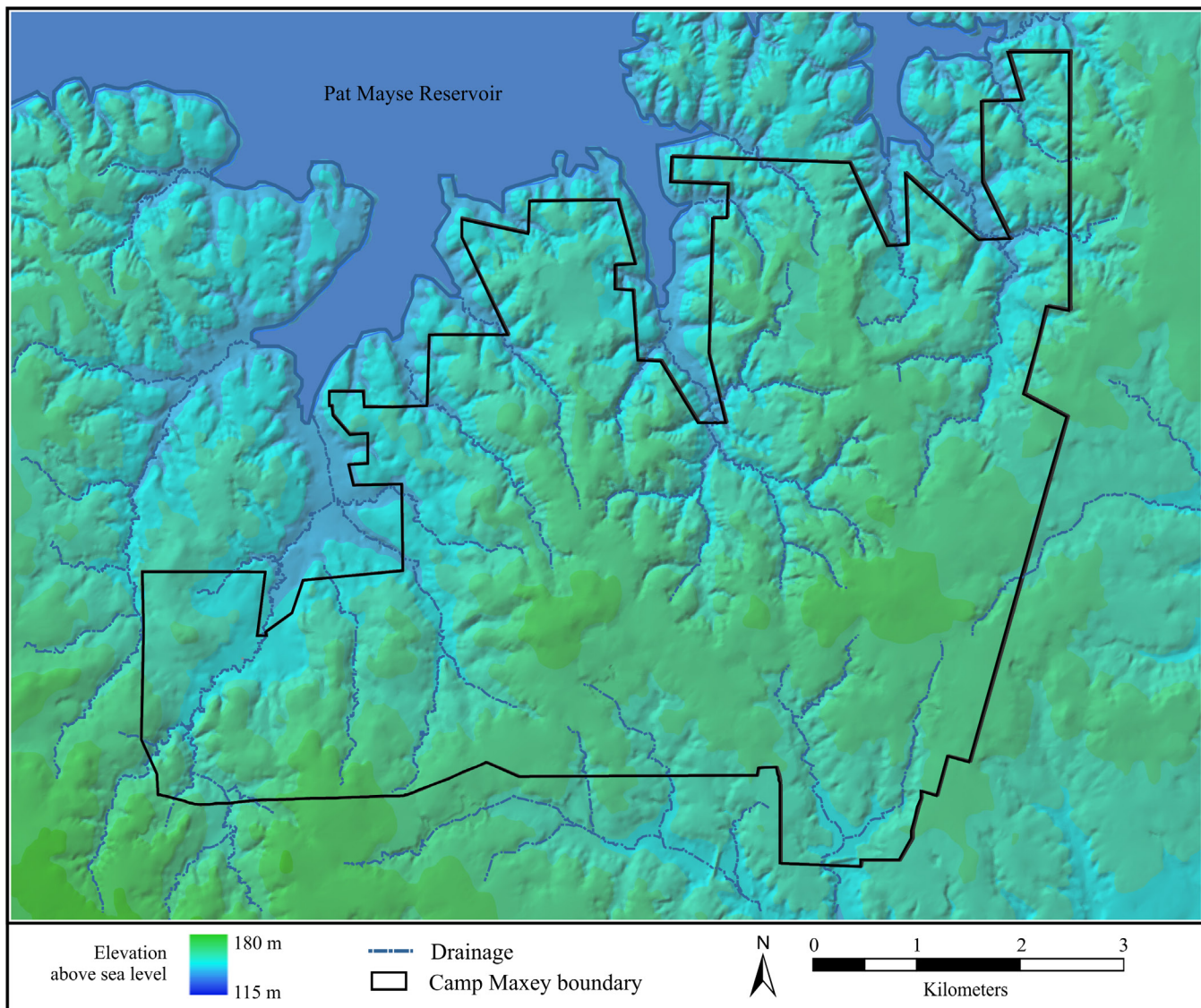


Figure 2-6. A raster map showing elevations and drainages of Camp Maxey.

2005:361]). Grasslands comprise 18% of the installation with little bluestem (*Schizachyrium scoparium*), Indiangrass (*Sorghastrum nutans*) and other grasses and forbs (Ford and Hampton 2005:361). Small and scattered patches of shortleaf pine (*Pinus echinata*) with an understory of oak and hickory trees comprise 3% of the base (Ford and Hampton 2005:361). Water oak (*Q. nigra*) and elms (*Ulmus* sp.) are found along the numerous drainages running through Camp Maxey.

Fauna

There is also a high diversity of animal life at Camp Maxey with 274 species of vertebrates. This is due, in part, to the abundant rainfall and the location of the Camp within a transition zone between southeast and southwest vegetation. Recorded are six carnivore species, 19 species of rodents, six species of bats, and eight species of other

mammals (Edwards and Johnson 2007). The white-tailed deer (*Odocoileus virginianus*) is the largest native species currently on Camp Maxey. Carnivores included the coyote (*Canis latrans*), two species of fox including the red fox (*Vulpes vulpes*) and the common gray fox (*Urocyon cinereoargenteus*), the common raccoon (*Procyron lotor*), the striped skunk (*Mephitis mephitis*), and the bobcat (*Lynx rufus*). Lagomorphs found on the facility included both the swamp rabbit (*Sylvilagus aquaticus*) and the eastern cottontail (*Sylvilagus floridanus*). Multiple species of Rodentia have been observed including American beaver (*Castor canadensis*), the Baird's Pocket Gopher (*Geomys breviceps*), three species of squirrels, and various species of mice and rats. In addition to mammals, there are 149 species of birds that either live on or migrate through Camp Maxey, 65 species of amphibians and reptiles, and 27 species of fish (NREB 2020:H-2, H-3, H-4).

Chapter 3: Cultural History of Northeast Texas and Past Archaeological Investigations of the Camp Maxey Region

Leonard Kemp

This first part of this chapter presents a synopsis of the cultural chronology of Northeast Texas to provide context for the investigated sites of the Camp Maxey project. As such, the chapter begins with the Paleoindian period and concludes with the development of Camp Maxey at the beginning of World War II. It is followed by a brief account of previous archaeological investigations of/or related to Camp Maxey.

North Texas Cultural Chronology

The region incorporating Camp Maxey falls within the middle Red River Basin of Northeast Texas. Table 3-1 is a generalized chronology of northeast Texas based on previous research by Kenmotsu and Pertulla (1993); Pertulla (2004), and Story (1981). The prehistoric occupation is divided into three broad periods, the Paleoindian, Archaic, Woodland, and Caddo, each of which is divided into finer temporal divisions.

Paleoindian Period

The Paleoindian period (11,500 to 9000 Radiocarbon Years Before Present [RCYBP]) is divided into two sub-periods Early and Late. Paleoindian occupations are found along the resource-rich major stream basin of the region (Anderson 1996; Pertulla 2004). These occupations consist of widely dispersed, small camps often containing a generalized tool kit. Pertulla (2004) suggest these characteristics are more akin to a mobile hunter and gatherer lifestyle rather than a specialized hunter of megafauna. While Paleoindian artifacts are found in Northeast Texas they are generally

found in mixed assemblages, or as surface or isolated finds (Pertulla 2004).

Clovis and Folsom points are lanceolate-shaped, fluted projectile points-definitive of the Early Paleoindian sub-period (11,500 to 10,000 BP). Both points are made of high quality lithic material not normally found in northeast Texas. Bousman et al. (2004 Table 2.2) documented one Clovis component in Lamar County. Four Clovis points have been documented in Lamar County (Bever and Meltzer 2007: Table 1). Largent et al. (1991) noted that only one Folsom point has been recorded in Lamar County.

The Late Paleoindian period (10,000 to 8800 BP) is marked by multiple point styles including lanceolate-shaped Plainview and corner-notched or stemmed points such as Big Sandy, Dalton, San Patrice, and Scottsbluff (Turner et al. 2011). Note that Dalton and San Patrice are also considered diagnostics of the Early Archaic period (Pertulla 2013). The SMU salvage archaeological survey found one site, 41LR11, with a substantial Late Paleoindian component containing Plainview and Dalton points, and quince-style scrappers (Lorrain and Hoffrichter 1967). On Camp Maxey proper, a reworked Dalton point was found on the surface east of 41LR158 (Mahoney 2001:40).

Archaic Period

The archaeological record of the Early and Middle Archaic is sparse, as contrasted with the prolific record of Late Archaic sites. This trend is consistent with the radiocarbon analysis conducted by Selden (2013) that shows a dramatic increase

Table 3-1. A Generalized Chronology of Northeast Texas (Kenmotsu and Pertulla 1993:Table 2.1.2)

Years RCYBP	Cultural Periods	Dates AD/BC
90-270 BP	Historic Caddo	AD 1680-1860
270-550 BP	Late Caddo	AD 1400-1680
550-750 BP	Middle Caddo	AD 1200-1400
750-950 BP	Early Caddo	AD 1000-1200
950-1150 BP	Formative Caddo	AD 800-1000
1150-2150 BP	Early Ceramic/Woodland	200 BC-AD 800
2150-4000 BP	Late Archaic	2000-200 BC
4000-6000 BP	Middle Archaic	4000-2000 BC
6000-9000 BP	Early Archaic	7000-4000 BC
9000-11,500 BP	Paleoindian	9500-7000 BC

in the number of dates from Early and Middle Archaic to Late Archaic sites. The Early Archaic period (9000 to 6000 BP) appears to be a continuation of the Late Paleo-Indian adaptations with low population density, high mobility within large river basins, and a generalized adaptation to a variety of animal and plant food (Perttula 2004, 2013). Diagnostics of this period are the Breckinridge, Scottsbluff, Keithville, as well as the Pelican, Graham Cave, and Rice lobed points (Perttula 2013).

During the Middle Archaic period (6000 to 4000 RCYBP), the hunter-gatherer populations are still highly mobile exploiting a wide range of food resources (Perttula 2013). Although at some point, there is an emergence of substantial and extensive occupations along the major river basins of the region (Perttula 2004; Perttula 2013). Burned rock features, ovens, and pits suggest the processing of plants for foods as documented at sites in the Sulphur River drainage (Perttula 2004). Another characteristic of the Middle Archaic is the exchange of finished tools made from non-local chert as suggested by sites found in the Lake Fork Reservoir (Bruseh and Perttula 1981). Common diagnostics of the Middle Archaic include Morrill, Cossatot, Calf Creek/Bell/Andice, and White River point types (Perttula 2013).

During the Late Archaic period (4000 to 2150 BP) sites become prolific, suggesting increasing populations, the development of defined territories, increasing sedentism, and the use of local economic resources (Perttula 2004). Late Archaic occupations are found on a wide variety of landform that include major stream terraces, spring-fed branches, upland ridges, and tributaries (Perttula 2004). Burned rock features are often found at these sites. Late Archaic diagnostics include Yarbrough, Wells, Ellis/Edgewood, and Williams points (Perttula 2004).

Woodland Period

The Woodland period begins around 2150 and continues to 1150 BP. In general, people from this period are characterized as hunter-gatherers, although qualified in that they were becoming more sedentary occupying places longer than previous Archaic cultures. Developing technologies include ceramics and, around AD 700, the bow and arrow (Perttula 2004). There is no evidence at this time that suggests the use of cultigens. The material culture is distinguished by the presence of a thick-walled, grog-tempered ceramic plain ware bowls and jars, Gary and Kent points, and later by corner-notched arrow points (Perttula 2004).

Bruseh and colleagues (2001) cite the development of small villages and campsites in the Middle Red River

Basin as evidenced by the Ray Site (41LR135). The Ray Site is a small occupation dating to the late Woodland period containing multiple house structures with middens (Bruseh 1998, 2001). Woodland diagnostics include Gary dart points, Homan, and other arrow points, and ceramics identified as Williams Plain and Cole Creeks varieties (Bruseh 1998:54).

Caddo Prehistory

Figure 3-1 is a map of the Caddo archaeological area (Perttula (2012:Figure 1). It purports to show the maximum spatial extent of the Caddo between AD 800 and 1688 that included portions of Texas, Oklahoma, Arkansas, and Louisiana. The Caddo chronology used in this report is specific to that of the Middle Red River Valley in which Camp Maxey is located (Bruseh 1998;Table 3-2).

Formative/Early Caddo Period

Caddo sites from the Formative to the Early Caddo periods are found on elevated landforms of uplands alluvial terraces adjacent to major and minor drainages (Perttula 2004). Hamlets and farmsteads are the most common site type with some having small family cemeteries (Perttula 2004). Important ceremonial sites of the Formative/Early Caddo period include the T. M. Coles (41RR3), Boxed Springs (41UR30), and Hudnall-Pirtle (41RK4) mound centers on the Sabine and Sulphur rivers, and the George C. Davis site (41CE19) on the Neches River (Bruseh 1998:54).

Bruseh (1998:55) argues that the initial development along the Middle Red River valley takes place around AD 900. Ceramic types of the period include Davis Incised, and other horizontal incised ceramics, Pennington Punctated-Incised, and Crockett Curvilinear are found at habitation sites. Holly Fine Engraved, Hickory Fine Engraved, and Spiro Engraved are found in funerary contexts (Bruseh 1998:55). Arrow points found in association with these ceramic types include Agee, Homan, and Scallorn (Bruseh 1998:55). The A.C. Mackin site (41LR36) is the only known mound site in this portion of the Red River Valley (Bruseh 1998:54).

Middle Caddo Period

The Middle Caddo Period is defined as beginning around AD 1200 to 1400 (Perttula 2012:Table 1-1). Large settlements with one to three mounds with cemeteries, as well as hamlets and dispersed farmsteads are characteristics of the Middle Caddo settlement pattern (Perttula 2004). These sites are dispersed throughout east and northeast Texas along the Red River, Sabine River, and the Big Cypress

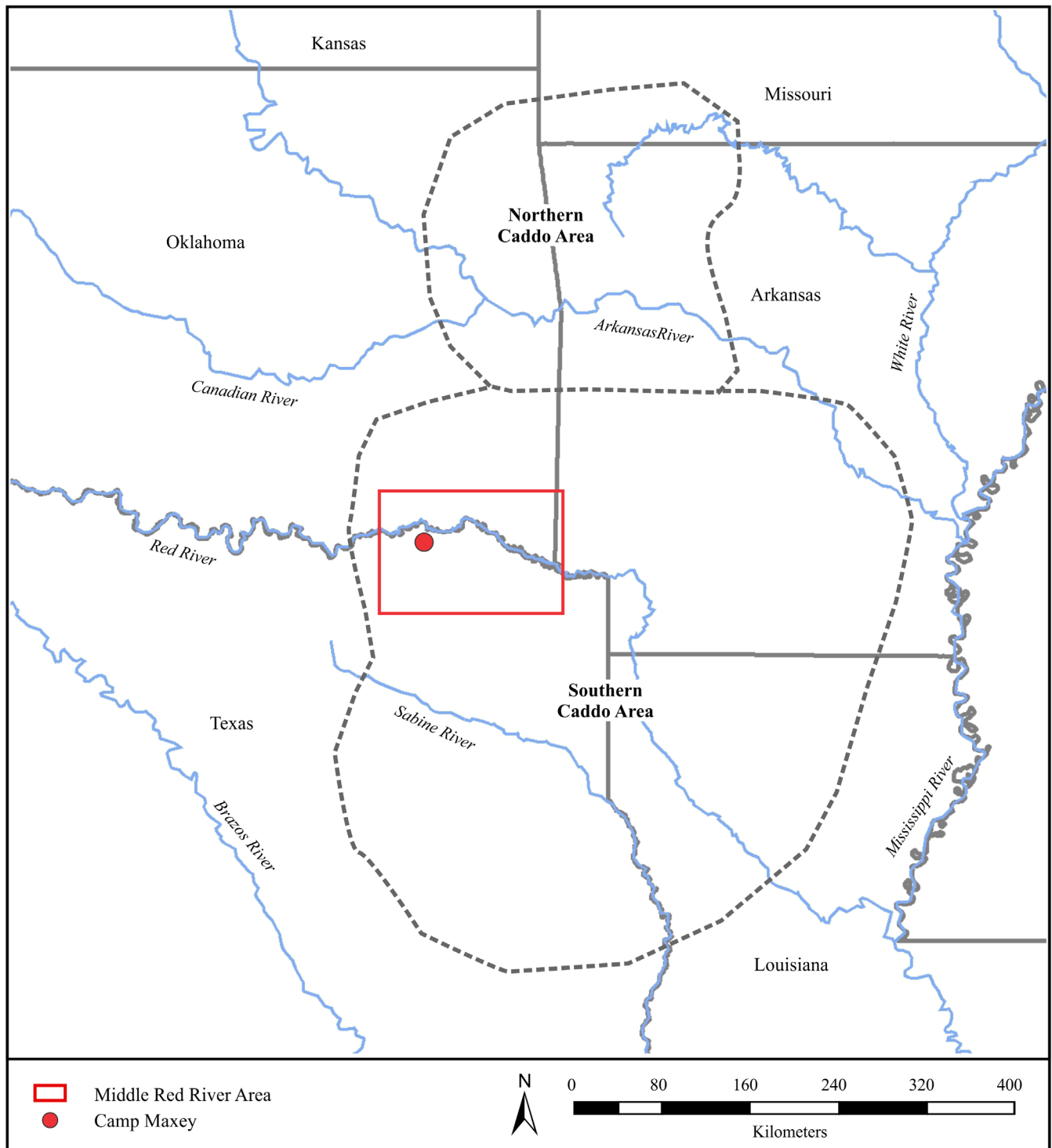


Figure 3-1. The Southern and Northern Caddo Areas as shown in Perttula (2012: Figure 1) with the Middle Red River Valley cultural area as defined by Bruseth in the red box (1998).

Bayous (Perttula 2004). Subsistence includes use of maize and squash supplemented with nuts, seeds, tubers, fishing and wildlife (Perttula 2004; 2010).

The Middle Red River valley chronology is referred to as the Sanders Phase and dates to AD 1100 to 1300 (Bruseth

1998:58-60). Note this chronology differs from the general chronology provided earlier in the chapter. The phase is based on the T.M. Sanders site (41LR2) located 27 km to the west of Camp Maxey on Bois D'Arc Creek and Red River. Sanders Phase diagnostics ceramics include Canton Incised, Maxey Noded Redware/Blackware, and Sanders

Table 3-2. The Caddo Chronology of Middle Red River Region (Bruseth 1998:Figure 3-4)

Cultural Periods	Middle Red River Phases	Dates AD/BC
Historic Caddo		AD 1700-1860
Late Caddo	Late McCurtain Early McCurtain	AD 1500-1700 AD 1300-1500
Middle Caddo	Sanders	AD 1100-1300
Early Caddo/Formative Caddo		AD 900-1100

Engraved (Bruseth 1998:58). Other diagnostics of this phase include Alba, Bonham, Morris, and Scallorn points, grinding stones, flake tools, celts, and sandstone abraders (Bruseth 1998:58). Sanders Phase site are found throughout the Middle Red River Valley and into southeastern Oklahoma along the Little River (Bruseth 1998:59).

Late Caddo Period

The Late Caddo sphere encompasses the east and northeast portions of Texas, northwestern Louisiana, western and central Arkansas, and southeast Oklahoma (Perttula 2004). The McCurtain phase is the Late Caddo manifestation found in the Middle Red River Valley and divided into early (AD 1300 to 1500) and late (AD 1500 to 1700) phases (Bruseth 1998). McCurtain phase sites include settlements and mound centers found to the east of Camp Maxey in Red River and McCurtain counties of Texas and the southeast corner of Oklahoma (Bruseth 1998). Perttula (2004) and Bruseth (1998) suggest mound construction may be limited to the early McCurtain phase. Bruseth (1998), after Schambach (1983), suggest that both the Early and Late McCurtain phase settlement pattern is more consistent with the Terán map (Sabo 2012) in which dispersed farmsteads center on vacant ceremonial centers.

The 400-year span of the McCurtain phases (early and late) resulted in greater variability in both design and quality of ceramics vessels. Bruseth (1998:60) notes the wide variety of vessels that include compound bowls, deep cylindrical bowls, and squat jars. Early McCurtain ceramics include Avery Engraved, Emory Punctated-Incised and Simms Engraved. While McCurtain ceramic types include Hudson Engraved, Foster Trilled-Incised, and Keno Trilled. Lithic diagnostics of Early McCurtain include Scallorn, Morris, Reed, and Alba points with Late McCurtain characterized by Fresno, Maud, and Talco point types (Bruseth 1998:60, 62). Bruseth (1998) dates the end of the Late McCurtain phase to approximately 1700 due in part to the lack of European trade and gift items found in burials dating to this time.

Historic Period

This section begins with European contact with the Caddo and ends with the construction of Camp Maxey in 1942 during World War II. The region's historic period is derived from multiple sources that provides an account of the people that lived in what becomes Lamar County and northeast Texas (see Chipman and Joseph 2010; Leffler 2001; Ludeman 2022; Perttula and Walker 2012; Smith 1998).

The historic Caddo consisted of three confederacies: the Hasinai, the Natchitoches, and the Kadohadacho. The Kadohadacho confederacy consisted of four tribes located on the bend of the Red River with an estimated population of 3000 individuals (Smith 1998:175). Contact between the Caddo and the Europeans were sporadic until the late seventeenth century (Chipman and Joseph 2010). In 1684-85, the French expedition to and settlement of the Texas Gulf Coastal region by Rene-Robert Cavelier, Sieur de La Salle of 1684-1885 prompted a military response by the Spanish (Chipman and Joseph 2010). These responses also included contacts and exchange with various Caddo tribes in East Texas and along the Red River. However, by the early eighteenth century European-introduced diseases and raids by the Chickasaws had reduced the Kadohadacho population to 1000 individuals (Smith 1998:176). The Kadohadacho confederacy was reduced to two tribes by the 1760s consisting of 450 individuals (Smith 1998). The Kadohadacho were forced to move multiple times due to attacks by the Osage essentially depopulating the Red River Valley (Smith 1998).

Euro-Americans began to settle in the Red River region in the early nineteenth following the Louisiana Purchase by the United States in 1803 (Leffler 2001). The Republic of Texas issued land grants for settlement between 1836 and 1845. By 1840 there was a sufficient population to create Lamar County from the Red River County with Paris becoming the county seat in 1844 (Ludeman 2022). Most of the settlers were English or Irish heritage migrating from Tennessee, Kentucky, Alabama, and South Carolina to establish small subsistence farms (Ludeman 2022).

In part, the development of Lamar County was due to its proximity to the Red River, one of the few navigable rivers in Texas. The Central National Road authorized by the Texas Congress in 1844 served as thoroughfare between the Trinity River in Dallas County through Paris to the northwest corner of Red River County (Anonymous 2022). The developing transportation infrastructure of road and shipping created regional economic development and encouraged immigration to Lamar County. Before the Civil War, Paris had become the commercial and industrial center of the region (Leffler 2001).

In 1850, the census of Lamar County recorded 3,978 residents with approximately 27% of that population listed as enslaved people (Leffler 2001; Texas Almanac 2022). The population grew to 10,136 residents in 1860 with an enslaved population of 2,800. In 1861, Lamar County was one of only fourteen Texas counties to vote against secession from the Union. However, multiple military units were formed in Lamar County that fought for the Confederacy, including Samuel Maxey's Lamar Rifles of the 9th Brigade of the Texas Militia (Leffler 2001).

Following the Civil War, the region rebounded with a steady increase of immigration from the southern states and the emancipation of enslaved people. In 1870, the population of Lamar County was 15,790 and by 1900 numbered 37,302 of which 9,358 lived in Paris (Texas Almanac 2022). In addition, multiple smaller farming communities were formed throughout the county comprised of a general store, post office, a school, and importantly a cotton gin (Leffler 2001). In the vicinity of Camp Maxey these towns included Center Springs (1865), Emberson (1878), Forest Chapel (1883), and Lenoir then named Powderly in the 1880s (Leffler 2001:19-24). The town of Rich Hill was formed by freedmen in the 1880s (Leffler 2001:19-24).

In 1875, the Texas and Pacific Railway was built connecting Paris to Texarkana (Ludeman 2022). In 1888, the Paris and Great Northern Railway connected with the St. Louis and San Francisco Railroad at the Red River (Ludeman 2022). The development of railroads through Paris connected the region to the national economy. The railroads in turn fostered the move from subsistence farming to cash crops specifically, cotton (Leffler 2001; Ludeman 2022). Cotton became the dominant industry of Lamar County in the late nineteenth and early twentieth century with the growing and production of cotton increasing from 24,623 bales in 1880 to its peak of 69,264 in 1920 (Leffler 2001; Ludeman 2022). In addition to cotton, corn and sorghum were grown. The majority of farms were small between 20 to 40 acres in size and owned by the farmer and not share-cropped (Leffler 2001). The population of Lamar County reached its peak of 55,742 in 1920 (Texas Almanac 2022).

In 1900, there were 6,514 farms valued at \$7.1 million peaking at 6,831 farms valued at \$56.5 million in 1920 (Ludeman 2022). The latter date is the apex of farming productivity which is then followed by dramatic decline through the 1920s and 1930s. There are multiple reasons for this decline including nutrient depleted soils, bad weather, the fall of cotton prices, and the Great Depression. In 1940 there were only 4,176 farms valued at \$13.6 million in Lamar County (Ludeman 2022). In 1930 the population fell by almost 7000 to 48,529 individuals, but made a moderate gain to 50,425 in 1940 (Texas Almanac 2022).

Following the building boom that occurred in the early decades of the twentieth century, construction slowed down in the 1930s due to the economic downturn. There were some Federal work projects including the construction of new water and sewer in Paris, as well as the construction of road infrastructure. The Paris Junior College building was constructed in 1940 (Ludeman 2022). It was in October of 1940 that the mayor of Paris solicited the U.S. Army to construct a camp in Paris following the passage of the Selective Training and Service Act of 1940 (Leffler 2001; Ludeman 2022). The act instituted the first peacetime draft in preparation for World War II. By May of 1941 there were plans to construct a U.S. Army training camp in northwest Lamar County in February of 1942. The camp was named for Confederate General and after the Civil War, a U.S. Senator, Samuel Maxey. .

Past Archaeological Investigations

Archaeological investigations of the middle Red River Basin that includes Lamar County began in the 1930s by the University of Texas at Austin, with additional work by the Dallas Archeological Society in the 1950s (Harris et al. 1965; Krieger 1946; Perttula 1998, 2015; Perttula et al. 2015). These investigations resulted in the documentation and reporting of the first sites in Lamar County, the Womack site (41LR1) and the T.M. Sanders site (41LR2). The former is primarily a historic Caddo settlement containing a large lithic assemblage used for hide processing, European trade goods, and a variety of ceramics that include Womack Engraved vessels that date ca. AD 1670–1730 (Harris et al. 1965; Perttula 2015). The latter is a large Caddo settlement that dates to ca. AD 1100–1300 containing mounds, as well as single and multiple burials (Krieger 1946; Schambach 2000).

The construction of the Pat Mayse Reservoir directly north of the current Camp Maxey boundary led to salvage archaeology surveys by UT Austin (Shafer 1965) and by Southern Methodist University (Lorrain and Hoffrichter 1967). Shafer (1965) documented twelve archaeological sites with Lorrain and Hoffrichter (1967) recording eleven

sites. The survey findings and limited testing suggests that the Sanders Creek landform was used from the Late Archaic through Middle Caddo periods (Lorrain and Hoffrichter 1967; Perttula 2001; Shafer 1965).

The first cultural resource surveys on Camp Maxey were implemented to comply with regulatory statutes for various development projects (Adjutant General's Department of Texas 1993, 1997; Corbin 1992; Sullo and Stringer 1998). The CAR conducted its first investigation of 1000 acres in the southwest portion of the base in 1998 (Nickels et al. 1998). This survey resulted in the documentation of 30

new archaeological sites. CAR returned to Camp Maxey to survey 5000 acres in 1999 documenting 98 new sites and investigated five previously recorded sites. CAR conducted eligibility testing on 36 sites between 2000 and 2002 (Greaves 2003; Mahoney 2001; Mahoney et al. 2002). Currently, there are 139 archaeological sites on Camp Maxey with seven of those sites eligible for inclusion to the National Register and 119 sites that are not eligible for inclusion. There are thirteen remaining sites listed as having unknown eligibility. The eligibility status of ten of those sites are resolved in this report with one site recommended as eligible and nine as not eligible for inclusion to the National Register (TMD 2021).

Chapter 4: Archaeological Patterns at Camp Maxey

Sarah Wigley and Leonard Kemp

The aim of this chapter is to synthesize archaeological patterns generated during previous testing phases (Greaves 2003; Mahoney 2001; Mahoney et al. 2002). In addition, this synthesis will provide a broader context for the assessment of the ten sites tested during the Maxey project. This chapter begins with establishing the chronology of the Middle Red River Valley by looking at the timing and intensity of use of the region through the Summed Probability Distribution (SPD) of radiocarbon dates. The Middle Red River Valley chronology is followed by examining the temporal diagnostics found on sites specific to Camp Maxey. An analysis of the data collected by the past testing of 36 sites with focus on the density and patterns of lithic material follows. This analysis draws upon the results and conclusions of previous investigations (Greaves 2003; Mahoney 2001; Mahoney et al. 2002) as well as methodologies used in previous regional analyses (Kemp et al. 2022; Mauldin et al 2018).

Regional Radiocarbon Dates and Camp Maxey Temporal Patterns

The summed probability distribution (SPD) of radiocarbon dates has been used to infer prehistoric population dynamics (Crema et al. 2017). SPD is calculated by the calibration of a region's radiocarbon dates and their individual probability summed into a probability curve. The SPD is based on the assumption that there is a relationship between population size, the generation of organic waste, and the sampling of that waste for radiocarbon dates. Qualifications to this assumption include a lack of sufficient number of dates, taphonomic loss, and calibration effects (Bamforth and Grund 2012; Lawrence et al. 2021). However, the SPD has served as a gross measure to examine population levels, population shifts and/ or changes in regional intensity of use (see Peros et al. 2010; Torfing 2015; Williams 2012).

Perttula initially compiled the East Texas Radiocarbon Database (ETRD) with a third iteration of the database developed by Perttula and Selden (2011). The current database has 1250 published and unpublished radiocarbon dates from 26 counties that form the East Texas region. CAR selected ETRD radiocarbon dates from four counties, Fannin, Lamar, Red River, and Bowie to construct an SPD analysis to estimate intensity of use along the Middle Red River in northeast Texas. Radiocarbon dates with standard deviation greater than 100 years were removed from the analysis. Four additional radiocarbon dates recently published by Perttula (2015, 2017) completed

the analytical data set of 87 assays shown in Figure 4-1. Table A-1 in Appendix A provides a summary of the 87 radiocarbon dates used.

The SPD was created using OxCal v4.4.4 software (Bronk Ramsey 2021) and is based on the 87 dates. Eighty-seven dates is a small sample size for this type of analysis. As such, patterns should be viewed with caution and treated as preliminary. The curve shows that regional occupation begins in the middle of the Middle Archaic period at approximately 5000 BP. The curve incorporates a transition to the early Late Archaic period at 4000 BP. However, the Middle and early Late Archaic (2100 BP) are represented by just five dates and only four sites. The early Late Archaic period is followed by a 700-year gap beginning at 3600 BP with the curve resuming at 2900 BP. The amplitude of the curve remains essentially the same to 1200 BP with the exception of two peaks, one at 2700 and the other 2300 BP. In addition, there is a 200-year gap beginning at 1700 BP. There is an exponential increase of dates at 1250 BP or AD 700 coinciding with the end of the Woodland period followed by a steep climb to approximately 900 BP characterized as the Early Caddo period. The curve suggests that from 900 to 700 BP the region reaches its maximum intensity of occupation during the Early and first part of the Middle Caddo periods. A steep 100-year decline is evident at 650 BP followed by a short-lived spike at 550 BP that marks the transition to the Late Caddo period. There is decline beginning at 500 BP matching Woodland and Formative Caddo levels of occupation marking the terminal Late Caddo period. There is a steep decline at approximately at 250 BP or AD 1700 followed by return to Woodland levels post-AD 1700 to AD 1800 coinciding with the Historic Caddo period.

Previous reports (Greaves 2003; Lyle et al. 2001; Mahoney 2001; Mahoney et al. 2002; Nickels 1998) were reviewed for radiocarbon dates and temporally diagnostic artifacts that might suggest occupation specific to Camp Maxey. Figure 4-2 shows results of the radiocarbon analysis for three sites, 41LR152, 41LR164, and 41LR187 that have been dated with eight assays (Mahoney 2001:Table 1). The radiocarbon dates were recalibrated using OxCal v4.4.4 software (Bronk Ramsey 2021). The earliest radiocarbon from 41LR187 yields a median date of 4000 cal BP or 2000 BC falling within the late Middle and early Late Archaic period. Four dates suggest use beginning at 2750 through 1800 cal BP (800 BC to AD 100) or the middle to late Late Archaic period. Three of these dates are associated with 41LR164 with the other date belonging to 41LR152.

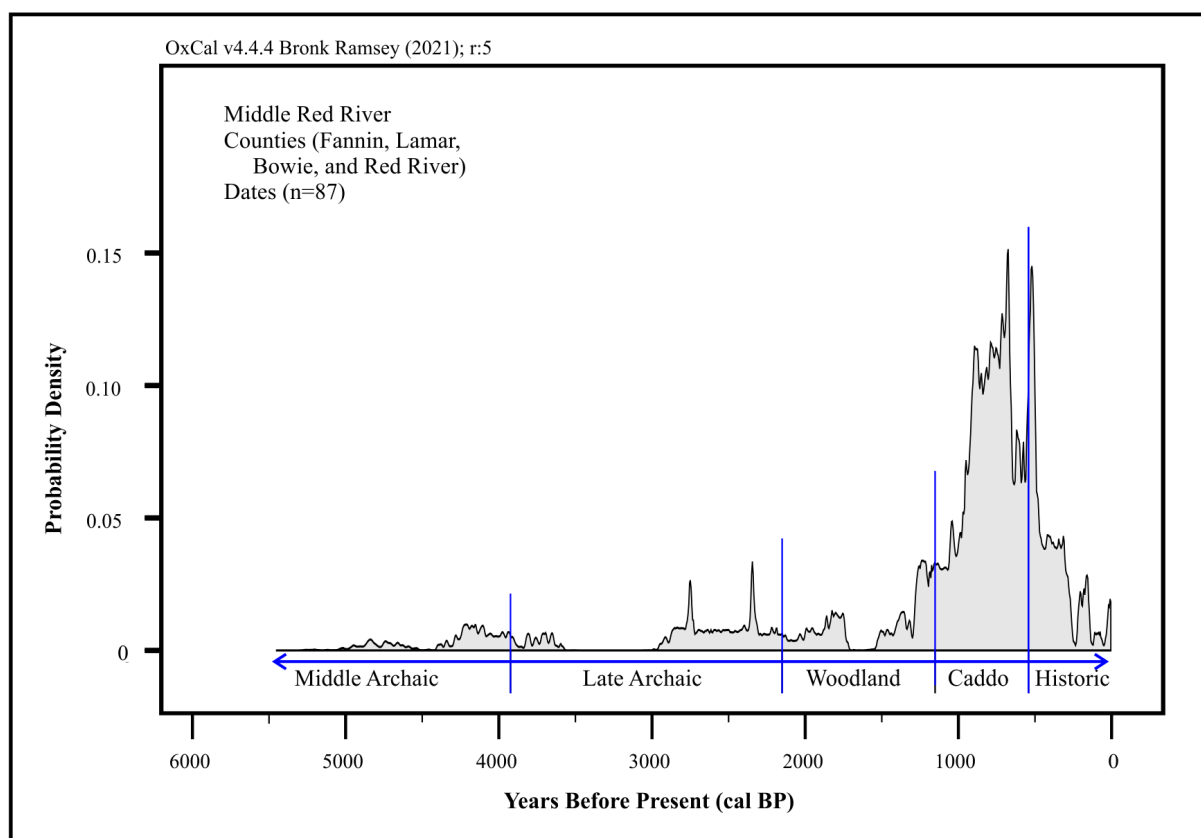


Figure 4-1. The summed probability distribution of 87 radiocarbon dates from the Middle Red River counties.

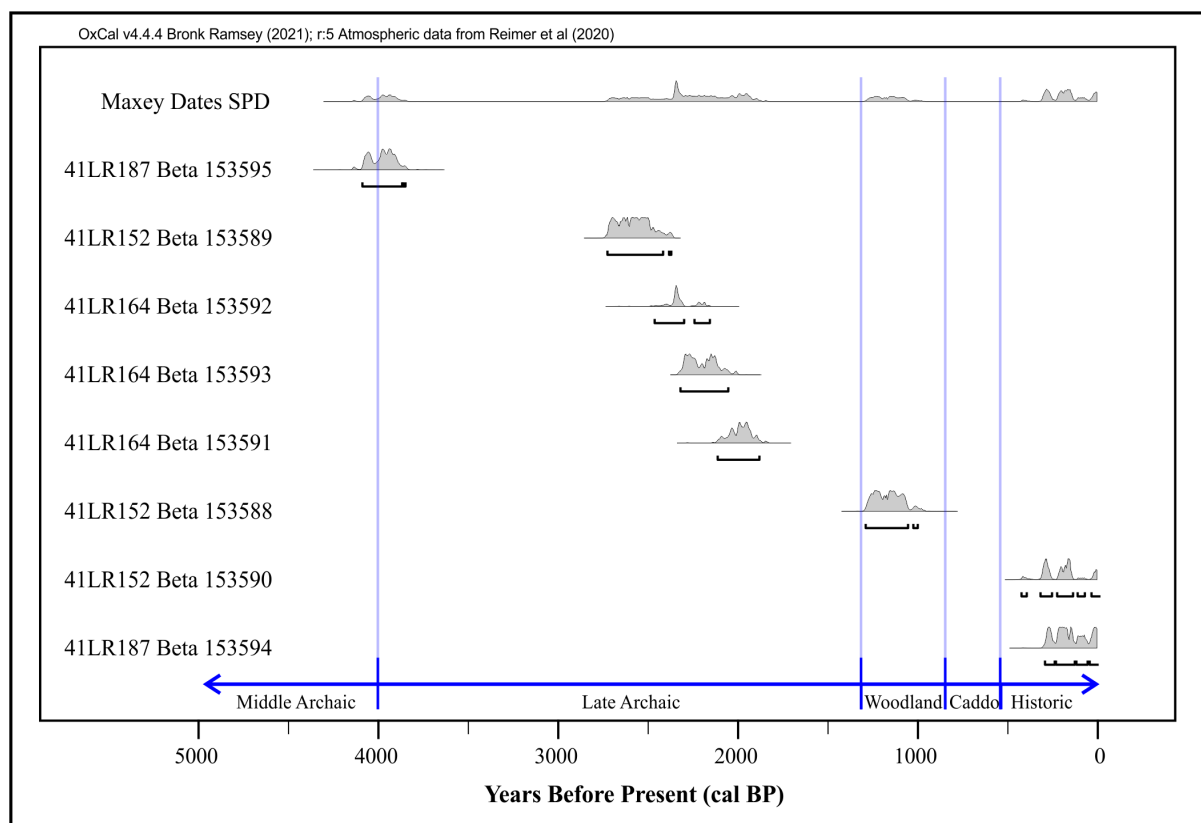


Figure 4-2. The temporal distribution of all previous analyzed radiocarbon dates from Camp Maxey.

Another date from 41LR152, (Beta 153588), suggests Woodland period use with a median value of AD 789 or 1162 cal BP. The remaining two dates suggest historic period use with median dates of AD1752 and AD1781 from sites 41LR152 and 41LR187, respectively. They are no dates for the prehistoric Caddo period.

A review of 138 sites on Camp Maxey produced only 35 (ca. 25%) that had artifacts diagnostic of a prehistoric period. Table 4-1 summarizes the temporal diagnostics recovered during the survey and testing phases of the 32 remaining sites. The sites are grouped by the earliest artifact and if a site is a multi-component, the chronological order of the site.

Table 4-1. Temporal Diagnostics found on Camp Maxey

Site	Temporal Diagnostic	Time Period	Simplified Time Period
41LR170	Dalton, Yarbrough; arrow point (3) ceramic plain;	Late Paleoindian/Late Archaic/Woodland-Caddo	LPaleo/LA-W-C
41LR190	Plainview; Kent; Gary	Late Paleoindian/Middle Archaic/Late Archaic-Woodland	LPaleo/MA-LA-W
41LR196	Kent	Middle Archaic	MA
41LR245	Wells	Middle Archaic	MA
41LR260	Wells; Gary; Perdiz; ceramic-plain grog tempered	Middle Archaic-Late Archaic- Woodland-Early, Middle, and Late Caddo	MA-LA-W-C
41LR164	Wells, Gary; arrow points; ceramic plain	Middle Archaic-Late Archaic-Woodland-Caddo	MA-LA-C
41LR168	Kent; Gary?	Middle Archaic/Late Archaic-Woodland	MA-LA-W
41LR208	Yarbrough	Late Archaic	LA
41LR254	Yarbrough	Late Archaic	LA
41LR169	Gary	Late Archaic-Woodland	LA-W
41LR213	Gary	Late Archaic-Woodland	LA-W
41LR214	Gary	Late Archaic-Woodland	LA-W
41LR268	Gary	Late Archaic-Woodland	LA-W
41LR286	Gary	Late Archaic-Woodland	LA-W
41LR163	Gary; ceramic	Late Archaic-Woodland/Woodland-Caddo	LA-W-C
41LR186	Gary, Crockett Curvilinear Incised; arrow point; ceramic plain	Late Archaic-Woodland/Early Caddo/Woodland-Caddo	LA-W-C
41LR225	Ellis/Edgewood; Gary; Alba; untyped arrow point	Late Archaic/Late Archaic- Woodland/Early Caddo/Woodland-Caddo	LA-W-C
41LR212	Gary; ceramic-grog tempered;	Late Archaic-Woodland-Early and Middle Caddo	LA-W-C
41LR187	Gary; ceramic plain red slipped; untyped arrow point	Late Archaic-Woodland/Middle Caddo/Woodland-Caddo	LA-W-C
41LR155	Gary; Talco	Late Archaic-Woodland/Late Caddo	LA-W-C
41LR158	untyped arrow point	Woodland-Caddo	W-C
41LR222	untyped arrow points	Woodland-Caddo	W-C
41LR150	ceramic	Woodland-Caddo	W-C
41LR157	ceramic	Woodland-Caddo	W-C
41LR226	ceramic	Woodland-Caddo	W-C
41LR233	ceramic	Woodland-Caddo	W-C
41LR244	ceramic	Woodland-Caddo	W-C
41LR204	ceramic-grog tempered	Early and Middle Caddo	C
41LR259	ceramic-grog tempered	Early and Middle Caddo	C
41LR152	ceramic-red slipped (Sanders Plain)	Middle Caddo	C
41LR152	Serrated corner-notched arrow point	Late Caddo	C
41LR137	Nash Neck Banded ceramic	Late Caddo	C

The temporal diagnostics suggests that occupation at Camp Maxey primarily encompasses the Middle Archaic through the Late Caddo periods. However, there are diagnostics that date to the Late Paleoindian. A Dalton and a Plainview point are noted, although the contexts of these artifacts are suspect. There are no Early Archaic diagnostics. There are six Middle Archaic points with three Kent point types and three Wells. The Late Archaic is characterized by the Yarbrough (n=2) and Edgewood/Ellis (n=1) points. The Gary point is the most common (n=15) found on Camp Maxey. The Gary point dates from the Late Archaic into the Woodland period. A Crockett Curvilinear Incised ceramic sherd found on Site 41LR186 is the sole Early Caddo diagnostic (Mahoney 2001). However, there are ten sites that contain grog tempered ceramics which are attributed to the Early and Middle Caddo periods. The Middle Caddo period is represented by the red-slipped Sanders Plain and engraved sherds recovered from 41LR152 and 41LR187 (Mahoney 2001; Nickels et al 1998). The Late Caddo period is represented by a single diagnostic-the Nash Neck Banded sherd found at 41LR137. The simplified chronology in Table 4-1 is used to date the sites for the following sections.

Intensity of Site Use

The radiocarbon dates and temporal diagnostics suggest that Camp Maxey was most intensively occupied during the Late Archaic and Woodland periods and less so during the prior Middle Archaic and later Caddo periods. The

phrase “intensively” may be an overstatement because there were long periods when the landscape was apparently not used. The following sections examines archaeological patterns of intensity of site use by analyzing available data for the 36 tested sites by CAR reported in Mahoney (2001), Mahoney et al. (2002), and Greaves (2003). Lab data on file at the CAR was revisited in order to analyze the debitage density by excavated cubic meter and develop a Maximum Level Density (MLD). This review focuses primarily on these measures.

Debitage Density

Density of debitage per cubic meter excavated was analyzed to discern the intensity of site use (Figure 4-3). Sites having a greater density of debitage were likely occupied for longer time periods and/or more frequently (Kelly et al. 2005). The density of debitage per cubic meter was calculated by obtaining test unit size and depths from field and lab paperwork on file at the CAR, as well as artifact counts by individual test unit. By this measure, site 41LR190 has the highest densities of debitage (197.6 per m³) by a significant amount. Sites 41LR196 (112.9 per m³), 41LR187 (104.4 per m³), and 41LR200 (90.3 per m³) also exhibit higher densities. At the low end, eleven sites exhibit very low densities of debitage, with fewer than 15 pieces of debitage recovered per cubic meter excavated. The measure of cubic debitage density suggests that in general sites are inhabited for only a short time and/or infrequently as suggested by the low density of debitage.

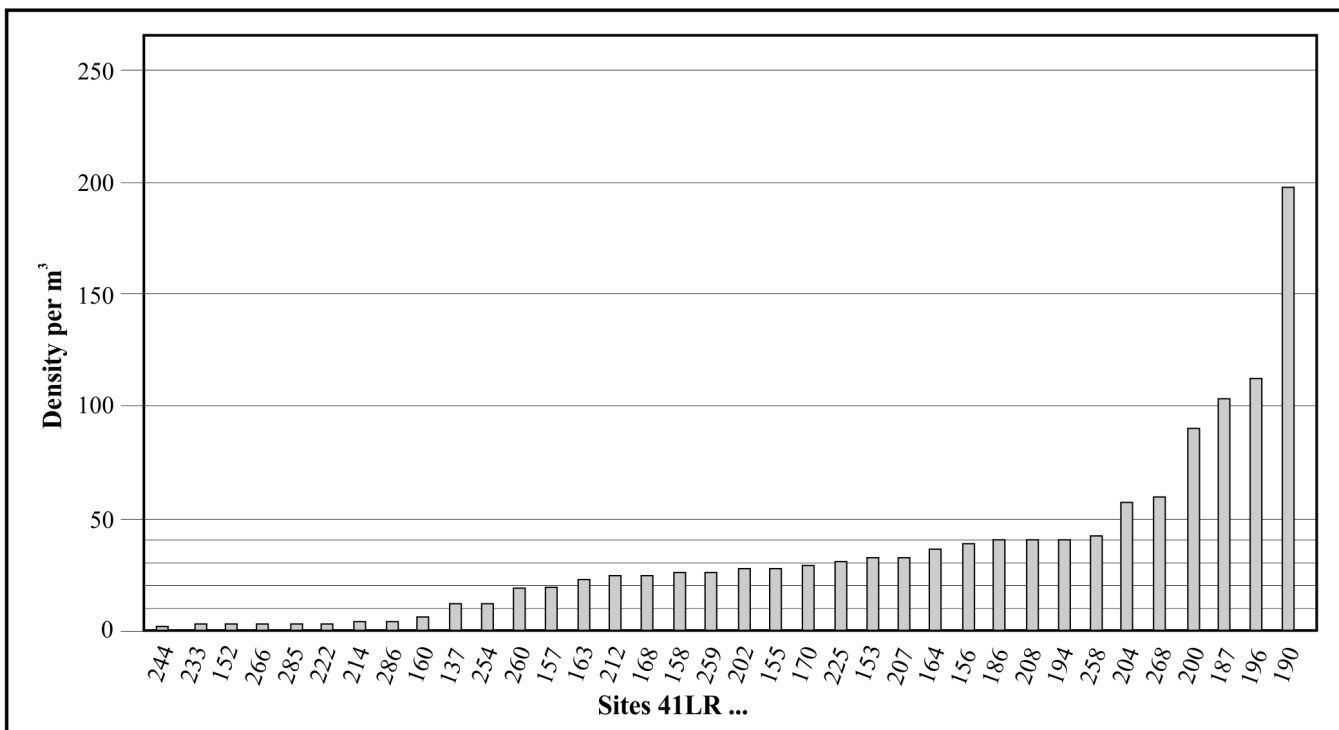


Figure 4-3. Density of debitage recovered by cubic meter for each site reviewed.

Maximum Level Density

Maximum Level Density (MLD) is a measure intended to provide a density comparison that is not as strongly

impacted by differences in excavation strategy (Kemp et al. 2019; Kim et al. 2022). The method compares the five highest totals from levels excavated at the site, which serves to eliminate levels with no recovery. Table 4-2 lists

Table 4-2. Site MLD average from highest to lowest

Site	Time Period	Highest count	Second highest	Third highest	Fourth highest	Fifth highest	Average
41LR190	MA-LA-W	62	60	55	43	43	52.6
41LR187	LA-W-C	31	23	23	21	20	23.6
41LR196	MA	18	18	16	16	15	16.6
41LR225	LA-W-C	29	16	15	11	9	16
41LR204	C	17	17	16	15	11	15.2
41LR170	LA-W-C	21	14	13	12	12	14.4
41LR200	--	20	14	14	11	11	14
41LR268	LA-W	16	15	15	10	9	13
41LR164	MA-LA-C	13	11	10	10	8	10.4
41LR259	C	20	12	7	6	6	10.2
41LR194	--	11	10	9	9	9	9.6
41LR258	--	11	9	9	9	8	9.2
41LR208	LA	14	11	8	6	6	9
41LR207	--	11	9	8	8	7	8.6
41LR186	LA-W-C	8	8	7	7	7	7.4
41LR155	LA-W-C	9	6	5	5	5	6
41LR137	C	7	6	5	5	5	5.6
41LR260	MA-LA-W-C	7	6	6	5	4	5.6
41LR157	W-C	8	6	4	4	4	5.2
41LR153	-	8	8	4	3	1	4.8
41LR254	LA	6	5	5	4	4	4.8
41LR163	LA-W-C	9	4	3	3	2	4.2
41LR212	--	5	4	3	3	3	3.6
41LR222	W-C	3	3	3	3	2	2.8
41LR214	LA-W	4	3	3	2	1	2.6
41LR156	--	4	2	2	1	1	2
41LR202	--	3	2	2	2	1	2
41LR152	C	3	3	1	1	1	1.8
41LR160	--	3	2	1	1	1	1.6
41LR168	MA-LA-W	2	2	2	1	1	1.6
41LR286	LA-W	3	2	1	1	1	1.6
41LR233	W-C	2	1	1	1	1	1.2
41LR285	--	2	2	1	1	0	1.2
41LR244	W-C	1	1	1	0	0	0.6
41LR266	--	2	0	0	0	0	0.5
41LR158	W-C	2	0	0	0	0	0.4

Blue = high MLD site; white = middle MLD sites, gray = low MLD sites as shown in Figure 4-4.

the highest counts and averages for the sites reviewed here, from highest MLD average to lowest. The results show some differences from the density by cubic meter results, likely reflecting differences in excavation strategy. In both cases, site 41LR190 (average 52.6) shows the highest densities by a significant amount. Site 41LR187 has a higher MLD average (23.6) than site 41LR196 (16.6), when the reverse is true when examining debitage density per cubic meter. Additionally, site 41LR225 falls to the middle of the density per cubic meter scale (31.4) but has the fourth highest MLD average (16). This is likely a reflection of the fact that multiple no-recovery test units were excavated at 41LR225, which would decrease the site's average density.

Figure 4-4 plots the MLD results of each site against the debitage density per cubic meter. Site 41LR190 is a significant outlier in both density and MLD, and is designated as the sole “high density” site. Seven sites fall into a medium density group. The remaining thirty sites fall into the low density, low MLD range. This low density, low MLD category represents 78% of the sites reviewed here that have been previously investigated at Camp Maxey.

A comparison on the MLD data and density by volume excavated data with the debitage peak data from the original reports highlights the differences between the two methods. Using the peak method, 41LR187 stands out due to having the highest count in a single level ($n=164$). However, as an example, site 41LR190 has an MLD average, as well as a density of debitage by volume excavated, more than twice that of 41LR187 due to the consistently high counts distributed vertically through test units in that site.

Overall, the examination of debitage density either by cubic meter or MLD establishes that the majority of sites at Camp Maxey are low-density in nature. In some cases, this density is exceptionally low, with at least six sites having debitage densities of less than five debitage pieces per cubic meter. However, a number of individual sites show high to medium artifacts densities extending through multiple levels.

Site density can be reflective of duration and/or intensity of site occupation, often connected with mobility patterns (Binford 1980, 2001; Kelly et al. 2005). Examination of site density in conjunction with other assemblage characteristics,

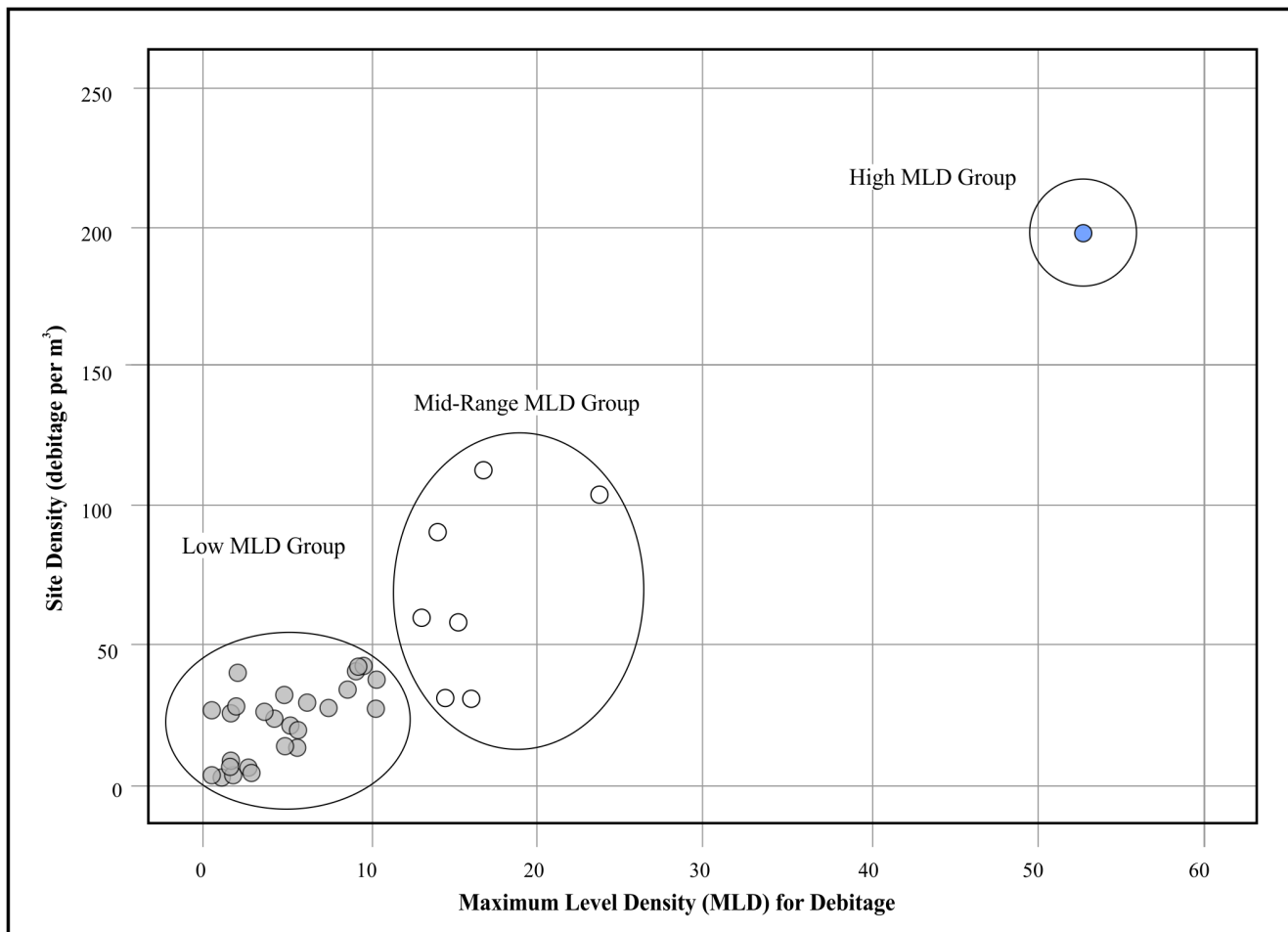


Figure 4-4. Debitage density by cubic meter plotted against site MLD average. Blue circles indicate high-density grouping, white circles indicate medium-density grouping, and gray indicate low-density grouping.

such as cortex percentage, material sources and artifact variety, can provide additional insight into mobility patterns, site function and subsistence practices (Binford 1980, 2001; Dibble et al. 2005; Mauldin and Figueroa 2006; Sullivan and Rozen 1985; Surovell 2003, 2012). While raw material access complicates any comparison, the predominance of low-density sites at Camp Maxey may be reflective of a series of short-term occupations in the area (Binford 1980; Kelly et al. 2005).

Debitage Characteristics

Debitage characteristics of an assemblage are often analyzed as an aspect of lithic assemblages as method of tracking shifts in lithic technologies and reduction patterns. The variations in behavior reflected in assorted characteristics recorded and measured by archaeologists can provide insight into prehistoric lifeways including mobility patterns, subsistence practices, and changes in technology. Information on debitage characteristics from each site reviewed here was provided in previous reports (Greaves 2003; Mahoney 2001; Mahoney et al. 2002). This data includes percentage of non-cortical flakes for each site, debitage material type, and average thickness to length ratios of flakes at each site. Previous studies have found that dorsal cortex percentage is associated with reduction stage as well as raw material access (Amick et al. 1988; Andrefsky 2005; Dibble et al. 2005; Figueroa et al. 2009; Mauldin and Figueroa 2006). Variety in debitage material, in particular local vs non-local materials, has been previously associated with variation

in mobility ranges (Mauldin et al. 2003; Mauldin et al. 2018; McCall and Horowitz 2015; Munoz et al. 2011). Variations in the average thickness to length ratios of flakes has previously been associated with differences in lithic reduction patterns. Broadly, assemblages dominated by biface thinning activity will have lower average ratios of thickness to length, while assemblages dominated by core reduction activity will exhibit the inverse (Sullivan and Rozen 1985; Surovell 2003, 2012). These differences in reduction pattern can be associated with changes in mobility patterns, site occupation, or site function, as well as aspects of site location such as resource availability (Bamforth and Bleed 1997; Binford 1980, 2001; Bleed 1986; Boydston 1989; Camilli 1989; Kelly 2013; Nelson 1987; Shott 1986; Surovell 2003, 2012).

Percentage of non-cortical flakes has previously been associated in Central Texas with raw material access (Mauldin and Figueroa 2006). Mauldin and Figueroa found that areas with high tool stone availability most often exhibit high percentages of non-cortical flakes. At Camp Maxey, no sites show a high (over 80% [Mauldin and Figueroa 2006]) percentage of non-cortical flakes (Figure 4-5). The range present spans a broad continuum without obvious groupings. Nine sites show non-cortical flake percentages above 60%. The remaining sites all have less than 50% non-cortical flakes. Site 41LR158 shows an extremely low percentage of non-cortical flakes (12%). This site is noted as a likely lithic procurement site due to a surface gravel deposit consisting primarily of quartzite (Mahoney 2001). Broadly, the pattern of medium to low percentages of non-cortical flakes observed

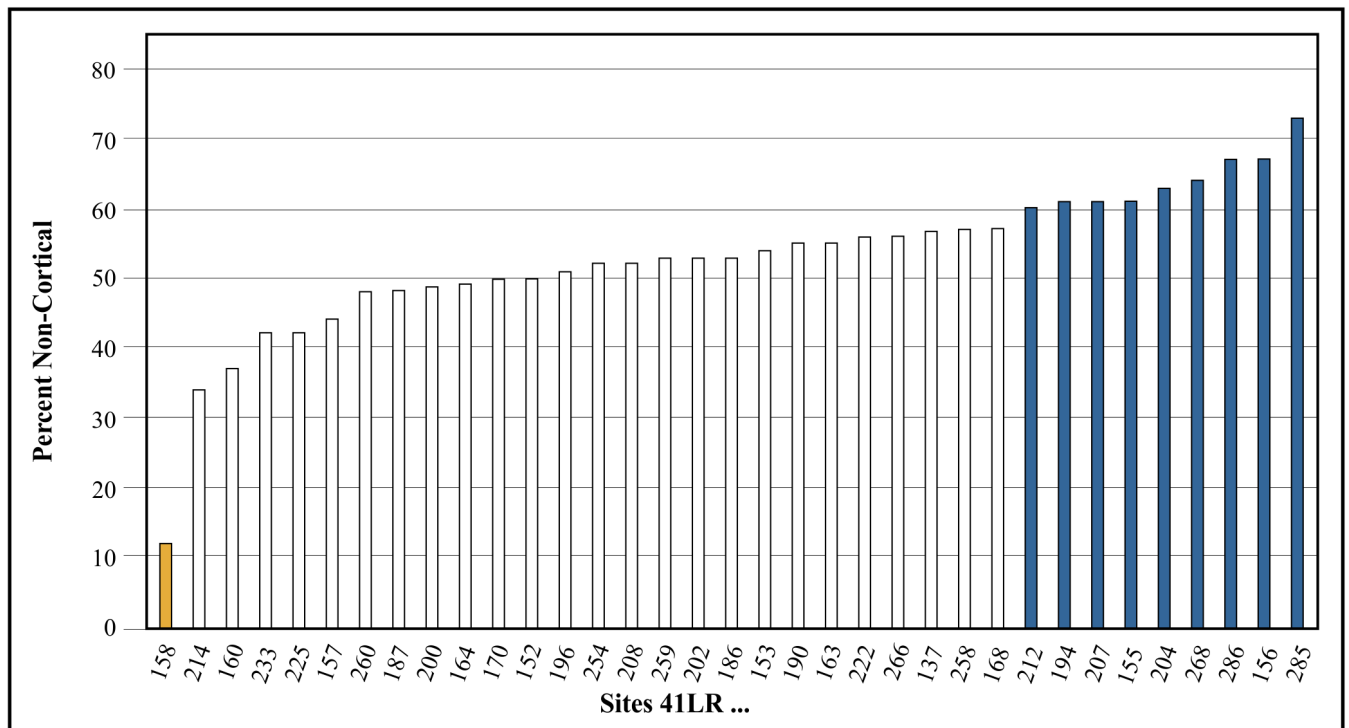


Figure 4-5. Percentage of non-cortical debitage by site.

at the sites reviewed here at Camp Maxey is associated with low to moderate chert availability (Mauldin and Figueroa 2006). It is also suggestive of reliance on local stone sources, rather than importing higher-quality materials.

The average thickness to length measurement of chert debitage recovered from the sites reviewed here is 0.18; the average thickness to length measurement of quartzite debitage recovered from the sites reviewed here is 0.22 (Table 4-3). This was determined by averaging the mean ratios of each site provided in the relevant report (Mahoney 2001; Mahoney et al. 2002). This data was not provided in Greaves (2003),

so those sites were excluded from this analysis. The majority of the sites cluster around these two averages. As discussed previously, differences in thickness to length ratios of debitage are associated with differences in lithic reduction patterns, with lower ratios indicative of later stages of reduction. This lack of variation suggests that similar reduction strategies were practiced across the Camp Maxey area. The lower average ratio for chert debitage versus quartzite is noted by previous investigators (Mahoney et al. 2002). A possible explanation provided (Mahoney et al. 2002:51) is that the available chert is a more suitable material for later-stage reduction activities, due to the coarse grain of the quartzite.

Table 4-3. Mean Thickness to Length Ratios (Mahoney 2001, Mahoney et al. 2002)

Site	Mean Thickness to Length Ratio: Chert	Mean Thickness to Length Ratio: Quartzite
41LR168	0.17	0.16
41LR207	0.16	0.17
41LR155	0.14	0.18
41LR156	0.18	0.18
41LR266	0.08	0.18
41LR268	0.18	0.18
41LR157	0.21	0.19
41LR170	0.19	0.19
41LR204	0.17	0.19
41LR208	0.17	0.19
41LR286	0.13	0.19
41LR186	0.19	0.2
41LR212	0.21	0.2
41LR260	0.16	0.2
41LR163	0.15	0.21
41LR187	0.2	0.21
41LR202	0.15	0.21
41LR164	0.21	0.22
41LR258	0.18	0.23
41LR152	0.21	0.24
41LR190	0.23	0.24
41LR158	0.27	0.25
41LR160	0.14	0.25
41LR196	0.21	0.25
41LR153	0.2	0.26
41LR285	0.14	0.27
41LR200	0.22	0.28
41LR194	0.18	0.29
41LR259	0.2	0.44
Average	0.18	0.22

Table 4-4 is a summary of the debitage material type. The majority (57%) of debitage recovered from the reviewed sites at Camp Maxey was quartzite (n=2442). A significant minority (38%) was chert (n=1629). Other material represented include silicified wood (n=40) and non-local novaculite (n=59). Twenty-five of the 36 sites

Table 4-4. Summary of Debitage Material Type

Site	Total Debitage	Quartzite	Quartzite percent	Chert	Chert percent	Silicified wood	Novaculite	Novaculite percent	Other	# material types present
41LR137	93	49	53%	44	47%	0	0	0%	0	2
41LR152	20	10	50%	8	40%	1	1	5%	0	4
41LR153	37	26	70%	9	24%	1	1	3%	0	4
41LR155	75	56	75%	17	23%	2	0	0%	0	3
41LR156	18	8	44%	10	56%	0	0	0%	0	2
41LR157	50	32	64%	17	34%	1	0	0%	0	3
41LR158	66	59	89%	3	5%	3	0	0%	1	4
41LR160	27	19	70%	4	15%	1	2	7%	1	5
41LR163	33	27	82%	5	15%	1	0	0%	1	4
41LR164	159	108	68%	50	31%	1	0	0%	1	4
41LR168	14	8	57%	4	29%	0	2	14%	0	3
41LR170	237	124	52%	107	45%	2	4	2%	0	4
41LR186	240	103	43%	124	52%	3	4	2%	4	3
41LR187	381	135	35%	230	60%	3	11	3%	2	5
41LR190	856	702	82%	114	13%	5	2	0%	33	5
41LR194	214	99	46%	95	44%	3	10	5%	7	5
41LR196	242	139	57%	93	38%	3	3	1%	4	5
41LR200	168	81	48%	78	46%	2	1	1%	6	5
41LR202	36	15	42%	21	58%	0	0	0%	0	2
41LR204	200	114	57%	80	40%	1	4	2%	1	5
41LR207	84	53	63%	25	30%	1	4	5%	1	5
41LR208	135	86	64%	46	34%	1	2	1%	0	4
41LR212	30	11	37%	18	60%	0	0	0%	1	3
41LR214	14	9	64%	5	36%	0	0	0%	0	2
41LR222	15	15	100%	0	0%	0	0	0%	0	1
41LR225	100	43	43%	55	55%	0	0	0%	2	3
41LR233	17	5	29%	11	65%	0	0	0%	1	3
41LR244	3	0	0%	2	66%	0	0	0%	1	2
41LR254	83	31	37%	50	60%	0	0	0%	2	3
41LR258	167	50	30%	112	67%	3	0	0%	2	4
41LR259	103	28	27%	65	63%	0	7	7%	3	4
41LR260	163	72	44%	83	51%	0	0	0%	8	3
41LR266	9	6	67%	1	11%	1	1	11%	0	4
41LR268	137	101	74%	32	23%	1	0	0%	3	4
41LR285	22	11	50%	11	50%	0	0	0%	0	2
41LR286	9	7	78%	2	22%	0	0	0%	0	2

reviewed specifically noted the inclusion of non-local material in the debitage assemblage, which included novaculite and non-local green and gray cherts. No exact quantity of debitage found to be non-local was provided, only presence or absence of non-local materials in the assemblage. While quartzite is dominant across the general area, there are 11 sites where chert debitage is the dominant material recovered. Camp Maxey is located in a zone of low chert availability (Mauldin and Figueroa 2006: 84). However, the materials analysis indicated that the majority of chert recovered was local in origin (Mahoney 2001; Mahoney et al. 2002).

Material variety in a debitage assemblage is an indicator of past mobility patterns. Mobility patterns with longer ranges are more likely to provide past peoples with access to non-local materials, resulting in a more varied assemblage (Mauldin et al. 2018; McCall and Horowitz 2015; Surovell 2003, 2012). The reliance on local materials at Camp Maxey suggests a somewhat limited range of mobility, but the inclusion of non-local materials such as novaculite in the majority of assemblages is indicative of some variety in access to lithic sources (Mauldin et al. 2010; Munoz et al. 2011).

In general, the material analysis broadly identified debitage as quartzite, chert, silicified wood, novaculite, or a variety of materials including jasper, quartz, and silicified sandstone, broadly grouped here as “Other,” for a total of five broad material groupings. In an attempt to assess the material diversity of each site, the number of broad material groups present at each site was counted. Sites at Camp Maxey include an average of 3.5 debitage material groups out of five possible groupings.

In numerous cases, material diversity appears to be a function of debitage count. Site 41LR190 has both the highest

debitage count and high diversity, while site 41LR222 has both low debitage count and the lowest diversity (Figure 4-6). However, a number of sites with higher diversity and low debitage counts exist, including sites 41LR160 and 41LR207. This pattern may represent groups with higher mobility. Under these conditions, accumulation of cultural material is less dense due to frequent residential moves, but a wider variety of material sources are encountered. In contrast, a number of sites with lower diversity but moderate debitage counts were identified, including 41LR186, and 41LR260. These sites may represent groups with less frequent or more restricted mobility patterns. Such groups may spend more time in one location, accumulating debris, and travel less widely, encountering less variety in sources of raw material. Site 41LR222, a low-density site including only one material type which is local in origin (quartzite), is almost certainly a procurement site for toolstone.

Lithic Tools and Ceramics

Artifact variety and count can provide insight into site function (Munoz et al. 2011). Distribution of tool types and number of lithic tools for each site was examined. Counts of prehistoric ceramic sherds are provided as well for context. Tools are presented based on the data provided in the reports of the investigations reviewed (Greaves 2003; Mahoney 2001; Mahoney et al. 2002).

Table 4-5 summarizes the 234 lithic tools and cores were recovered from the 36 reviewed sites. The most commonly recovered categories were bifaces (n=78, 33%), cores (n=64, 27%), and projectile points (n=52, 22%), suggesting that the lithic tool assemblage is dominated by more formalized lithic technologies. The large number of cores suggests lithic procurement activity as well. No groundstone was recovered from any of the sites reviewed at Camp Maxey.

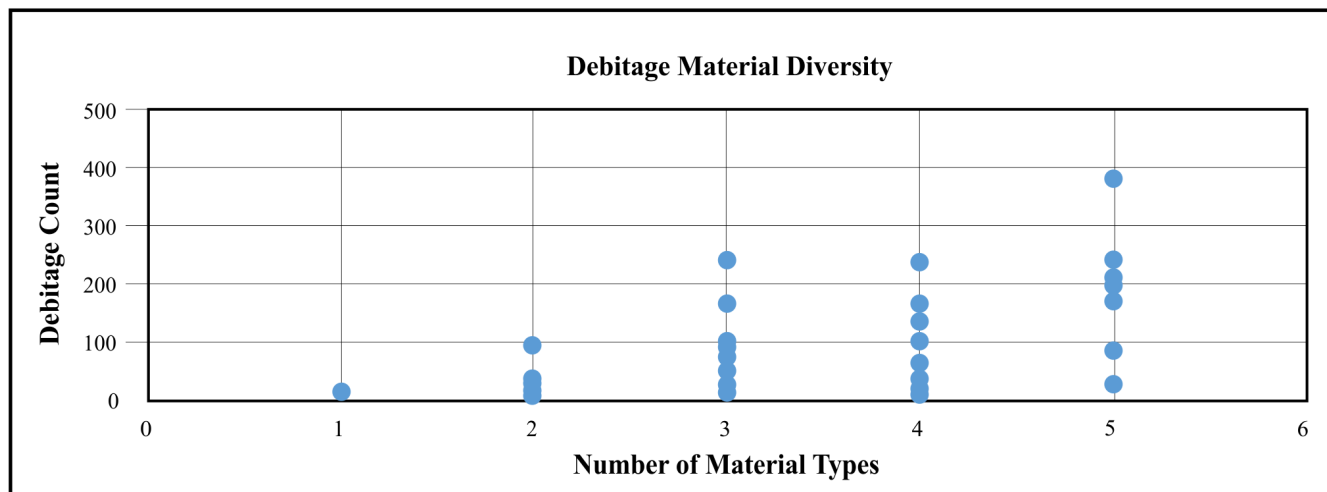


Figure 4-6. Number of material types by total debitage count.

Table 4-5. Summary of Lithics and Prehistoric Ceramics Recovered from Sites Reviewed at Camp Maxey

Site	Time Period	Core/ core tool/ chopper/tested cobble	Biface	Point	Uniface/ scraper/gouge/ adze	Edge modified/ retouched/ utilized	Drill/ Perforator	Hammer Stone/battered stone	Total Tools	Total Types	Total Debitage	Total Prehistoric Ceramics
41LR137	C	1	1	1	0	1	0	0	4	4	92	0
41LR152	C	0	1	0	0	1	0	0	2	2	20	31*
41LR153		0	0	1	0	0	0	0	1	1	37	0
41LR155	LA-W-C	1	1	2	0	0	0	0	4	3	75	0
41LR156		0	0	0	0	0	0	0	0	0	18	0
41LR157	W-C	0	0	0	0	0	1	0	1	1	50	17
41LR158	W-C	7	2	0	0	0	0	0	9	2	66	0
41LR160		1	0	0	0	0	0	0	1	1	27	0
41LR163	LA-W-C	0	1	1	0	2	0	0	4	3	33	0
41LR164	MA-LA-C	2	3	3	2	0	0	1	11	5	159	1
41LR168	MA-LA-W-C	0	1	2	0	0	0	0	3	2	14	0
41LR170	LPaleo/LA-W-C	9	6	8	0	4	0	1	28	5	237	77
41LR186	LA-W-C	3	4	2	1	3	1	3	17	7	240	47
41LR187	LA-W-C	6	11	5	2	5	0	0	29	5	381	319
41LR190	LPaleo/MA-LA-W	6	15	10	0	1	0	1	33	5	856	0
41LR194		1	0	0	0	0	0	0	1	1	214	0
41LR196	MA	4	2	2	1	0	0	0	9	4	242	0
41LR200		1	0	0	0	0	0	0	1	1	168	0
41LR202		2	0	0	0	0	0	1	3	2	36	1
41LR204	C	3	5	1	0	0	0	0	9	3	200	7
41LR207		0	1	0	0	0	0	0	1	1	84	0
41LR208	LA	0	3	1	0	0	0	0	4	2	135	0
41LR212		1	4	2	0	1	0	0	8	4	30	2
41LR214	LA-W	0	0	0	0	1	0	0	1	1	14	0
41LR222	W-C	1	0	1	0	0	0	0	2	2	25	0
41LR225	LA-W-C	1	0	3	0	1	0	0	5	3	100	0
41LR233	W-C	0	0	0	0	0	0	0	0	0	17	1
41LR244	W-C	0	1	0	0	0	0	0	1	1	3	0
41LR254	LA	1	4	0	0	1	0	0	6	3	83	0
41LR258		0	2	0	0	0	0	0	2	1	167	2
41LR259	C	2	2	2	3	0	0	0	9	4	103	9
41LR260	MA-LA-W-C	4	4	3	0	0	0	1	12	4	163	37
41LR266		0	0	0	0	0	0	0	0	0	9	0
41LR268	LA-W	4	2	1	0	0	0	0	7	3	137	0
41LR285		3	0	0	0	0	0	0	3	1	22	0
41LR286		0	2	1	0	0	0	0	3	2	9	0

*1 intact vessel

No lithic tools of any kind were recovered from three sites; 41LR156, 41LR266, and 41LR233.

Tool Distribution

Figure 4-7 presents the number of tools at each site plotted against the number of tool types, or variety of artifacts recovered. Four sites clearly stand out on the graph. Site 41LR186 stands out as having the most artifact variety of the sites reviewed for this study. High variety of artifacts is associated with residential sites (Binford 1980, 2001; Munoz et al. 2011). By debitage count, this site is categorized as low-density. Sites 41LR190, 41LR187, and 41LR170 have less variety in artifacts types, but higher numbers of lithic tools. These sites are all medium to high in debitage recovery. Generally, less variety in tools but increased count is suggestive of sites that are more highly specialized in their function (Binford 1980, 2001; Munoz et al. 2011). Sites 41LR190 and 41LR187 both have lithic tool assemblages that are dominated by projectile points (41LR190: $n=10$, 41LR187: $n=3$) and bifaces (41LR190: $n=14$, 41LR187: $n=4$). This is consistent with many of the sites reviewed at Camp Maxey, where assemblages dominated by formal tools

are common. However, at site 41LR170 more cores ($n=9$) than projectile points ($n=8$) were recovered, and bifaces were few ($n=2$). This suggests that site 41LR170 may serve a different function than sites 41LR190 and 41LR187.

The other sites reviewed generally fall into a medium diversity, medium artifact count category or low, diversity, low artifact count. Sites in the medium category make up 36% of sites included in this review. Sites in the low category make up 50% of sites included in this review. This zone is more of a continuum than a sharp break/grouping. The patterning mostly clusters in the top left of the graph, suggesting a series of lower density residential sites.

Tool Material

Information on tool material and locality was provided for 162 lithic tools recovered from 25 sites in the reports reviewed (Greaves 2003; Mahoney 2001; Mahoney et al. 2002) from Camp Maxey. Assignments of material as “local” or “nonlocal” is based on the identification given in the relevant reports. The vast majority of lithic tool material was identified as local in origin (91%). The

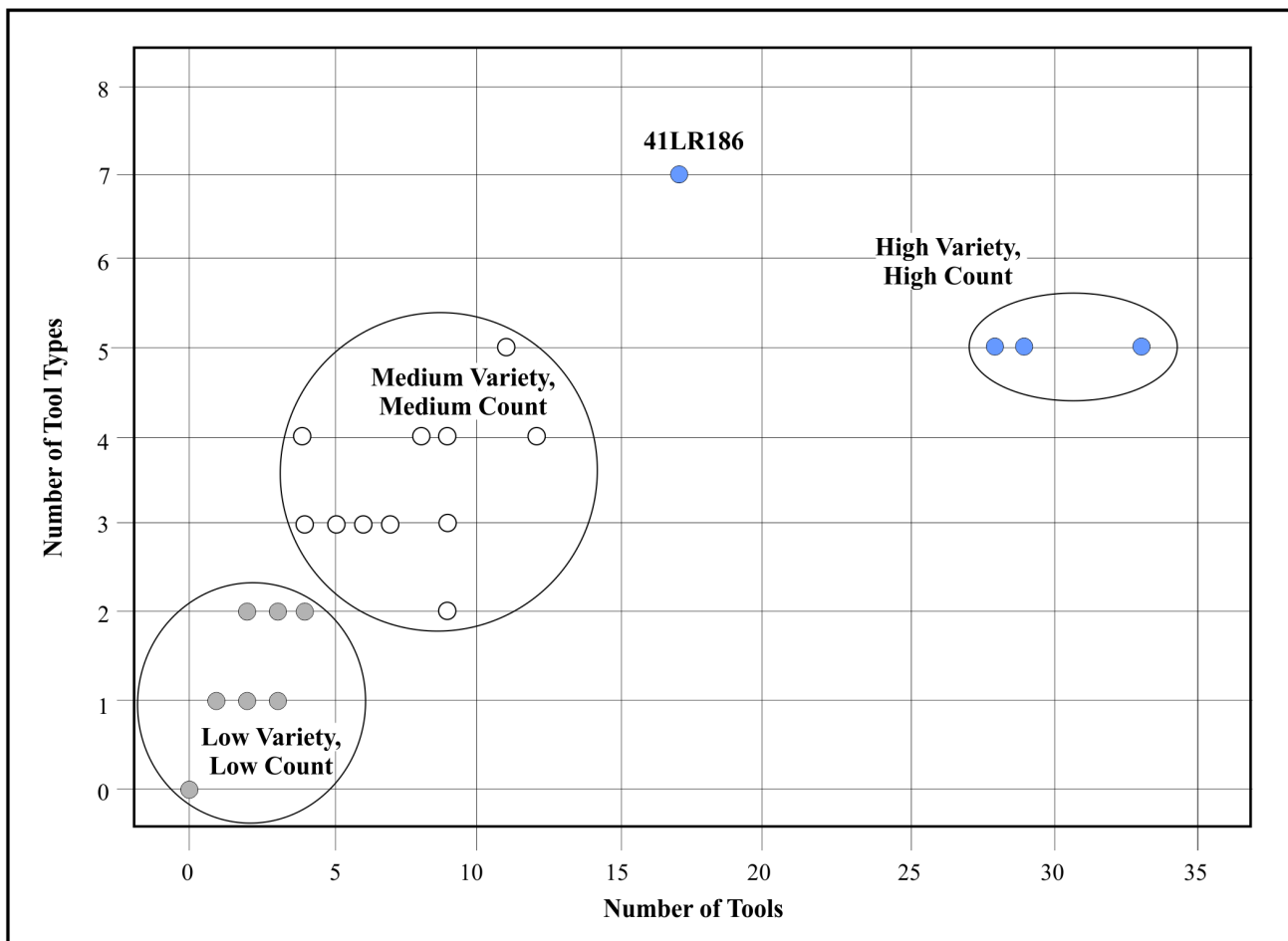


Figure 4-7. Number of tools recorded at each site plotted against number of tool types.

majority of tools were manufactured from quartzite (63%, n=102) or chert (31%, n=51). Other materials used include silicified wood, novaculite and jasper. All cores recovered and reported on were manufactured of local materials. Thirty-five of the 47 cores were quartzite, 10 were chert, and one was silicified wood.

Toolstone that was identified as non-local included green and gray chert and novaculite. Thirteen of the non-local tools were formal in nature; projectile points (n=5), bifaces (n=7), and a drill recovered from site 41LR157. One edge-modified flake from site 41LR212 was identified as non-local chert. Nine sites had tools manufactured of nonlocal material. These nine sites have a low to medium MLD average, with 41LR170 and 41LR196 falling into the medium category. This suggests the possibility of increased mobility at these lower-density sites.

In addition to the primary focus of this review, lithics, Native American ceramics have been recorded at 13 of the 36 sites previously investigated. At 41LR152 this assemblage included an intact vessel (Mahoney 2001), and at site 41LR233 the

ceramic assemblage consists of a long-stemmed pipe sherd (Greaves 2003). The majority of ceramics recovered are described as grog tempered, but some sherds include bone, grit, hematite, and/or shell (Greaves 2003; Mahoney 2001; Mahoney et al. 2002). Burned daub was also recovered from 41LR164 (Mahoney 2001).

Summary

Broadly, the archaeological landscape at Camp Maxey is dominated by low density, low diversity prehistoric sites. Lithic debitage and tools are comprised of predominately local materials, and formal tools such as bifaces and projectile points are more common than expedient tool types. However, some individual sites exhibit higher artifact densities and more diverse assemblages. In addition, thermal features, preserved organic material suitable for radiocarbon dating and temporally diagnostic artifacts are all present at various sites. This assessment of site and assemblage characteristics across Camp Maxey indicates potential at some sites to contribute significant research data.

This page intentionally left blank.

Chapter 5: Field and Laboratory Methods

Leonard Kemp

The Camp Maxey project was conducted in multiple phases that included a pre-field review, site reconnaissance, shovel testing, and site eligibility testing. This chapter describes the field and laboratory methods, as well as the curation strategy used on this project.

Field Methods

Pre-Field and Reconnaissance

Prior to the start and throughout the fieldwork, the PI and PA reviewed reports of previous investigations (Lyle et al. 2001; Nickels et al. 1998), topographic maps, site maps, and aerial photographs to determine the locations of the proposed project sites. Twelve sites were visited in May 2021 that included 41LR154, 41LR159, 41LR161, 41LR162, 41LR165, 41LR175, 41BR177, 41LR184, 41LR203, 41LR213, 41LR226, and 41LR238. Based on the pre-field reviews and reconnaissance, additional ground investigation was needed to assess the validity of the given site location for sites 41LR154, 41LR162, 41LR165, and 41LR175. In addition, there was a need to investigate further the findings from the initial surveys prior to any commencement of eligibility testing. Shovel testing was proposed for sites were 41LR154, 41LR159, 41LR161, 41LR162, 41LR165, 41LR213, and 41LR226. It was assumed that the remaining four sites, 41LR177, 41LR184, 41LR203, and 41LR238 were in their correct locations and sufficiently shovel tested so that the location of test units could be determined.

Shovel Testing

The PA and two Field Archaeologists excavated shovel tests on seven sites, 41LR154, 41LR159, 41LR161, 41LR162, 41LR165, 41LR213, and 41LR226 from July 15

through July 20, 2021. Note two locations were tested to determine the location of 41LR165. Table 5-1 summarizes the quantity and results of that testing. A detailed account of this testing phase is presented in the following chapter that reports on the investigation.

The locations of proposed shovel tests were placed on a Trimble Juno in ArcMap to guide the archaeologist to the location(s) of the shovel test. Shovel tests were excavated 30 cm in diameter and to a maximum depth of 80 cm below surface in 20 cm levels per THC standards. All excavation matrix from each level was screened through ¼" hardware cloth. All artifacts from each level were collected and bagged with that bag labelled with provenience. A unique identifier was assigned to each artifact bag and this information was recorded into a field log. A standard form was completed for each shovel test noting the description of the soil matrix and the presence of cultural material by level. In those shovel tests that contained prehistoric and/or historical cultural material, CAR excavated additional shovel tests to determine the extent of the deposit per THC guidelines. The location of each shovel test was recorded on Trimble GPS data collector.

NRHP Eligibility Testing

CAR outlined its NRHP testing plan for the sites in an email to then TMD Cultural Resources Manager Kristen Mt. Joy who concurred with the proposal (email on August 4, 2021). CAR conducted eligibility testing of ten sites in four sessions in August and September of 2021, followed by a final session in May 2022. Table 5-2 summarizes the testing effort. Note the test unit locations for 41LR165 was placed outside of its boundaries with an additional unit subsequently placed in the correct location.

Table 5-1. Summary of Shovel Tests on Seven Maxey Sites

41LR....	Number of Shovel Tests	Number of Positive Shovel Tests
154	11	2
159	29	14
161	10	7
162	20	3
165	3	0
165 alternate	3	0
213	7	0
226	10	0
Totals	83	16

Table 5-2. Summary of Tests Units on Ten Maxey Sites

Site 41LR...	Number of Test Units
154	1
159	4
161	3
162	2
165	2
175	1
177	1
203	3
226	4
238	2
Totals	23

CAR archaeologists consisting of the PA and one to two field archaeologists used the following methods to conduct the excavation of test units. Each test unit was excavated in arbitrary 10-cm levels referenced to the unit datum. In most cases, the first level was excavated to the nearest even 10-cm increment meaning it was usually removed as a partial level so that excavations could proceed in 10-cm increments for each subsequent level. Excavation was performed using shovel skimming with troweling when necessary to expose features and in situ artifacts. The collected sediment from each level was sifted through ¼" hardware cloth. Artifacts found in the screen were collected, labeled by provenience, given a unique identifier, and recorded in a field log. A standardized test unit form was completed for each level. When artifacts were found in situ, they were drawn on the unit grid on the excavation form. All units were photographed at the completion of each level. All prehistoric cultural material encountered in test units was collected and returned to the CAR laboratory for processing and analysis. Ammunition was noted as present when encountered but not collected.

Magnetic Soil Susceptibility (MSS) samples were taken from test units that had sufficient depth beyond the bioturbated zone (approximately 40 to 50 cm below surface). The MSS samples were collected from the wall profile of each test unit upon completion of the unit's excavation. Plastic vials were inserted into a 1-m board with holes drilled at 5-cm increments. The board was placed against the profile wall, and the vials were tapped into the profile. The vials were carefully removed from the test unit wall, labeled, and placed into separate bags for each unit. All test units were backfilled upon completion of each session.

Laboratory Methods

Upon completion of fieldwork, all recovered artifacts, sediment samples, and organic samples were transported

to the CAR laboratory for processing. Proveniences for the materials were double-checked by comparing the unique field number to the field log. Prior to analysis, artifacts were washed, air-dried, and placed into zip-locking, archival-quality bags. Each bag contained a label with provenience information and a corresponding lot number. The artifacts were then separated into appropriate categories (e.g., debitage, tools, burned rock) for analysis.

Lithic Analysis

This study takes an attribute analysis approach to allow for basic summary of technological variability, reduction intensity, and reduction efficiency between different raw materials, while also allowing for direct comparison between this sample and previous descriptions of stone tool technologies (Greaves et al. 2003; Mahoney 2001; Mahoney et al. 2002). The assemblage was separated into either debris elements (chunks, pieces of knapping shatter) or debitage elements (flakes, biface thinning flakes, cores), and edge modified pieces (flakes with edge modification, bifaces). Debris elements were grouped together by raw material type, and weighed in bulk, while the remainder of the assemblage was measured individually. Across elements measured, raw material type, color, transparency, and quality were assessed. Length, width, thickness, platform width and platform depth were measured using a pair of Pro-grade digital calipers. The weight of each piece was measured to the nearest 1/100 of a gram. The degree of cortex on each piece was characterized in an interval scale (0%, 1-50%, 51-99%, 100%), and the number of dorsal scars was also counted. Any distinctive technological features (presence of features consistent with bipolar percussion, or platform preparation) were noted. Cores were measured in terms of their length, width, and thickness, number of scar removals, size of the largest scar removed, and the amount of cortical cover in addition to raw material type, as well as other notes about the reduction

strategy employed. Bifaces were also measured in terms of their length, width, and thickness, and further described.

Magnetic Soil Susceptibility Analysis

Magnetic Soil Susceptibility (MSS) analysis measures the potential magnetic signature of a sediment sample, with higher values suggesting greater magnetic potential. In this study, MSS analysis can provide information on the overall integrity of a site as well as a means to infer buried cultural surfaces.

In the CAR lab, the MSS samples were air dried and packed into a pre-weighed 10-cm³ plastic vial. The sample was weighed with the sample mass recorded less the weight of the empty vial. The sample was then placed into a Bartington MS2 frequency sensor attached to a MS2 magnetic susceptibility meter. Low frequency volume susceptibility (κ) was measured on each sample. Two readings were taken, and the results were averaged. The mass corrected magnetic susceptibility (χ) values were then calculated using the sample mass (see Dearing 1999). These results are discussed in Chapter 9, and MSS data are presented in Appendix B.

Flotation

Flotation samples were taken from the fill of two features defined in the field on this project. Previous testing of float procedures with unburned poppy seeds indicates a recovery rate of approximately 90%. Table 5-3 lists the sites, features, provenience, amount of sample collected, and material collected from the light and heavy fraction. The material consisted of charcoal and micro debitage. Charcoal samples from features were used to date the three features (see following section on Radiocarbon). The debitage was added to the artifact counts but was not included in the analysis due to the small size.

Radiocarbon Dating

Two charcoal samples associated with two features one on 41LR159 (Feature 1) and another on 41LR161 (Feature 1)

were submitted for radiocarbon analysis. The results of the analysis are discussed in Chapter 7 with additional information provided in Appendix A. The remaining charcoal samples collected during testing were placed in aluminum and curated.

Curation

All cultural materials and records obtained and/or generated during the project were prepared in accordance with federal regulation 36 CFR part 79 and THC requirements for State Held-in-Trust collections. The accession file number for the Maxey project is 2603. The materials were curated in accordance with current CAR guidelines. Artifacts were stored in archival-quality bags with acid-free labels including a provenience and corresponding lot number. Materials needing extra support were double-bagged. Paper labels were applied to all tools using a clear coat of acrylic with an additional coat applied to protect the label. In addition, 50% of unmodified debitage greater than 25 mm from each lot was labeled with the appropriate provenience data. All artifacts were stored in acid-free boxes.

Digital photographs were printed on acid-free paper, labeled with archival appropriate materials, and placed in archival-quality sleeves. All field forms were completed with pencil. Field notes, forms, photographs, and drawings were printed on acid-free paper, placed in archival folders, and stored in acid-free boxes. A copy of this report and all computer media pertaining to the investigation were stored in an archival box and curated with the field notes and documents.

Following analyses and quantification, artifacts associated with this project possessing little scientific value will be discarded pursuant to Chapter 26.27(g)(2) of the Antiquities Code of Texas and in consultation with the TMD. The only artifact class to be discarded specific to this project was non-feature burned rock. It was documented with counts and is included in curation documentation.

Table 5-3. Flotation Samples Collected During the Present Project

Trinomial	Feature	Provenience (Test Unit and Level)	Depth (cmbd)	Amount Floated (liters)	Recovered Material
41LR159	1	TU 4	59-71	8.5	charcoal
41LR161	1	TU2	28-37	8.6	charcoal, fossil shell

This page intentionally left blank.

Chapter 6: Site Descriptions, Work Accomplished, and Material Recovered

Leonard Kemp

This chapter presents an overview of the twelve archaeological sites investigated during the Maxey project. The first section describes the archaeological efforts associated with the NRHP eligibility testing of ten archaeological sites, 41LR154, 41LR159, 41LR161, 41LR162, 41LR165, 41LR175, 41LR177, 41LR203, 41LR226, and 41LR236 for NRHP eligibility (Figure 6-1). It contains a site description for each of the ten tested sites, the results of the previous investigations, and summarizes the findings from the current site investigation. A second section describes the current efforts at two sites, 41LR184 and 41LR216 that were revisited and shovel tested

during this project (Figure 6-1). Neither site was tested for NRHP eligibility during this project due to time and budget constraints.

41LR154

Site 41LR154 was recorded in 1998 by CAR archaeologists and is estimated to be 5600 m² in size (Nickels et al. 1998:51). The site is located in a grassy area with scattered sumac trees and low brush (Figure 6-2) within the Freestone-Hicota complex, 0-3% slopes alfisols. An ephemeral drainage was

Redacted Image

Figure 6-1. Locations of the twelve Camp Maxey sites (Lyle et al. 2001: Figure 8-1; Nickels et al. 1998: Figure 7-1).



Figure 6-2. View to the south of 41LR154 from the current investigation.

observed just south of the site. The site ranges in elevation from approximately 168 to 170 m AMSL.

Background

Site 41LR154 was defined with eight shovel tests with one shovel test positive for an Ogallala quartzite flake and two pieces of brown glass fragments as shown in Figure 6-3 (Nickels et al. 1998:Figure 8-9). In addition, a surface scatter of Ogallala quartzite ($n=3$) and chert ($n=2$) flakes was documented on the site. Historic whiteware ceramic and two clear glass fragments were also recorded on the surface. The buried cultural zone is estimated to be in the upper 20 cm of the site (Nickels et al. 1998:51-52).

Current Investigation

CAR visited 41LR154 in May 2021. A review of the previous investigation suggested that the location of 41LR154 as depicted in the TMD GIS database was wrong. The TMD location shows the site on the southern boundary of the base adjacent to a large pond. The overall project map (Nickels et al. 1998: Figure 8-1) shows it 200 m north of the pond. An aerial on file at CAR used during the initial investigation also shows the site in that second location. The site description and map does not reference or show the pond. CAR archaeologists visited both locations during the initial reconnaissance and determined that the location

along the two-track road was correct based on the original site map and the aerial.

CAR archaeologists returned to 41LR154 on July 15, 2021 and excavated eleven shovel tests to test the validity of the location (Figure 6-4). Shovel test depths ranged from 55 to 75 cmbs averaging 55 cmbs before encountering clay, sandy clay or sandstone. Only two (ST 4 and ST 5) of the shovel tests were positive for a limited quantity of historic and prehistoric material that included debitage, burned rock, and clear glass fragments in the western portion of the tested area. Table 6-1 summarizes the findings of 41LR154 positive shovel test. These artifacts are similar to the findings of Nickels et al. (1998). The eastern area of the site that included ST 12 through 14 appear to be bladed and contained dense new growth vegetation.

CAR excavated one test unit at 41LR154 on August 19, 2021. Test Unit 1 was placed near the two positive shovel tests from the July 2022 testing (Figure 6-4). The soil matrix was a fine to very fine sand primarily very pale brown (10YR7/4) terminating at 60 cmdb in a sandy clay with gravels. CAR screened 0.5 m³ of excavated sediments.

A piece of debitage, a 1903 U.S. penny, two fragments of glass (clear and purple, respectively), and a cast iron stove fragment were found in Level 2 (20-30 cmdb) of TU 1. No other artifacts were found in the unit. Magnetic soil susceptibility (MSS) samples were collected from the test unit. The results of the MSS samples will be discussed in Chapter 9.

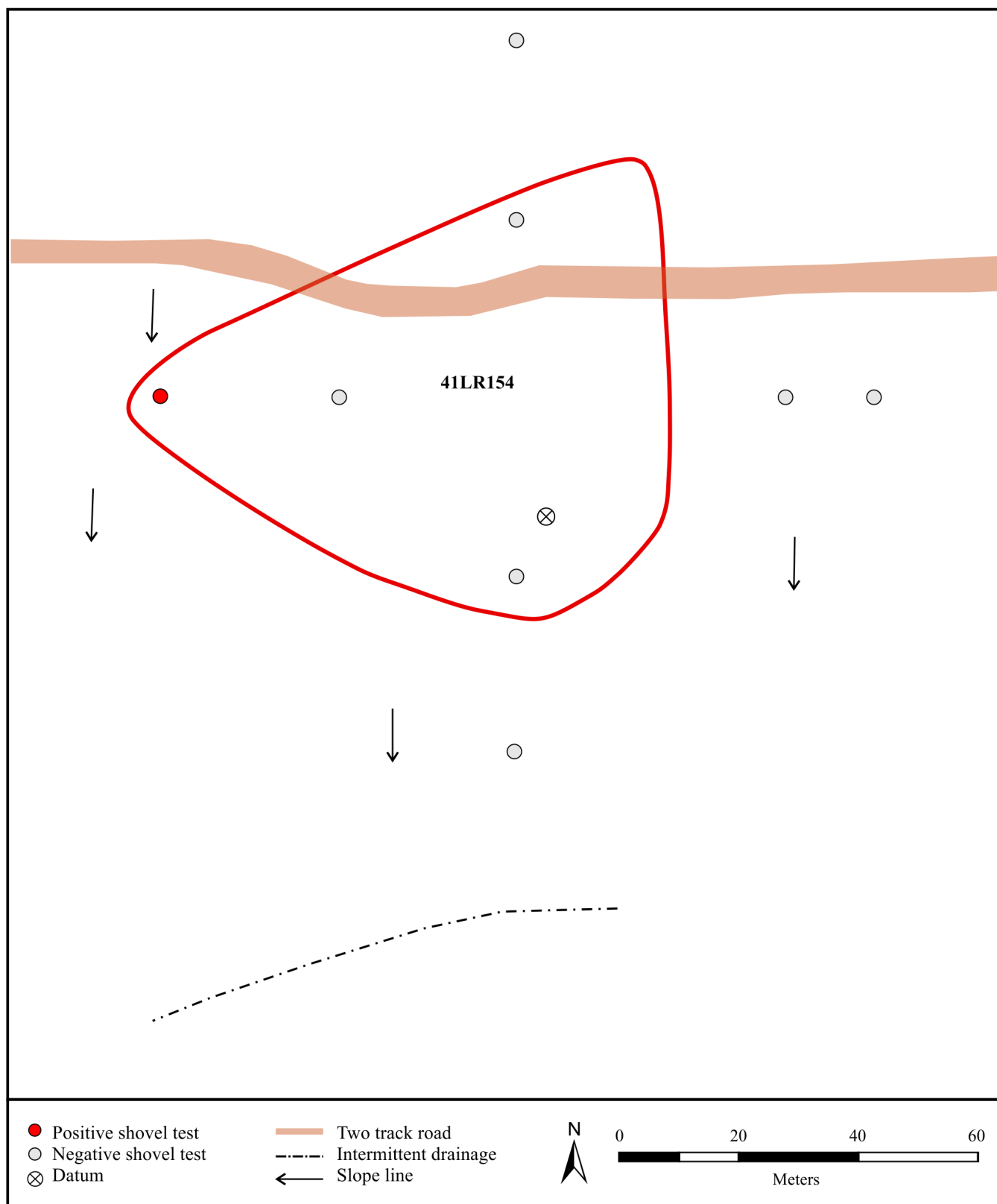


Figure 6-3. Site map of 41LR154 showing previous work by CAR as depicted in Nickels et al. (1998: Figure 8- 9).

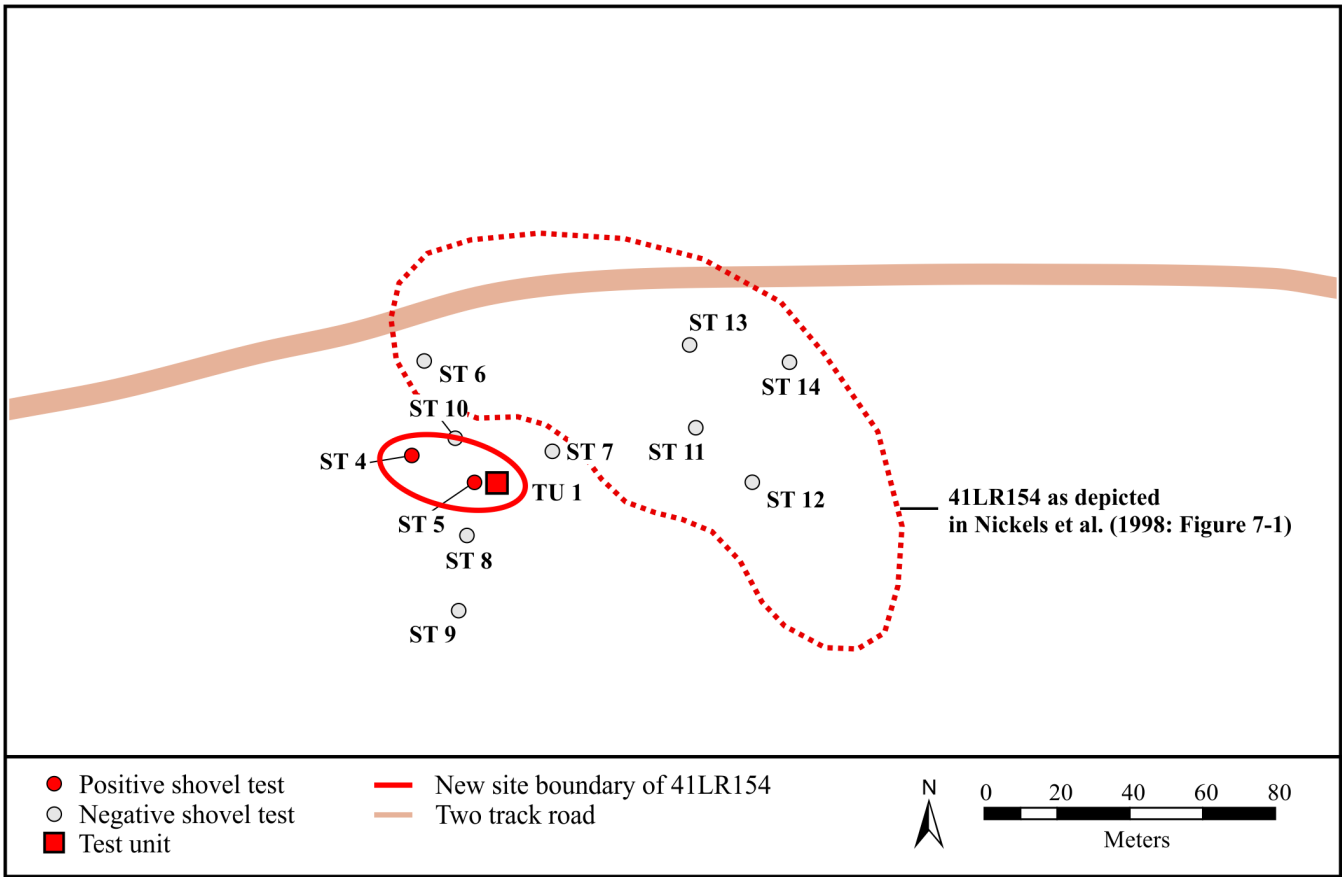


Figure 6-4. New site boundary of 41LR154 with shovel tests and unit excavated by CAR during this investigation.

Table 6-1. Summary of Positive Shovel Tests at 41LR154

Shovel Test	Terminal Depth Below Surface (cmbs) and Soil Type	Findings
4	52 (clay)	clear glass (1) at 20-40 cmbs
5	68 (sandy clay)	debitage (1) at 20-40 cmbs burned rock (0.48 g), clear glass (1) at 40-60 cmbs

41LR159

Site 41LR159 was recorded in 1998 by CAR archaeologists and approximately 2080 m² in size (Nickels et al. 1998:60). The site is located at the confluence of two creeks. It was described at the time a grassy field with scattered trees and briars (Nickels et al. 1998:60). Figure 6-5 shows a current view of the site with grassy vegetation and scattered trees. The northern half of the site falls within the Woodtell loam soil, 5-12% slopes and the southern half the Freestone-Hicota complex, 0-3% slopes. Both soils are alfisols. The site ranges in elevation from approximately 162 to 164 m AMSL.

Background

Site 41LR159 was first identified by the presence of a surface scatter of chert (n=8), Ogallala quartzite (n=3),

and novaculite (n=1) flakes (Nickels et al. 1998:60). Ten shovel tests were excavated with five of those shovel tests positive for lithics (Figure 6-6). The 12 artifacts included flakes (n=9) and three pieces of angular debris of Ogallala quartzite, two of which were heat-treated. The flakes are a diverse mix of raw material that included Ogallala quartzite (n=3), coarse- grained quartzite (n=2), chert (n=2; Red River and local brownish-grey), petrified wood (n=1), and red claystone/ siltstone (n=1). Nickels and colleagues (1998:60) suggest based on the findings that artifacts are found in the upper 15 cm and between 30 to 40 cm below surface.

Current Investigation

CAR visited 41LR159 in May 2021. They original site datum was not found. The assumed site location was



Figure 6-5. View to the northeast of 41LR159.

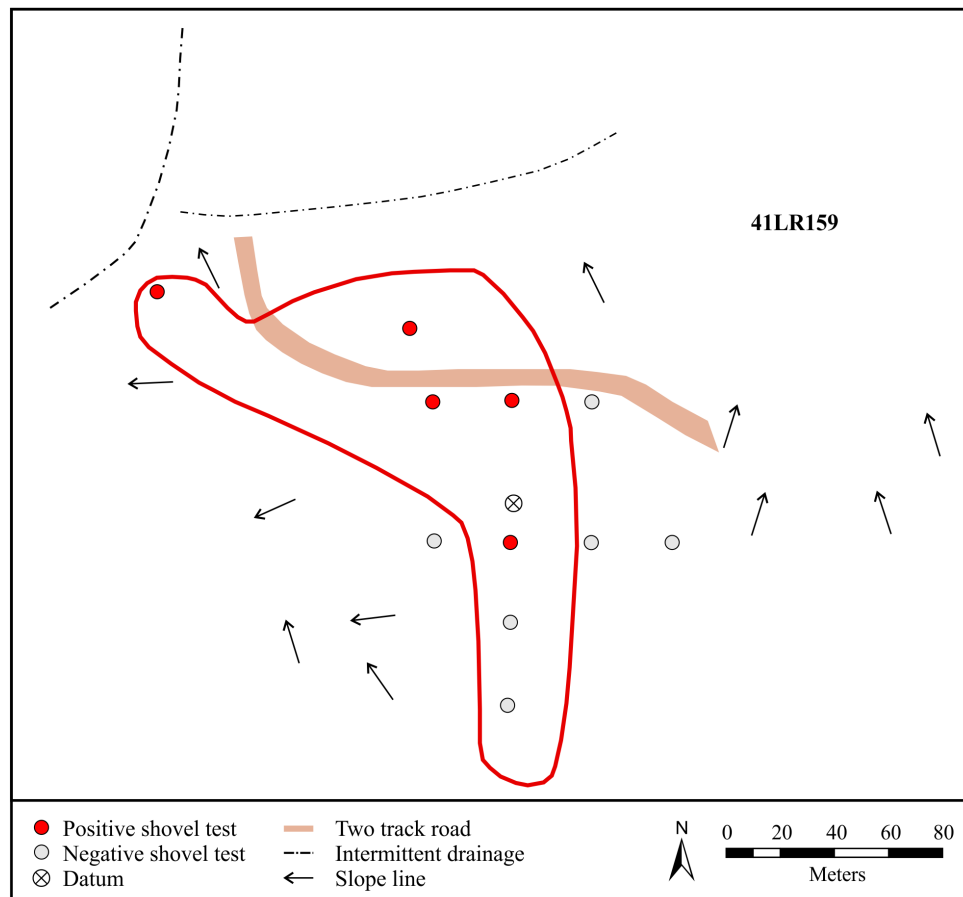


Figure 6-6. Site map of 41LR159 showing previous work by CAR as depicted in Nickels et al. (1998: Figure 8-14).

recorded with a GPS and flagged. The shapefile of the site and original site map differ in size and shape. The original site (Nickels et al. 1998: Figure 8-14) includes a distinctive east to west boundary along the northern portion of the site. The site description is generally the same as described by Nickel et al. (1998), differing only in that they reported a “grassy field with scattered trees” and we observed a relatively wooded area of younger and older trees. Given the twenty-plus years separating the two surveys, this is not unexpected. The landform is a relatively flat area with a sheer overlook of Visor Creek and an intermittent drainage in the north-northwest portion of the site as described by Nickels et al. (1998). A previously documented two-track road was not found during the reconnaissance. However, the road was located during shovel testing.

CAR archaeologists returned to 41LR159 on July 18-19, 2021 and excavated 29 shovel tests that included the southern ridge as described earlier (Figure 6-7). No shovel tests were positive on the northern portion of site

41LR161. All positive shovel tests were found on the southern portion of the east to west ridge suggesting the site location is likely further to the south as depicted on the original site map (see Figure 6-6).

Shovel test depths ranged from 10 to 80 cmbs averaging 44 cmbs before encountering clay, sandy clay, or gravels. Thirteen of the 29 shovel tests were positive for prehistoric artifacts. Table 6-2 summarizes the positive shovel test with the termination depth, soil matrix in the terminal level, the type of artifacts(s), and the level in which the artifacts were found. A burned rock feature was recognized in ST 57 in Level 3 (40 to 60 cmbs). It was subsequently identified as Feature 1 during eligibility testing. Sixteen lithics were recovered that included a biface, an edge modified flake and 14 pieces of chipped stone with the majority of these artifacts (n=10) found in Level 2 (20 to 40 cmbs). Burned rock (total weight= 840.08 g) was distributed throughout the upper levels (1-3; 0 to 60 cmbs) of the shovel tests.

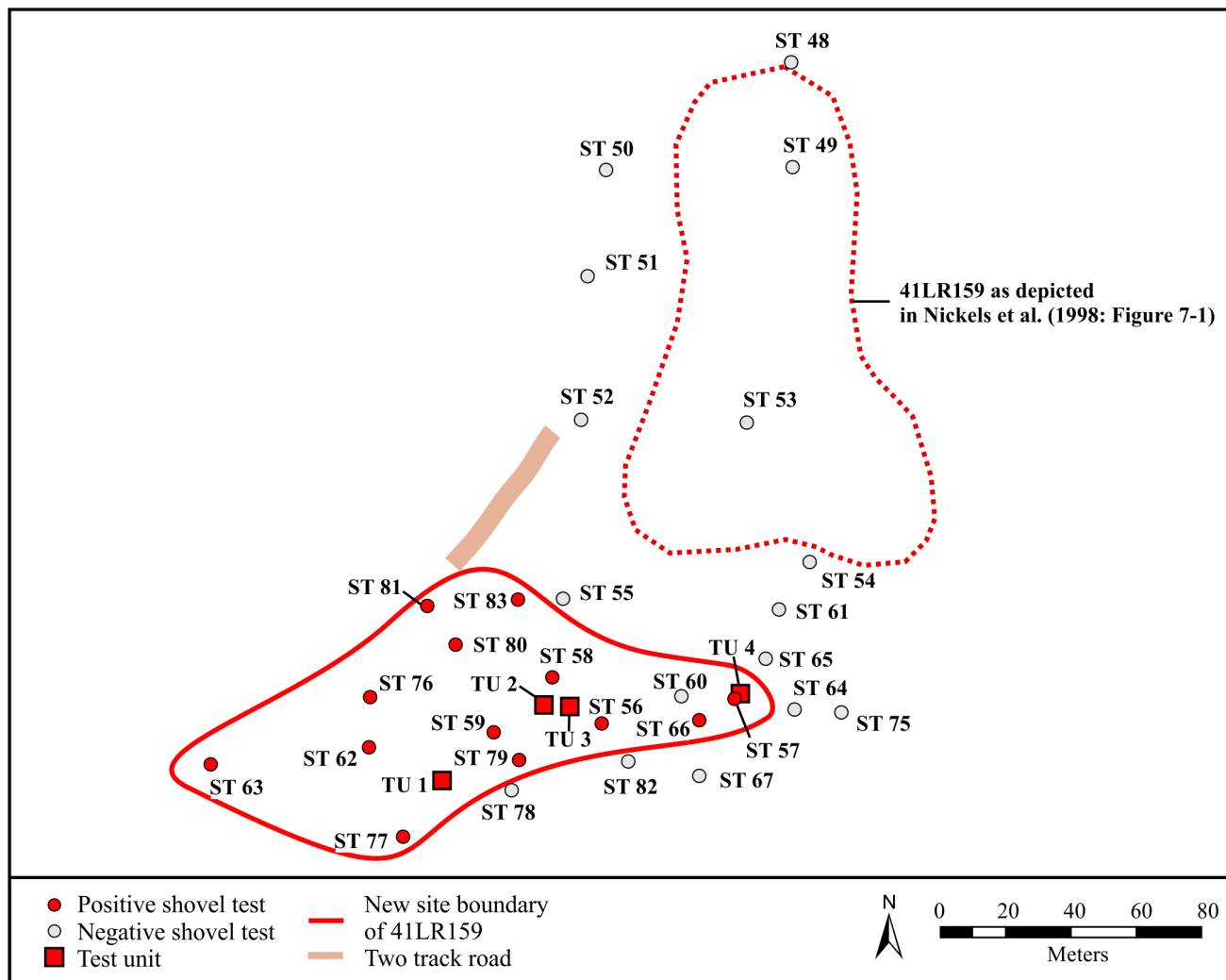


Figure 6-7. New site boundary of 41LR159 with shovel tests and units excavated by CAR during this investigation.

Table 6-2. Summary of Positive Shovel Tests at 41LR159

Shovel Test	Terminal Depth Below Surface (cmbs) and Soil Type	Findings
56	40 (clay/sand)	burned rock (108.48 g) at 20 to 40 cmbs
57	80 clay/sand)	burned rock (426.05 g) at 40 to 60 cmbs; Feature 1; burned rock (3.01 g) at 60 to 80 cmbs
58	55 (clay/sand)	debitage (1) at 0 to 20 cmbs
59	58 (clay/sand)	debitage (2), burned rock (4.3 g) at 20 to 40 cmbs; debitage (1), burned rock (34.95 g) at 40 to 60 cmbs; debitage (3) at 60 to 80 cmbs
62	50 (clay/sand)	debitage (1), burned rock (4.41 g) at 20 to 40 cmbs
63	49 (clay/sand)	debitage (2), burned rock (37.76 g) at 20 to 40 cmbs
66	35 (clay/sand)	biface at 30 cmbs
76	45 (clay/sand)	edge modified flake (1), debitage (1), burned rock (3.3 g) at 0 to 20 cmbs, debitage (3), burned rock (0.63 g) at 20 to 40 cmbs
77	65 (sand)	debitage (1) at 20 to 40 cmbs
79	25 (clay)	burned rock (2.26 g) at 20 to 40 cmbs
80	30 (sand)	burned rock (198.79 g) at 0 to 20 cmbs
81	35 (clay/sand)	burned rock (7.07 g), burned faunal bone at 0 to 20 cmbs
83	35 (clay)	burned rock (9.87 g) at 0 to 20 cmbs

CAR excavated four 1-x-1 m test units between September 18 and September 21, 2021. Figure 6-7 shows the locations of the units relative to the shovel tests excavated by CAR in July 2021. TU 1 was placed between ST 62, 77, and 78. Test Units 2 and 3 were placed between ST 56, 58, and 59. CAR placed TU 4 over ST 57 that contained Feature 1.

Excavated soils ranged in color between gray (10YR5/1) to light yellowish brown (10YR6/4) of loose to soft sand. All test units terminated at clay between 54 and 122 cmbd. CAR screened 3.01 m³ of excavated sediments. Table 6-3 provides a summary of the excavation effort.

The four units produced a burned rock feature, three bifaces, a uniface, a core, 118 pieces of debitage, 1,986 g of non-feature burned rock, a quartzite crystal, and charcoal. A

burned rock feature initially found in ST 57 was confirmed in TU 4 Level 6. The feature appears to be a single layer of burned rock in a tight cluster between 59 cmbd and 63 cmbd. It was found in the southwest corner of the unit and continues into the wall of the unit (Figure 6-8). The feature was composed of 2916 g of burned rock. In addition, eight pieces of debitage were found in the screened matrix from Level 6. A sample of charcoal from Feature 1 was submitted to DirectAMS (D-AMS 047725) for radiocarbon dating returning an uncorrected date of 1056 ±23 RCYBP. The results of are discussed in Chapter 7.

Table 6-4 summarizes the artifacts recovered from 41LR159 by unit and level. Magnetic soil susceptibility samples were also collected from each of the four units. The results of the MSS analysis are discussed in Chapter 9.

Table 6-3. Summary of Test Units Excavations at 41LR159

Test Unit	Number of Levels Excavated	Maximum Terminal Depth Below Datum (cmbd) and Soil Type	Excavated Sediments (m ³)
1	11	122 (clay)	1.12
2	5	55 (clay)	0.45
3	5	54 (clay)	0.44
4	10	110 (clay)	1.00

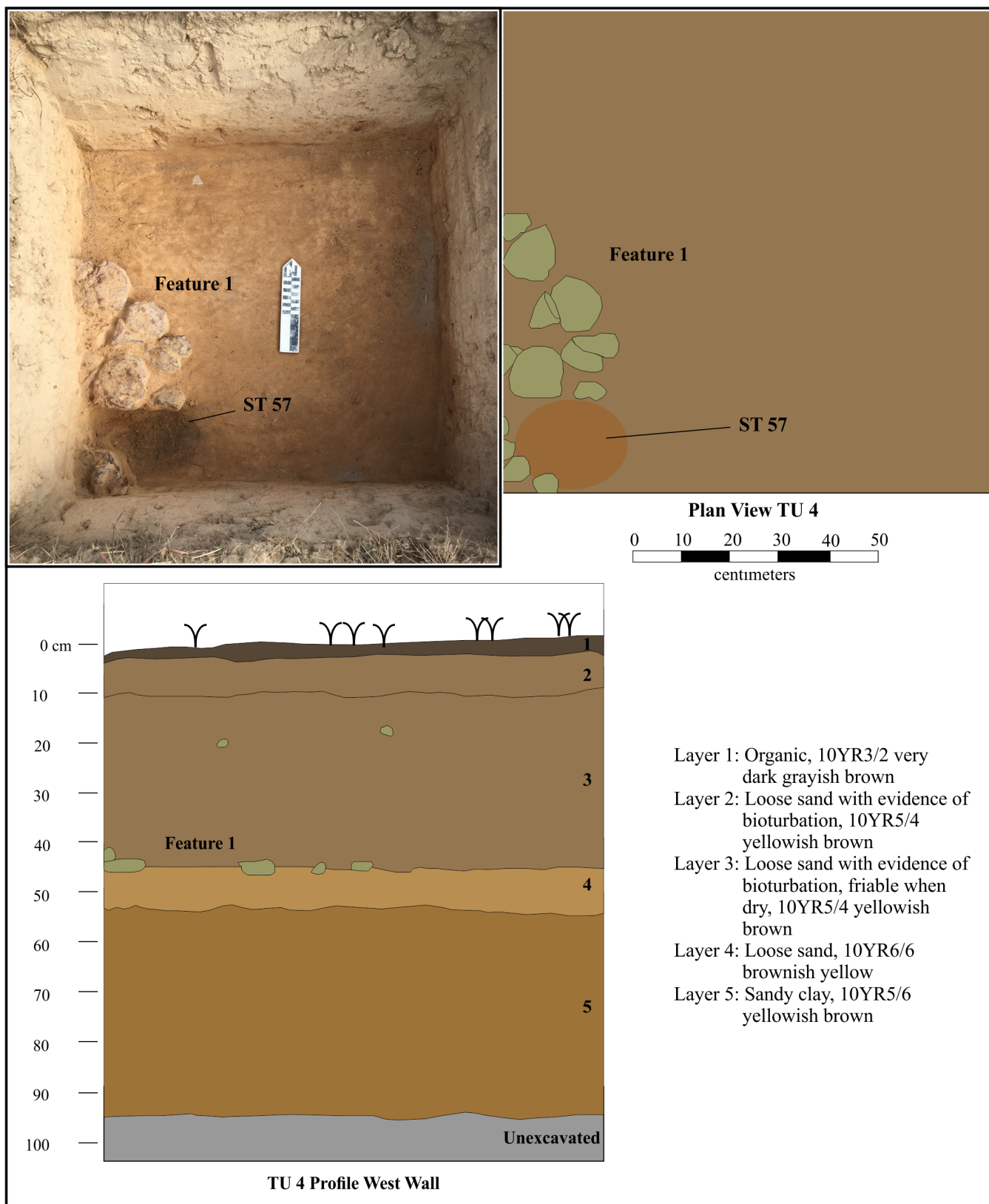


Figure 6-8. Plan and profile views of Feature 1 on 41LR159.

Table 6-4. Summary of Artifacts by Unit and Level from 41LR159

Level	Test Unit 1	Test Unit 2	Test Unit 3	Test Unit 4
1	debitage (10)	null	burned rock (2.09 g)	null
2	debitage (7); burned rock (1.85 g)	debitage (7); burned rock (109.31 g); ¹⁴ C	biface; debitage (10); burned rock (9.43 g)	debitage (2); burned rock (39.8 g)
3	debitage (5); burned rock (2.40 g)	core; debitage (2); burned rock (162.61 g)	debitage (7); burned rock (339.75 g); ¹⁴ C	debitage (2); burned rock (31.7 g)
4	uniface; debitage (4); burned rock (15.72 g)	debitage (5); burned rock 254.52 g); ¹⁴ C	debitage (1); burned rock (18.88 g)	debitage (6); burned rock (31.99 g)
5	debitage (12); burned rock (88.91 g)	null	null	debitage (3); burned rock (74.59 g); ¹⁴ C
6	debitage (5); burned rock (34.96 g)	not excavated	not excavated	feature 1; debitage (8); burned rock (2949.97 g); ¹⁴ C
7	debitage (2); burned rock (139.11 g)	not excavated	not excavated	debitage (3); burned rock (5.14 g)
8	debitage (2); burned rock (166.62 g)	not excavated	not excavated	biface; burned rock (33.4 g)
9	debitage (4); burned rock (209.68 g)	not excavated	not excavated	biface; debitage (3); burned rock (21.67 g)
10	debitage (4); burned rock (106.24 g)	not excavated	not excavated	debitage (4); burned rock (32.66 g)
11	debitage (2); burned rock (28.60 g)	not excavated	not excavated	not excavated
12	null	not excavated	not excavated	not excavated

41LR161

Site 41LR161 was recorded in 1998 by CAR archaeologists as approximately 7700 m² in size (Nickels et al. 1998:62). The site is located on a finger ridge between two drainages with Visor Creek just to the northwest of the site. The site is wooded with grass and areas of dense brush (Figure 6-9). The northwestern third of the site falls within the Woodtell loam soil, 5-12% slopes with the remaining two-thirds of the site in the Freestone-Hicota complex, 0-3% slopes. Both soils are alfisols. The site ranges in elevation from approximately 158 to 160 m AMSL.

Background

Site 41LR161 was defined by seven shovel tests with five of those shovel tests positive for lithics as shown in Figure 6-10 (Nickels et al. 1998:62). The lithics consisted of chert core fragment, a split quartzite pebble, and five flakes. The flakes were derived from Red River cherts (n=2), Ogallala quartzite (n=2), and a coarse-grained quartzite (n=1). The cultural zone may extend to 80 cm below surface (Nickels et al. 1998:62).

Current Investigation

CAR visited 41LR161 in May 2021. The original site datum was not found. The location of the site was recorded

with a GPS and flagged. Given the geographic features (Visor Creek and an intermittent drainage) on the site map and topography, the location of the TMD site shapefile appears to be incorrect and placed somewhat further north of the finger ridge shown on the topographic map. The area is relatively open with widely scattered mature trees. The 1-m road cut documented during the 1998 was not identified during this reconnaissance. In addition, the



Figure 6-9. View to the north of 41LR161 in the footprint of a two-track road.

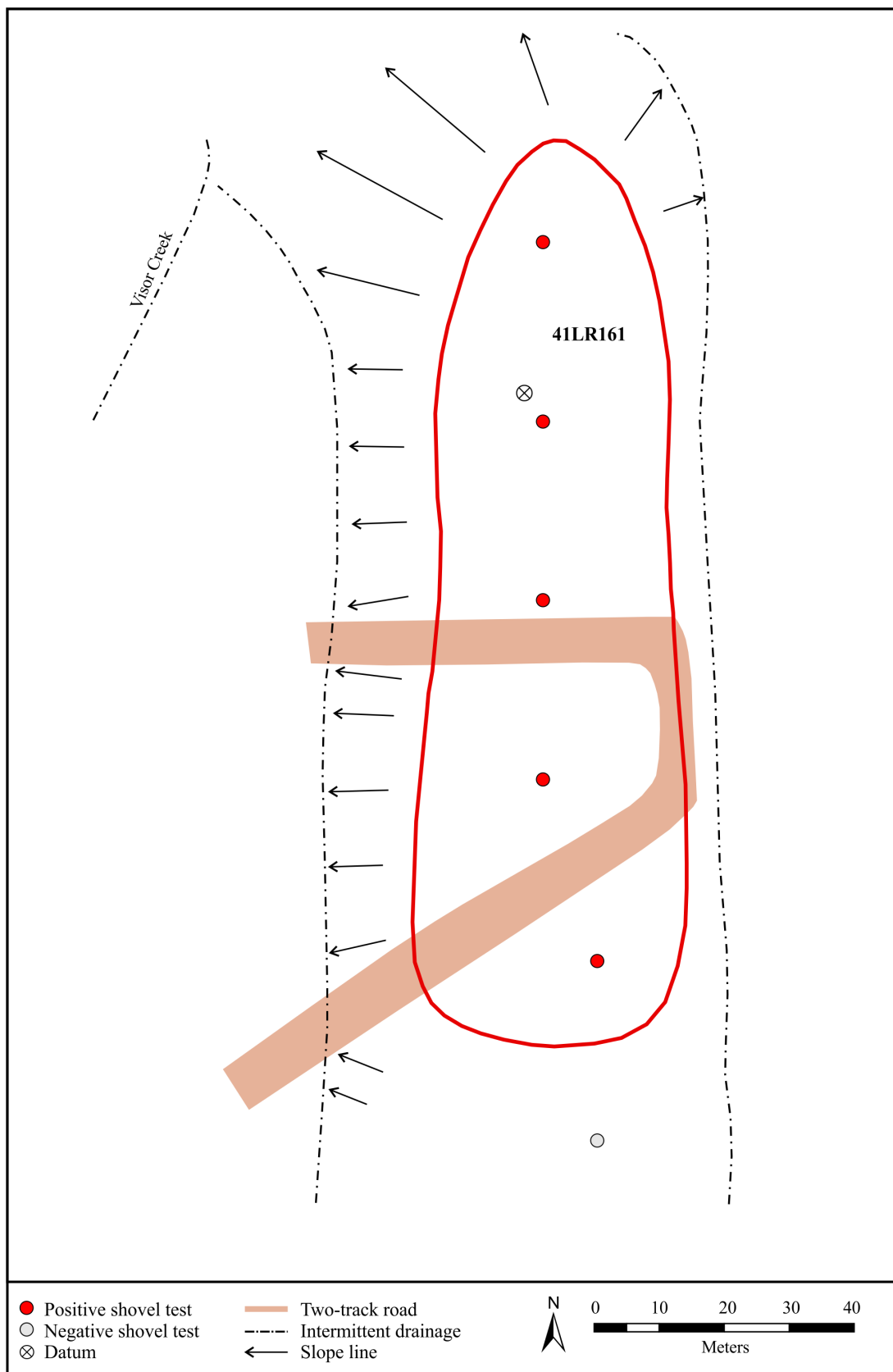


Figure 6-10. Site map of 41LR161 showing previous work by CAR as depicted in Nickels et al. (1998: Figure 8-16).

original site map and the TMD GIS shapefile boundaries differ in shape and size.

On July 20, 2021, CAR returned to 41LR161 and excavated ten shovel tests (Figure 6-11). Shovel test depth ranged between 43 and 80 cmbs with an average depth of 62 cmbs. Table 6-5 summarizes the positive shovel test with the termination depth, soil matrix in the terminal level, the type of artifact(s) and the level in which the artifacts were found. Seven of the shovel tests were positive with

six for prehistoric artifacts and one for a historic artifact- a metal spool. The prehistoric artifacts included four pieces of debitage and burned rock weighing 8.26 g. The majority of prehistoric material was found 20 to 40 cmbs with the exception of one shovel test containing burned rock at 40 to 60 cmbs. A piece of debitage was also found in one shovel test between 60 to 70 cmbs. While prehistoric artifacts were generally found in the upper level of the shovel tests, the depth of shovel tests suggests there are areas that may contain deeper deposits.

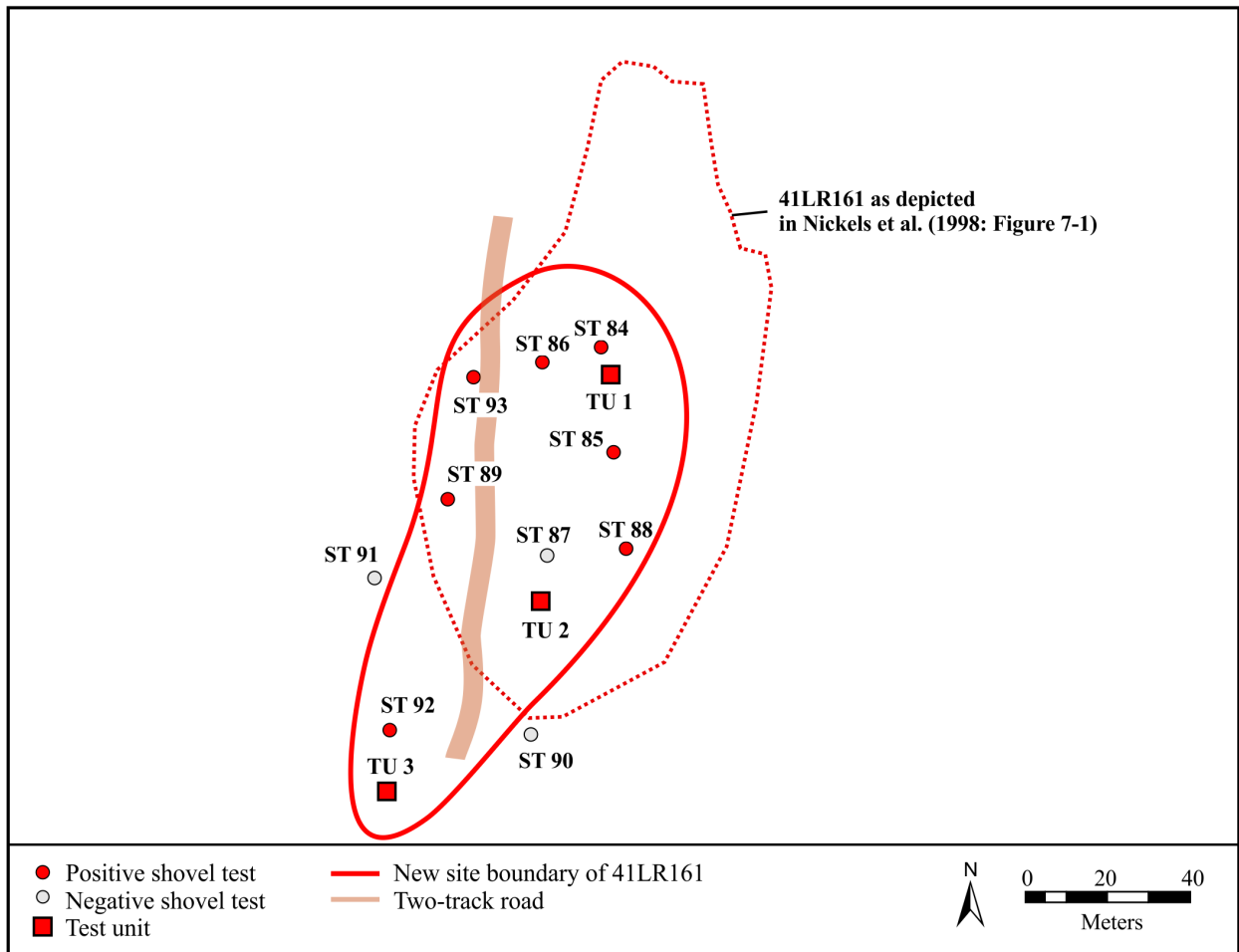


Figure 6-11. New site boundary of 41LR161 with shovel tests and units excavated by CAR during this investigation.

Table 6-5. Summary of Positive Shovel Tests at 41LR161

Shovel Test	Terminal Depth below Surface (cmbs) and Soil Type	Findings
84	80 (sand)	burned rock (0.87 g) at 20-40 cmbs
85	80 (sand)	metal spool at 0-20 cmbs
86	70 (clay)	burned rock (0.71 g) at 20-40 cmbs; debitage (1) at 60-70 cmbs
88	80 (sand)	debitage (1) at 20-40 cmbs
89	50 (clay)	debitage (1) at 20-40 cmbs
92	63 (unknown)	burned rock (6.68 g) at 40-60 cmbs
93	80 (sand)	debitage (1) at 20-40 cmbs

CAR excavated three 1-x-1 m test units between August 16 and August 17, 2021. Figure 6-11 shows the locations of the units relative to the shovel tests excavated by CAR in July 2021. Test Unit 1 was placed in the norther portion of the site between ST 84 and 85. Test Unit 2 was placed south and southwest of ST 87 and 88, respectively. The final unit, TU 3 was placed south of ST 92.

Excavated soils ranged in color between brownish yellow (10YR6/6) to brown (7.5YR4/4). Sediment is a loose to soft sand. Two of the test units (TU 1 and 2) terminated at clay at 50 and 102 cmbd, respectively. Test Unit 3 was terminated

due to dense gravels at 50 cmbd. CAR screened 1.72 m³ of excavated sediments. Table 6-6 provides a summary of the excavation effort.

The three units produced one burned rock feature, a core, an edge modified flake, nine pieces of debitage, 1,617 g of burned rock, and charcoal. Feature 1, a burned rock feature was found in Level 4 of TU 2 (Figure 6-12). The feature is an irregular shaped scatter consisting of burned rock, burned clay, and charcoal. It measures approximately 1-x-1 m in size. The feature was composed of 1447 g of burned rock. A core and one piece of debitage was also collected

Table 6-6. Summary of Test Units Excavations at 41LR161

Test Unit	Number of Levels Excavated	Maximum Terminal Depth Below Datum (cmbd) and Soil Type	Excavated Sediments (m ³)
1	10	102 (clay)	0.92
2	5	50 (clay)	0.40
3	5	50 (gravel)	0.40

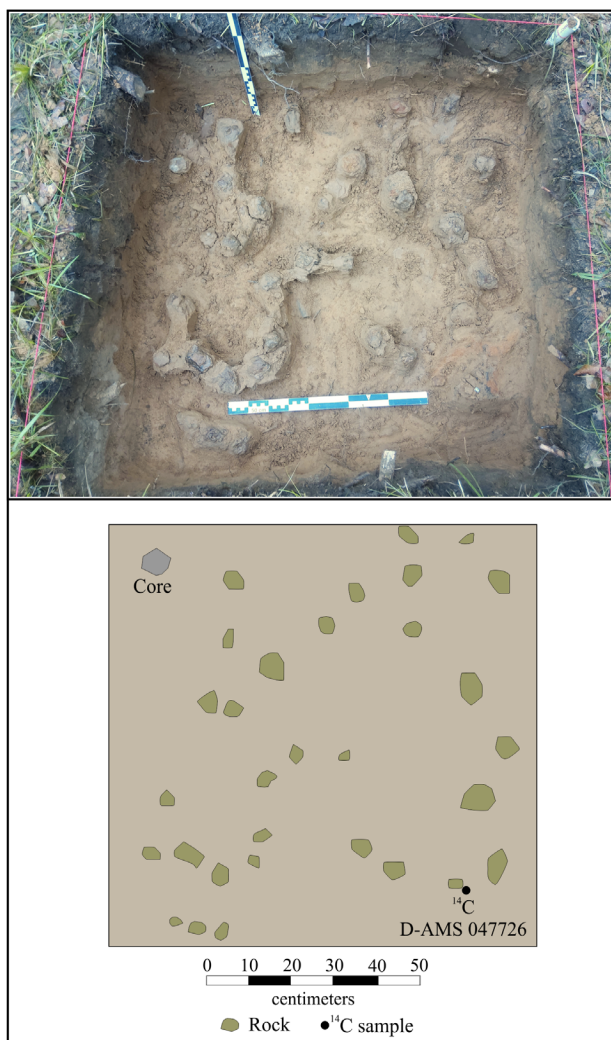


Figure 6-12. Plan views of Feature 1 on 41LR161.

in the same level. A sample of charcoal from Feature 1 was submitted to DirectAMS (D-AMS 047726) for radiocarbon dating returning an uncalibrated date of 239 ± 22 . The results of which are discussed in Chapter 7.

Table 6-7 summarizes the artifacts recovered from 41LR161 by unit and level. Magnetic soil susceptibility samples were also collected from each of the four units. The results of the MSS analysis is discussed in Chapter 9.

Table 6-7. Summary of Artifacts by Unit and Level from 41LR161

Level	Test Unit 1	Test Unit 2	Test Unit 3
1	debitage (2)	null	null
2	null	null	burned rock (69.69 g)
3	debitage (1)	debitage (1); burned rock (77.81 g)	null
4	debitage (1)	Feature 1; core; debitage (1); burned rock (1447 g); ^{14}C	burned rock (20.78 g)
5	debitage (1)	debitage (1); burned rock (2.39 g)	null
6	null	not excavated	not excavated
7	edge modified flake; debitage (1)	not excavated	not excavated
8	null	not excavated	not excavated
9	null	not excavated	not excavated
10	null	not excavated	not excavated

41LR162

Site 41LR162 was recorded in 1998 by CAR archaeologists. It was estimated at 7100 m² in size (Nickels et al. 1998:63). The site is located on a finger slope abutting the southern boundary of the facility. An intermittent drainage forms the east and northeast site boundary. The site is heavily wooded with dense brush (Figure 6-13). The site falls within the Woodtell loam, 5-12% slopes and the Annona loam, 1-4% slopes. Both soils classes are alfisols. The site ranges in elevation from approximately 156 to 158 m AMSL.

Background

Ten shovels test defined site 41LR162. Four of the 10 were positive with 15 lithics recovered (Figure 6-14). Ten of the artifacts came from one shovel test (ST EEEE-34) in the western portion of the site in the upper level (0-20 cmbs). The assemblage contains three pieces of Ogallala angular debris, ten flakes, and two fire-cracked cobbles. Seven of the ten flakes are Ogallala quartzite, two of Red River chert, and the last flakes is derived from a coarse-grained quartzite. Nickels and colleagues (1998:62) recovered artifacts to 60 cm below surface.

Current Investigation

CAR visited 41LR162 in May of 2021. CAR did not find the original site datum. The assumed site location was recorded with a GPS and flagged. There are significant shape differences in the TMD GIS shapefile and the original site

map that cannot be explained (Figures 6-14 and 6-15). The former shows essentially a north-south site orientation with continuing across the two-track road with the southern portion situated on the base boundary (Figure 6-14). The latter shows the site south of the two-track road. The southern portion of the site along the fence was recorded as a reference line to help determine the location of the site. Visor Creek lies to the east of the site and was observed during this reconnaissance. The road shown in Figure 6-14 is observable on earlier aerials of the site location and falls south of an existing road. The area is wooded and previously impacted by blading with push piles (firebreaks) evident throughout the site.

On July 17 and 19, 2021, CAR excavated 20 shovel tests on 41LR162 to determine the site boundary of 41LR162 and for the future placement of test units (Figure 6-15). Shovel test depth ranged between 15 and 80 cmbs with an average depth of 65 cmbs. Table 6-8 summarizes the positive shovel tests with the termination depth, soil matrix in the terminal level, the type of artifact(s), and the level in which the artifacts were found. Four of the 20 shovel tests were positive for small quantity of artifacts that included a core, debitage (n=5), burned rock weighing 2.5 g, and a bullet casing.

CAR excavated two 1-x-1 m test units on August 18, 2021 at site 41LR162. Figure 6-15 shows the locations of the units relative to the shovel tests excavated by CAR in July 2021. Test Unit 1 was placed east of ST 20 and TU 2 was placed in the southern portion of the tested sites in the vicinity of ST 17 and 69, an area that appeared to be less disturbed.



Figure 6-13. View to the south of the dense vegetation found on 41LR162.

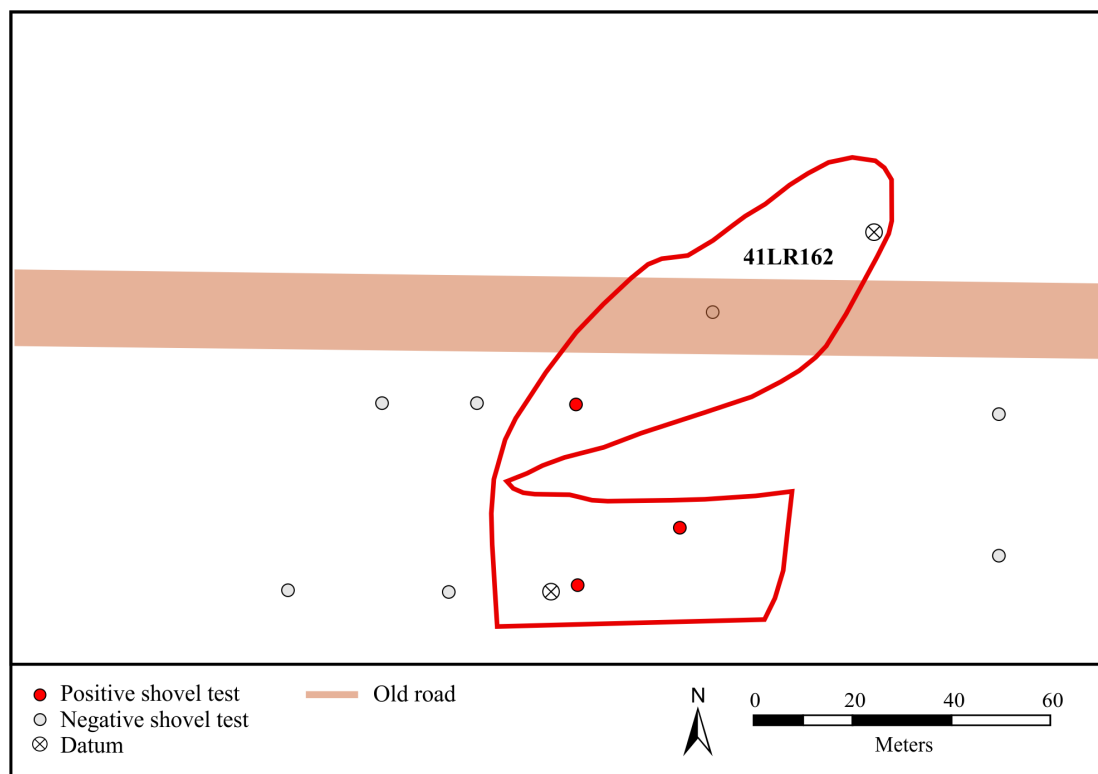


Figure 6-14. Site map of 41LR162 showing previous work by CAR as depicted in Nickels et al. (1998: Figure 8-17).

Excavated soils ranged in color between yellowish brown (10YR5/4) to (10YR5/6). Sediment is loose to soft sand. The test units (1 and 2) terminated at clay at 41 and 40

cmdbd, respectively. CAR screened 0.61 m³ of excavated sediments. Table 6-9 provides a summary of the excavation effort. No artifacts were found in either test unit.

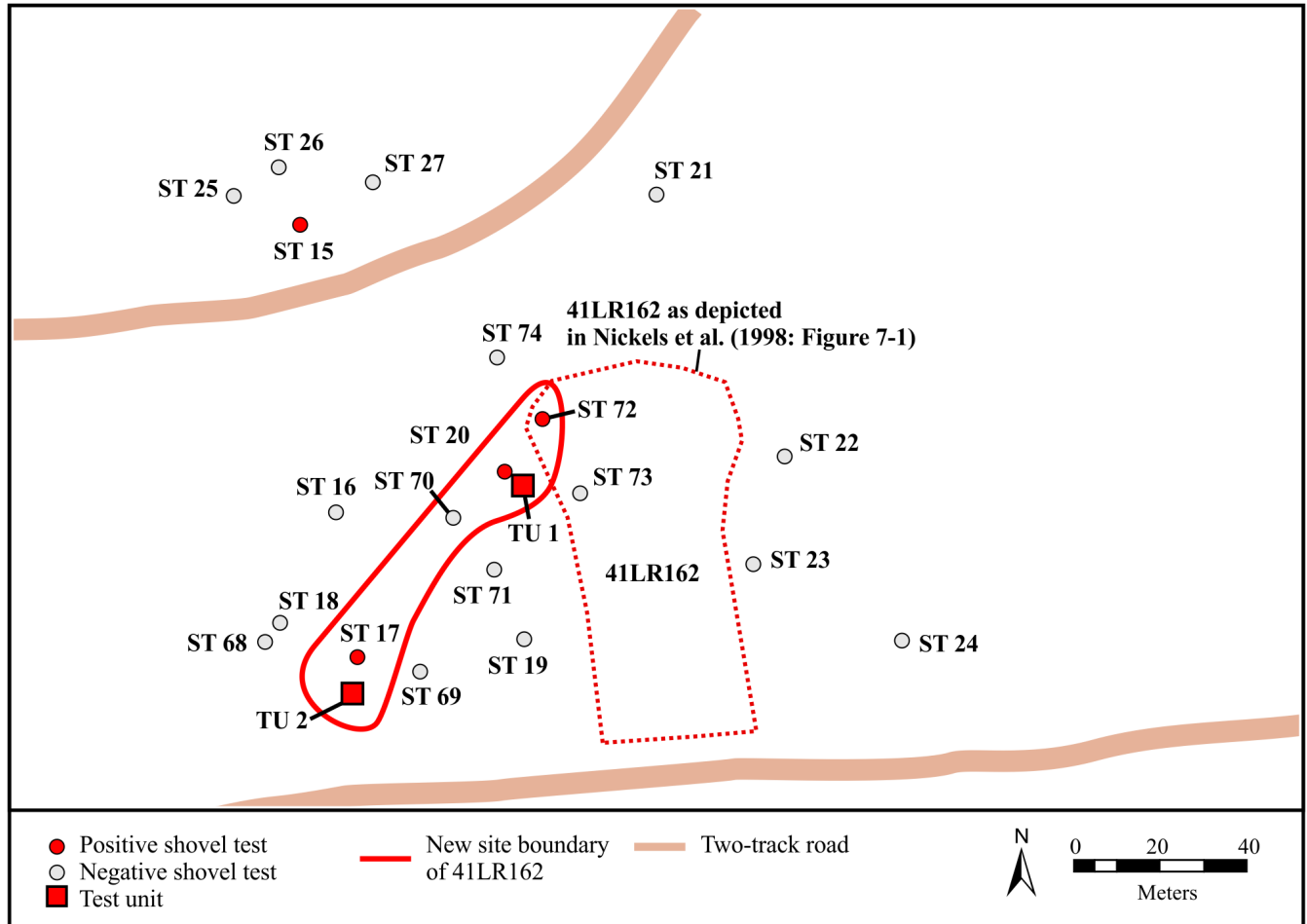


Table 6-8. Summary of Positive Shovel Tests at 41LR162

Shovel Test	Terminal Depth Below Surface (cmbs) and Soil Type	Findings
15	80 (sand)	debitage (1) at 20-40 cmbs
17	80 (sand)	core (1) at 40-60 cmbs
20	80 (sand)	debitage (1) at 40-60 cmbs
72	70 (clay)	debitage (2), burned rock (2.57 g), bullet casing at 20-40 cmbs; debitage (1) at 40-60 cmbs

Table 6-9. Summary of Test Units Excavations at 41LR162

Test Unit	Number of Levels Excavated	Maximum Terminal Depth below Datum (cmdbd) and Soil Type	Excavated Sediments (m ³)
1	4	41 (clay)	0.31
2	3	40 (clay)	0.30

41LR165

Site 41LR165 was recorded in 1998 by CAR archaeologists. The site is approximately 400 m² in size (Nickels et al. 1998:67). It is located along the terrace of Visor Creek within Lassiter silt loam 0-1% slopes. The site is heavily wooded with dense brush and is situated along Visor Creek (Figure 6-16). The site ranges in elevation from approximately 148 to 150 m AMSL.

Background

As shown in Figure 6-17, site 41LR165 was defined by nine shovel tests with three of those shovel tests positive (Nickels et al. 1998:67). Three flakes from two of the shovel tests were found in the upper 20 cm of the excavation and a fourth flake was 20 to 40 cm below surface. The flakes were novaculite (n=3) and Frisco chert (n=1). Nickels and colleagues (1998:62) recovered artifacts to 40 cm below surface.

Current Investigation

CAR visited site 41LR165 in May of 2021. During that initial reconnaissance, CAR did not find the original site datum. The presumed site, based on the TMD GIS shapefile, was recorded with a GPS and flagged. However, there are differences in the topography and the size of the site that suggest this location is wrong. The site map shows a prominent point bar extending into Visor Creek that matches the topo lines shown on the site map. The point bar is approximately 140 m southwest of the current

location and may be a result of GPS error. CAR elected to test two locations along Visor Creek to try to determine the actual location of site 41LR165.

On July 15 and 16, 2021, CAR excavated six shovel tests on the two presumed locations of 41LR165 (Figure 6-18). At the first locale, shovel tests were excavated to 60 to 90 cmbs. At the second locale, shovel tests were excavated to 80 cmbs. No artifacts were found in either location. As such, CAR could not determine the location of 41LR165 based on the lack of findings. However, after the completion of fieldwork, an aerial from the original investigation was found which showed the location of Field Site 17, later given the trinomial, 41LR165. This aerial compared with historical imagery on Google Earth Pro suggests that the current TMD GIS location is correct.

CAR excavated two 1-x-1 m test units on September 18, 2021 and May 4, 2022 at site 41LR165. The September excavation of the test unit (TU 1) fell outside the site boundary, as such another unit (TU 2) was excavated in May 2022. Figure 6-18 shows the locations of the units relative to the shovel tests excavated by CAR in July 2021. The results of both excavations are presented here.

The soils of TU 1 were a brownish yellow (10YR6/6) soft sand that terminated at clay horizon at 30 cmdbd. The soils of TU 2 were a yellowish brown (10YR5/4) sand that also terminated at clay horizon at 36 cmdbd. CAR screened 0.46 m³ of excavated sediments. Table 6-10 provides a summary of the excavation. No artifacts were found in the test units. No MSS samples were collected due to the shallow depth of the units.



Figure 6-16. View of Visor Creek that borders the south and east portions of 41LR165.

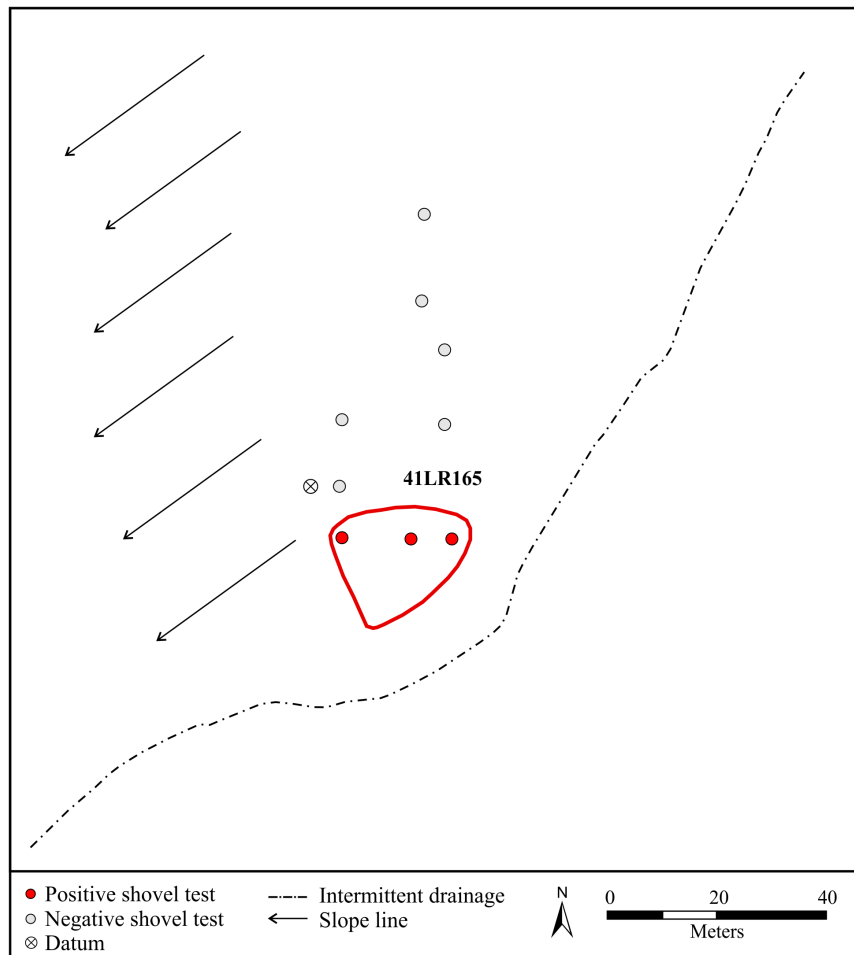


Figure 6-17. Site map of 41LR165 showing previous work by CAR as depicted in Nickels et al. (1998: Figure 8-20).

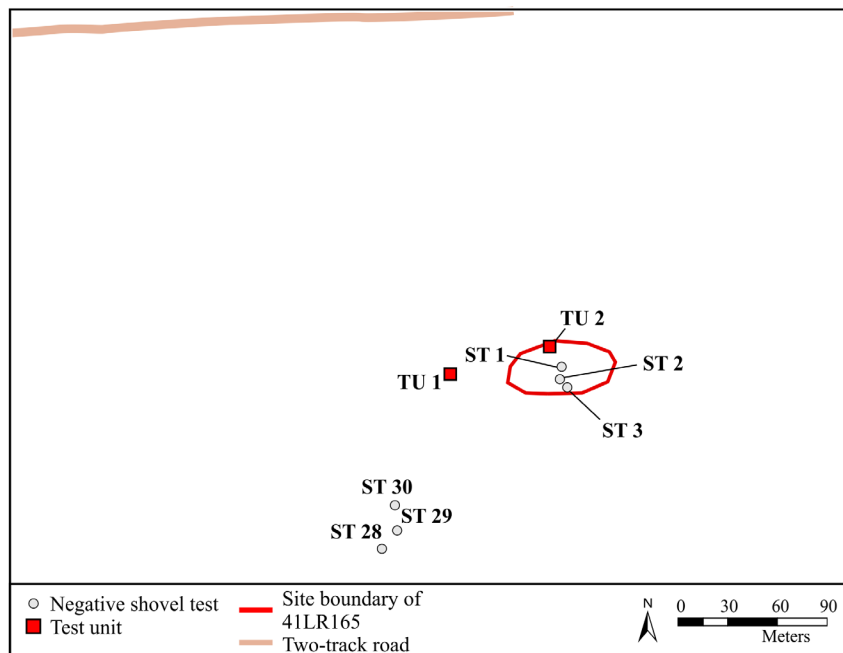


Figure 6-18. Locations of shovel test and units excavated to determine the location of 41LR165.

Table 6-10. Summary of Test Units Excavations at 41LR165

Test Unit	Number of Levels Excavated	Maximum Terminal Depth below Datum (cmbd) and Soil Type	Excavated Sediments (m ³)
1	2	30 (clay)	0.20
2	3	36 (clay)	0.26

41LR175

Site 41LR175 was recorded in 1998 by CAR archaeologists and approximately 400 m² in size (Nickels et al. 1998:73). It is located along the terrace of Visor Creek within Freestone-Hicota 0-3% alfisols. The site is heavily wooded with areas of dense brush (Figure 6-19). The site's elevation is approximately 156 m AMSL.

Background

Site 41LR175 was defined by five shovel tests with one of those shovel tests positive (Figure 6-20). Four lithics were

recovered (Nickels et al. 1998). The assemblage consists of two Ogallala quartzite flakes and two heat-treated Ogallala quartzite pieces of angular debris. Nickels and colleagues (1998:62) recovered artifacts to 80 cm below surface.

Current Investigation

CAR visited site 41LR175 in May of 2021. The site was recorded with a GPS and the presumed location was flagged. The TMD GIS shapefile and site map placed the site west of an intermittent creek on a small rise. However, this location is incorrect. The actual location is south of the road as shown on the project aerial image referenced earlier and the archaeological sites map in Figure 8-1 of Nickels et al.



Figure 6-19. View from Test Unit 1 excavated on 41LR175.

(1998). CAR did not excavate any shovel tests on 41LR175 due to the small size of the site.

CAR excavated one 1-x-1 m test unit on September 17, 2022 at site 41LR175. Figure 6-21 shows the location of the unit.

The soils of TU 1 were a brownish yellow (10YR6/8) soft sand that terminated at a clay horizon within the first level (20 cmbd). CAR screened 0.10 m³ of excavated sediments. No artifacts were found in the test unit. No MSS samples were collected due to the shallow depth of the unit.

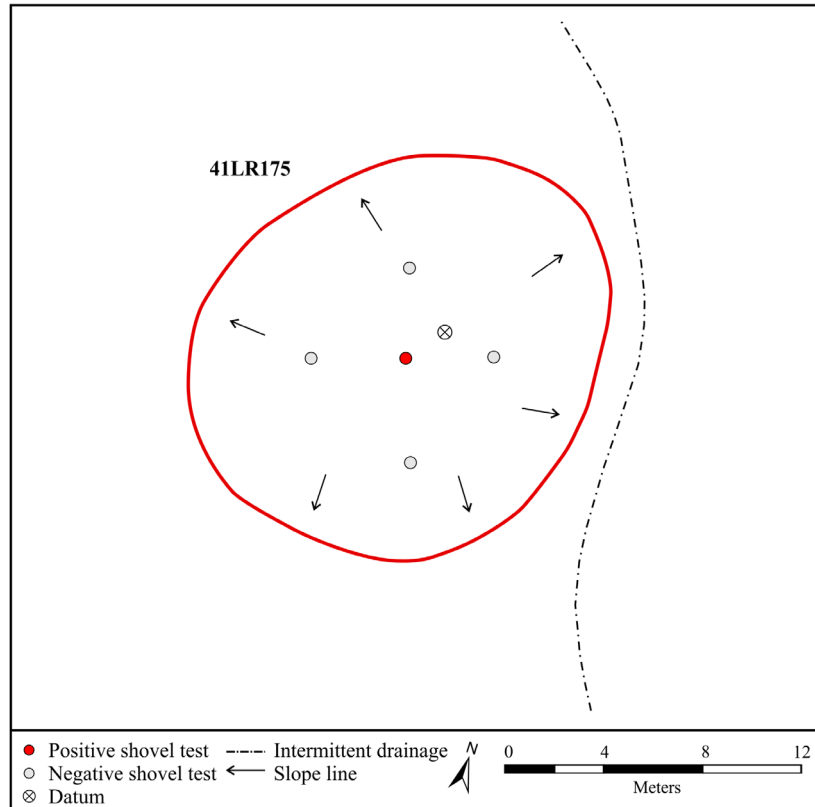


Figure 6-20. Site map of 41LR175 showing previous work by CAR as depicted in Nickels et al. (1998: Figure 8-24).

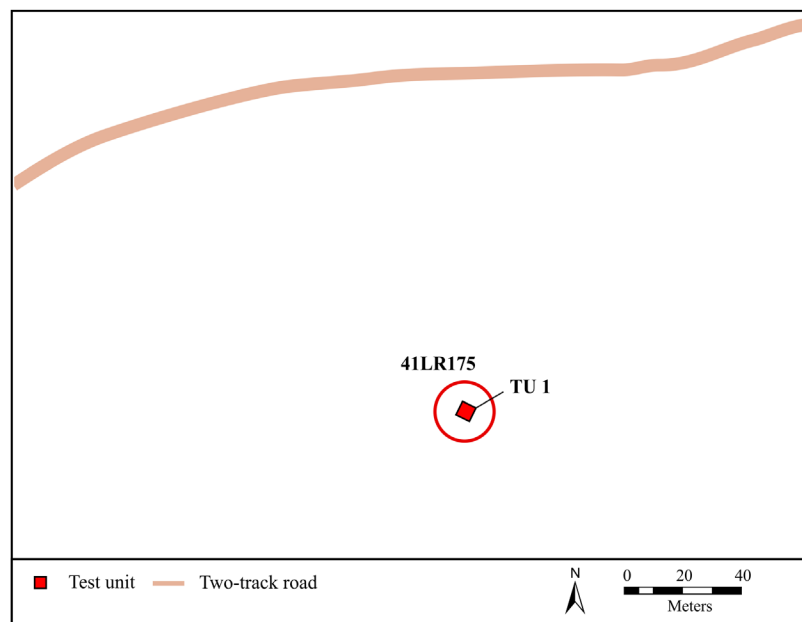


Figure 6-21. The current site map of 41LR175 showing the location of the test unit and identifying landmarks.

41LR177

Site 41LR177 was recorded in 1998 by CAR archaeologists as being approximately 160 m² in size (Nickels et al. 1998:74). The site is located on a grassy finger slope (Figure 6-22)



Figure 6-22. View to the north of 41LR177 from the excavated test unit.

within the Whakana fine sandy loam 1-5% slope alfisols. Two gullies are just north and south of the site. The site ranges in elevation from approximately 154 to 156 m AMSL.

Background

Nine shovel tests defined site 41LR177 with three shovel tests positive for lithics (Figure 6-23). The assemblage contains three flakes of Ogallala angular debris and one coarse-grained quartzite. Nickels and colleagues (1998:74; Appendix A) recovered artifacts to 80 cm below surface.

Current Investigation

CAR visited site 41LR177 in May of 2021. The presumed site location was recorded with a GPS and flagged. CAR archaeologists observed the north and south gully features shown on the site map. In addition, the location matched the landform as shown on the site map. A service road is 275 m to the west of the site. CAR did not excavate any shovel tests on 41LR177 due to the small size of the site.

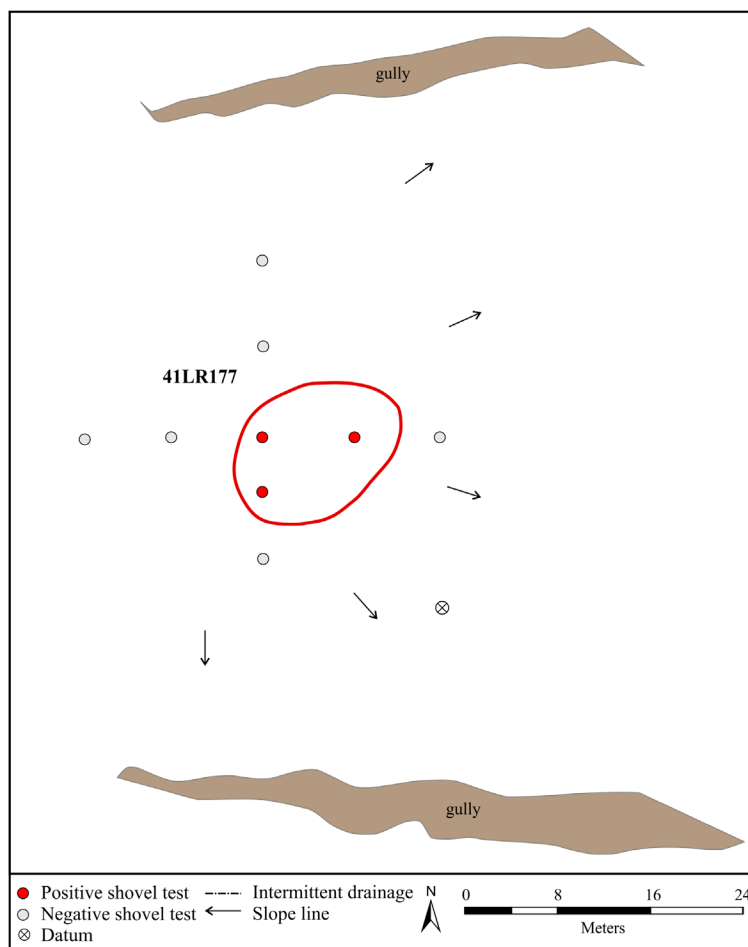


Figure 6-23. Site map of 41LR177 showing previous work by CAR as depicted in Nickels et al. (1998: Figure 8-26).

CAR excavated one 1-x-1 m test units on August 16, 2021 at site 41LR177. Figure 6-24 shows the locations of the unit. The excavated soil was a brown (10YR5/3), loose to soft sand. The test unit terminated at clay at 56 cmbd. CAR screened 0.46 m³ of excavated sediments.

Test Unit 1 produced a small quantity of artifacts that included debitage in Levels 2 (n=2) and 3 (n=2). An unknown metal fragment was also found in Level 2. Magnetic soil susceptibility samples were collected from the unit. The results of the MSS analysis are discussed in Chapter 8.

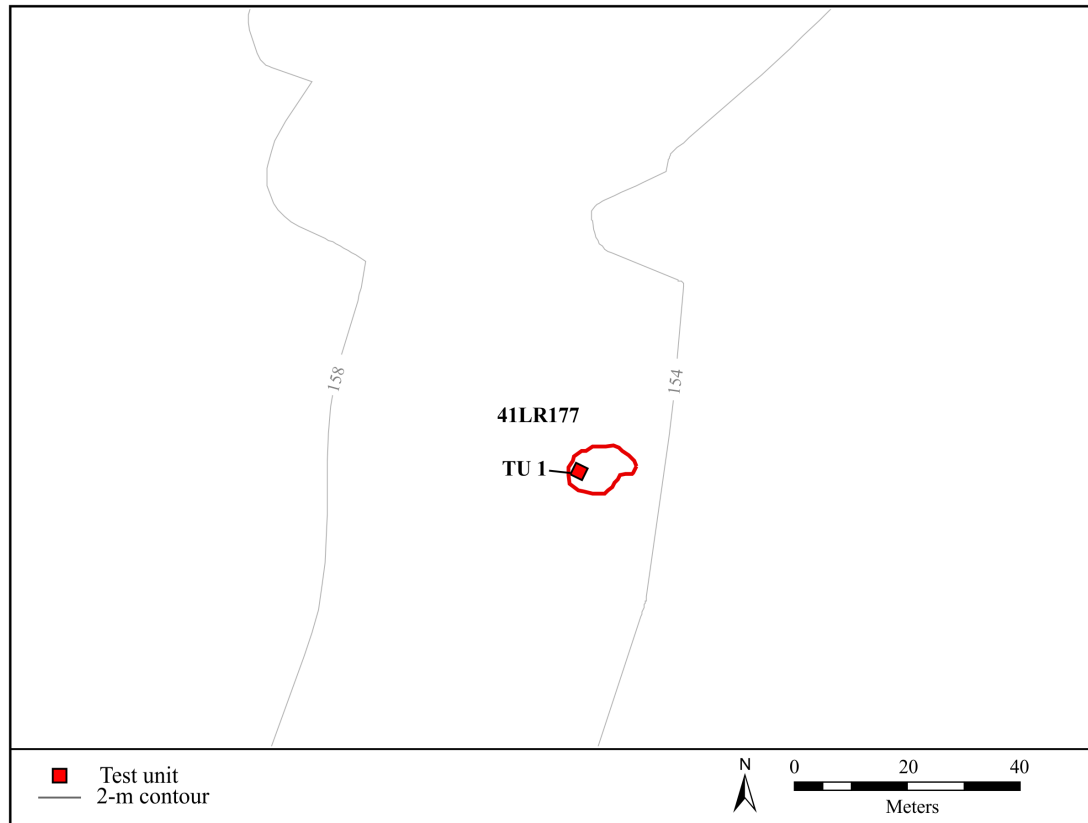


Figure 6-24. Location of the test unit excavated on 41LR177.

41LR203

Site 41LR203 was recorded in 1999 by CAR archaeologists as approximately 23,700 m² in size (Lyle et al. 2001:84). The site is located on a relatively level landform with intermittent drainages to the east and west. It abuts the facility's boundary on its north and east sides. The site vegetation is composed of little bluestem grass and small sumac brush (Figure 6-25). The site falls within the Freestone-Hicota, 0-3% slope alfisols. Site 41LR203 ranges in elevation from approximately 150 to 152 m AMSL.

Background

Site 41LR203 was defined by 26 shovel tests with ten shovel tests positive for artifacts as shown in Figure 6-26 (Lyle et al. 2001:Figure 8-6). These artifacts included seven flakes, heat spalls (n=2), a piece of fire crack rock (95.3 g), and carbonized nutshell fragment (Lyle et al. 2001:85). The flakes consisted of Ogallala quartzite (n=6) with half of those flakes heat-treated (Lyle et al. 2001:85). The remaining flake

was derived from a red chert (Lyle et al. 2001:85). Lyle and colleagues (2001:85) recovered artifacts extending to a depth of 60 cm below surface.



Figure 6-25. View to the north of 41LR 203 to the base boundary in the background.

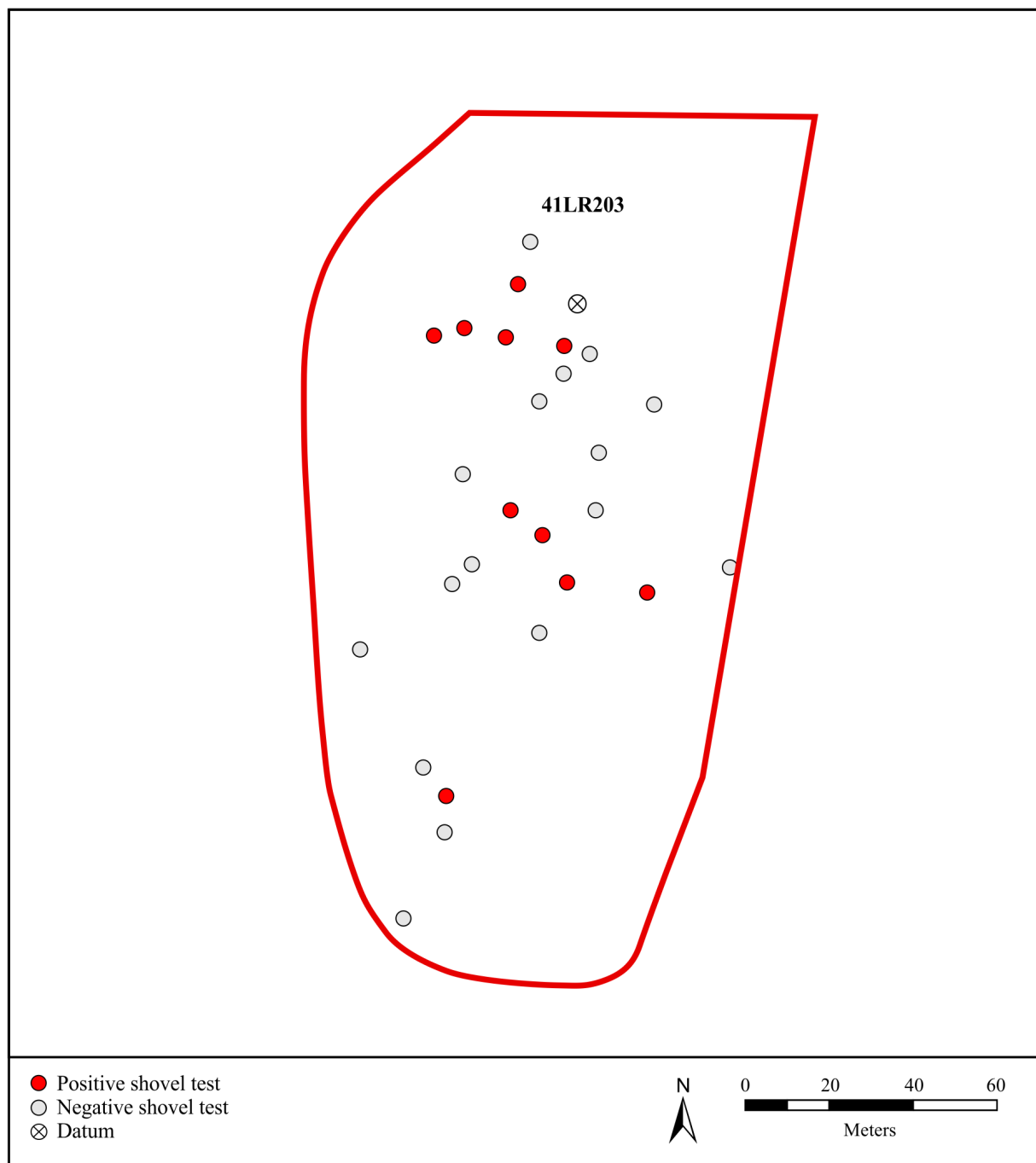


Figure 6-26. Site map of 41LR203 showing previous work by CAR (Lyle et al. 2001: Figure 8-6).

Current Investigation

CAR visited site 41LR203 in May of 2021. The location was recorded with a GPS. The site location is certain given that the site abuts the northeastern boundary of the facility marked by fences. Landscape is an open field and at the time was inundated with water. Numerous vehicle ruts were observed during the survey. A service road is 300 m to the south of the site. CAR did not excavate any shovel tests

on 41LR203 due to the certainty of the location and the adequate distribution of previously excavated shovel test.

CAR excavated three 1-x-1 m test units on August 14 and 15, 2021 at site 41LR203. Figure 6-27 shows the locations of the three test units. Excavated soils ranged in color from yellowish brown to very pale brown (10YR5/4 to 10YR7/3). Sediment was a loose to soft sand. All units terminated at clay. CAR screened 1.45 m³ of excavated sediments. Table 6-11 provides a summary of the excavation effort.

The three units produced four pieces of debitage and charcoal. Table 6-12 summarizes the artifacts recovered from 41LR203 by unit and level. Magnetic soil

susceptibility samples were also collected from each of the units. The results of the MSS analysis are discussed in Chapter 8.

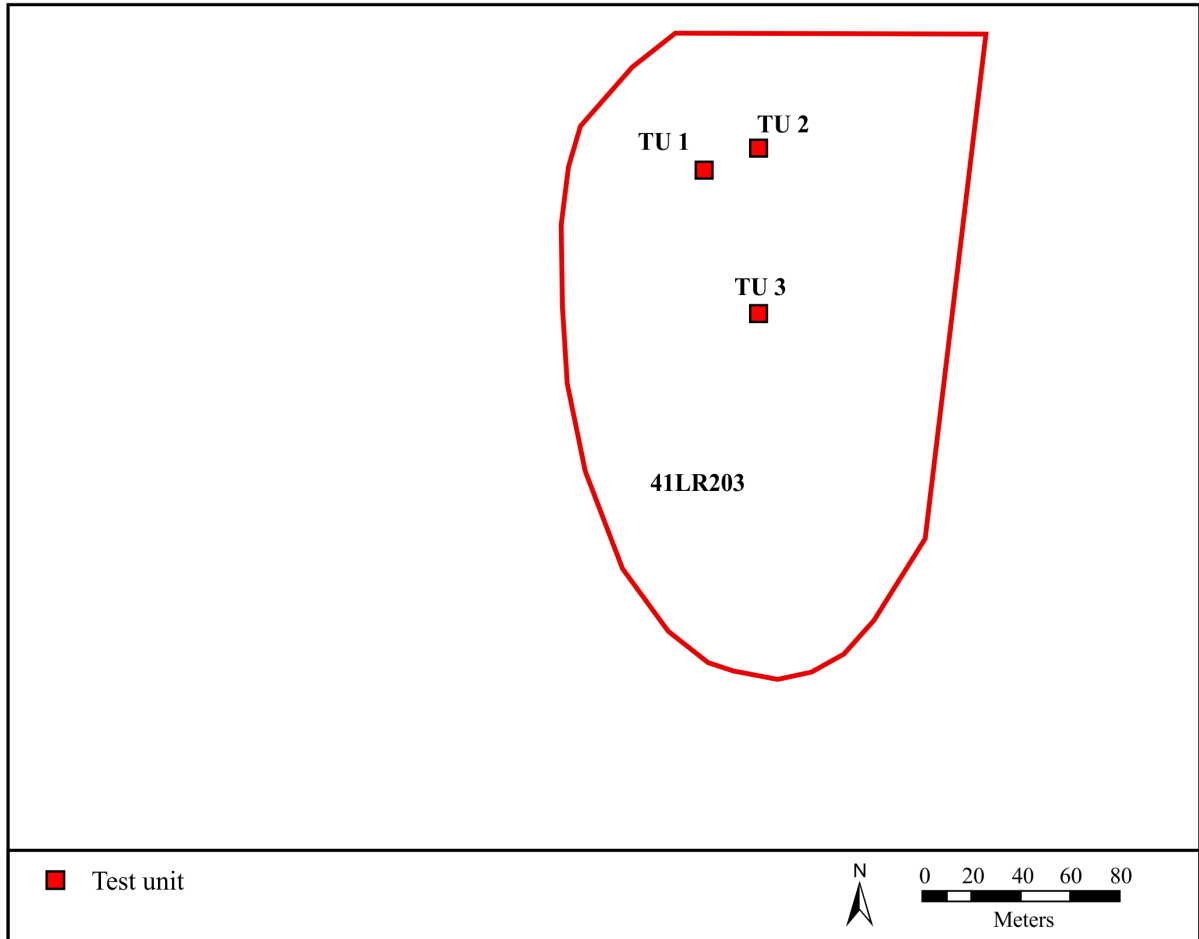


Figure 6-27. The location of test units excavated on 41LR203. The site boundary shown here is from the TMD geodatabase and different from the one in Figure 6-26.

Table 6-11. Summary of Test Units Excavations at 41LR203

Test Unit	Number of Levels Excavated	Maximum Terminal Depth Below Datum (cmbd) and Soil Type	Excavated Sediments (m ³)
1	5	56 (clay)	0.46
2	5	60 (clay)	0.50
3	5	50 (clay)	0.49

Table 6-12. Summary of Artifacts by Unit and Level from 41LR203

Level	Test Unit 1	Test Unit 2	Test Unit 3
1	null	null	null
2	null	debitage (1)	null
3	debitage (1)	debitage (1)	debitage (1); ¹⁴ C
4	null	null	null
5	null	null	null

41LR226

Site 41LR226 was recorded in 1999 by CAR archaeologists. The site is approximately 27,450 m² in size (Lyle et al. 2001:94). Site 41LR226 is located on an upland in the north central portion of the base and overlooks Pat Mayse Reservoir. An intermittent drainage is on the west site of the boundary. The site's vegetation is mixed oak, juniper, and hickory trees with brush and briar (Figure 6-28). The upland portion of the site falls within the Whakana fine sandy loam, 1-5% slopes and the finger slopes in the Woodtell loam, 5-12% slopes. Both groups are alfisols. The site ranges in elevation from approximately 150 to 160 m AMSL.

Background

Twenty-seven shovels test were excavated to define site 41LR226. Five shovels were positive recovering 15 artifacts (Figure 6-29). Eleven artifacts were found in a single shovel test (ST A-28) in the north central portion of the site. Each of the remaining four shovels test recovered a single

artifact (Lyle et al. 2001:Table D-21). Five ceramics were found with four of these in ST A-28 (Lyle et al. 2001:Table D-21). Four of the ceramics are plain ware with one sherd having a single engraved line (Lyle et al. 2001:95). The site is assigned to the Caddo period based on the decorated ceramics, but the temporal period could not be refined further. There were five pieces of debitage of coarse-grained quartzite (n=2), gray chert (n=1), and red claystone/siltstone (n=1; Lyle et al. 2001:95). Two heat spalls and four pieces of fire-cracked rock (weight=36 g) were also found during shovel testing (Lyle et al. 2001:95). Lyle and colleagues (2001:62) recovered artifacts to 80 cm below surface.

Current Investigation

CAR visited site 41LR226 in May of 2021. The site datum was not located. The north central portion of the site containing ST A-28 was recorded with a GPS. The site location is presumed accurate based on the topography and the presence of the north and south fences marking the base boundary.



Figure 6-28. View to the north of 41LR226 towards the base boundary.

On July 17, 2021, CAR excavated ten shovel tests to help determine the location of future test units (Figure 6-30). Shovel tests were excavated to 40 to 80 cmbs with an average depth of 60 cmbs. No artifacts were found in any of the shovel tests.

CAR excavated four 1-x-1 m test units on August 12 and 13, 2021 on site 41LR226. Figure 6-30 shows the locations of the four test units. Excavated soils ranged in color from light yellowish brown to very pale brown (10YR6/4 to 10YR7/3 and 7/4). Sediment was loose to soft sand.

All units terminated at clay. CAR screened 1.35 m³ of excavated sediments. Table 6-13 provides a summary of the excavation effort.

The four units produced six fragments of undecorated ceramics (four fragments refitted into one piece), five pieces of debitage, burned rock weight 2.19 g, and charcoal. Table 6-14 summarizes the artifacts recovered from 41LR226 by unit and level. Magnetic soil susceptibility samples were also collected from each of the units. The results of the MSS analysis are discussed in Chapter 8.

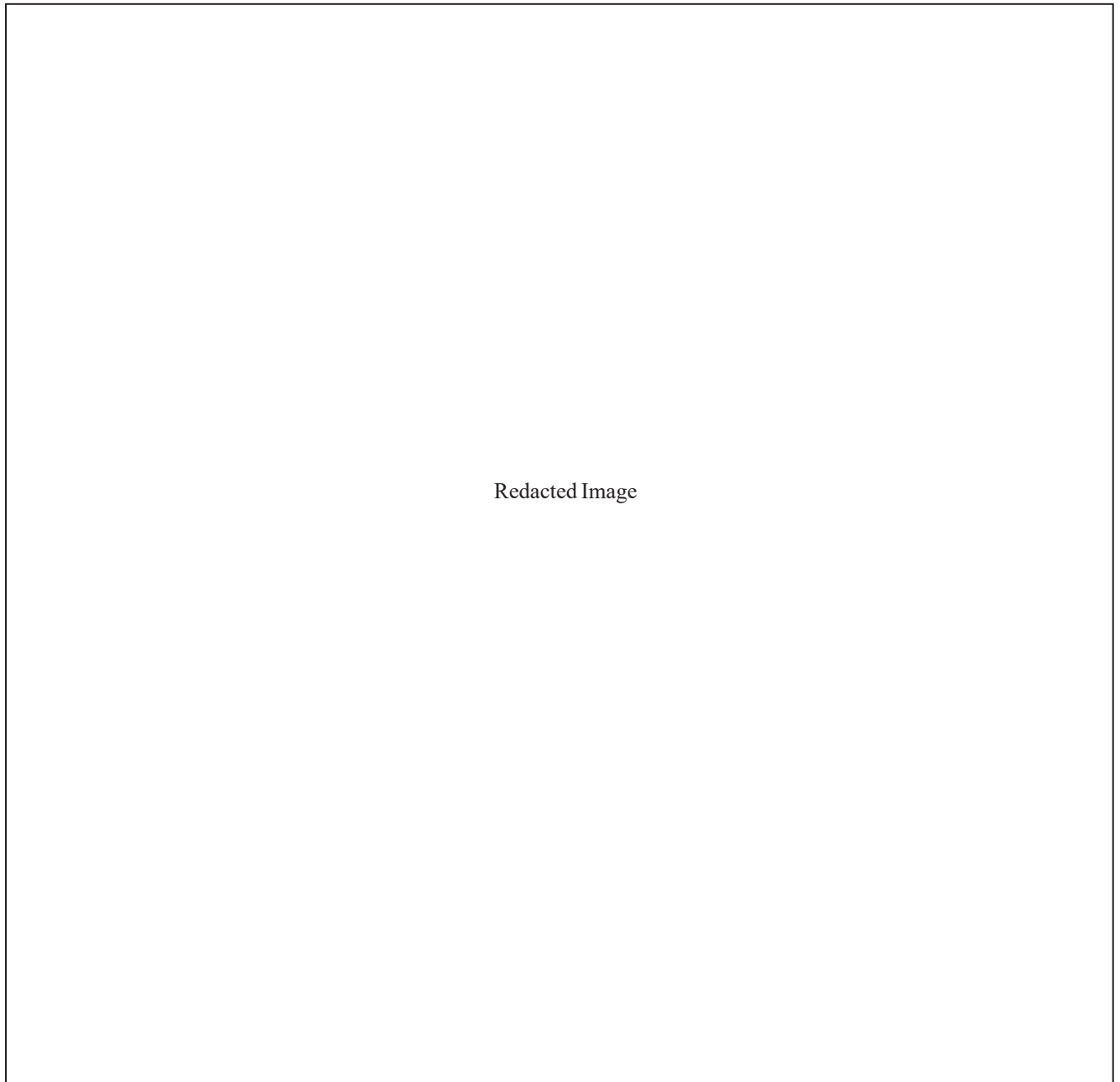


Figure 6-29. Site map of 41LR226 showing previous work by CAR (Lyle et al. 2001: Figure 8-14). Shovel test A-28 is identified.

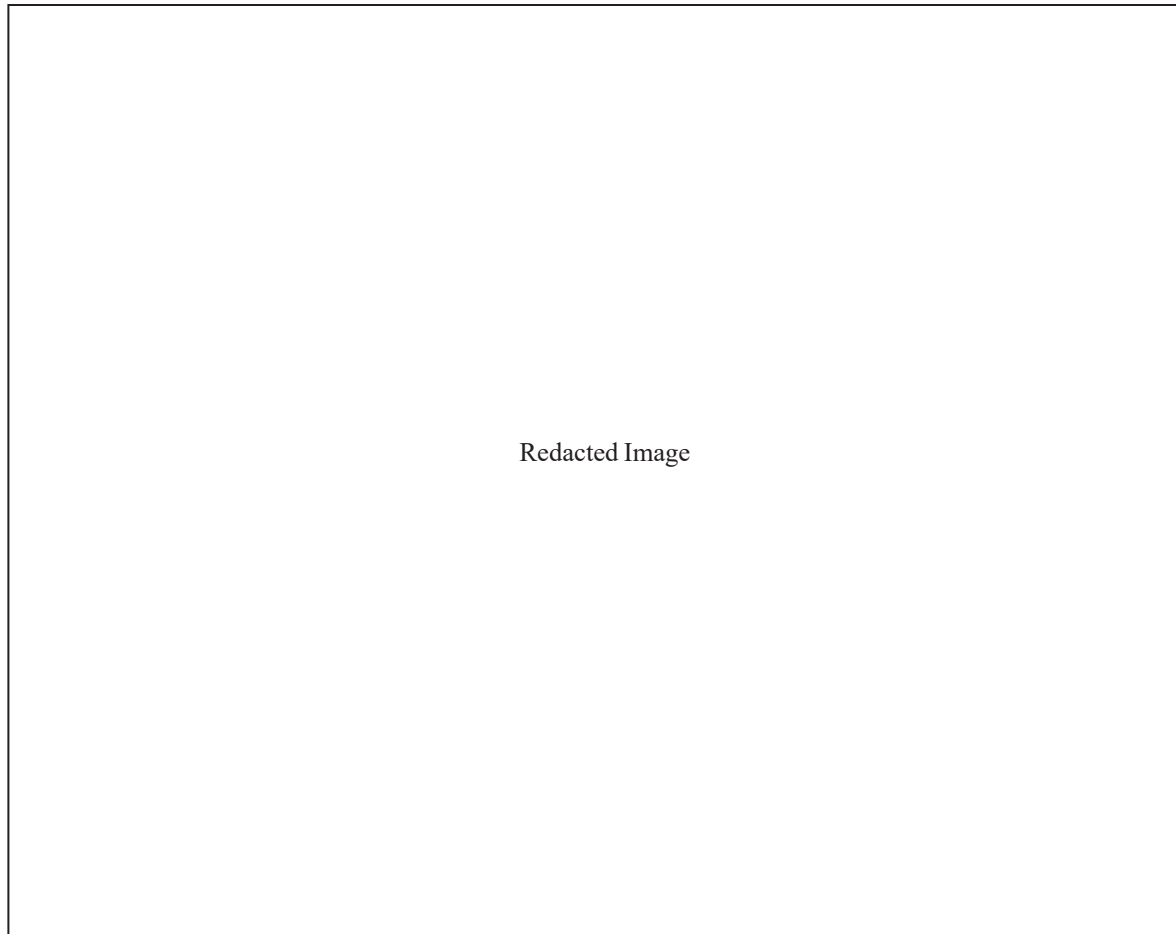


Figure 6-30. The locations of shovel tests and test units excavated by CAR during the current investigation.

Table 6-13. Summary of Test Units Excavations at 41LR226

Test Unit	Number of Levels Excavated	Maximum Terminal Depth below Datum (cmbd) and Soil Type	Excavated Sediments (m ³)
1	3	39 (clay)	0.29
2	5	50 (clay)	0.40
3	3	40 (clay)	0.30
4	5	46 (clay)	0.36

Table 6-14. Summary of Artifacts by Unit and Level from 41LR226

Level	Test Unit 1	Test Unit 2	Test Unit 3	Test Unit 4
1	ceramics (5 in total-4 of which refitted)	null	null	null
2	null	debitage (1); burned rock (0.65 g)	null	debitage (1)
3	null	burned rock (0.16 g)	null	debitage (1); burned rock (0.52 g); ¹⁴ C
4	not excavated	ceramics (1);debitage (1);	not excavated	debitage (1)
5	not excavated	burned rock (0.36 g)	not excavated	null

41LR238

Site 41LR238 was recorded in 1999 by CAR archaeologists as covering 23,575 m² in size (Lyle et al. 2001:99). The site is located on an upland to the east and on the west a series of finger slopes extending into an intermittent drainage. Vegetation is mixed oak and pine with grassy open areas (Figure 6-31). The site falls primarily in the Bernalso fine sandy loam, 1-3% slopes and the site periphery in the Woodtell loam, 5-12% slopes. Both groups are alfisols. The elevation ranges from roughly 154 to 148 m AMSL.

Background

Twenty-seven shovel tests were excavated to define site 41LR238. Five shovel tests were positive (Figure 6-32). Two of those five contained military bullets. Three prehistoric artifacts were recovered from three shovel tests. The distal portion of a chert, corner-notched dart point was found in ST 62-8. A bifacial drill of brown chert was found in another shovel test (ST CC-6). The final artifact is a large piece of burned clay approximately 52 cm³ found in ST CC-4. Lyle and colleagues (2001:99)

suggest that it may be a remnant from a hearth or cooking feature. Prehistoric artifacts were found to 60 cm below surface (Lyle et al. 2001:99).

Current Investigation

CAR visited site 41LR238 in May of 2021. CAR did not find the original site datum. The central portion containing the datum of the site was shot in with a GPS and flagged. Based on the site map and landform, the site appears to be in the correct location. The site was relatively open with mature oak and pine trees. A service road is 940 m to the east of the site.

CAR excavated two 1-x-1 m test units on May 3 and 4, 2022 on site 41LR226. Figure 6-33 shows the locations of the two test units. Excavated soils ranged in color from yellowish brown to light yellowish brown (10YR5/4 to 10YR6/4). Sediment was soft sand. All units were terminated due to high water levels. CAR screened 0.65 m³ of sediment. Table 6-15 provides a summary of the excavation effort. No artifacts were found in either of the test units. No MSS samples were collected due to the saturated soils.



Figure 6-31. View to the northwest of 41LR238 and towards to Unit 1.

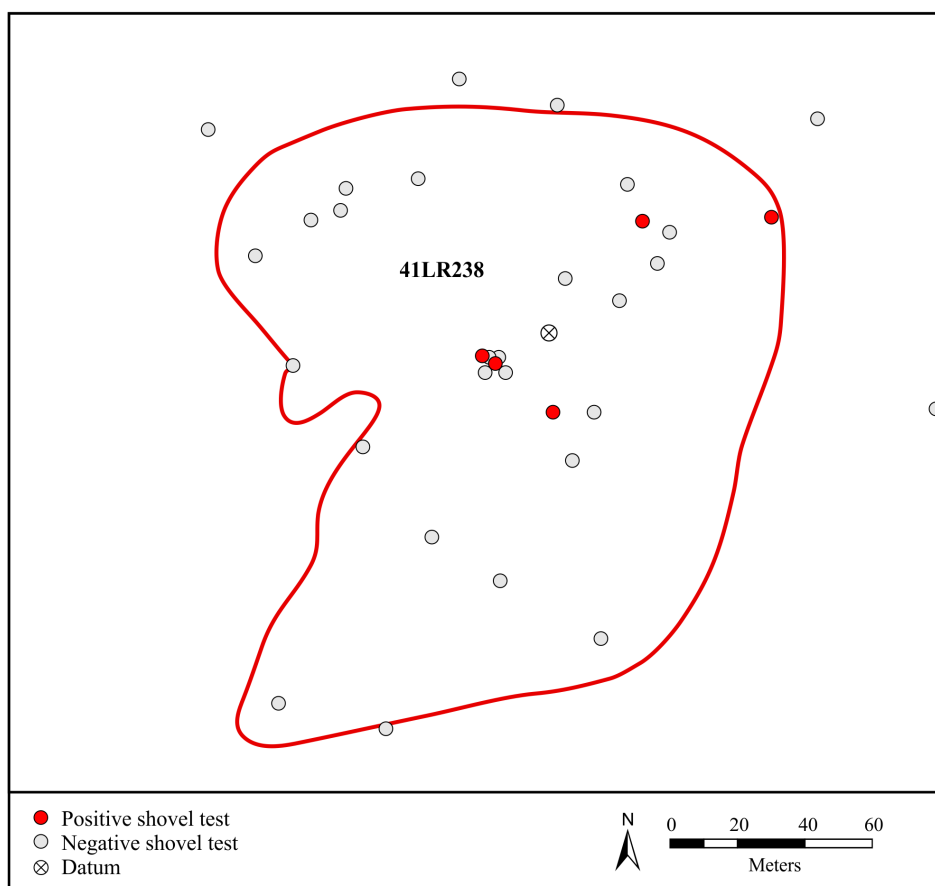


Figure 6-32. Site map of 41LR238 showing previous work by CAR (Lyle et al. 2001: Figure 8-16).

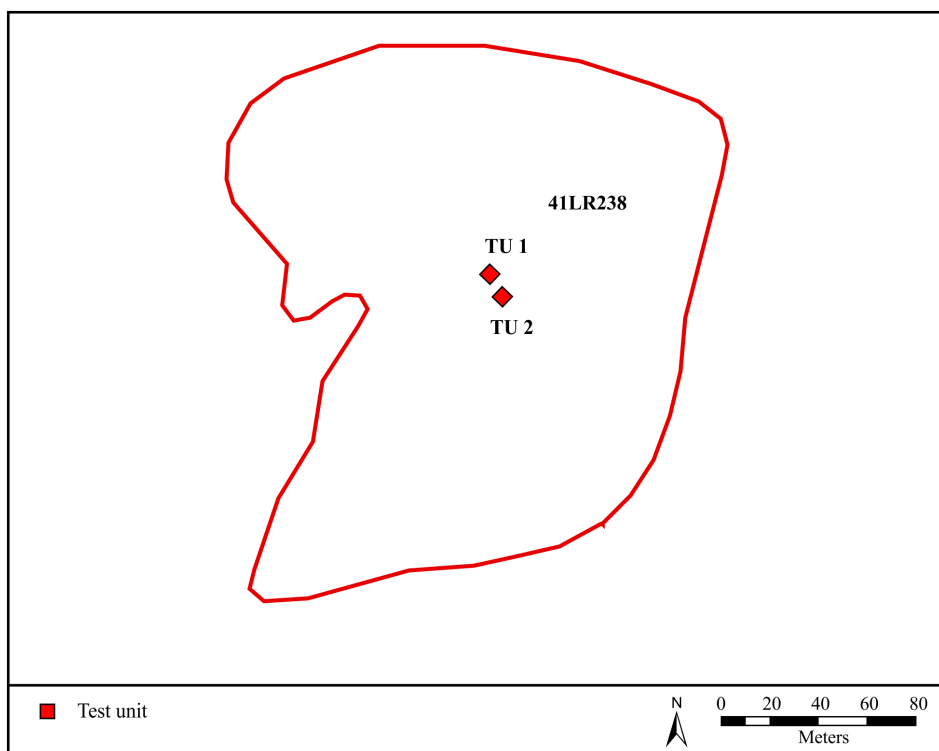


Figure 6-33. Location of two test units excavated on 41LR238.

Table 6-15. Summary of Test Units Excavations at 41LR238

Test Unit	Number of Levels Excavated	Maximum Terminal Depth Below Datum (cmbd) and Soil Type	Excavated Sediments (m ³)
1	5	50 (water)	0.40
2	3	35 (water)	0.25

Preliminary Investigation of 41LR184 and 41LR213

As discussed earlier in Chapter 5 and the beginning of this chapter, CAR revisited 12 sites during the initial reconnaissance. In addition to the ten sites previously discussed, sites 41LR184 and 41LR213 were revisited. Site 41LR213 was also shovel tested during this investigation to help place future test units.

41LR184 Background and Current Investigation

Site 41LR184 was recorded in 1999 by CAR archaeologists as 5751 m² in size (Lyle et al. 2001:62). The site is on a ridge approximately 1300 m south of what was Sanders Creek. It now overlooks Pat Mayse Reservoir. The site is heavily wooded and contains moderate to dense undergrowth (Figure 6-34). It falls within the Woodtell loam soil, 5-12% slopes alfisols. The site ranges in elevation from approximately 148 to 152 m AMSL.



Figure 6-34. View to the north from 41LR184 in the vicinity of positive shovel tests excavated by Lyle et al. (2001).

As shown in Figure 6-35, 41LR184 was defined with ten shovel tests, seven of which were positive (Lyle et al. 2001:80). These artifacts included a biface, three cores, 89 flakes, and approximately 500 g of FCR. Approximately 90% of the artifacts were found in three shovel tests (STs 4-2, 4-3, and A-15; Lyle et al. 2001:80). The biface was made from heat-treated coarse-grained quartzite, as were two of the cores (Lyle et al. 2001:81). The third core was made from Ogallala quartzite (Lyle et al. 2001:81). The flake material was diverse being dominated by coarse-grained quartzite, followed by Ogallala quartzite, novaculite, claystone/siltstone, multiple

varieties of chert, and petrified wood. (Lyle et al. 2001:81). Lyle and colleagues (2001:80) recovered artifacts extending to a depth of 80 cm below surface.

CAR revisited site 41LR184 in May of 2021. The presumed site location was recorded with a GPS and flagged. The site was relocated based on north and west fence features shown on the site map, as well as the landform. It sits in a relatively open wooded area. A service road is 400 m to the east. No further work was done on this site. There is no change in the undetermined eligibility status.

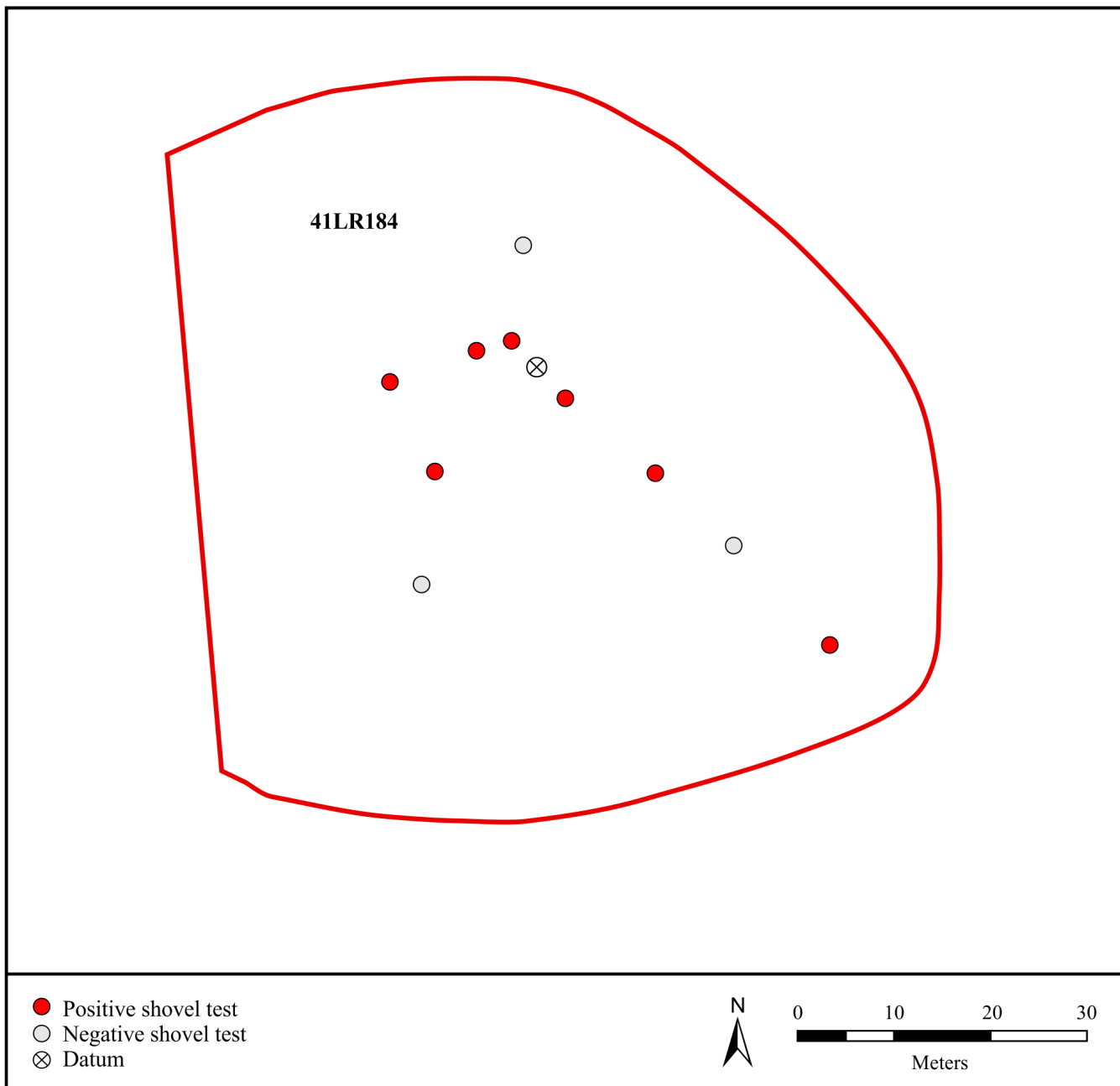


Figure 6-35. Site map of 41LR184 showing previous work by CAR (Lyle et al. 2001: Figure 8-2).

41LR213 Background and Current Investigation

Site 41LR213 was recorded in 1999 by CAR archaeologists as approximately 18,653 m² in size (Lyle et al. 2001:84). The site is on an upland with steep slopes and a large creek on the east and southeast portions of the site. The site vegetation is composed of oak and pine tree mix with little to no undergrowth (Figure 6-36). The eastern two-thirds of the site falls within the Freestone-Hicota complex, 0-3% slopes and the remaining southwestern portion in the Woodtell loam soil, 5-12% slopes. Both soil classes alfisols. The site ranges in elevation from approximately 152 to 142 m AMSL.

Site 41LR213 was defined by 21 shovel tests, five of which were positive (Figure 6-37). These artifacts included a Gary dart point, seven flakes, and a piece of fire-cracked rock (Lyle et al. 2001:89). The Gary point was made from chert likely derived from Red River chert. The site is assigned to the Early Ceramic or Woodland period based on the associated Gary point. The flakes were made from coarse-grained quartzite (n=3), petrified wood (n=2), chert (n=1), and novaculite (n=1; Lyle et al. 2001:89). Lyle and colleagues (2001:89) recovered artifacts extending to a depth of 60 cm below surface.

CAR revisited site 41LR213 in May of 2021 but did not find the original site datum. A fallen military sign reported in the Lyle et al. (2001) report was observed in the southern portion of the site. This area of the site containing the artifact concentration and sign was recorded with a GPS and flagged. The site is situated along a finger ridge and extends to the northeast with drainages along the south and east sides of the site. The landform and drainages were observed during the current survey. The site is in a relatively open area with an over story of oak, elm and pine trees. A service road is 400 m to the northeast of the site

CAR archaeologists returned to 41LR213 on July 17-18, 2021 and excavated seven shovel tests (Figure 6-38). Shovel tests were placed in the northern portion of the site to investigate a positive shovel test, the central portion of the site that was not shovel tested, and in the southern portion of the site. Shovel tests were excavated to 30 to 80 cmbs with an average depth of 58 cmbs. The two shovel tests (44 and 45) on the southern portion were shallow at 30 and 39 cmbs, respectively. Those shovel tests in the central portion were deeper ranging from 70 to 80 cmbs. Two of the three shovel tests in the northern shovel test were deep at 80 cmbs with one excavated to 40 cmbs. No artifacts were found in any of the shovel tests.



Figure 6-36. View to the northeast from the southern portion of 41LR213.

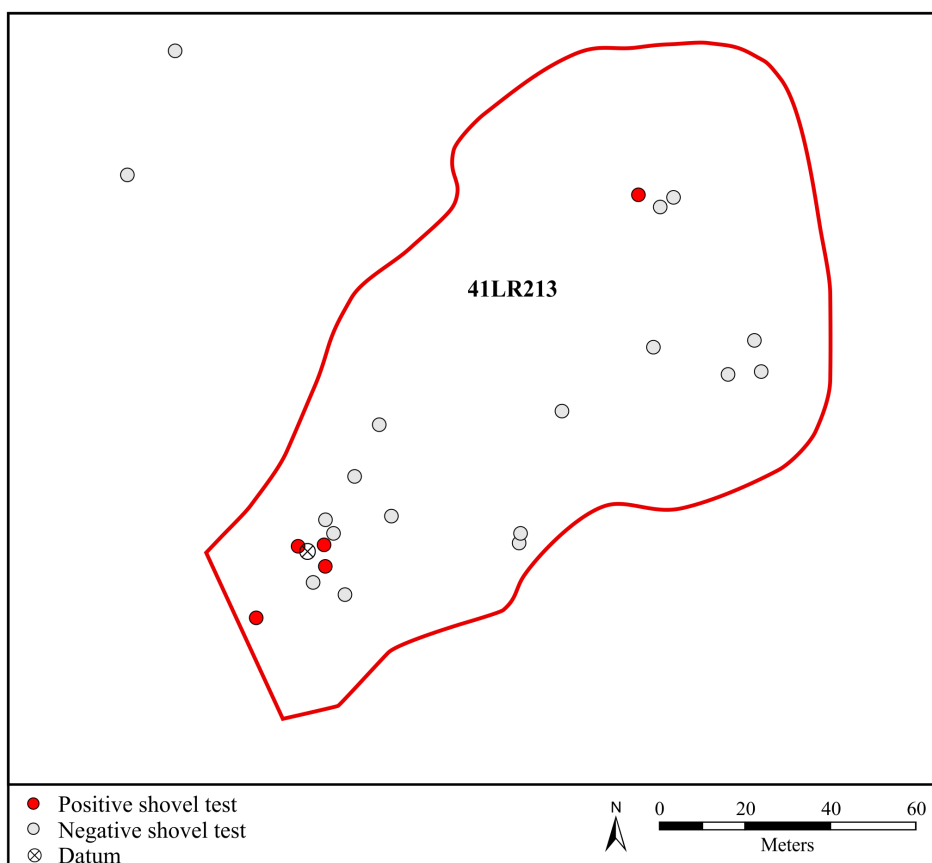


Figure 6-37. Site map of 41LR213 showing previous work by CAR (Lyle et al. 2001: Figure 8-11).

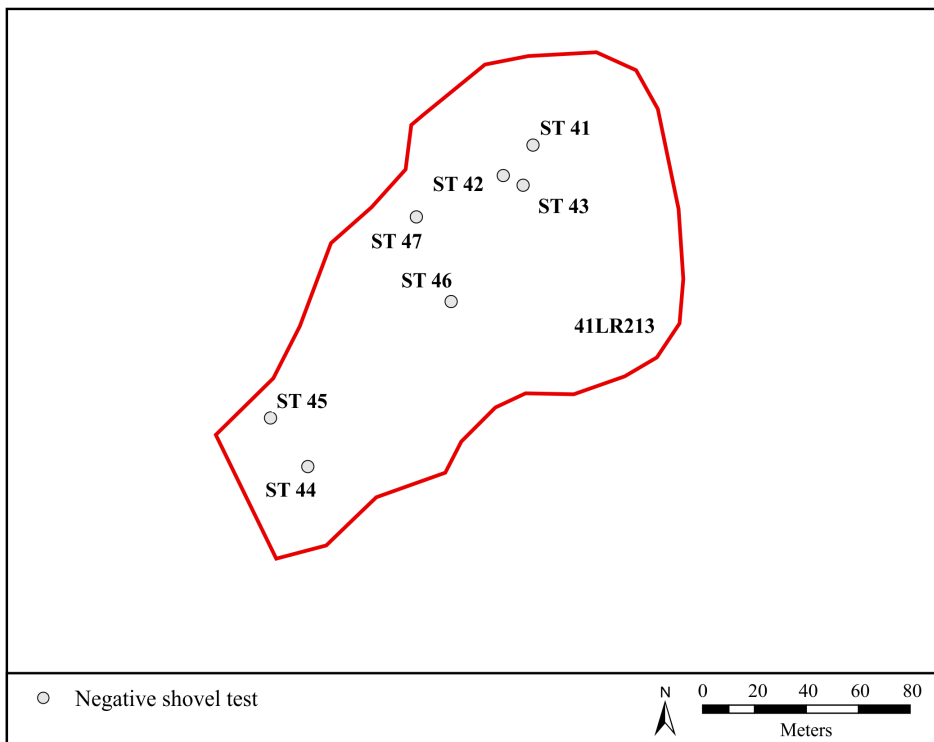


Figure 6-38. Site map of 41LR213 showing shovel test excavated during the current investigation.

Summary

This chapter summarized the findings from current and past investigations of Maxey sites. During the current investigation, CAR archaeologists excavated 23 test units on ten sites and screened 10.1 m³ of sediment during NRHP eligibility testing. Overall, the quantity of artifacts from nine of the ten tested sites is low. The exception is 41LR159. Several sites returned no artifacts from either shovel tests or test units including 41LR165, 41LR175, and 41LR238. From both shovel tests and test units CAR collected four bifaces, a uniface, two cores, two edge modified flakes, five native ceramics, 165 pieces of debitage, 2.45 kg of non-feature burned rock, burned faunal bone, and a quartzite

crystal, as well as historic artifacts including a 1903 U.S. penny, glass fragments, and bullet. Two burned rock features were identified, one at 41LR159 and the second at 41LR161. Radiocarbon samples were submitted from both features to Direct AMS for dating. In addition, CAR redefined the boundaries of four sites, 41LR154, 41LR159, 41LR161, and 41LR162 reflecting findings from the current investigation. CAR revisited sites 41LR184 and 41LR213 with seven shovel tests excavated on 41LR213. No shovel tests were excavated on 41LR184. CAR did not excavate any test units on either of these sites and their NRHP eligibility status remains to be determined. Table 6-16 summarizes levels of effort and results from current and previous investigations at the twelve sites.

Table 6-16. Summary of the Previous and Current Investigations

Site	Previous Investigations		Current Investigations		
	Number of Shovel Tests	Artifacts	Level of Work	Features	Total Artifacts and Counts
41LR154	1	surface-debitage (5); historic ceramic, glass fragment (2) subsurface-debitage (1); glass fragment (2)	revisit; shovel tests (11); test unit (1)	0	subsurface-debitage (2); burned rock (0.48 g); 1903 U.S. penny, glass fragments (4); metal-possible stove fragment
41LR159	6	surface-debitage (8); subsurface-debitage (9)	revisit; shovel tests (29); test units (4)	1	subsurface-burned rock feature; bifaces (4); uniface; edge modified flake; core; debitage (132); non-feature burned rock (2400 g); burned faunal bone; quartz crystal; ¹⁴ C
41LR161	5	subsurface-core; debitage (5)	revisit; shovel tests (10); test units (3)	1	Subsurface-burned rock feature; edge modified flake; core; debitage (13); non-feature burned rock (178.9 g); unidentified metal; ¹⁴ C
41LR162	4	subsurface-debitage (5); burned rock (0.03 g)	revisit; shovel tests (20); test units (2)	0	subsurface-debitage (5); non-feature burned rock (2.57 g); bullet casing
41LR165	3	subsurface-debitage (4)	revisit; shovel tests (6); test units (2)	0	no artifacts
41LR175	1	subsurface-debitage (4)	revisit; test units (1)	0	no artifacts
41LR177	3	subsurface-debitage (3)	revisit; test units (1)	0	subsurface-debitage (4); unidentified metal
41LR184	7	surface-burned rock (121 g) subsurface-biface; cores (3); debitage (89); burned rock (499.1 g); heat spall (3); ocher	revisit only	n/a	n/a
41LR203	10	subsurface-debitage (7); heat spall (3); burned rock (95.3 g); burned nutshell	test units (3)	0	subsurface-debitage (4); ¹⁴ C
41LR213	5	subsurface-Gary dart point; debitage (6); burned rock (131 g);	revisit; shovel tests (7)	n/a	no artifacts in shovel tests
41LR226	5	subsurface-native ceramics (5); debitage (7); heat spall (3); burned rock (95.3 g); burned nutshell	revisit; shovel tests (10); test units (4)	0	subsurface-native ceramics (6); debitage (5); burned rock (2.19 g)
41LR238	5	subsurface-non- diagnostic dart point; biface “drill”; burned clay	revisit; test units (2)	0	no artifacts

This page intentionally left blank.

Chapter 7: Chronological Potential

Leonard Kemp

This chapter assesses a site's potential to contribute to the chronological understanding of prehistoric occupations at Camp Maxey. As summarized in Chapter 4, 35 of the 138 sites have either a prehistoric or a mix deposit of prehistoric and historic components. However, only three of the thirty-six tested sites have been radiocarbon dated with eight assays. This chapter presents the results of temporally diagnostic artifacts as well as the radiocarbon results from the two features found during the current testing.

Temporal Diagnostics

During the current investigation, six fragments of Caddo ceramics were found on 41LR226 with four of those fragments refitting to one piece. No other diagnostics were found on any of the other nine sites with the exception of a 1903 U.S. penny at 41LR154. A small number of temporal diagnostics were found during a previous investigation (Lyle et al. 2001) on sites 41LR226 and 41LR238. Ceramics (n=5) were found during the previous shovel testing of 41LR226. One of the sherds was engraved with a line designating an affiliation with the prehistoric Caddo (Lyle et al. 2001:95). Lyle et al. (2001) also found a distal portion of a non-diagnostic corner notched dart point on 41LR238 which they date to the Late Archaic period. It was made from locally sourced Red River chert (Lyle et al. 2001:99).

Radiocarbon Dates and Potential Radiocarbon Samples

Charcoal was found on four of the ten investigated sites. These sites are 41LR159, 41LR161, 41LR203, and

41LR226. Table 7-1 shows the presence of charcoal found at and below Level 4 (approximately 30 cmbs) by site and unit. We make the assumption that material in the upper three levels are likely out of context due to bioturbation based on field observations and past experience on Sandy Mantle sites. Potentially, charcoal samples at and below this depth would be less likely to be disturbed by modern bioturbation. Three sites (41LR159, 41LR161, and 41LR226) have charcoal at and below the depth of Level 3. In addition, a piece of burned faunal bone was found during shovel testing at 41LR159 in Level 1 (0-20 cmbs).

Two features were found during the current testing with one at 41LR159 and another at 41LR161. Charcoal was recovered from both features and a sample from each was submitted to Direct-AMS (D-AMS) for radiocarbon dating. The D-AMS report is found in Appendix A. The radiocarbon dates were calibrated using the OxCal, version 4.4 online program and the calibration curve IntCal 2020 for a 2 σ value (Bronk Ramsey 2021) Table 7-2 presents the results of this analysis. The median radiocarbon date for 41LR159 is cal AD 1003. The calibration for the radiocarbon sample from Feature 1 of 41LR159 is shown in Figure 7-1. This date places 41LR159 in the middle Formative period using the Middle Red River chronology (Bruseh 1998). The calibration for the radiocarbon sample from Feature 1 of 41LR161 is shown in Figure 7-2. The sample dates to cal BP 418 to 150 (AD 1533 to 1800). The calibration suggests that at 61.8% probability the sample dates to cal AD 1636 to 1676 and 32.3% probability that it dates to cal AD 1765 to 1800. Assuming the higher probability, the sample dates during the transition from

Table 7-1. Presence of Charcoal by Site and Units at and below Level 4

Site 41LR...	TU 1	TU 2	TU 3	TU 4
159	none	none	yes	yes
161	none	yes	none	
203	none	none	yes	
226	none	none	none	yes

Table 7-2. Radiocarbon Results from 41LR159 and 41LR161

D-AMS Assay Number	Site	Provenience	Material	Radiocarbon Years Before Present	Std Error	Calibrated Date Range: cal BP and cal AD at 2- σ
D-AMS 047725	41LR159	Feature 1	Charcoal	1056	23	cal BP 1052 to 921; cal AD 898 to 1029
D-AMS 047726	41LR161	Feature 1	Charcoal	239	22	cal BP 418 to 150; cal AD 1533 to 1800

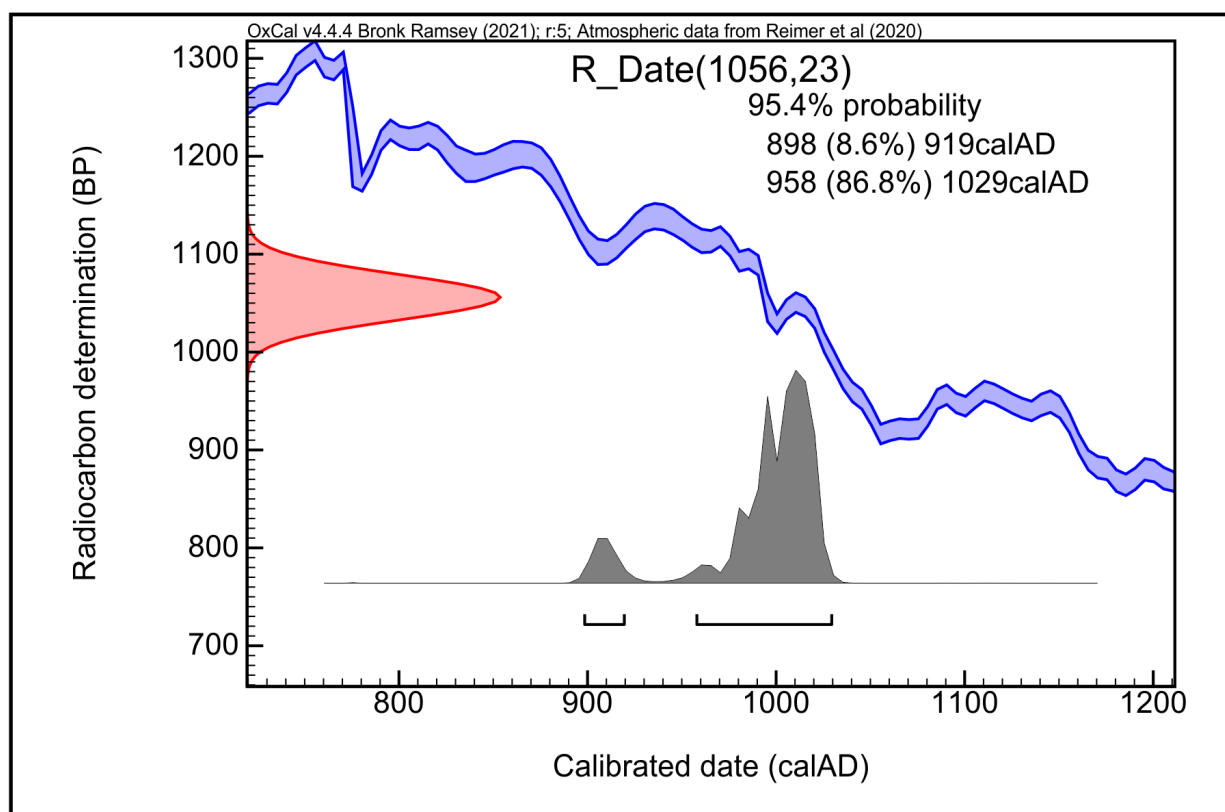


Figure 7-1. The calibrated radiocarbon sample from Feature 1 of 41LR159.

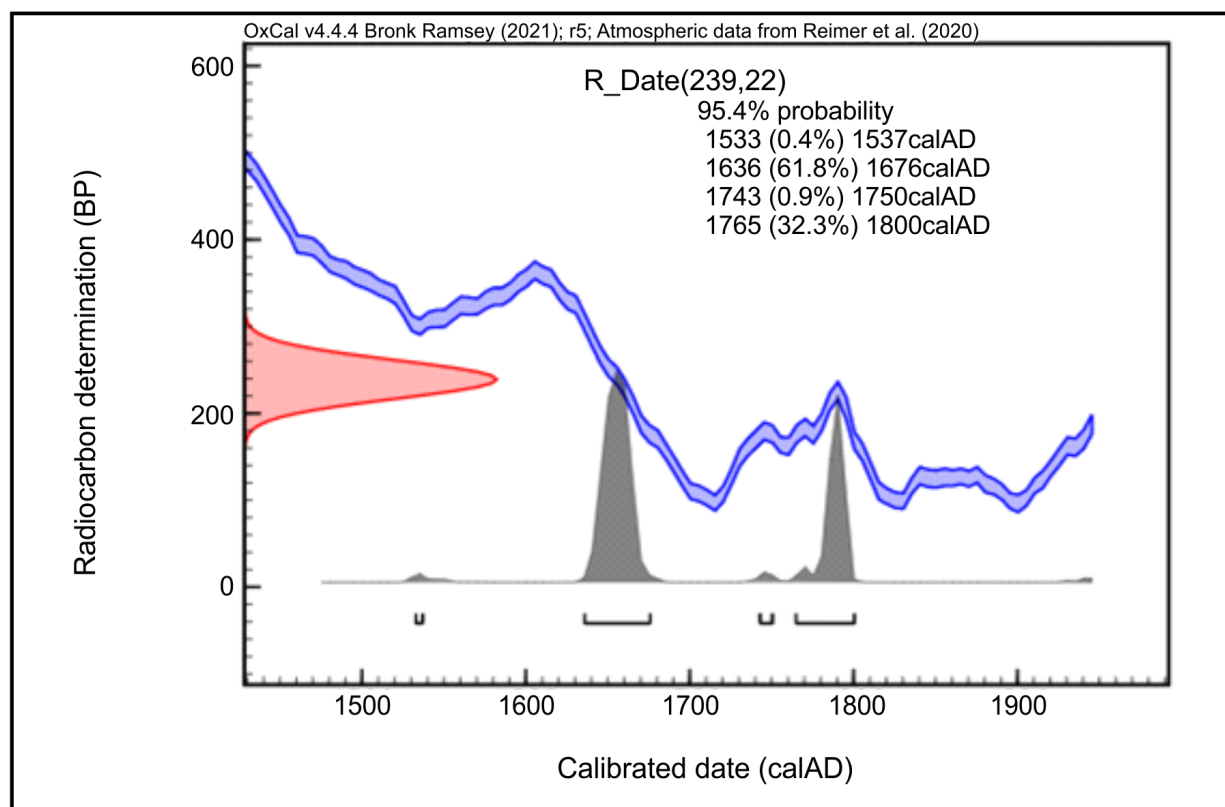


Figure 7-2. The calibrated radiocarbon sample from Feature 1 of 41LR161.

the late McCurtain Phase to the beginning of the Historic Caddo period (Bruseh 1998).

Summary

Table 7-3 summarizes the chronological data present for the ten tested Maxey sites. Only three sites during either this or previous investigations contain temporal diagnostics. These sites are 41LR154, which contained a 1903 U.S. penny,

41LR226, that contained native prehistoric ceramics, and 41LR238 that contained a Late Archaic corner- notched dart point. Charcoal was recorded at four sites, 41LR159, 41LR161, 41LR203, and 41LR226. However, at only two sites, 41LR159 and 41LR161, was the charcoal associated with features. Both features produced radiocarbon dates. CAR suggests that three sites, 41LR159, 41LR161, and 41LR226 have moderate chronological potential. The remaining seven sites have low chronological potential.

Table 7-3. Chronological Potential of the Ten Tested Maxey Sites

Site (41LR...)	Diagnostics Recovered	Charcoal	Bone	Number of Radiocarbon Dates	Chronological Potential
154	yes	no	no	0	low
159	no	yes	yes	1	moderate
161	no	yes	no	1	moderate
162	no	no	no	0	low
165	no	no	no	0	low
175	no	no	no	0	low
177	no	no	no	0	low
203	no	yes	no	0	low
226	yes	yes	no	0	moderate
238	yes	no	no	0	low

This page intentionally left blank.

Chapter 8: Site Content

Jonathan Paige

The second eligibility criterion concerns the assemblage of the seven tested sites that contained artifacts. These sites are 41LR154, 41LR159, 41LR161, 41LR162, 41LR177, 41LR203, and 41LR226. Lithics were the only prehistoric artifacts recovered from the seven sites with the exception of ceramics from 41LR226. The latter was discussed in Chapter 7. This chapter focuses first on providing a brief overview of the nature of assemblages and how lithic raw material was used on Camp Maxey and summarizes the finding on each of the seven sites. It then focuses on 41LR159 which had the largest and most diverse lithic assemblage. The chapter then focuses on a modelling approach to measure how much of the raw material reduction sequences is likely present on 41LR159. The last section summarizes the assemblage of the ten tested sites and their potential to add to our understanding of the past.

Overview

The most readily available tool-stones in the Camp Maxey area are found in the form of quartzite, petrified wood, and brown/tan gravels in the uplands area (Lyle et al. 2001). Further north, on the Red River Terrace, jasper and mudstone can be found and the red river deposits novaculite, chert, and shale into the Muddy Bottom Creek drainage. The relative abundance of quartzite in the area may be, in part, why tools like bifaces, were often manufactured on quartzite. Prior work has highlighted that coarse grained quartzites were often heat treated prior to being reduced to manufacture dart points, as was the case at 41LR190. 41LR190 also had some evidence of earlier stage biface reduction of quartzite nodules, and 41LR194 had similarly early evidence of quartzite reduction relative to other raw materials like chert, which showed later stage reduction (Mahoney et al. 2002).

In the Camp Maxey area, chert tools, cores and bifaces tend to be larger than the immediately available chert gravels, which tend to be no greater than 60-80 mm in maximum dimension (Lyle et al. 2001:6). This suggests that larger raw chert cobbles, as well as cores and tools, were brought in from elsewhere. For example, at 41LR190 a complete chert biface (55-x-30-x-14 mm) was recovered, and Mahoney et al. (2002:20) note that it was deposited in the middle of its reduction sequence. At 41LR194, a chert core with seven removals was recovered from TU 2, Level 11, with a maximum dimension of 37 mm. Cherts, like quartzite, were also heat treated, though the practice was less frequent, and likely not as necessary to aid in the workability of the raw material (Mahoney et al. 2002:22).

In other areas, groups who rely on small rounded river pebbles as a raw material would often practice bipolar percussion, which is argued to be more efficient than free-hand when available raw materials are smaller gravels and pebbles (Horta et al. 2022; Pargeter et al. 2019). This avoids the problem of attempting to free-hand knap small artifacts, and is argued to be common adaptation to raw material poor environments, or may serve as a method of extending the use lives of already heavily reduced pieces. Bipolar percussion tends to be associated with flakes with bidirectional scar orientations on the dorsal surface, crushed platforms, and sheared bulbs of percussion (Eren et al. 2013; Hayden 1980; Shott 1989b, 1999). However, prior work at Camp Maxey has not identified the use of bipolar percussion (Greaves 2003; Lyle et al. 2001; Mahoney 2001; Mahoney et al. 2002).

The Maxey Lithic Assemblage

One hundred and seventy-five artifacts (ca. 702 g), including flakes, cores, edge modified pieces, and flaking debris were recovered across the seven tested sites (Table 8-1). These materials were recovered across 80 shovel tests, and 16 1-x-1 meter test units. The total volume screened in the excavation units was roughly 10.22 m³. Site 41LR159 had 139 of the 175 items, with 41LR161 yielding 16 pieces of chipped stone. These two sites also had the highest densities, with 45.3 and 9.4 items recovered per m³. Most of the raw material represented by count and by weight is dominated by chert and quartzite (Figures 8-1 and 8-2).

Most of the pieces were small. The naturally occurring quartzite nodules in the area of Camp Maxey average 100 to 120 mm in their longest dimension (Lyle et al. 2001:6). For example, the burnt quartzite scatter in Feature 3, Test Unit 5 of 41LR190 consisted of nodules ranging between 30-70 mm in diameter (Mahoney et al. 2002:19), and chert nodules tend to be even smaller. This pattern is similar to that observed in the burnt rock recovered across the seven sites sampled in this project.

The relatively high frequency of quartzite and chert, the large amount of cortex that tends to be present, the relatively small size of flakes and edge modified pieces, and the stream-rolled nature of cortex all point to a strategy of procuring and knapping mostly locally available river gravels of small size. Despite it being a common strategy for reducing small stream rolled pebbles elsewhere no definitive evidence of bipolar percussion was identified. Some evidence of biface thinning

Table 8-1. Summary of Chipped Stone Across Sites Separated by Raw Material

Site (41LR...)	Flakes				Biface Thinning Flakes				Bifaces				Cores				Debris					
	Chert	Quartzite	Claystone/Sandstone	Total	Chert	Quartzite	Claystone/Sandstone	Total	Chert	Quartzite	Claystone/Sandstone	Total	Chert	Quartzite	Claystone/Sandstone	Total	Chert	Quartzite	Claystone/Sandstone	Quartz	Petrified Wood	Total
154	1	0	0	1	0	0	0	0	0	0	0	0	0	0	0	0	0	0	1	0	0	1
159	34	31	5	70	0	1	1	2	3	1	0	4	0	1	0	1	25	31	6	0	0	62
161	7	3	0	10	0	0	0	0	0	0	0	0	0	1	0	1	3	1	0	0	1	5
162	1	2	0	3	0	0	0	0	0	0	0	0	0	0	0	0	1	0	0	1	0	2
177	1	3	0	4	0	0	0	0	0	0	0	0	0	0	0	0	0	0	0	0	0	0
203	3	0	0	3	0	0	0	0	0	0	0	0	0	0	0	0	0	1	0	0	0	1
226	2	0	2	4	0	0	0	0	0	0	0	0	0	0	0	0	1	0	0	0	0	1

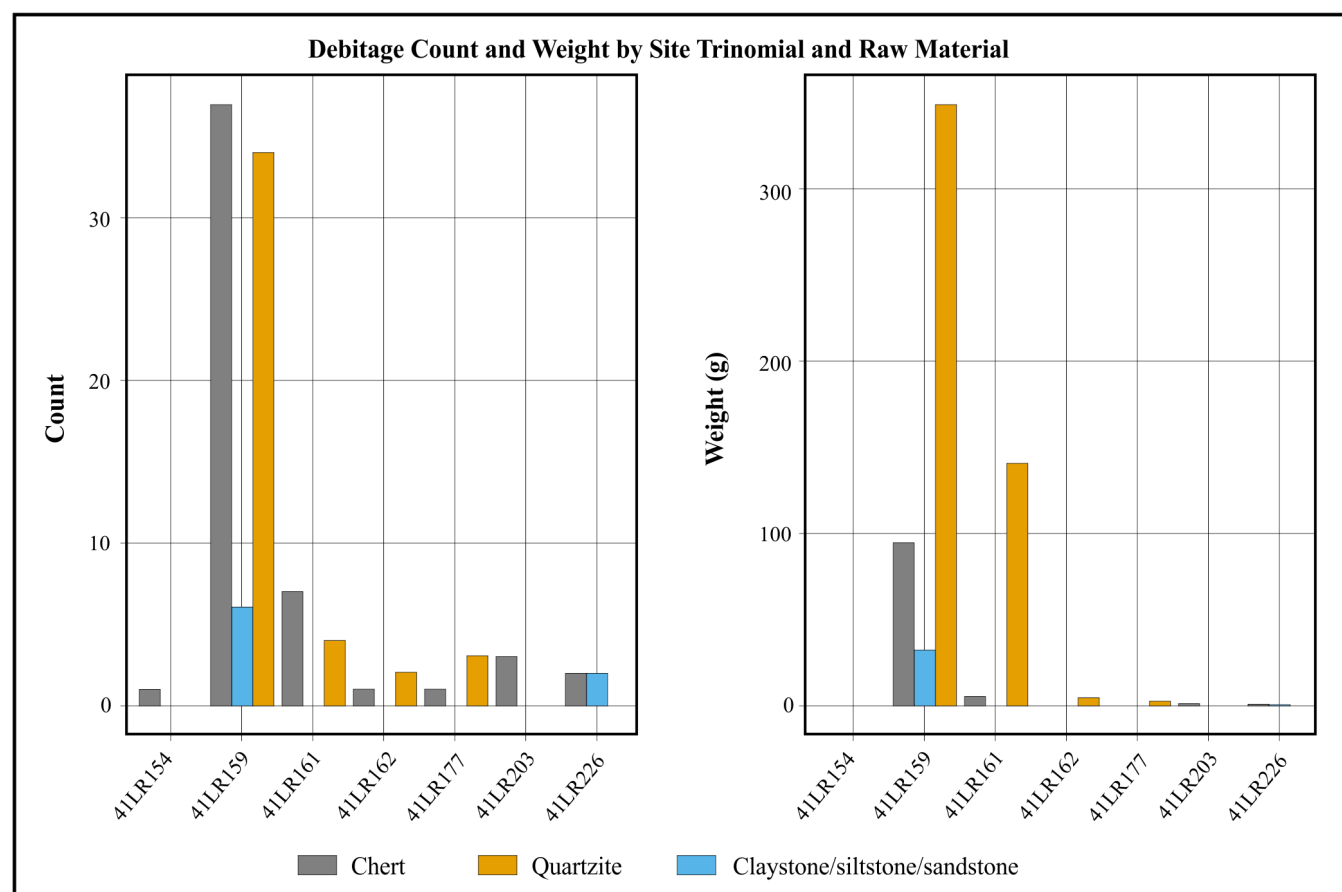


Figure 8-1. Left: Amount of debitage elements per raw material type, and by site. Right: weight of raw material by raw material, and by site.

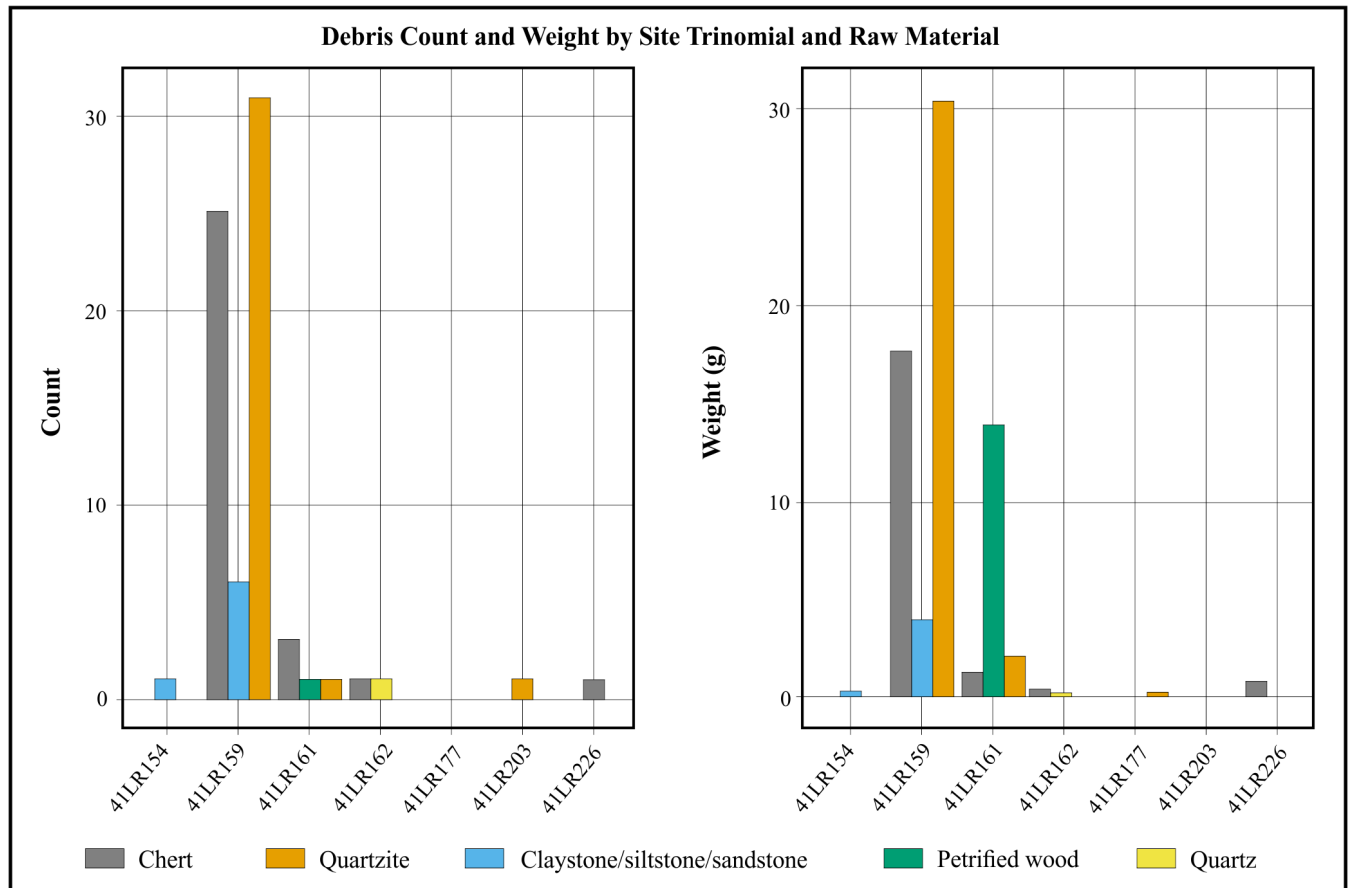


Figure 8-2. Left: number of chipped stone debris elements per raw material across the seven sites sampled. Right: total weight of chipped stone debris by raw material.

was identified at 41LR159, in the form of two biface thinning flakes, one of chert, and one of quartzite. No temporally diagnostic pieces were recovered, and there were only seven edge modified pieces recovered, including four bifaces (three on chert, and one on quartzite), and three retouched pieces, two quartzite flakes with unifacial retouch, and one quartzite flake with bifacial retouch, all of which were recovered from 41LR159, except one quartzite flake with unifacial retouch recovered from 41LR161.

41LR159

Site 41LR159 is the largest site sampled over the course of this project. It was first recorded in 1998 by CAR as a debitage surface scatter. Subsequently, 10 shovel tests were excavated, of which five were positive with 12 chipped stone artifacts. The site was initially reported as roughly 2080 m² in area (Nickels et al. 1996:60). In July 2021, CAR excavated 29 shovel tests, of which 13 were positive for chipped stone or burnt rock. In total, 16 artifacts were recovered, all prehistoric. A burnt rock feature (Feature 1) was identified in ST 57 in Level 3 (40-60 cmbs). Four subsequent test units recovered an additional 123 chipped stone artifacts. The chipped stone

material was recovered throughout the excavated sequence, from the first level starting at 20 cmbs, though 120 cmbs.

A total of 3.07 m³ of sediment was excavated from 41LR159 in 2021, across four 1-x-1 meter test units. This total does not include volume from 29 shovel tests. One burnt rock feature was identified in TU 4 at a depth of 45 cmbs. One hundred and thirty-nine chipped stone artifacts, weighing 527.6 g, were recovered from 41LR159. While this is the largest assemblage of the seven sites with artifacts tested on this project, it is still a low to moderate amount of material per unit of volume excavated (45.3 artifacts, or 172 g of toolstone per m³). Figure 8-3 shows the debitage density of 41LR159 (43.7 of debitage per m³) compared to the debitage density of 36 sites reviewed in Chapter 4. The figure shows 41LR159 is placed in the middle of the distribution of reviewed sites.

Of the 139 pieces recovered, 77 were debitage elements, either cores, flakes, or flake fragments, and 62 were debris elements (shattered pieces, chunks, and other fragments; Table 8-1). The assemblage weighs 527 g total, of which the debris elements weigh 52 g, and the debitage elements weigh 475 g. Most artifacts recovered from 41LR159 were made on either chert (n=62, 45% of assemblage),

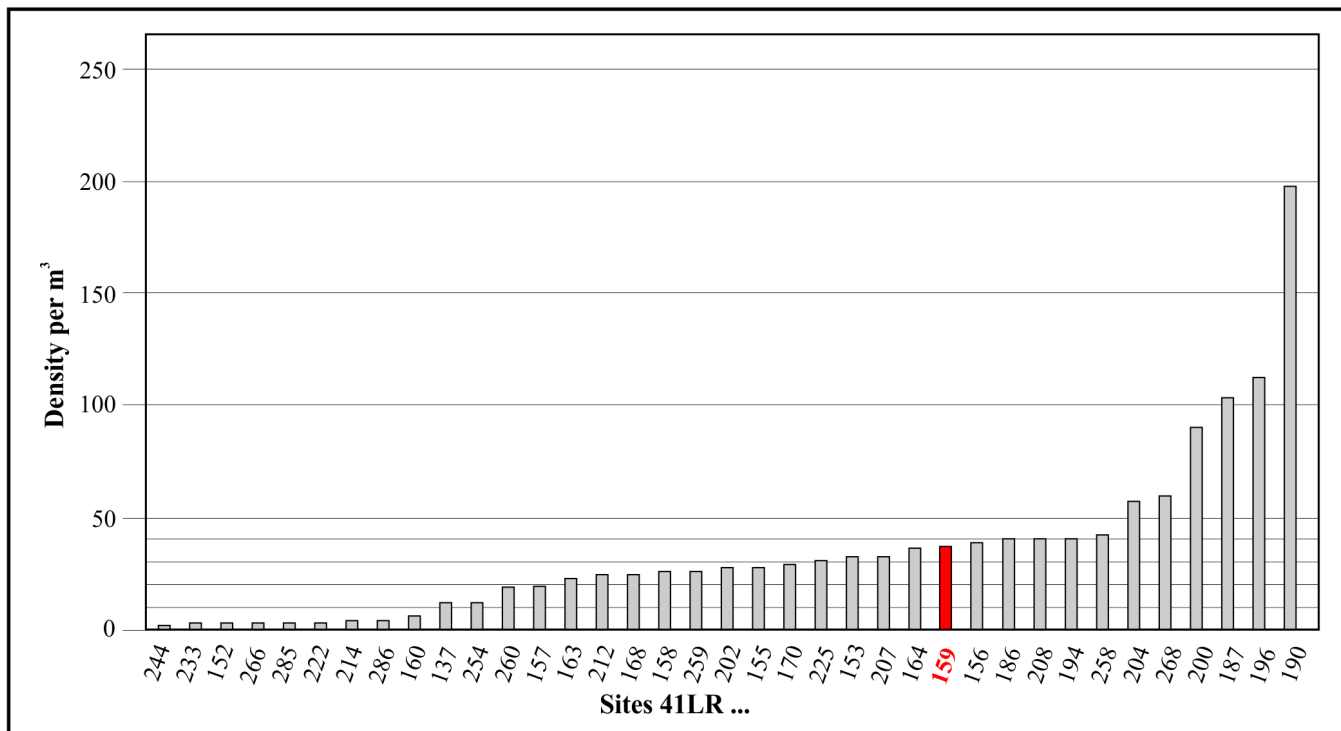


Figure 8-3. Density of debitage recovered by cubic meter for 41LR159 and 36 previously tested sites on Camp Maxey (see Chapter 4). 41LR159 is highlighted in red.

or quartzite (n=65, 47% of assemblage). The remainder were some variation of tan sedimentary mud or claystone representing 8% of the assemblage.

The distribution of complete flake sizes, and their degree of cortical cover highlights that much of the reduction sequence was likely present at 41LR159. Flakes longer than 25 mm, or wider than 15 mm, tended to have at least some amount of cortex (Figure 8-4). However, relatively small nodules were also likely reduced. Some 100% cortical covered complete flakes were small, less than 25 mm long (Figure 8-4).

One quartzite core was recovered from 41LR159, Test Unit 2 in Level 3 (30- 40 cmbs). The raw material was a coarse-grained quartzite, light brown in color, and had more than half of its surface covered in rounded cortex. The core has a single platform, with rounded cortex all over, except for where three removals were taken from a cortical platform with no preparation. The largest flake scar on this core is 53-x-23 mm, which is slightly larger than the range of sizes of quartzite flakes recovered from 41LR159.

Two complete chert bifaces were recovered from 41LR159 (Figure 8-5). These were likely too thick to represent projectile points. They lack side notches, or a thinned cross section. Both were recovered from Test Unit 4, one within Level 9 (FS 87) is made on a light brown fine-grained chert, with no evidence of heat treatment. It is 30-x-22-x-8 mm in

size, and weighs 5.7 g. Despite its small size, this piece has rounded, remnant cortex on both of its faces, which suggests a flattened pebble of less than a centimeter in thickness was knapped to produce this piece. The second complete biface was recovered from Level 8 of Unit 4 (FS 86). This piece was made on a banded brown fine-grained chert, and also lacked evidence for heat modification. This piece is also similar in its size to FS 87, 27-x-16-x-7 mm.

41LR161

Site 41LR161 was defined in 1998 by CAR archaeologists through five positive shovel tests, out of seven excavated. Seven stone artifacts were recovered as deep as 80 cmbs (Nickels et al. 1998:62). In July 2021, CAR excavated ten additional shovel tests in Site 41LR161. Of those, six were positive with stone artifacts, including burnt rock and debitage. In August 2021, CAR excavated three 1-x-1 m test units, each of which contained prehistoric artifacts, including debitage, burnt rock, cores. One burnt rock feature was also identified in Test Unit 2 at level 4 (30-40 cmdb).

Roughly 1.74 m³ of sediment was excavated from 41LR161 across two test units. This site had the second highest amount of chipped stone of the sites tested during this project though only 16 pieces were recovered. The artifact density per m³ is only approximately 9.2. These included 10 flakes,

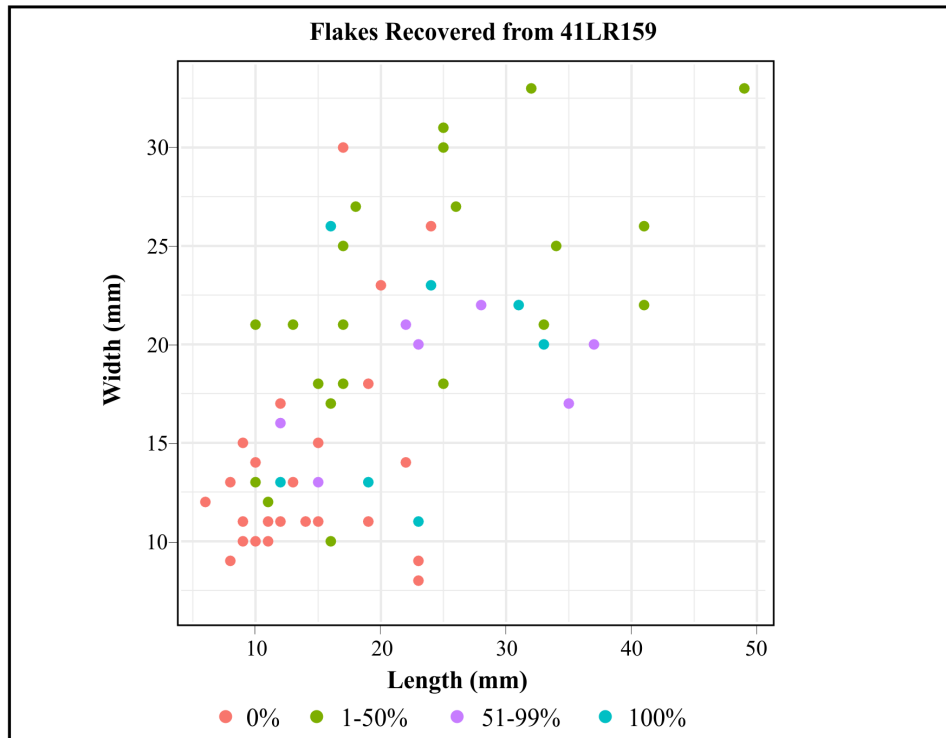


Figure 8-4. Dimensions of complete flakes recovered from 41LR159 differentiated by amount of cortex.



Figure 8-5. Top: FS 87, a biface on a fine-grained brown chert. Note relict cortex on both faces, despite the piece being only 8 mm in thickness. Bottom: FS 86. A similar small and relatively thick biface manufactured on a banded fine grained brown chert.

one core, and five pieces of debris. These were recovered from near the surface, at 8-20 cmbs, to as deep as 80 cmbs. Most of the artifacts recovered are made of chert (n=10, 62% of assemblage), followed by quartzite (n=5, 31% of assemblage). The remainder of the assemblage consists of one-piece knapping debris made of petrified wood.

One core was recovered from Test Unit 2, at a depth of 31 cmbs. This piece was made on a fine grained, light brown quartzite material, and like the core recovered from 41LR159, was largely covered in cortex. It is also similar in dimension to the 41LR159 core: 62-x-47-x-39 mm, and weighs 129.3 g. Technologically it is a single platform core with no preparation. The knapper attempted a change in orientation after running into step fractures, but these failed and the core was abandoned. The largest flake scar on the core is 38-x-31 mm.

While there are only a handful of artifacts present, all but one of the flakes have some amount of cortex present, and two have more than 50% cortical cover. The complete flakes all have some amount of cortex, despite their relatively small size (Figure 8-6), which suggests smaller gravels were brought to the area whole and reduced.

One edge-modified piece (FS 52) was recovered from 41LR161. This piece was recovered from Test Unit 1, in

Level 7, between 70 and 80 cmbs. This piece is a light brown, and fine-grained quartzite flake almost completely covered in cortex, weighing 6.3 g, and is 37-x-26-x-14 mm. The retouch on this flake is relatively abrupt, and scraper-like.

Measuring reduction intensity at 41LR159 using the Cortex Ratio Method

Prior research has argued for variability in raw material preference, and reduction intensity over time in the Camp Maxey Area (Nickels 1998; Lyle et al. 2001:147). Based on the above summary of the seven sites tested at Camp Maxey, we can say little about those preferences aside from their being a greater reliance on both quartzite and chert relative to other raw materials. The results of an application of the cortex ratio method to try to assess whether there might be differences between how quartzite and chert was used within the largest assemblage of the seven tested, that from 41LR159.

The cortex ratio method is frequently used in Pleistocene contexts to assess the degree of transport of locally available raw materials (Dibble et al. 2005; Lin et al. 2015). This method assesses how much an assemblage deviates from an expected amount of cortex assuming the entire reduction sequence happened on site. For example, sites could have less cortex represented than expected. This could be the case if most

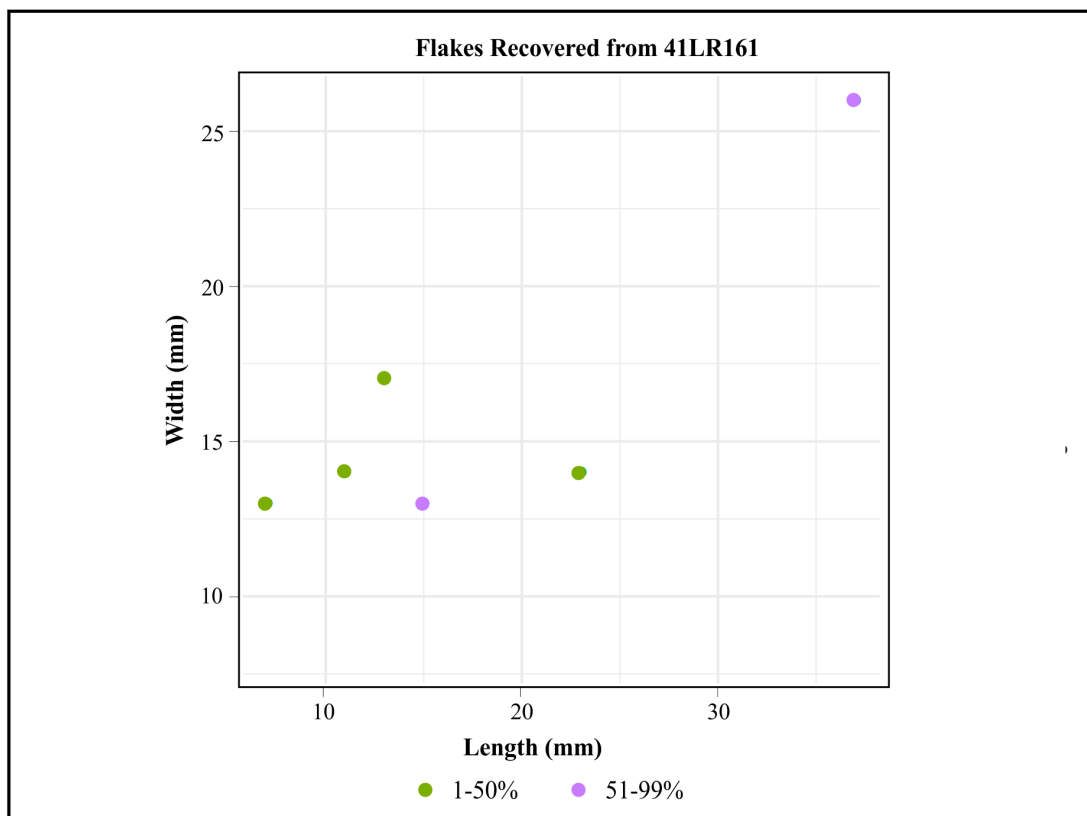


Figure 8-6. Dimensions of complete flakes recovered from 41LR161 separated by cortex cover.

of the initial stage reduction occurred off site, and partially reduced elements were brought into the site to be further reduced. Sites could also have more cortex than expected. This could be the case at a site where cobbles were tested, and partially reduced before being transported elsewhere for later secondary and tertiary reduction. Or the assemblage could have roughly the amount of cortex assuming that the entire reduction sequence happened at the site. This would indicate that most of the tool-making behaviors were more spatially limited to a particular point on the landscape, and that lithic transport was minimal. The methodology applied, following Lin et al. (2015) is outlined in Appendix D.

Results

The chert assemblage has an estimated volume of 45.09 cm³, and a surface area of 112.73 cm². Assuming the largest flakes in the chert assemblage are representative of nodule size, and assuming an ellipsoid model fairly characterizes the relationship between volume and surface area, the minimum number of nodules that could account for the observed volume of the chert assemblage is 1.47, with an estimated nodule volume of 30.7 cm³, and a total surface area of 84.36 cm². Based on these estimations, the total amount of cortex represented in the assemblage represents just under half of what we expect based on the modelled nodule surface area (cortex ratio = 0.45)(Table 8-2).

The results are similar for the quartzite assemblage, though the total assemblage volume and surface area are both slightly higher (Table 8-2). Nonetheless, the largest quartzite flakes are similar in size to the largest chert flakes, meaning that the estimated volume of nodules is also similar (38.8 cm³). The volume of quartzite represented in the assemblage can be accommodated by 3.6 such nodules, with a total surface area of 241.51 cm² (Table 8-2). Similar to the chert assemblage, there is also roughly half the cortex present compared to what is expected to be present assuming nodules similar to the modelled nodules were entirely reduced on site.

While both assemblages have an under-representation of cortex, the effect appears slightly more pronounced in the chert artifacts, which would be consistent with some differences in how chert was transported relative to quartzite. For example, it could be that chert was transported longer distances, and earlier stages of the chert reduction sequence more often happened elsewhere, rather than at 41LR159. In contrast, quartzite may have been more locally procured, and more often whole nodules were brought to the site to be reduced. However, is the difference between chert and quartzite cortex ratios greater than we would expect by chance?

Using the Monte-Carlo approach outlined in Lin et al. (2015), a test distribution was generated by pooling all the chert artifacts and quartzite artifacts into one dataset. From this dataset, two random samples were drawn without replacement, one set equal in number to the number of chert artifacts in the dataset, and one equal to the number of quartzite artifacts. The cortex ratio measurement was performed for each pair of sampled groups, and that difference in the cortex ratio between both groups was added to the test distribution. This process was repeated 10,000 times, resulting in a total of 10,000 permuted cortex ratio difference estimates (Appendix E, Figure 8-7). The test distribution highlights that cortex ratio differences of 0.1 or less are the most common, while there are very few instances of differences greater than 0.4. This test distribution was then used to test whether the observed difference in cortex ratio between the chert and quartzite datasets (0.09), was unusually high. An alpha of 0.05 was used for significance. In the test distribution generated, this means differences in cortex ratios higher than the 95th percentile, or differences in cortex ratios greater than 0.26 represent unusually high, and statistically significant differences (Figure 8-7). The observed difference in chert and quartzite cortex ratios is close to the mean of the test distribution, and thus is broadly what should be expected if the cortex ratio differences were due to chance. The observed cortex ratio difference between chert and quartzite was only greater than the differences measured across 45% of the 10,000 permuted datasets (p-value = 0.45)(Lin et al. 2012).

Table 8-2. Assemblage volume and surface area, compared to the amount of cortical area represented across artifacts grouped by raw material. The observed cortical area is compared to a modelled cortical area we would expect if the entirety of core reduction happened on site.

Group	Assemblage volume (cm ³)	Assemblage surface area (cm ²)	Assemblage cortical area (cm ²)	Modelled nodule volume (cm ³)	Modelled nodule N	Modelled cortex area (cm ²)	Cortex ratio (assemblage cortex/modelled cortex)
Chert	45.09	112.73	38.3	30.7	1.47	84.36	0.45
Quartzite	139.57	249.49	131.55	38.8	3.6	241.51	0.54

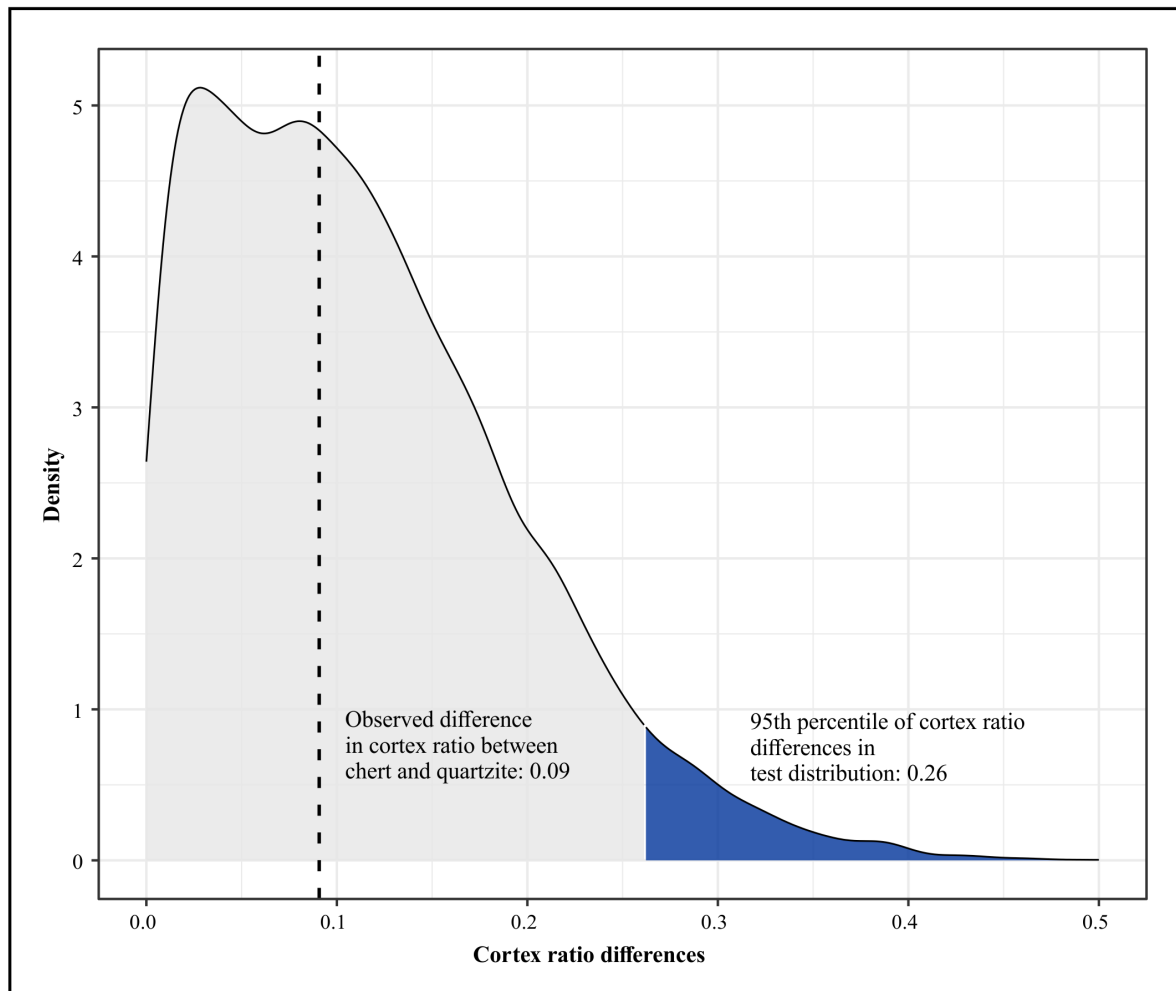


Figure 8-7. Test distribution generated by pooling all artifacts at 41LR159, and randomly sampling new pairs of assemblages and their respective cortex ratio differences 10,000 times. The dashed vertical line highlights the observed difference in cortex ratio between chert and quartzite assemblages. The area in blue represents values more extreme than 95% of cortex ratio differences generated through resampling the pooled data. The difference between quartzite and chert cortex ratios are unlikely to be statistically significant (p -value=0.57).

Overall, the results of the cortex ratio analysis suggest that both raw materials have cortex under-represented in the lithic assemblage relative to what we would expect if the entire reduction sequence was sampled. This means that some initial reduction in both raw materials likely occurred elsewhere, and partially reduced nodules were transported to some degree before reduction occurred in the area sampled by the 41LR159 test units. However, based on the Monte Carlo simulation, there is little evidence for there being a significant difference in the cortex ratio between the quartzite and chert assemblages at 41LR159. This is somewhat surprising, as prior work has highlighted that there may have been differences in transport between both, with quartzites seeing less transport than the larger chert nodules that are not available in the immediate area. The lack of significant difference, however, could also be due to relatively small sample size of both raw material assemblage. A more intensive investigation using

the cortex ratio method across other sites in the Camp Maxey area with larger numbers of chipped stone artifacts, may help to clarify evidence for differences in transport between both quartzite and chert.

Discussion

The assemblages recovered from seven sites at Camp Maxey tended to be low in density, and tended to be made up of relatively small artifacts. This is consistent with the reduction of smaller chert and quartzite nodules for the purposes of making tools. No diagnostic pieces were recovered, and few edge modified pieces were recovered. While there is little, we can say about most of the assemblages, the largest assemblage, 41LR159 had some consistent evidence for all stages of the reduction sequence being present. Many of the flakes recovered with cortex, tended to be larger than flakes without much cortex, and this

pattern was the same for both chert and quartzite pieces. To assess whether there may have been differences in transportation of both of these raw materials at 41LR159, a popular method of assessing reduction intensity, the cortex ratio method, was applied. The results indicate that cortex was likely underrepresented in both the chert and quartzite assemblages of 41LR159, though there was no statistically significant difference in cortex ratio between the chert and quartzite assemblages. These findings suggest that both chert and quartzite saw some degree of transport, with earlier stages of reduction happening off site, resulting in less cortex than we would expect if the entire reduction sequences happened at 41LR159. No raw material specific patterns were identified, though this could be a result of the relatively small sample size of the assemblage. If applied more generally in Texas, the cortex ratio method could be applied to many more lithic assemblages, and could help, along with other indices of mobility and land use (Wigley

2018), further assess how people modified tool-making behaviors in different times and circumstances.

Summary

This chapter considers the artifact assemblage characteristics at a site level as the second eligibility measure for the ten tested Maxey sites. Except for 41LR159, the Camp Maxey sites discussed here have few or in several cases no artifacts. Very few tools or cores were found during the current and previous investigations. All sites that have artifacts have little diversity as far as raw material type. Only one site contained prehistoric diagnostics, Caddo ceramics, found on 41LR226. Two sites, 41LR159 and 41LR161 contained burned rock features with charcoal that was radiocarbon dated. Table 8-3 summarizes the site level analysis of the ten sites.

Table 8-3. Summary of Site-Level Content Analysis

Site 41LR...	Chipped Stone Densities	Raw Material Variety	Total Tool Core and/or Ceramic Count	Number of Features	Total Burned Rock (g)
154	low	low	0	0	0.48
159	low-moderate	low	7	1	5742.95
161	low	low	3	1	1721.42
162	low	low	0	0	0
165	none	low	0	0	0
175	none	low	0	0	0
177	low	low	0	0	0
203	low	low	0	0	95.30
226	low	low	7	0	97.49
238	none	low	2	0	0

This page intentionally left blank.

Chapter 9: Site Integrity

Leonard Kemp

The final criterion used to assess the eligibility status of archaeological sites investigated here is integrity. CAR will use three methods to assess the archaeological integrity of the ten sites. These methods include field observation of the ten sites and test units made during the investigation, the distribution of artifacts (chipped stone and burned rock) within test units, and finally, the patterning in magnetic soil susceptibility (MSS) values. Note that whether the last two methods are employed is dependent on the findings from the unit excavations.

Natural and Human Impacts to Sites

Past investigations by CAR (Greaves 2003; Mahoney 2001; Mahoney et al. 2002) have noted that both natural and human processes have affected archaeological sites to some degree on Camp Maxey. Natural impacts include bioturbation and soil erosion. Human impacts have included the construction

of roads and the development of small farmsteads in the late nineteenth and early twentieth century. The construction of the base itself and subsequent military training was likely the most harmful for archaeological preservation. Table 9-1 summarizes site level disturbance observed by previous and the current investigations (Lyle et al. 2001; Nickels et al. 1998).

Table 9-2 summarizes field observations of bioturbation made during and following testing through a review of photographs taken at the end of each level. Rodent burrowing was observed during excavation on site 41LR159 (Figure 9-1, left). Bocek (1986) states that gopher burrowing can be as deep as 30 to 40 cmbs. We assume that the context of the upper 40 cm of any given unit is likely impacted by bioturbation. Insect burrowing were also observed on 41LR159 and 41LR203. Roots were found in all test units and varied from fine ($x < 2$ mm) to very course (≥ 10 mm) (Figure 9-1, right). Roots can also relocate artifacts up and down the unit profile (Waters 1992).

Table 9-1. Site- Level Observations of Natural and Human Impacts

Site	Natural Impacts	Human Impacts
41LR154	bioturbation	two-track road, fire breaks or berms
41LR159	bioturbation, cutbank and slope erosion	two-track road, vehicle traffic
41LR161	bioturbation, slope erosion	1-meter road cut through site, push piles
41LR162	bioturbation, slope erosion	two-track road, push piles, military activities
41LR165	bioturbation, cutbank erosion,	n/a
41LR175	bioturbation, cutbank erosion,	n/a
41LR177	bioturbation, cutbank and creek erosion,	possible vehicle traffic
41LR203	bioturbation	possible vehicle traffic
41LR226	bioturbation, slope erosion	n/a
41LR238	bioturbation, slope erosion	n/a

Table 9-2. Test Unit-Level Observations of Bioturbation

Site	TU 1	TU 2	TU 3	TU 4	Potential
41LR154	roots				low
41LR159	roots/insects	roots/rodents/insects	roots/rodents	roots/rodents	low
41LR161	roots	roots	roots		low
41LR162	roots	roots			low
41LR165	roots	roots			low
41LR175	roots				low
41LR177	roots				low
41LR203	roots/rodents	roots	roots/insects		low
41LR226	roots	roots	roots	roots	low
41LR238	roots	roots			low



Figure 9-1. Image on the right show roots of various sizes throughout the unit profile of TU 1 on 41LR154. Image on the left shows active rodent borrowing in the upper levels of TU 3 on 41LR159.

Artifact Distribution

This section examines the vertical distribution of debitage and burned rock in each excavation unit as one of several measures designed to assess unit and site integrity. Debitage is characterized by counts while burned rock is assessed

by weight. This analysis assumes that in sediments such as found at Camp Maxey, increased turbation will tend to displace more material to the terminal clay level. Conversely, units that have less turbation may preserve artifacts at or near the occupation surfaces resulting in isolated peaks in debitage and burned rock. Figure 9-2 illustrates these two

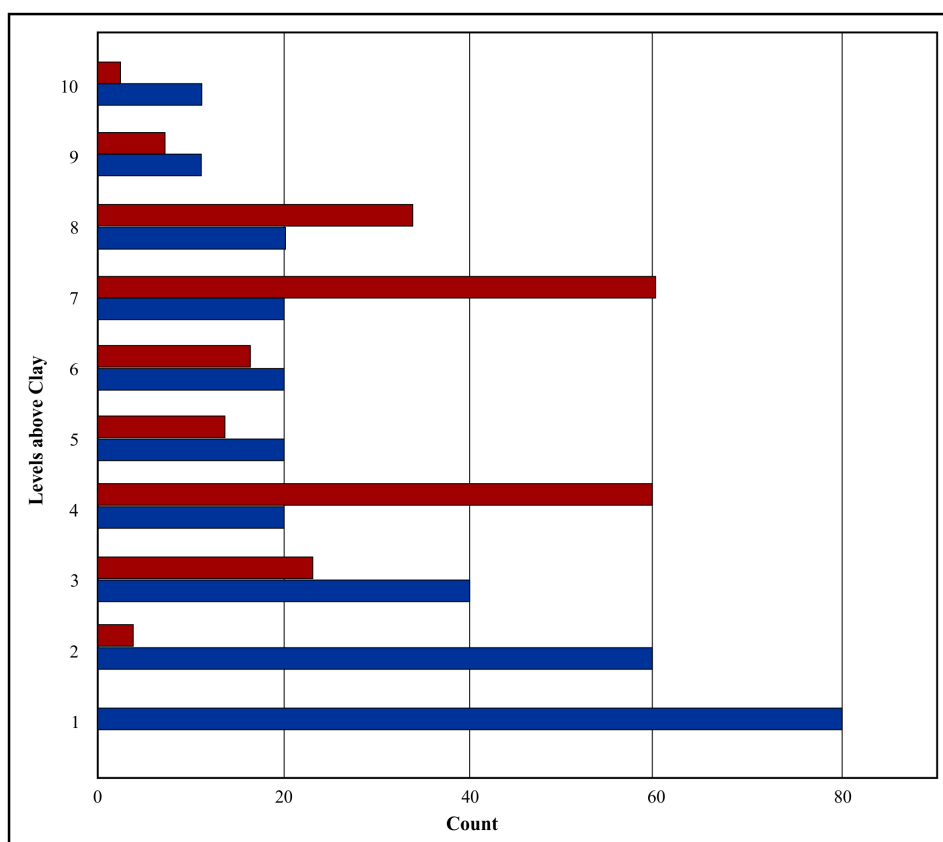


Figure 9-2. Two scenarios of debitage distribution by site. In blue, artifacts cluster at the bottom of the units near the clay floor suggesting that these artifacts are in secondary contexts and have low integrity. The other pattern in red indicates some degree of integrity where two peaks are represented suggesting two occupations.

scenarios using debitage counts. The distribution shown in red would potentially reflect two occupations with integrity, while the blue distribution would reflect high levels of disturbance (Figure 9-2). Most assemblages will not reflect these extreme examples, and there are varieties of processes that can produce clustering of material that would mimic the distribution highlighted in red, but that still lack integrity.

Table 9-3 provides summary data from test units used in this and subsequent analysis in this chapter. It includes by unit from each site the number of levels, the terminal sediment and maximum depth of excavation. In addition, the table provides a count of the chipped stone recovered and the weight of burned rock. Only two sites 41LR159 and 41LR161 contained sufficient chipped stone and/or burned rock to make an assessment based on artifact distributions. In a similar vein, 60% of the excavated test units were shallow or relatively shallow making interpretation of MSS values tentative given the degree of bioturbation in the upper levels. CAR employed an arbitrary cut-off of 50 cmbd as acceptable with selected units from six sites analyzed. These are shaded

in blue. One unit at 41LR238 was excavated to this depth, but the saturated soils prevented MSS sampling from the unit. Cells shaded in gray are not considered in this analysis.

41LR159

Test Units 1 and 4 contained enough material to conduct an assessment on both type of artifacts. Test Units 2 and 3 contained enough burned rock for assessment, but not chipped stone. All units terminated at clay. Figure 9-3 shows the distribution of chipped stone and/or burned rock for Test Units 1, 2, 3 and 4 on site 41LR159.

The amount of chipped stone in TU 1 peaks in Level 1, declines, and then peaks in Level 5. The weight of burned rock gradually increases beginning in Level 7, peaks in Level 9, and then decreases. The mixed results suggest low integrity due to the increase of burned rock towards the bottom of the units. Test Units 2 and 3 have a similar pattern with burned rock increasing towards the bottom of each unit. This accumulation of burned rock suggest that both Units 2

Table 9-3. Summary of Excavated Test Units from the Maxey Project

41LR...	Unit	Number of Levels	Chipped Stone (count)	Burned Rock (g)	Terminal Sediment	Maximum Depth (cmbd)
154	1	5	2	0.48	clay/sand	60
159	1	12	55	793.73	clay	122
159	2	5	14	517.44	clay	55
159	3	5	18	370.15	clay	54
159	4	10	10	3220.92	clay	110
161	1	9	6	0	clay	102
161	2	5	3	1527.39	clay	50
161	3	5	0	90.47	gravel	50
162	1	4	0	0	clay	41
162	2	3	0	0	clay	40
163	1	2	0	0	clay	30
163	2	3	0	0	clay	36
175	1	1	0	0	clay	20
177	1	5	4	0	clay	56
203	1	5	1	0	clay	56
203	2	5	2	0	clay	60
203	3	4	1	0	clay	50
226	1	3	0	0	clay	39
226	2	5	2	1.17	clay	50
226	3	3	0	0	clay	40
226	4	5	4	1.02	clay	46
238	1	5	0	0	clay	50
238	2	3	0	0	unknown	35

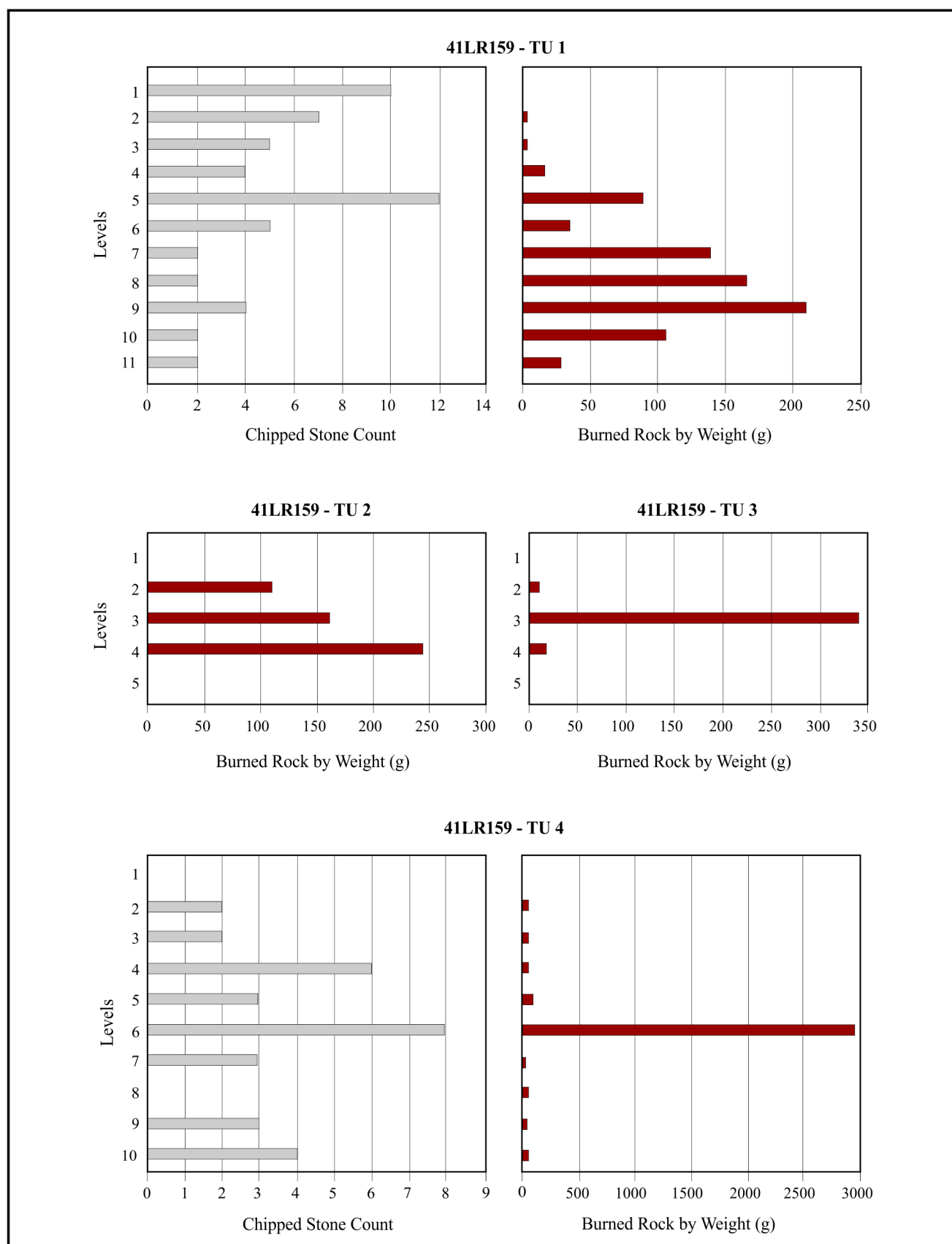


Figure 9-3. Vertical distributions of chipped stone and or burned rock from test units on 41LR159.

and 3 have low integrity. Test Unit 4 shows an increasing in chipped stone in Levels 4 and 6. There is also an increase in burned rock in Level 6 in which Feature 1 was found. The low amount of burned rock in the higher and lower levels of TU 4 suggests relatively good integrity.

41LR161

Of the three test units excavated on 41LR161, only TU 2 contained enough burned rock to conduct an assessment of integrity (Figure 9-4). Levels 1 through 3 contained relatively little burned rock. TU 2 contained a burned rock feature with two cores in Level 4 with burned clay under the feature. A sample from the feature was radiocarbon dated suggesting early historic use. In this scenario, despite our assumption that burned rock at or near the bottom of the unit suggests low integrity, we argue that the feature, when coupled with artifacts and a radiocarbon date, reflects good unit integrity.

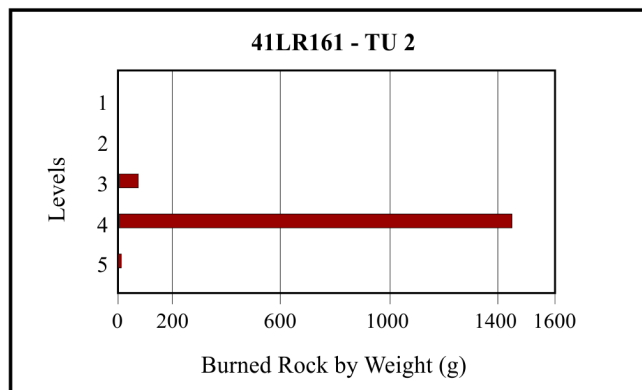


Figure 9-4. Vertical distribution of burned rock recovered from TU 2 on 41LR161.

Artifact Distribution Summary

Table 9-4 summarizes the degree of integrity using the count of chipped stone and weight of burned rock distributed through the units. Of the ten tested sites, only two, 41LR159 and 41LR161 contained enough material to conduct this analysis. Of the four units on 41LR159, only one unit, TU 4 suggested an intact surface. The results from TU 1 were mixed with debitage suggesting a surface, while burned rock collecting at the bottom of the unit suggesting turbation. The

Table 9-4. Summary of Test Unit Integrity Determination Based on Chipped Stone and Burned Rock Distribution

Test Unit	41LR159	41LR161
1	mixed results	n/a
2	low	good
3	low	n/a
4	good	

results from TU 2 at 41LR161 suggests that unit is relatively intact based on the presence of a recognizable feature with associated artifacts and radiocarbon date despite its proximity to the bottom of the unit.

Magnetic Soil Susceptibility

The third and final consideration of the integrity of deposits uses patterning in Magnetic Soil Susceptibility (MSS) values. MSS provides evidence of more localized, intra-site level patterns. MSS analyses has been conducted as part of the eligibility testing at Camp Maxey during prior investigations (Mahoney 2001; Mahoney et al. 2002; Greaves 2003). MSS samples were collected and analyzed from 20 sites (Mahoney 2001; Mahoney et al. 2002; Greaves 2003). Potential buried surfaces were identified at 15 of the 20, while four sites exhibited values where no clear stable surfaces could be identified, and one site where the values were so skewed by ferrous inclusions that no conclusions could be drawn. The overall results suggest that despite the sandy soils and extensive roots and rodent activity at Camp Maxey, the majority of the 20 analyzed sites exhibited at least some stratigraphic integrity (Mauldin 2001, 2002, 2003).

Mauldin et al. (2018) presented four hypothetical patterns of MSS values to aid in the interpretation (Figure 9-5). In the upper left box, there are two peaks in MSS values, one at the surface and one shown approximately eight to nine levels below the surface. The first peak is likely a result of organic enrichment found on the surface that migrating into the profile. This peak would be suspect because it is also within the rodent activity zone. The second peak consisting of multiple successive levels may indicate a buried occupational surface. Mauldin et al. (2018) suggest that rapid burial could potentially place the occupation surface below the rodent zone, thereby maintaining assemblage integrity. Box B shows a spike near the surface level. This near-surface spike is common and is often due to organic enrichment from modern plants. Below the spike, the Box B pattern shows decreasing values. This suggests that constant sediment deposition may have prevented the formation of an enriched occupation surface. Box C shows a nearly vertical pattern of values interpreted as a profile impacted by a mixing of sediments caused by bioturbation. Box D shows a large spike in MSS values within a single level. This spike is likely a result of the soil chemical composition containing iron oxide that would return a high value (see Dearing 1999:36-38). Mauldin et al. (2018) state that MSS results are qualified in that the interpretation of the data is somewhat subjective and that there may be multiple processes that may cause a similar signal. However, it is useful when considered in conjunction with other methods, such as artifacts patterning, to help determine the degree of integrity.

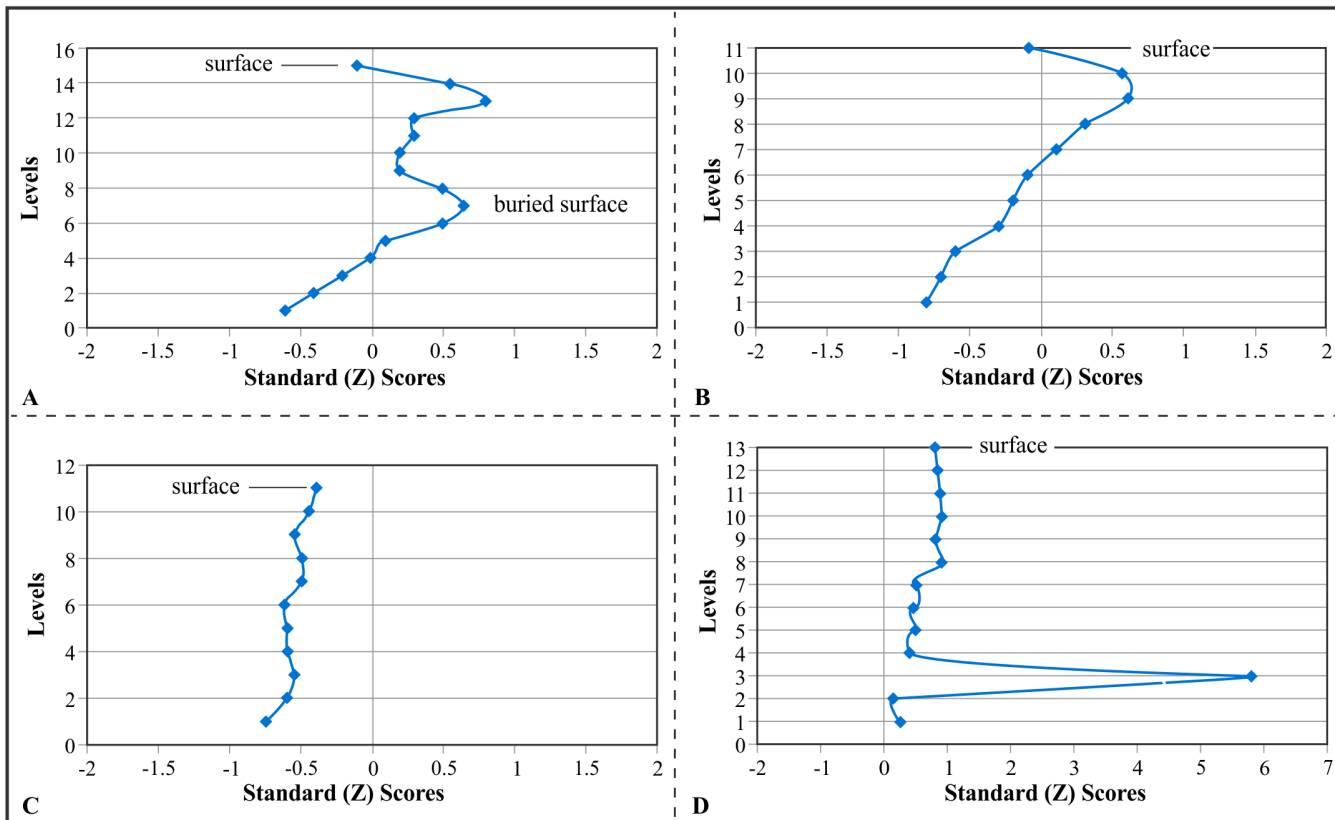


Figure 9-5. Four hypothetical patterns of MSS values (Mauldin et al. 2018: Figure 7-12).

On the current project, 152 sediment samples were processed from six of the ten sites. These sites are 41LR154, 41LR159, 41LR161, 41LR177, 41LR203 and 41LR226. Only one of the four units excavated on 41LR226 was deep enough for MSS analysis. The excavated depth of remaining four sites were too shallow or inundated to permit meaningful MSS analysis. The raw data and additional information on the 152 MSS samples used in the test unit discussions are presented in Appendix B. The MSS analysis focuses on indicators of buried surfaces at depths below 20 cm (Figure 9-5, Box B) and evidence of extensive bioturbation (Figure 9-5, Box C). Of note is the generally low MSS value from the collected samples. These findings are similar to the MSS values reported by past reports of sandy soil (see Kemp et al. 2022; Mauldin et al. 2018). The following section interprets the MSS value at the unit level to assess the integrity of the site as a whole.

41LR154

Figure 9-6 presents the MSS values for the test unit at 41LR154. There is a large spike in Sample 6 which falls within the modern organic surface suggesting a ferrous inclusion. This spike is followed by a near vertical column of values suggestingurbation throughout the bottom portion of the unit.

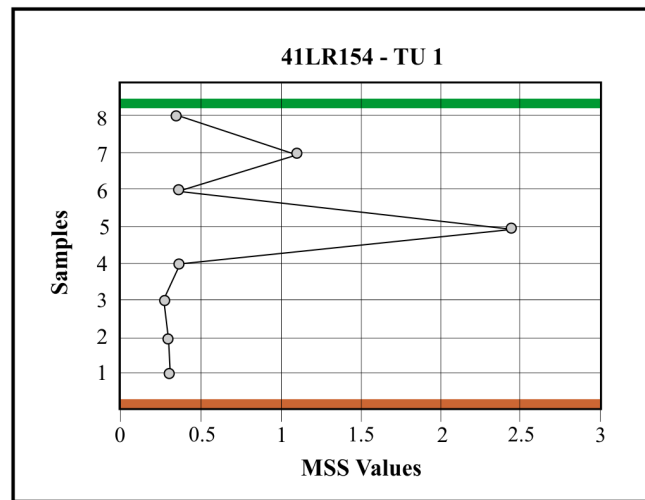


Figure 9-6. MSS values of test unit sampled at 41LR154. Green bar represents surface. Orange bar represents terminal depth.

41LR159

All four units on 41LR159 were sampled for MSS analysis. Figure 9-7 presents the MSS values for the test units. TU 1 shows an increase in signal in Samples 5 through 15 that may suggest a surface or surfaces, although the strength of those signals is relatively low and fluctuate. Both TU 2 and 3 show spikes in the upper organic zone with moderate spikes in Samples 6 and 5 approximately 30 to 35

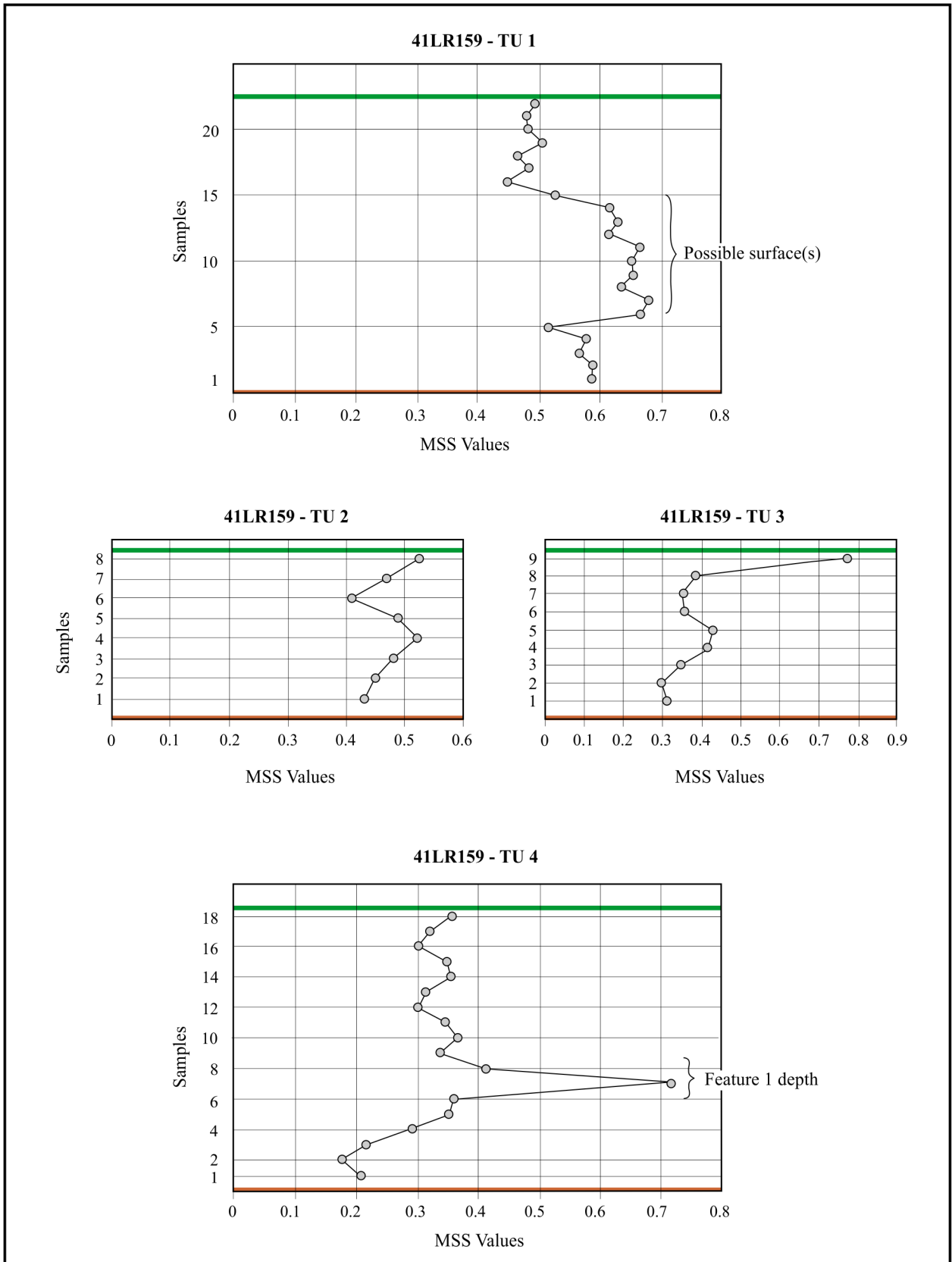


Figure 9-7. MSS values of test units sampled at 41LR159. Green bar represents surface. Orange bar represents terminal depth.

cmbs. These moderate spikes may suggest a contiguous subsurface given the proximity of one unit to the other. The signals from TU 4 fluctuates in the upper levels with a single substantial spike in Sample 7 within a feature level. However, given its value and the singularity of the spike, it is assumed to be a result of iron oxide in the soil.

41LR161

All three units on 41LR 161 were sampled for MSS analysis with Figure 9-8 presenting the MSS values for the test units. TU 1 is the deepest unit excavated, however in general the samples fluctuate between the 0.3 to 0.5 values. There is a strong spike in the bottom level suggesting high iron oxide concentration. The MSS values

for TU 2 fluctuate between approximately 0.5 and 0.75 suggesting some turbation. There is a slight increase in Sample 4 followed by a decline in values that may suggest a possible surface. Sample 4 is associated with Feature 1. The values of TU 3 show an upper organic surface with a steady decline suggesting no further organic enrichment.

41LR177

The MSS values from TU 1 excavated on 41LR177 is shown in Figure 9-9. All values are relatively low with a gradual increase from the surface to Sample 4 approximately 35 cm below grade. The remaining values fluctuate to the terminal level. No obvious surface(s) is present.

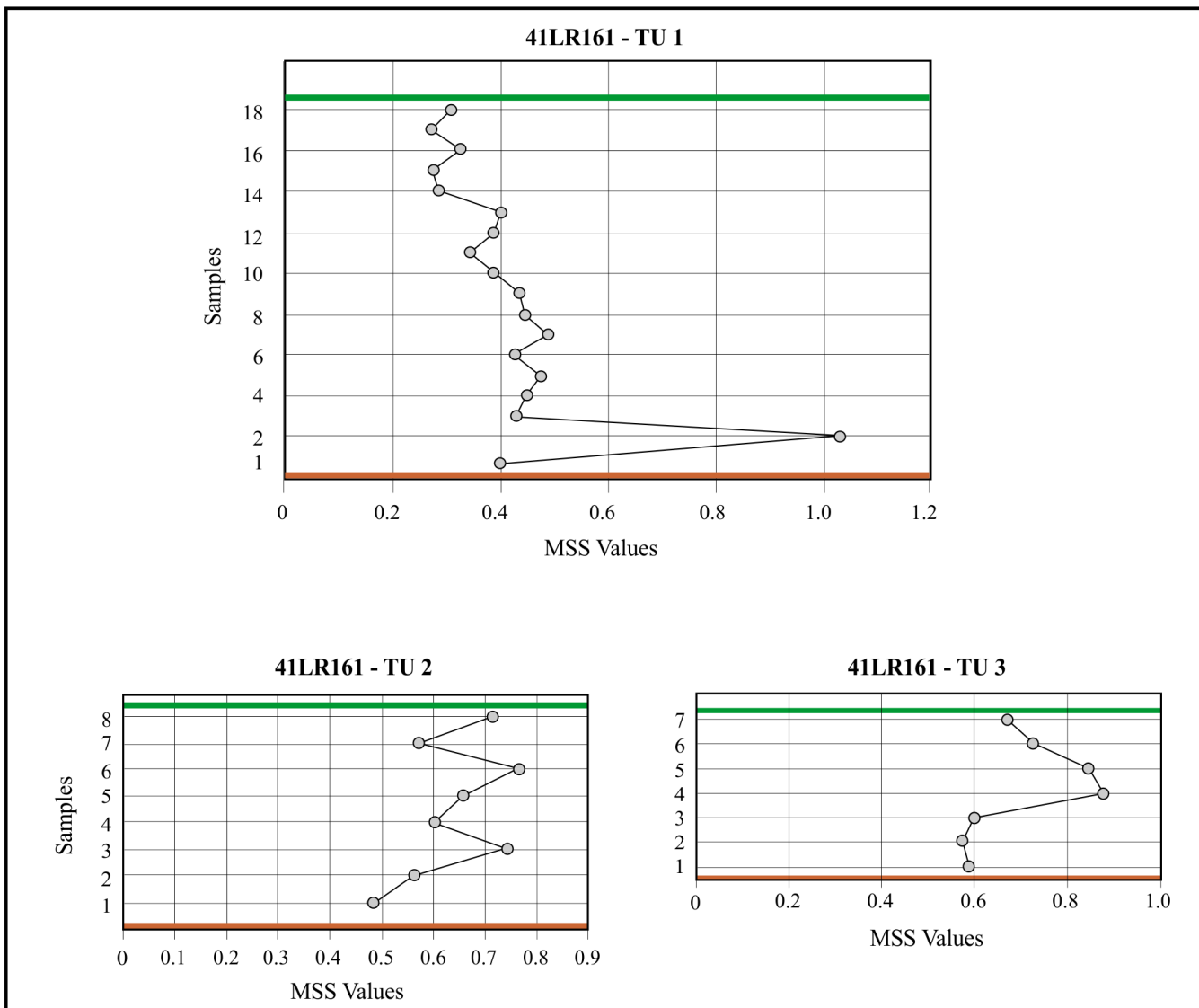


Figure 9-8. MSS values of test units sampled at 41LR161. Green bar represents surface. Orange bar represents terminal depth.

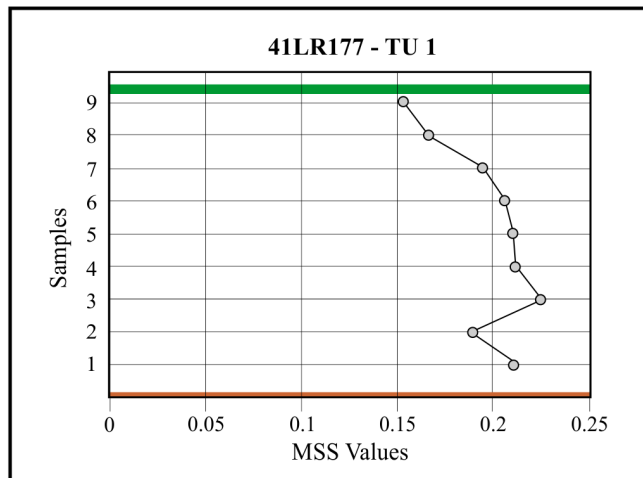


Figure 9-9. MSS values of test unit sampled at 41LR177. Green bar represents surface. Orange bar represents terminal depth.

41LR203

All three units on 41LR203 were sampled for MSS analysis. Figure 9-10 presents the MSS values for the test units. All units follow a similar trend with higher value in the upper levels associated with the surface followed by a decline in value. There appears to be no obvious indicators of a surface at 41LR203.

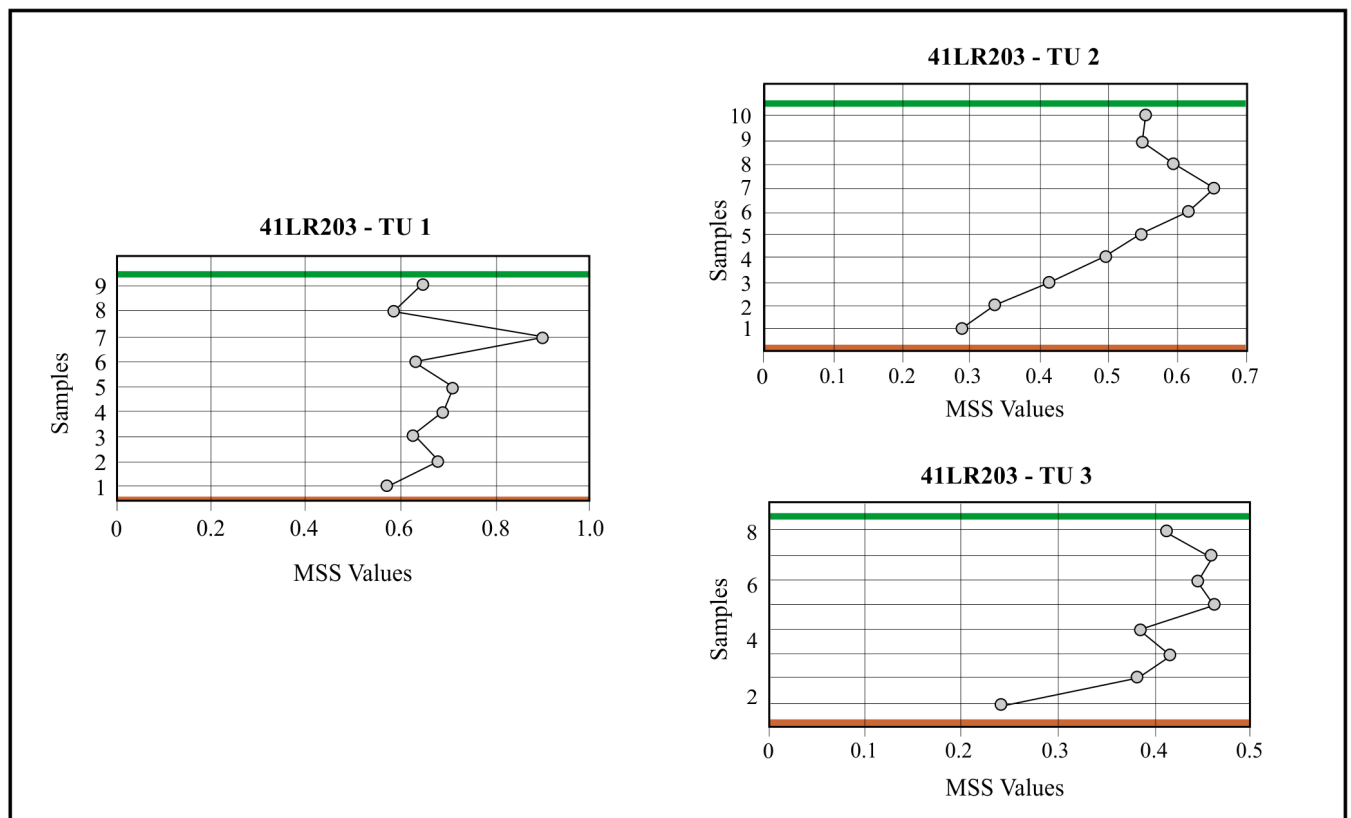


Figure 9-10. MSS values of test units sampled at 41LR203. Green bar represents surface. Orange bar represents terminal depth.

41LR226

Only one of the units at 41LR226 had sufficient depth for MSS analysis. Figure 9-11 presents the MSS values of TU 2. The upper levels suggest modern disturbance followed by a decline in values suggesting no intact surface.

MSS Summary

Table 9-5 summarizes the results of MSS analysis of test units that sufficient depth from six sites. The MSS values from three test units on two sites, 41LR159 (TU 1 and 4) and 41LR161(TU 2) may have potential surfaces. The MSS values from the remaining four sites suggest there is a low probability of having any intact sub-surfaces.

Conclusions

This chapter discussed the criteria of integrity as a component for determining a site's eligibility to the National Register. While "integrity" is qualitative to a degree, CAR has employed three methods to quantify that determination. These methods are field observation made by archaeologists, the vertical distribution of artifacts

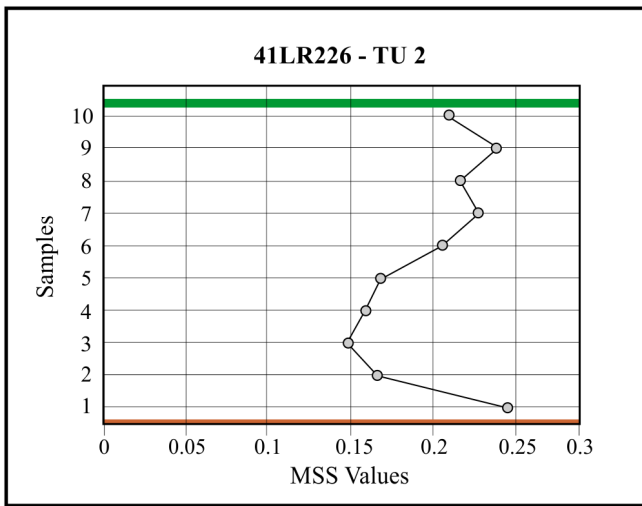


Figure 9-11. MSS values of test unit sampled at 41LR226. Green bar represents surface. Orange bar represents terminal depth.

through the unit, and lastly, MSS analysis taken from the profiles of the test units. No site or unit was classified as having high integrity, and most were classified as having low integrity.

Field observations at a site and unit level suggest that all ten sites have been impacted by both human and natural impacts resulting in low integrity. These impacts include roads running the sites, past military activities, and erosion. At a unit level field observations and a photographic analysis of all units by level suggest that roots were common and at two sites active rodents were recorded during excavation.

The second approach, using the distribution of the amount of chipped stone and weight of burned rock, was used to discern patterns that may suggest intact surfaces (Table 9-6). Only two of the ten sites contained sufficient cultural material to conduct this analysis. The results suggest buried surfaces in TU 1 of 41BP159 and TU 2 of 41LR161. The results from TU 1 of 41LR159 are mixed with chipped stone suggesting a surface and an accumulation of burned rock on the unit floor suggest otherwise. The overall ranking of the two sites suggests that portions of the two sites have a moderate degree of integrity.

The final method, using MSS, suggests buried surfaces may be present on 41LR159 TUs 1 and 4 (Table 9-7). The

Table 9-5. Summary of Test Unit Integrity Determination Based on MSS Analysis

Test Unit	41LR154	41LR159	41LR161	41LR177	41LR203	41LR226
1	low	possible surface	low	low	low	n/a
2		low	possible surface		low	low
3		low	n/a		low	n/a
4		possible surface				n/a

Table 9-6. Chipped Stone and Burned Rock Site Summary Data from Unit Profiles

Sites	Number Excavated	Number of Units Assessed	Percentage with Moderate Integrity	Percentage with Low Integrity	Overall Site Integrity Assessment
41LR159	4	4	50	50	moderate
41BP161	3	1	100	0	moderate

Table 9-7. MSS Site Summary Data from Unit Profiles

Site	Number of Units Assessed	Percentage with Moderate Integrity	Percentage with Low Integrity	Overall Site Integrity Assessment
41LR154	1	0	100	low
41LR159	4	50	50	moderate
41LR161	2	33.33	66.66	low
41LR177	1	0	100	low
41LR203	3	0	100	low
41LR226	1	0	100	low

MSS values from the remaining five sites suggest that intact buried surfaces are not present within those analyzed units.

To conclude, all ten sites have been impacted by human and natural factors with only one site, 41LR159 having some

degree of integrity. Based on these analyses, TUs 1 and 4 on 41LR159 contains areas with moderate integrity. Site 41LR161 may also contain one possible area of moderate integrity in TU 2 based on the relatively intact, although shallow, feature.

This page intentionally left blank.

Chapter 10: Summary and Recommendations

Leonard Kemp, Sarah Wigley, and Jonathan Paige

The Center for Archaeological Research (CAR) at The University of Texas at San Antonio (UTSA) conducted fieldwork associated with NRHP eligibility determination on 12 prehistoric sites located on Camp Maxey in Lamar County, Texas. These sites are 41LR154, 41LR159, 41LR161, 41LR162, 41LR165, 41LR175, 41LR177, 41LR184, 41LR203, 41LR213, 41LR226, and 41LR238. The CAR carried out the work in accordance with Section 106 of the NHPA of 1966.

During these investigations, CAR revisited all 12 sites and excavated 95 shovel tests on eight of those sites. The CAR excavated 23 1-x-1 m test units on ten sites to determine NRHP eligibility. The ten sites are 41LR154, 41LR159, 41LR161, 41LR162, 41LR165, 41LR175, 41LR177, 41LR203, 41LR226, and 41LR238. CAR screened roughly 10.1 m³ of deposits from the ten sites. CAR did not conduct NRHP eligibility testing on sites, 41LR184

and 41LR213 and as such their NRHP eligibility status is still to be determined.

Recommendations

CAR's recommendations regarding eligibility for inclusion to the NRHP are based on Criterion D of 36 CFR 60.4, which covers properties that have yielded, or may be likely to yield, information important in prehistory or history. The CAR relied on three interrelated criteria to determine site eligibility (Mauldin et al. 2018). These criteria consist of the chronological potential of a site, discussed in Chapter 7, the content of a site, discussed in Chapter 8, and integrity of a site, discussed in Chapter 9.

Table 10-1 summarizes the findings of each of these domains and presents CAR's eligibility recommendations. Highlighted cells identify those elements that contribute

Table 10-1. Summary of the Ten Archaeological Sites Tested for NRHP Eligibility

Site (41LR...)	Shovel Test Excavated	Test Units Excavated	Amount Excavated (m ³)	Temporal Diagnostics	Radiocarbon Dates/ Potential	Debitage Density (m ³)	Number of Features	Artifact Patterning	MSS Assessment of Integrity	NRHP Eligibility Recommendations
154	11	1	0.5	yes, historic	no/low	low	0	n/a	low	not eligible
159	29	4	3.01	not present	yes/moderate	low-moderate	1	moderate	moderate	eligible
161	10	3	1.72	not present	yes/moderate	low	1	moderate	low	not eligible
162	29	2	0.61	not present	no/low	low	0	n/a	low	not eligible
165	6	1	0.26	not present	no/low	none	0	n/a	n/a	not eligible
175	0	1	0.1	not present	no/low	low	0	n/a	n/a	not eligible
177	0	1	0.46	not present	no/low	none	0	n/a	low	not eligible
203	0	1	1.45	not present	no/low	low	0	n/a	low	not eligible
226	10	4	1.35	present, prehistoric	no/moderate	low	0	n/a	low	not eligible
238	0	2	0.65	present, prehistoric	no/low	none	0	n/a	n/a	not eligible

positively (green) or negatively (orange) to the three criteria, while cells that are inconclusive are not highlighted. Sites that were lacking in one or more of criteria were judged to have little or no potential to contribute to resolutions of broader research questions, and therefore, would be unlikely to yield information important in prehistory.

Concerning chronology, sites 41LR159 and 41LR161 each produced a radiocarbon date from a burned rock feature. These two sites, and site 41LR226, appear to have potential for radiocarbon dates based on the presence of charcoal and/or bone. During this testing phase, only two sites, 41LR154 and 41LR226, were found to have temporally diagnostic artifacts. Site 41LR154 contained a U.S. penny dating to 1903 and 41LR226 contained prehistoric ceramics. Prehistoric ceramics were also found at 41LR226 during the Lyle et al. (2001) investigation. Previous investigation at 41LR238 revealed a possible burned clay feature and a corner-notched dart point. The remaining six sites have poor potential for either radiocarbon dating or temporal diagnostics.

The second measure to address eligibility is the artifactual data generated by the site excavations. As reported in Chapter 4 of this report, the assemblages from Camp Maxey sites tend to be small in quantity and lack diversity in both tool type(s) and raw material. The current investigation produced similar results with only one site, 41LR159, having a low to moderate number of artifacts. Six sites contained no tools and three sites had no artifacts. Only two sites, 41LR159 and 41LR161, contained features.

Camp Maxey is in the Sandy Mantle formation of Texas. As such, there is debate as to whether a site found in this formation has any integrity. In past investigations of sites located in the same formation, CAR and others have found sites or components of sites may contain some integrity. CAR used multiple lines of analysis to quantify integrity including field observations and analysis of unit photos, the vertical distribution of artifacts, and magnetic soil susceptibility (MSS) analysis. Only one site, 41LR159 was rated as having moderate integrity in both artifact patterning and MSS values. Although all 4 units were impacted to some degree by bioturbation. The results from 41LR161 are mixed with artifact patterning that is categorized as having moderate integrity, while the MSS results are classified as having low integrity results. The remaining eight sites are classified as having low to no integrity.

CAR recommends that sites 41LR154, 41LR161, 41LR162, 41LR165, 41LR175, 41LR177, 41LR203, 41LR226, and 41LR238 are not eligible for NRHP listing due to the lack of chronological potential, poor integrity, and/or limited site content. CAR further recommends that site 41LR159 be considered as eligible for listing on the NRHP. Based on testing, this site had moderate integrity and a feature that reflect Late Prehistoric use. Site 41BLR159 should be avoided if possible and protected from damage related to future development or military activities. If avoidance is not possible, then additional research is warranted to mitigate adverse effects from these impacts. In addition, CAR redefined the boundaries of four sites, 41LR154, 41LR159, 41LR161, and 41LR162 reflecting findings from the current investigation.

References Cited:

Adjutant General's Department

1993 *Archeological Survey Report, October 4, 1993*, Adjutant General's Department, Austin.

1997 *Archeological Survey Report, July 1, 1997*, Adjutant General's Department, Austin.

Ahr, S.W., L.C. Nordt, and S.G. Driese

2012 Assessing Lithologic Discontinuities and Parent Material Uniformity within the Texas Sandy Mantle and Implications for Archaeological Burial and Preservation Potential in Upland Setting. *Quaternary Research* 78:60-71

Amick, D.S., R.P. Mauldin and S.A. Tomka

1988 An Evaluation of Debitage Produced by Experimental Bifacial Core Reduction of a Georgetown Chert Nodule. *Lithic Technology* 17(1): 26-36.

Anderson, D.G.

1996 Approaches to Modeling Regional Settlement in the Archaic Period Southeast. In *Archaeology of the Mid- Holocene Southeast*, edited by K.E. Sassaman and D.G. Anderson, pp. 157-176, University Press of Florida, Gainesville.

Andrefsky, W. Jr.

2005 *Lithics: Macroscopic Approaches to Analysis*. 2nd edition. Cambridge University Press.

Anonymous

2022 Central National Road. In Handbook of Texas Online. Electronic document, <https://www.tshaonline.org/handbook/>, accessed September 2022.

Bamforth, D.B and P. Bleed

1997 Technology, Flaked Stone Technology, and Risk. In *Rediscovering Darwin; Evolutionary Theory and Archaeological Explanation*, edited by C. M. Barton and G. A Clark, pp. 109-40. Archaeological Papers of the American Anthropological Association No. 7.

Bamforth, D.B. and B. Grund

2012 Radiocarbon calibration curves, summed probability distributions, and early Paleoindian population trends in North America. *Journal of Archaeological Science* 39:1768–1774.

Bever, M.B. and D.J. Meltzer

2007 Exploring Variation in Paleoindian Lifeways: The Third Revised Edition of the Texas Clovis Fluted Point Survey. *Bulletin of Texas Archeological Society* 78:65-100.

Binford, L.

1980 Willow Smoke and Dog's Tails: Hunter-Gatherer Settlement Systems and Archaeological Site Formation. *American Antiquity* 45:4-20.

2001 *Constructing Frames of Reference: An Analytical Method for Archaeological Theory Building Using Hunter-Gatherer and Environmental Data Sets*. University of California Press, Berkeley, California.

Bleed, P.

1986 The Optimal Design of Hunting Weapons: Maintainability or Reliability. *American Antiquity* 51(4):737-747.

Bocek, B.

1986 Rodent Ecology and Burrowing Behavior: Predicted Effects on Archaeological Site Formation. *American Antiquity* 51:589-603.

References Cited

Bousman, C.B., B.W. Baker, and A.C. Kerr

2004 Paleoindian Archaeology in Texas. In *The Prehistory of Texas*, edited by T.K. Perttula, pp. 15-97. Texas A&M University Press, College Station.

Bousman, C.B., and R.C. Fields

1991 Environmental Setting. In *Excavations at the Bottoms, Rena Branch, and Moccasin Springs Sites, Jewett Mine Project, Freestone and Leon Counties, Texas*, edited by R.C. Fields, pp. 5-20. Reports of Investigations No. 82. Prewitt and Associates, Inc., Austin.

Boydston, R. A.

1989 A Cost-Benefit Study of Functionally Similar Tools. In *Time, Energy, and Stone Tools* edited by R. Torrence, pp. 67-78. Cambridge University Press, Cambridge, UK.

Bronk Ramsey, C.

2021 OxCal Calibration Version 4.4. Online Program. Electronic document, <https://c14.arch.ox.ac.uk/>, accessed July 2022.

Bruseeth, J.E.

1998 The Development of Caddoan Polities along the Middle Red River Valley of Eastern Texas and Oklahoma. In *Native History of the Caddo: Their Place in Southeastern Archaeology and Ethnohistory*, edited by T.K. Perttula and J.E. Bruseeth, pp 47-68, Studies in Archeology 30, Texas Archeological Research Laboratory, The University of Texas at Austin.

Bruseeth, J. E., L. Banks, and J. Smith

2001 The Ray Site (41LR135). *Bulletin of the Texas Archeological Society* 72:197-213.

Bruseeth, J.E., and W.A. Martin

2001 OSL Dating and Sandy Mantle Sites in East Texas. *Current Archeology in Texas* 3:12-17.

Bruseeth, J.E. and T.K. Perttula

1981 Prehistoric Settlement Patterns at Lake Fork Reservoir. Southern Methodist University and Texas Antiquities Committee, Texas Antiquities Permit Series, Report No. 2, Dallas and Austin.

Camilli, E.

1989 The Occupation History of Sites and the Interpretation of Prehistoric Technological Systems: An Example from Cedar Mesa, Utah. In *Time, Energy, and Stone Tools* edited by Robin Torrence, pp. 17-27. Cambridge University Press, Cambridge, UK.

Chipman, D. E., and H.D. Joseph

2010 *Spanish Texas, 1519-1821*. Revised ed. University of Texas Press, Austin.

Corbin, J.E.

1992 Archaeological Survey of a Proposed Raw Water Line (EDA, B4) for the City of Paris, Lamar County, Texas. Nacogdoches, Texas.

Crema, E.R., A. Bevin, and S. Shennan.

2017 Spatio-temporal Approaches to Archaeological Radiocarbon Dates Application. *Journal of Archaeological Science* 87:1-19.

Dearing, J.

1999 *Environmental Magnetic Susceptibility*. Chi Publishing, Kenilworth, England.

Dibble, H.L, U.A. Schurmans, R.P. Iovita and M.V. McLaughlin

2005 The Measurement and Interpretation of Cortex in Lithic Assemblages. *American Antiquity* 70(3):545-560.

Edwards, CW. and S.A. Johnson

2007 Report on a Mammal Survey at Camp Maxey, Lamar County, Texas (Texas Army National Forces Facility). Occasional Papers No. 267, Museum of Texas Tech University, Lubbock.

Eren, M., F. Diez-Martin, and M. Dominguez-Rodrigo

2013 An empirical test of the relative frequency of bipolar reduction in Beds VI, V, and III at Mumba Rockshelter, Tanzania: implications for the East African Middle to Late Stone Age transition. *Journal of Archaeological Science* 40(1):248–256.

Figuerroa, A, C. Munoz, S. Smith, and R. Mauldin

2009 Exploring the Impacts of Raw Material Availability and Size on Prehistoric Chipped Stone Assemblages in Central and South Texas. Paper presented at the Texas Academy of Science Meeting, Junction, Texas.

Fisher, R.S., R.E. Mace, E. Boghici, C.A. Kuharic, and M. Blum.

1996 Ground-water and surface-water hydrology of Camp Maxey, Lamar County, Texas. Report o. THCB-95-1-05-01. Austin (TX): Bureau of Economic Geology, University of Texas at Austin.

Ford, N.B. and P.M. Hampton

2005 The Amphibians and Reptiles of Camp Maxey, Lamar County, Texas with Comments on Census Methods. *Texas Journal of Science* 57(4):359-370.

Frederick, C.D., and M.D. Bateman

2001 OSL Dating and Sandy-Mantle Sites in East Texas: A Reply. *Current Archeology in Texas* 3(2):14-18.

Greaves, R.D.

2003 *Camp Maxey V: Archaeological Testing of Seven Sites in the Camp Maxey Training Facility, Lamar County, Texas*. Archaeological Survey Report No. 330. Center for Archaeological Research, the University of Texas at San Antonio.

Griffith, G. S. Bryce, J. Omernik, and A. Rogers

2007 *Ecoregions of Texas*. Texas Commission on Environmental Quality, Austin.

Harris, R.K., I.M. Harris, J.C. Blaine, and J. Blaine

1965 A preliminary Archeological and Documentary Study of the Womack Siter, Lamar County, Texas. *Bulletin of Texas Archeological Society* 36:287-365.

Hayden, B.

1980 Confusion in the Bipolar World: Bashed Pebbles and Splintered Pieces. *Lithic Technology* 9(1):2–7.

Horta, P., N. Bicho, and J. Cascalheira

2022 Lithic bipolar methods as an adaptive strategy through space and time. *Journal of Archaeological Science: Reports* 41:103263.

Kelly, R.L

2013 *The Lifeways of Hunter Gatherers; The Foraging Spectrum*. Cambridge University Press, New York.

Kelly, R.L., L. Poyer and B. Tucker

2005 An Ethnoarchaeological Study of Mobility, Architectural Investment, and Food Sharing among Madagascar's Mikea. *American Anthropologist* 107(3):403-416.

Kemp, L., L. Kim, and R. Mauldin

2023 *National Register Eligibility Testing of Sites 41BP471, 41BP477, and 41BP666 on Camp Swift, Bastrop County, Texas*. Archaeological Report No. 495. Center for Archaeological Research, the University of Texas at San Antonio.

Kemp, L., R. P. Mauldin, and C. M. Munoz

2019 *National Register Eligibility Testing of Three Archaeological Sites on Camp Swift, Bastrop County, Texas*. Archaeological Report, No. 465, The University of Texas at San Antonio.

Kenmotsu, N.A. and T.K. Perttula, editors

1993 Archeology in the Eastern Planning Region, Texas: A Planning Document Department of Antiquity Protection, Cultural Resources Management Report 3, Texas Historical Commission Austin.

Kim, L., R. Mauldin, and L. Kemp.

2023 Chapter 9: Site Content. In *National Register Eligibility Testing of Sites 41BP471, 41BP477, and 41BP666 on Camp Swift, Bastrop County, Texas* by L. Kemp, L. Kim, and R. Mauldin. Archaeological Report No. 495. Center for Archaeological Research, the University of Texas at San Antonio.

Krieger, A. D

1946 *Cultural Complexes and Chronology in Northern Texas with Extensions of Puebloan Datings to the Mississippi Valley*. The University of Texas Publication No.4640, Austin.

Largent, F.B., M.R. Waters and D.L. Carlson

1991 The Spatiotemporal Distribution and Characteristics of Folsom Projectile Points in Texas. *Plains Anthropologist* 36(137):323–341.

Lawrence D, A. Palmisano A, and M.W. de Gruchy

2021 Collapse and continuity: A multi-proxy reconstruction of settlement organization and population trajectories in the Northern Fertile Crescent during the 4.2kya Rapid Climate Change event. *PLoS ONE* 16(1): e0244871. <https://doi.org/10.1371/journal.pone.0244871>

Leffler, J.J.

2001 History of Camp Maxey and its Environs, 1830-1970. In *Camp Maxey II: A 5000 Acre Cultural resources Survey of Camp Maxey, Lamar County, Texas*, by A.S. Lyle, S.A. Tomka, and T.K. Perttula, pp. 13-43. Archaeological Survey Report, No. 312. Center for Archaeological Research, The University of Texas at San Antonio.

Lin, S., S. McPherron, and H. Dibble

2015 Establishing statistical confidence in Cortex Ratios within and among lithic assemblages: a case study of the Middle Paleolithic of southwestern France. *Journal of Archaeological Science* 59:89–109.

Lorrain, D. and N. Hoffrichter

1967 *Archeological Survey and Excavation at Pat Mayse Reservoir, Texas*. Archeological Salvage Project, Southern Methodist University, Dallas.

Ludeman, M.M.

2021 Lamar County. Handbook of Texas Online. Electronic document, <https://www.tshaonline.org/>, accessed September 2022.

Lyle, A.S., S.A. Tomka and T.K. Perttula

2001 *Camp Maxey II: A 5000 Acre Cultural Resources Survey of Camp Maxey, Lamar County, Texas*. Archaeological Survey Report No. 312. Center for Archaeological Research, University of Texas at San Antonio.

Mahoney, R.B.

2001 *Camp Maxey III: Archaeological Testing of 23 Prehistoric Sites, Lamar County, Texas*. Archaeological Survey Report No. 314. Center for Archaeological Research, University of Texas at San Antonio.

Mahoney, R.B., S.A. Tomka, J.D. Weston, and R.P. Mauldin.

2002 *Camp Maxey IV: Archaeological Testing of Six Sites, Lamar County, Texas*. Archaeological Survey Report No. 326. Center for Archaeological Research, University of Texas at San Antonio.

Mauldin, R.P. and A.L. Figueroa

2006 Chapter 9: Chipped Stone Technology. In *Data Recovery Excavations at 41PR44, Fort Wolters, Parker County, Texas*, pp. 83-96. Archaeological Survey Report No. 369. Center for Archaeological Research, University of Texas at San Antonio.

Mauldin, R.P., R.D. Greaves, J.L. Thompson, C.M. Munoz, L. Kemp, B.A. Meissner, B.K. Moses, and S.A. Tomka

2010 *Archaeological Testing and Recovery at 41ZV202, Zavala County, Texas*. Archaeological Survey Report No. 409. Center for Archaeological Research, University of Texas at San Antonio.

- Mauldin, R.P., C.M. Munoz, and L. Kemp
2018 *National Register Eligibility Testing of Eight Sites on Camp Swift, Bastrop County, Texas*. Archaeological Report, No. 436. Center for Archaeological Research, University of Texas at San Antonio.
- Mauldin, R.P., D.L. Nickels, and C.J. Broehm
2003 *Archaeological Testing to Determine the National Register Status of 18 Prehistoric Site on Camp Bowie, Brown County, Texas*. Archaeological Survey Report, No. 334, Center for Archaeological Research, University of Texas at San Antonio.
- McCall, G.S. and R.A. Horowitz
2015 Comparing Forager and Pastoralist Technological Organization in the Central Namib Desert, Western Namibia. In *Works in Stone: Contemporary Perspectives on Lithic Analysis*, edited by M.J. Shott, pp. 63-78. University of Utah Press, Salt Lake City.
- National Oceanic and Atmospheric Administration (NOAA)
2022 Paris Climatology-30 Year Normals (1991-2020). National Weather Service. Electronic document, accessed July 2022.
- National Parks Service (NPS)
2016 Title 36-Parks, Forests, and Public Property. Part 60-National Register of Historic Places. National Park Service, Department of the Interior. Electronic document, <https://www.nps.gov/>, accessed September 2022.
- Natural Resources Environmental Branch
2020 *Integrated Natural Resources Management Plan-Camp Maxey, Powderly, Lamar County, Texas*. Texas Military Department, Austin.
- Nelson, M.
1987 Site Content and Structure: Metate Quarries and Workshops in the Maya Highlands. In *Lithic Studies Among the Contemporary Highland Maya*, edited by B. Hayden, pp. 120-147. University of Arizona Press, Tucson.
- Nickels, D.L.
2008 *Archaeological Excavations on 20 Prehistoric Sites at Camp Swift, Bastrop County, Texas: 2002*. Archaeological Studies Report No. 5, Center for Archaeological Studies, Texas State University, San Marcos.
- Nickels, D.L., L.C. Nordt, T.K. Perttula, C.B. Bousman, and K. Miller
1998 *Archaeological Survey of Southwest Block and Selected Roads and Firebreaks at Camp Maxey, Lamar County, Texas*. Archaeological Survey Report No. 290. Center for Archaeological Research, University of Texas at San Antonio.
- Pargeter, J., P. Peña, and M. I. Eren,
2019 Assessing raw material's role in bipolar and freehand miniaturized flake shape, technological structure, and fragmentation rates. *Archaeological and Anthropological Sciences* 11(11):5893–5907.
- Peros, M.C., S.E. Munoz, K. Gajewski, and A.E. Viau
2010 Prehistoric Demography of North America Inferred from Radiocarbon Data. *Journal of Archaeological Science* 37:656-664.
- Perttula, T. K.
1998 Previous Archaeological Research and Historic Context. In *Archaeological Survey of Southwest Block and Selected Roads and Firebreaks at Camp Maxey, Lamar County, Texas*, by Nickels, D.L., L.C. Nordt, T.K. Perttula, C.B. Bousman, and K. Miller pp. 16-20. Archaeological Survey Report, No. 290. Center for Archaeological Research, University of Texas at San Antonio.
- 2001 Previous Archaeological Research and Historic Context. In *Camp Maxey II: A 5000 Acre Cultural resources Survey of Camp Maxey, Lamar County, Texas*, by A.S. Lyle, S.A. Tomka, and T.K. Perttula, pp. 13-43. Archaeological Survey Report, No. 312. Center for Archaeological Research, University of Texas at San Antonio.
- 2004 The Prehistoric and Caddoan Archeology of the Northeastern Texas Pineywoods. In *The Prehistory of Texas*, edited by T.K. Perttula, pp. 370-407. Texas A&M University Press, College Station.

- 2012 The Archaeology of the Caddo in Southwest Arkansas, Northwest Louisiana, Eastern Oklahoma, and East Texas. In *The Archaeology of the Caddo*, edited by T.K. Perttula and C.P. Walker, pp. 1-25, University of Nebraska Press, Lincoln.
- 2013 Paleoindian to Middle Archaic Projectile Points from East Texas. *Journal of Northeast Texas Archeology*, 42:47-54.
- 2015 The Womack Site (41LR1), An Ancestral Caddo Settlement on the Red River in Lamar County, Texas. *Journal of Northeast Texas Archeology*, 52:1-38.
- 2017 New Radiocarbon Dates from the Sanders Site (41LR2), Lamar County, Texas. *Journal of Northeast Texas Archeology*, 47:79-80.
- Perttula, T.K. B. Nelson, M. Walters, and R.Z. Selden, Jr.
2015 The Sanders Site (41LR2): A Middle to Historic Caddo Settlement and Mound Center on the Red River in Lamar County, Texas. *Journal of Northeast Texas Archeology*, 52:1-38.
- Perttula, T.K. and R.Z. Selden, Jr
2011 East Texas Radiocarbon Database November 2011. Electronic document <https://counciloftexasarcheologists.org/>, accessed July 2022.
- Perttula, T.K. and S.A. Tomka
2001 The Project Area. In *Camp Maxey II: A 5000 Acre Cultural resources Survey of Camp Maxey, Lamar County, Texas*, by A.S. Lyle, S.A. Tomka, and T.K. Perttula, pp. 5-12. Archaeological Survey Report, No. 312. Center for Archaeological Research, University of Texas at San Antonio.
- Perttula, T.K. and C.P. Walker (editors)
2012 *The Archaeology of the Caddo*, University of Nebraska Press, Lincoln.
- Ressel, D.
1979 *Soil Survey of Lamar and Delta Counties, Texas*. Soil Conservation Service, U.S. Department of Agriculture, Washington, D.C.
- Sabo III, G.
2012 The Terán Map and Caddo Cosmology. In *The Archaeology of the Caddos*, edited by T.K. Perttula and C.P. Walker, pp. 431-447. University of Nebraska Press, Lincoln.
- Schambach F.F
1983 The Archeology of the Great Bend Region in Arkansas. In *Contribution to the Archaeology of the Great Bend Region*, edited by F.F. Schambach and F. Rackerby, pp. 1-11. Research Series No. 22 ,Arkansas Archeological Survey, Fayetteville.
- 2000 Introduction: The Significance of the Sanders Site in the Cultural History of the Mississippi Period Southeast and the Southern Plains, AD 1100-1750, In *The 1931 Excavations at the Sanders Site, Lamar County, Texas*, by A.T. Jackson, M.S. Goldstein, and A.D. Krieger, pp. 1-17. Archival Series No. 2, Texas Archeological Research Laboratory, University of Texas at Austin.
- Selden, Jr. R.Z.
2013 Consilience: Radiocarbon, Instrumental Neutron Activation analysis, and Litigation on the Ancestral Caddo Region. PhD dissertation, Texas A&M University, College Station.
- Shafer, H.J.
1965 Archeological Surveys of Honea, Pat Mayse, and Halsell Reservoirs, Texas. Texas Archeological Salvage Project Survey Reports, No.1, Austin.
- Shott, M. J.
1986 Technological Organization and Settlement Mobility: An Ethnographic Examination. *Journal of Anthropological Research* 42(1):15-51.
- 1989a On Tool-Class Use Lives and the Formation of Archaeological Assemblages. *American Antiquity* 54:9-30.

- 1989b Bipolar Industries: Ethnographic Evidence and Archaeological Implications. *North American Archaeologist* 10(1):1–24.
- 1999 On Bipolar Reduction and Splintered Pieces. *North American Archaeologist* 20(3):217–238.
- Smith, F.T.
1998 The Political History of the Caddo Indians, 1686-1874. In *Native History of the Caddo: Their Place in Southeastern Archaeology and Ethnohistory*, edited by T.K. Perttula and J.E. Bruseeth, pp. 175-181, Studies in Archeology 30, Texas Archeological Research Laboratory, University of Texas at Austin.
- Story, D.A.
1981 An Overview of the Archaeology of East Texas. *Plains Anthropologist* 26(92):139-156.
- Sullivan, A.P. III and K.C. Rozen
1985 Debitage Analysis and Archaeological Interpretation. *American Antiquity* 50(4):755-779.
- Sullo, D.M. and S.C. Stringer
1998 Cultural Resource Investigations for Minor Construction Projects, Camp Maxey, Lamar County, Texas. Adjutant General's Department, Austin.
- Surovell, T.
2003 The Behavioral Ecology of Folsom Lithic Technology. PhD dissertation, Department of Anthropology, University of Arizona, Tucson.

2012 *Toward a Behavioral Ecology of Lithic Technology: Cases from Paleoindian Archaeology*. University of Arizona Press, Tucson.
- Texas Almanac
2022 City Population History from 1850-2010. Texas State Historical Association. Electronic document, <https://www.texasalmanac.com/>, accessed September 2022.
- Texas Military Department (TMD)
2021 Texas Military Department Cultural Database. GIS database on file, Center for Archaeological Research, University of Texas at San Antonio.
- Torfin, T.
2015 Neolithic Population and Summed Probability Distribution of ¹⁴C-dates. *Journal of Archaeological Science* 63:193-198.
- Turner, S.E., T.R. Hester, R.L. McReynolds, and H.J. Shafer
2011 *Stone Artifacts of Texas Indians*. Taylor Trade Publishing, Boulder, Colorado.
- U.S. Geological Survey (USGS)
2022 Geologic Database of Texas. The University of Texas Bureau of Economic Geology and Texas Natural Resources Information System. Electronic document, <https://txpub.usgs.gov/txgeology/>, accessed July 2022.
- Waters, M.R.
1992 *Principles of Geoarchaeology: A North American Perspective*. The University of Arizona Press, Phoenix.
- Wigley, S.
2018 Hunter-gatherer Mobility at the Granberg Site (41BX17), Bexar County, Texas. Master's thesis, Department of Anthropology, University of Texas at San Antonio.
- Williams, A.N.
2012 The Use of Summed Probability Distributions in Archaeology: A Review of Methods. *Journal of Archaeological Science* 39:578-589.

This page intentionally left blank.

Appendix A: Radiocarbon Dates

Table A-1 are radiocarbon dates primarily derived from the East Texas Radiocarbon Database compiled by Perttula and Selden (2011), as well as additional dates for the Womack and Sanders sites reported by Perttula (2015, 2017) to create the Middle Red River SPD in Chapter 4.

Table A-1. Radiocarbon Dates Used to Create the Middle Red River SPD

Site Name	Trinomial	Assay No.	Raw Age	±	δ ¹³ C	Corrected ¹⁴ C Age	±
Hatchel	41BW003	Beta-173085	780	40	-24.0‰	800	40
Hatchel	41BW003	Beta-173086	940	40	-26.9‰	910	40
Hatchel	41BW003	Beta-173087	880	40	-25.5‰	870	40
Hatchel	41BW003	Beta-173088	320	40	-25.6‰	310	40
Hatchel	41BW003	Beta-176676	340	40	-26.1‰	320	40
Hatchel	41BW003	Tx-1903	1250	70		1250	81
Hatchel	41BW003	Tx-1904	810	40		810	57
Hatchel	41BW003	Tx-1905	1000	40		1000	57
Hatchel	41BW003	Tx-1906	660	40		660	57
Cranfill	41BW171	Beta-189640	650	70	-21.1‰	710	70
Cranfill	41BW171	Beta-92921	510	50	-25.9‰	490	50
Dogwood Mound	41BW226	Beta-206837	520	40	-11.7‰	740	40
	41BW553	Beta-94626**	920	80	-27.4‰	880	80
	41BW553	Beta-94627**	930	70	-27.1‰	890	70
	41BW553	Beta-94628**	450	70	-26.0‰	430	70
	41BW553	Beta-94629**	580	90	-26.9‰	550	90
Weaver Creek	41BW692	UGA-13419	210	40	-25.4‰	200	40
Weaver Creek	41BW692	UGA-13420	1270	40	-24.7‰	1280	40
Weaver Creek	41BW692	UGA-13421	2690	40	-24.6‰	2630	40
Weaver Creek	41BW692	UGA-13422	3450	40	-24.5‰	3450	40
Weaver Creek	41BW692	UGA-13423	2760	40	-25.1‰	2760	40
Weaver Creek	41BW692	UGA-13424	960	40	-26.1‰	940	40
	41FN066	Beta-205705	4110	80	-16.5‰	4250	90
	41FN066	Beta-206954	1800	40	-17.8‰	1920	40
Two Hearth Site	41FN125	Beta-304938	530	30	-26.2‰	510	30
Stephanie's Point	41FN127	Beta-304940	830	40	-7.8‰	1110	40
Shell Lens Site	41FN130	Beta-304936	3450	40	-5.7‰	3770	40
Shell Lens Site	41FN130	Beta-304937	3530	40	-6.5‰	3830	40
Prehistoric Site #24	41FN136	Beta-304939	1820	30	-20.7‰	1890	30
Mackin	41LR039	Tx-2167	710	40		710	57
Mackin	41LR039	Tx-2171	890	60		890	72
Mackin	41LR039	Tx-2172	1000	70		1000	81
Mackin	41LR039	Tx-2174	1100	70		1100	81
Mackin	41LR039	Tx-2175	940	40		940	57

Table A-1. Radiocarbon Dates Used to Create the Middle Red River SPD (continued)

Site Name	Trinomial	Assay No.	Raw Age	±	δ ¹³ C	Corrected ¹⁴ C Age	±
Mackin	41LR039	Tx-2176	970	40		970	57
Mackin	41LR039	Tx-2179	1010	80		1010	90
Womack	41LR1	D-AMES 007077	580	21		580	21
Womack	41LR1	D-AMES 007078	294	25		294	25
Ray	41LR135	Beta-46264	1210	90	-25.0‰	1210	90
Ray	41LR135	Beta-46265	1070	70	-25.6‰	1060	70
Ray	41LR135	Beta-46266	850	60	-27.9‰	800	60
Ray	41LR135	Beta-88418**	780	50	-11.8‰	1000	50
Ray	41LR135	Beta-88419**	700	50	-12.1‰	910	50
Ray	41LR135	Beta-88420	890	80	-27.9‰	850	80
Ray	41LR135	Beta-88421	1250	80	-26.1‰	1230	80
Ray	41LR135	Beta-88422	760	80	-26.6‰	740	80
Ray	41LR135	Beta-88423**	670	50	-11.6‰	890	50
Camp Maxey	41LR152	Beta-153588			-28.7‰	1240	60
Camp Maxey	41LR152	Beta-153589			-24.8‰	2490	40
Camp Maxey	41LR152	Beta-153590			-26.7‰	220	40
Camp Maxey	41LR164	Beta-153591			-21.0‰	2040	40
Camp Maxey	41LR164	Beta-153592			-20.6‰	2320	40
Camp Maxey	41LR164	Beta-153593			-21.2‰	2180	40
Camp Maxey	41LR187	Beta-153594			-25.4‰	170	40
Camp Maxey	41LR187	Beta-153595			-25.6‰	3650	40
Sanders	41LR2	D-AMES 017189	777	27		777	27
Sanders	41LR2	D-AMES 017190	738	36		738	36
Stallings Ranch	41LR297	Beta-208519	240	40	-11.2‰	470	40
	41LR297	Beta-220453	1030	40	-24.5‰	1040	40
Stallings Ranch	41LR297	Beta-237677	1570	50	-24.9‰	1570	50
Stallings Ranch	41LR297	Beta-237678	2340	50	-25.1‰	2340	50
Stallings Ranch	41LR297	Beta-237679	2470	50	-24.6‰	2480	50
Stallings Ranch	41LR297	Beta-237680	1480	40	-24.9‰	1480	40
Stallings Ranch	41LR297	Beta-239524	1290	40	-25.9‰	1280	50
Stallings Ranch	41LR297	Beta-239525	1110	40	-26.1‰	1090	40
Stallings Ranch	41LR297	Beta-239526	1200	40	-25.2‰	1200	40
Stallings Ranch	41LR297	Beta-239527	950	40	-26.0‰	930	40
Holdeman	41RR011	Beta-75059	330	50	-16.9‰	460	50
Holdeman	41RR011	Beta-75060	310	60	-14.5‰	480	60
Holdeman	41RR011	Beta-75061	790	60	-20.2‰	870	60
Holdeman	41RR011	Beta-79446	350	70	-15.5‰	510	70
Fasken	41RR014	Beta-91234	850	50	-24.0‰	870	50
Fasken	41RR014	Beta-91235	850	60	-21.5‰	910	60
Roitsch/Sam Kaufman	41RR016	Beta-46267**	705	45		705	45

Table A-1. Radiocarbon Dates Used to Create the Middle Red River SPD (continued)

Site Name	Trinomial	Assay No.	Raw Age	±	δ ¹³ C	Corrected ¹⁴ C Age	±
Rowland Clark	41RR016	Beta-75053	150	70	-17.0‰	280	70
Roitsch/Sam Kaufman	41RR016	Tx-8074	170	63	-8.0‰	448	65
Roitsch/Sam Kaufman	41RR016	Tx-8075	151	53	-8.2‰	426	55
Roitsch/Sam Kaufman	41RR016	Tx-8076	404	84	-8.2‰	679	86
Roitsch/Sam Kaufman	41RR016	Tx-882	870	70		870	81
Roitsch/Sam Kaufman	41RR016	Tx-883	1000	70		1000	81
Roitsch/Sam Kaufman	41RR016	Tx-884	910	70		910	81
Roitsch/Sam Kaufman	41RR016	Tx-885	900	70		900	81
Rowland Clark	41RR077	Beta-79447	410	60	-14.5‰	580	60
Rowland Clark	41RR077	Beta-79448	80	70	-14.0‰	260	70
Rowland Clark	41RR077	Beta-79449	320	60	-11.5‰	540	60
Saltwell Slough	41RR204	Beta-46269	640	100	-27.4‰	600	100
Saltwell Slough	41RR204	Beta-92199**	380	60	-24.3‰	390	60



Report: **1391-047725-047726**


20 July 2022

Customer: 1391
Leonard Kemp
Center for Archaeological Research
University of Texas at San Antonio
One UTSA Circle
San Antonio, TX 78249
USA

Samples submitted for radiocarbon dating on 30 June 2022 have been processed and measured by AMS.
The following results were obtained:

DirectAMS code	Submitter ID	Sample type	$\delta(^{13}\text{C})$	Fraction of modern		Radiocarbon age	
			per mil	pMC	1 σ error	BP	1 σ error
D-AMS 047725	41LR159_Fea1	charcoal	-22.6	87.68	0.25	1056	23
D-AMS 047726	41LR161_Fea1	charcoal	-26.3	97.07	0.26	239	22

Results are presented in units of percent modern carbon (pMC) and the uncalibrated radiocarbon age before present (BP). The results relate only to the sample material submitted and the portion analyzed. All results have been corrected for isotopic fractionation with a $\delta^{13}\text{C}$ value measured on the prepared carbon by the accelerator. These $\delta^{13}\text{C}$ values provide the most accurate radiocarbon ages, but cannot be used to investigate environmental conditions, nor for trophic and nutritional interpretations. The pMC reported requires no further correction for fractionation.


Alyssa M Tate, MS
Director of Laboratory Operations
Data Analyst


Brittany Ricketts, MA
Director of Archaeological Services
Quality Review


Tye Lacey
Laboratory Manager
Quality Review

Appendix B: MSS Sampling Information

Table B-1. MSS Sampling Information

41LR...	Test Unit	Sample	Total Weight (g)	VSS 1	VSS 2	Average VSS	Sample weight (g)	MSS Value
154	1	0	12.86	25.6	25.4	25.5	9.77	0.261
154	1	1	12.93	30.5	30.3	30.4	9.84	0.309
154	1	2	11.28	23.5	23.8	23.65	8.19	0.289
154	1	3	11.64	23.6	23.6	23.6	8.55	0.276
154	1	4	11.45	31.6	30.9	31.25	8.36	0.374
154	1	5	12.27	221.3	225.8	223.55	9.18	2.435
154	1	6	12.03	32.6	32.7	32.65	8.94	0.365
154	1	7	12.17	99.1	99.6	99.35	9.08	1.094
154	1	8	12.86	29.8	29.99	29.9	9.77	0.348
159	1	0	12.49	46.5	46.7	46.6	9.41	0.495
159	1	1	12.54	55.4	55.6	55.5	9.46	0.587
159	1	2	11.54	49.6	49.9	49.75	8.46	0.588
159	1	3	12.25	52	51.8	51.9	9.17	0.566
159	1	4	11.98	51	51.3	51.15	8.9	0.575
159	1	5	11.69	44.5	43.9	44.2	8.61	0.513
159	1	6	13.51	69.2	69.4	69.3	10.43	0.664
159	1	7	12.52	64.3	63.5	63.9	9.44	0.677
159	1	8	12.25	58.1	58.2	58.15	9.17	0.634
159	1	9	11.98	58.2	58	58.1	8.9	0.653
159	1	10	11.7	55.6	56.4	56	8.62	0.650
159	1	11	11.94	58.6	59.1	58.85	8.86	0.664
159	1	12	12.29	56.5	56.5	56.5	9.21	0.613
159	1	13	12.21	57.3	57.4	57.35	9.13	0.628
159	1	14	12.66	58.8	58.9	58.85	9.58	0.614
159	1	15	11.9	46.4	46.4	46.4	8.82	0.526
159	1	16	12.34	41.4	41.4	41.4	9.26	0.447
159	1	17	12.21	43.9	44.4	44.15	9.12	0.484
159	1	18	12.83	45	45.6	45.3	9.74	0.465
159	1	19	11.75	43.7	43.5	43.6	8.66	0.503
159	1	20	11.89	42.5	42.3	42.4	8.8	0.482
159	1	21	11.67	42	40.3	41.15	8.58	0.480
159	1	22	12.11	44.5	44.5	44.5	9.02	0.493
159	2	0	11.11	34.6	34.9	34.75	8.02	0.493
159	2	1	10.78	33.3	33.2	33.25	7.69	0.433
159	2	2	12.47	42.2	42.2	42.2	9.38	0.432
159	2	3	12.42	44.8	45	44.9	9.33	0.450
159	2	4	11.62	44.3	44.7	44.5	8.53	0.522

Table B-1. MSS Sampling Information (continued)

41LR...	Test Unit	Sample	Total Weight (g)	VSS 1	VSS 2	Average VSS	Sample weight (g)	MSS Value
159	2	5	11.76	42.4	42.4	42.4	8.67	0.489
159	2	6	12.27	37.6	37.7	37.65	9.18	0.410
159	2	7	11.31	38.2	38.8	38.5	8.22	0.468
159	2	8	9.8	35.2	35.3	35.25	6.71	0.525
159	3	0	14.48	32	31.9	31.95	11.43	0.280
159	3	1	14.75	36.5	36.3	36.4	11.7	0.311
159	3	2	15.3	36.4	36.6	36.5	12.25	0.298
159	3	3	15.95	44.5	44.9	44.7	12.9	0.347
159	3	4	15.36	51	51.2	51.1	12.31	0.415
159	3	5	15.68	54.2	53.8	54	12.63	0.428
159	3	6	15.6	44.5	45.4	44.95	12.55	0.358
159	3	7	15.43	43.4	44.2	43.8	12.38	0.354
159	3	8	15.1	46.3	46.4	46.35	12.05	0.385
159	3	9	15.39	95.1	95.5	95.3	12.34	0.772
159	4	0	13.6	11.7	11.9	11.8	10.54	0.112
159	4	1	13.86	22.5	22.3	22.4	10.8	0.207
159	4	2	13.65	18.2	18.7	18.45	10.59	0.174
159	4	3	14.33	24	24.3	24.15	11.27	0.214
159	4	4	14.41	32.7	33.1	32.9	11.35	0.290
159	4	5	14.72	41	41	41	11.66	0.352
159	4	6	14.79	41.7	42.6	42.15	11.73	0.359
159	4	7	15.6	89.6	89.9	89.75	12.54	0.716
159	4	8	15.24	50	50	50	12.18	0.411
159	4	9	15.22	40.9	40.9	40.9	12.16	0.336
159	4	10	14.22	40.8	40.6	40.7	11.16	0.365
159	4	11	14.59	39.7	39.8	39.75	11.53	0.345
159	4	12	15.4	36.9	37.2	37.05	12.34	0.300
159	4	13	15.5	38.9	38.7	38.8	12.44	0.312
159	4	14	15.23	42.8	43.4	43.1	12.17	0.354
159	4	15	15.23	42.5	42.3	42.4	12.17	0.348
159	4	16	14.33	34	34.2	34.1	11.27	0.303
159	4	17	14.07	35	35.6	35.3	11.01	0.321
159	4	18	13.01	31.7	31.9	31.8	8.95	0.355
161	1	1	11.73	34.8	34.4	34.6	8.65	0.400
161	1	2	11.92	89.1	93	91.05	8.84	1.030
161	1	3	11.64	36.5	36.6	36.55	8.56	0.427
161	1	4	12.16	40.8	40.6	40.7	9.08	0.448
161	1	5	11.67	40.6	40.6	40.6	8.59	0.473
161	1	6	11.99	37.6	38.1	37.85	8.91	0.425
161	1	7	10.54	36.6	36.3	36.45	7.46	0.489
161	1	8	9.85	30	30.1	30.05	6.77	0.444

Table B-1. MSS Sampling Information (continued)

41LR...	Test Unit	Sample	Total Weight (g)	VSS 1	VSS 2	Average VSS	Sample weight (g)	MSS Value
161	1	9	10.65	32.8	32.8	32.8	7.57	0.433
161	1	10	12.07	34.4	34.7	34.55	8.99	0.384
161	1	11	10.39	24.8	25.3	25.05	7.31	0.343
161	1	12	11.72	33.2	33.2	33.2	8.64	0.384
161	1	13	11.77	34.6	34.6	34.6	8.69	0.398
161	1	14	12.54	27.1	26.9	27	9.46	0.285
161	1	15	11.99	24.3	24.2	24.25	8.91	0.272
161	1	16	11.62	27.8	27.5	27.65	8.54	0.324
161	1	17	11.04	21.6	21.5	21.55	7.96	0.271
161	1	18	9.36	19.6	19.4	19.5	6.28	0.311
161	2	0	14.29	77.5	77.6	77.55	11.24	0.690
161	2	1	15.59	60.9	60.8	60.85	12.54	0.485
161	2	2	15.64	70.6	71	70.8	12.59	0.562
161	2	3	16.02	96.1	96.5	96.3	12.97	0.742
161	2	4	15.49	74.5	75	74.75	12.44	0.601
161	2	5	15.98	85.1	84.8	84.95	12.93	0.657
161	2	6	15.22	92.9	93.6	93.25	12.17	0.766
161	2	7	14.93	67.7	68.2	67.95	11.88	0.572
161	2	8	13.08	71.2	71.6	71.4	10.03	0.712
161	3	1	15.11	70.4	71.2	70.8	12.06	0.587
161	3	2	15.42	70.7	71.1	70.9	12.37	0.573
161	3	3	15.86	76.7	77	76.85	12.81	0.600
161	3	4	15.52	109.1	108.9	109	12.47	0.874
161	3	5	15.06	101.5	101.7	101.6	12.01	0.846
161	3	6	14.77	84.8	85.5	85.15	11.72	0.727
161	3	7	14.01	73.5	73.8	73.65	10.96	0.672
177	1	1	13.15	19.1	19.4	19.25	10.1	0.191
177	1	2	13.98	22.7	23.4	23.05	10.93	0.211
177	1	3	14.17	20.9	21	20.95	11.12	0.188
177	1	4	15.12	26.9	27.1	27	12.07	0.224
177	1	5	15.63	26.3	26.9	26.6	12.58	0.211
177	1	6	15.45	25.9	26.2	26.05	12.4	0.210
177	1	7	15.42	25.2	25.6	25.4	12.37	0.205
177	1	8	14.54	19.1	19.2	19.15	11.49	0.167
177	1	9	14.07	16.7	17.1	16.9	11.02	0.153
203	1	1	15.05	67.9	68.5	68.2	12	0.568
203	1	2	14.12	74.8	75.2	75	11.07	0.678
203	1	3	15.4	77	77.2	77.1	12.35	0.624
203	1	4	13.62	72.2	72.6	72.4	10.57	0.685
203	1	5	14.8	83.3	83.2	83.25	11.75	0.709
203	1	6	14.39	71.5	71.2	71.35	11.34	0.629

Table B-1. MSS Sampling Information (continued)

41LR...	Test Unit	Sample	Total Weight (g)	VSS 1	VSS 2	Average VSS	Sample weight (g)	MSS Value
203	1	7	9.22	55.7	55.6	55.65	6.17	0.902
203	1	8	13.41	60.6	60.2	60.4	10.36	0.583
203	1	9	11.02	51.5	51.5	51.5	7.97	0.646
203	2	0	13.21	26.8	27.4	27.1	10.15	0.267
203	2	1	13.29	29.1	29.4	29.25	10.23	0.286
203	2	2	13.44	34.6	35	34.8	10.38	0.335
203	2	3	14.28	46.3	46.3	46.3	11.22	0.413
203	2	4	14.24	55.2	55.4	55.3	11.18	0.495
203	2	5	14.78	64.3	63.9	64.1	11.72	0.547
203	2	6	14.78	72	72	72	11.72	0.614
203	2	7	14.31	73.2	73.8	73.5	11.25	0.653
203	2	8	14.25	66.3	66.5	66.4	11.19	0.593
203	2	9	13.45	56.9	57.4	57.15	10.39	0.550
203	2	10	12.33	51.2	51.3	51.25	9.27	0.553
203	3	1	14.83	28.2	28.2	28.2	11.78	0.239
203	3	2	14.97	45.4	45.8	45.6	11.92	0.383
203	3	3	14.29	46.3	47.2	46.75	11.24	0.416
203	3	4	14.54	43.8	44.4	44.1	11.49	0.384
203	3	5	14.24	51.1	52	51.55	11.19	0.461
203	3	6	13.55	46.5	46.9	46.7	10.5	0.445
203	3	7	13.1	45.8	46.7	46.25	10.05	0.460
203	3	8	12.73	39.8	39.7	39.75	9.68	0.411
226	1	1	10.99	12.1	11.9	12	7.91	0.152
226	1	2	11.28	12.2	12.5	12.35	8.2	0.151
226	1	3	9.26	12.4	12.4	12.4	6.18	0.201
226	1	4	11.6	14.4	14.3	14.35	8.52	0.168
226	1	5	9.96	12.3	12.3	12.3	6.88	0.179
226	2	0	10.7	18.5	18.8	18.65	7.61	0.245
226	2	1	12.13	15	14.9	14.95	9.04	0.165
226	2	2	11.55	12.6	12.5	12.55	8.46	0.148
226	2	3	11.5	13.2	13.5	13.35	8.41	0.159
226	2	4	11.83	14.6	14.8	14.7	8.74	0.168
226	2	5	11.34	16.9	16.9	16.9	8.25	0.205
226	2	6	11.73	19.7	19.6	19.65	8.64	0.227
226	2	7	11.5	18.2	18	18.1	8.41	0.215
226	2	8	11.23	19.4	19.4	19.4	8.14	0.238
226	2	9	10.24	15.2	14.8	15	7.15	0.210
226	3	1	11.63	13.8	13.9	13.85	8.55	0.162
226	3	2	11.71	13.2	13.5	13.35	8.63	0.155
226	3	3	11.99	16.6	16.5	16.55	8.91	0.186
226	3	4	12.13	17	17.1	17.05	9.05	0.188

Table B-1. MSS Sampling Information (continued)

41LR...	Test Unit	Sample	Total Weight (g)	VSS 1	VSS 2	Average VSS	Sample weight (g)	MSS Value
226	3	5	11.74	18.7	18.3	18.5	8.66	0.214
226	3	6	10.11	13.9	14	13.95	7.03	0.198
226	4	0	11.06	12.9	12.7	12.8	7.98	0.160
226	4	1	12.49	13.6	13.7	13.65	9.41	0.145
226	4	2	12.77	12.5	12.7	12.6	9.69	0.130
226	4	3	11.89	13.4	13.3	13.35	8.81	0.152
226	4	4	11.7	14.3	13.8	14.05	8.62	0.163
226	4	5	11.06	16.8	16.8	16.8	7.98	0.211
226	4	6	11.89	17.4	17.4	17.4	8.81	0.198
226	4	7	11.28	18.8	18.4	18.6	8.2	0.227
226	4	8	11.05	16.2	16.6	16.4	7.97	0.206

This page intentionally left blank.

Appendix C: Debitage Attribute Data

Table C-1. Debitage Attribute Data

Trinomial (41LR...)	FS #	Extension	Provenience	Level	Depth range (cmbs)	Element	Count	Fragment	Edge modified	Raw material	Raw material finish	Raw material heated	Raw material texture	Raw material color	Cortex (%)	Cortex midpoint	Dorsal scars	Length	Width	Thickness	Platform Thickness	Platform Width	Weight (g)
154	59	na	TU 1	2	20-30	flake	1	no		chert	matte finish	evidence	fine grained	grey	51-99	0.00	3	13	11	1	1	5	0.25
177	61	1	TU 1	3	30-40	flake	1	distal		quartzite	matte finish	no evidence	coarse grained	grey	0	0.00	3						0.9
177	61	2	TU 1	3	30-40	flake	1	proximal		quartzite	matte finish	no evidence	coarse grained	grey	0	0.00	2	18	15	3	2	6	0.82
177	60	3	TU 1	2	20-30	flake	1	no		chert	translucent finish	no evidence	fine grained	light brown	0	0.00	3	16	7	2	1	2	0.3
177	60	4	TU 1	2	30-40	flake	1	no		quartzite	matte finish	no evidence	coarse grained	light brown	0	0.00	2	13	15	3	2	6	0.6
226	42	na	TU 4	4	30-40	flake	1	distal		chert	matte finish	no evidence	fine grained	white	0	0.00	3						0.2
226	35	na	TU 2	2	10-20	flake	1	no		chert	matte finish	no evidence	fine grained	light brown	0	0.00	2	11	13	2	2	8	0.23
226	38	na	TU 2	4	30-40	flake	1	no		claystone/siltstone/sandstone	matte finish	no evidence	coarse grained	dark red	0	0.00	1	9	10	1	1	9	0.12
226	41	na	TU 4	3	20-30	flake	1	no		claystone/siltstone/sandstone	matte finish	no evidence	coarse grained	dark red	0	0.00	1	11	14	2	2	4	0.41
162	16	1	ST 72	2	20-40	flake	1	no		quartzite	matte finish	no evidence	coarse grained	light red	1-50	0.25	2	23	13	4	2	9	1.17

Table C-1. Debitage Attribute Data (continued)

Trinomial (41LR...)	FS #	Extension	Provenience	Level	Depth range (cmbs)	Element	Count	Fragment	Edge modified	Raw material	Raw material finish	Raw material heated	Raw material texture	Raw material color	Cortex (%)	Cortex midpoint	Dorsal scars	Length	Width	Thickness	Platform Thickness	Platform Width	Weight (g)
162	16	2	ST 72	2	20-40	flake	1	no		chert	matte finish	evidence	coarse grained	dark red	0	0.00	3	17	8	2	1	2	0.31
162	3	17	ST 72	3	40-60	flake	1	distal		quartzite	matte finish	no evidence	coarse grained	light brown	1-50	0.25	3		30	6			3.08
203	46	na	TU 3	3	30-40	flake	1	medial		chert	matte finish	no evidence	fine grained	grey	0	0.00	3		15	3			0.43
203	45	na	TU 1	3	30-40	flake	1	distal		chert	matte finish	evidence	fine grained	dark red	51-99	0.75	1		12	10			0.35
203	44	na	TU 2	3	30-40	flake	1	no		chert	matte finish	no evidence	fine grained	light red	0	0.00	2	8	10	1	1	3	0.12
161	54	na	TU 2	3	20-30	flake	1	no		chert	matte finish	evidence	fine grained	brown	1-50	0.25	2	23	14	3	3	7	0.87
161	50	na	TU 1	4	40-50	flake	1	proximal		chert	matte finish	evidence	fine grained	brown	1-50	0.25	2		19	5	6	17	1.72
161	49	na	TU 1	3	30-40	flake	1	no		quartzite	matte finish	no evidence	coarse grained	brown	1-50	0.25	2	13	17	4	2	10	0.96
161	89	na	ST 89	2	20-40	flake	1	proximal		quartzite	matte finish	no evidence	coarse grained	dark red	1-50	0.25	3		24	9	9	20	5.08
161	32	na	ST 93	2	20-40	flake	1	medial		chert	matte finish	evidence	fine grained	dark red	0	0.00	2		8	3			0.39
161	30	na	ST 88	2	20-40	flake	1	no		chert	matte finish	evidence	fine grained	light red	51-99	0.75	1	15	13	1	3	12	0.58
161	29	na	ST 86	4	60-80	flake	1	no		chert	matte finish	no evidence	fine grained	grey	1-50	0.25	2	7	13	3	3	10	0.24
161	56	na	TU 2	5	40-50	flake	1	distal		chert	matte finish	evidence	fine grained	dark red	1-50	0.25	1		14	2			0.32

Table C-1. Debitage Attribute Data (continued)

Trinomial (41LR...)	FS #	Extension	Provenience	Level	Depth range (cmbs)	Element	Count	Fragment	Edge modified	Raw material	Raw material finish	Raw material heated	Raw material texture	Raw material color	Cortex (%)	Cortex midpoint	Dorsal scars	Length	Width	Thickness	Platform Thickness	Platform Width	Weight (g)
161	57	1	TU 1	1	8-20	flake	1	siret		chert	matte finish	evidence	fine grained	dark red	1-50	0.25	2	11	14	5	4	8	1
159	78	1	TU 3	3	30-40	flake	1	no		chert	matte finish	no evidence	fine grained	light red	1-50	0.25	2	17	21	3	5	16	1.3
159	78	2	TU 3	3	30-40	flake	1	no		quartzite	matte finish	no evidence	coarse grained	light red	1-50	0.25	2	17	25	3	1	2	1.45
159	78	4	TU 3	3	30-40	flake	1	no		chert	matte finish	evidence	fine grained	dark red	0	0.00	2	10	10	1	1	1	0.19
159	78	5	TU 3	3	30-40	flake	1	no		quartzite	matte finish	no evidence	coarse grained	light red	100	1.00	0	16	26	5	5	22	2.13
159	78	6	TU 3	3	30-40	flake	1	no		quartzite	matte finish	no evidence	coarse grained	black	0	0.00	3	23	8	2	2	7	0.53
159	78	7	TU 3	3	30-40	flake	1	proximal		quartzite	matte finish	no evidence	coarse grained	dark red	100	1.00	0		7	2	2	4	0.23
159	70	1	TU 1	6	60-70	flake	1	no		claystone/siltstone/sandstone	matte finish	no evidence	coarse grained	yellow	1-50	0.25	1	18	27	8	2	5	1.96
159	70	2	TU 1	6	60-70	flake	1	distal		quartzite	matte finish	no evidence	coarse grained	light red	1-50	0.25	3		25	4			1.66
159	14	1	ST 63	2	20-40	flake	1	no		quartzite	matte finish	no evidence	coarse grained	light brown	0	0.00	2	20	23	5	2	12	1.99
159	87	1	TU 4	9	90-100	flake	1	no		chert	matte finish	no evidence	fine grained	brown	1-50	0.25	1	16	17	4	5	16	1.7
159	87	2	TU 4	9	90-100	flake	1	proximal		quartzite	matte finish	no evidence	coarse grained	light brown	1-50	0.25	1		33	6	7	15	6.92

Table C-1. Debitage Attribute Data (continued)

Trinomial (41LR...)	FS #	Extension	Provenience	Level	Depth range (cmbs)	Element	Count	Fragment	Edge modified	Raw material	Raw material finish	Raw material heated	Raw material texture	Raw material color	Cortex (%)	Cortex midpoint	Dorsal scars	Length	Width	Thickness	Platform Thickness	Platform Width	Weight (g)
159	87	3	TU 4	9	90-100	flake	1			chert	matte finish	no evidence	fine grained	green	0	0.00	3	23	9	2	2	7	0.65
159	67	3	TU 1	3	30-40	flake	1			quartzite	matte finish	no evidence	coarse grained	light brown	0	0.00	1	9	15	2	4	9	0.47
159	67	4	TU 1	3	30-40	flake	1			chert	matte finish	no evidence	fine grained	dark red	0	0.00	2	8	13	2	1	6	0.23
159	74	1	TU 1	10	100-110	flake	1	proximal		claystone/siltstone/sandstone	matte finish	no evidence	coarse grained	yellow	0	0.00	3		17	3	1	3	1.26
159	74	2	TU 1	10	100-110	flake	1			chert	matte finish	no evidence	fine grained	dark red	100	0.75	0	31	22	10	4	12	7.82
159	66	1	TU 1	2	20-30	biface thinning flake	1	no		quartzite	matte finish	no evidence	coarse grained	light red	0	0.00	2	6	12	2	4	14	0.32
159	66	2	TU 1	2	20-30	flake	1	no		chert	matte finish	no evidence	fine grained	light brown	0	0.00	3	9	11	1	1	2	0.16
159	66	5	TU 1	2	20-30	flake	1			quartzite	matte finish	no evidence	coarse grained	light red	1-50	0.25	1	11	12	3	4	9	0.57
159	66	6	TU 1	2	20-30	flake	1			quartzite	matte finish	no evidence	coarse grained	light brown	1-50	0.25	2	12	11	2	2	8	0.42
159	66	7	TU 1	2	20-30	flake	1	distal		quartzite	matte finish	no evidence	coarse grained	light brown	0	0.00	3		29	7			5.67
159	83	1	TU 4	5	50-60	flake	1	no		chert	translucent finish	no evidence	fine grained	light brown	0	0.00	3	15	11	2	3	7	0.34

Table C-1. Debitage Attribute Data (continued)

Trinomial (41LR...)	FS #	Extension	Provenience	Level	Depth range (cmbs)	Element	Count	Fragment	Edge modified	Raw material	Raw material finish	Raw material heated	Raw material texture	Raw material color	Cortex (%)	Cortex midpoint	Dorsal scars	Length	Width	Thickness	Platform Thickness	Platform Width	Weight (g)
159	83	2	TU 4	5	50-60	flake	1	no		quartzite	matte finish	no evidence	coarse grained	light brown	1-50	0.25	3	25	30	5	4	13	4.59
159	88	1	TU 4	10	100-110	flake	1	no		claystone/siltstone/sandstone	matte finish	no evidence	coarse grained	light brown	1-50	0.25	3	49	33	5	10	16	10.13
159	88	2	TU 4	10	100-110	flake	1	prox		chert	matte finish	no evidence	fine grained	light brown	100	1.00	0	24	23	7	2	14	35.3
159	88	3	TU 4	10	100-110	flake	1	no		quartzite	matte finish	no evidence	coarse grained	brown	1-50	0.25	1	25	18	6	5	11	5.28
159	88	4	TU 4	10	100-110	flake	1	no		quartzite	matte finish	no evidence	coarse grained	brown	1-50	0.25	1	10	13	2	4	6	0.5
159	69	1	TU 1	5	50-60	flake	1	no		quartzite	matte finish	no evidence	coarse grained	brown	0	0.00	2	24	26	9	7	22	4.3
159	69	2	TU 1	5	50-60	flake	1	no		chert	matte finish	no evidence	fine grained	dark red	51-99	0.75	1	28	22	3	3	6	1.7
159	69	3	TU 1	5	50-60	flake	1	no		chert	matte finish	no evidence	fine grained	light red	51-99	0.75	1	12	11	2	2	7	0.48
159	69	4	TU 1	5	50-60	flake	1	no		quartzite	matte finish	no evidence	coarse grained	light brown	0	0.00	2	12	11	2	2	8	0.31
159	69	5	TU 1	5	50-60	flake	1	no		chert	matte finish	no evidence	fine grained	light brown	0	0.00	1	8	9	1	2	9	0.13
159	69	6	TU 1	5	50-60	flake	1	proximal		chert	matte finish	no evidence	fine grained	light brown	0	0.00	2		9	5	3	8	0.44
159	69	7	TU 1	5	50-60	flake	1	proximal		quartzite	matte finish	no evidence	fine grained	dark red	0	0.00	2		13	2	2	7	0.37

Table C-1. Debitage Attribute Data (continued)

Trinomial (41LR...)	FS #	Extension	Provenience	Level	Depth range (cmts)	Element	Count	Fragment	Edge modified	Raw material	Raw material finish	Raw material heated	Raw material texture	Raw material color	Cortex (%)	Cortex midpoint	Dorsal scars	Length	Width	Thickness	Platform Thickness	Platform Width	Weight (g)
159	68	1	TU 1	4	40-50	flake	1	no		chert	matte finish	no evidence	fine grained	dark red	0	0.00	3	9	10	1	2	5	0.16
159	68	2	TU 1	4	40-50	flake	1	no		quartzite	matte finish	no evidence	coarse grained	dark red	0	0.00	3	10	10	2	1	1	0.25
159	68	3	TU 1	4	40-50	flake	1	medial		chert	matte finish	no evidence	fine grained	light brown	1-50	0.25	1		10	2			0.53
159	68	4	TU 1	4	40-50	flake	1	distal		chert	matte finish	no evidence	fine grained	light brown	1-50	0.25	2		26	2			1.09
159	77	1	TU 3	2	20-30	debris	4			quartzite					na								3.43
159	77	2	TU 3	2	20-30	debris	2			chert					na								1.32
159	77	3	TU 3	2	20-30	flake	1	no		chert	matte finish	no evidence	fine grained	grey	1-50	0.25	2	10	21	4	3	7	0.89
159	77	4	TU 3	2	20-30	flake	1	no		chert	matte finish	no evidence	fine grained	grey	0	0.00	2	13	13	2	1	6	0.29
159	77	5	TU 3	2	20-30	flake	1	no		chert	matte finish	no evidence	fine grained	dark red	1-50	0.25	1	17	18	2	2	6	0.70
159	77	6	TU 3	2	20-30	flake	1	no		quartzite	matte finish	no evidence	coarse grained	light brown	51-99	0.75	1	12	16	4	1	6	0.54
159	71	1	TU 1	7	70-80	flake	1	no		quartzite	matte finish	no evidence	coarse grained	brown	1-50	0.25	2	26	27	7	8	17	4.61
159	71	2	TU 1	7	70-80	debris	1			quartzite					na								0.27
159	82	1	TU 4	4	40-50	flake	1	no		claystone/siltstone/sandstone	matte finish	no evidence	coarse grained	brown	1-50	0.25	2	34	25	12	8	12	11.57

Table C-1. Debitage Attribute Data (continued)

Trinomial (41LR...)	FS #	Extension	Provenience	Level	Depth range (cmbs)	Element	Count	Fragment	Edge modified	Raw material	Raw material finish	Raw material heated	Raw material texture	Raw material color	Cortex (%)	Cortex midpoint	Dorsal scars	Length	Width	Thickness	Platform Thickness	Platform Width	Weight (g)
159	82	2	TU 4	4	40-50	flake	1	no		chert	matte finish	evidence	fine grained	black	0	0.00	3	15	15	2	1	3	0.4
159	82	3	TU 4	4	40-50	debris	3			quartzite					na								2.05
159	82	4	TU 4	4	40-50	debris	1			chert					na								0.7
159	72	1	TU 1	8	80-90	flake	1	no		quartzite	matte finish	no evidence	coarse grained	light brown	0	0.00	2	19	18	2	2	4	0.68
159	72	2	TU 2	8	80-90	debris	1			quartzite					na								0.97
159	13	na	ST 62	2	20-40	flake	1	prox		quartzite	matte finish	no evidence	coarse grained	light brown	0	0.00	2	10	14	3	2	5	0.41
159	80	1	TU 4	2	20-30	flake	1			chert	matte finish	no evidence	fine grained	dark red	100	0.75	0	23	11	4	4	6	1.01
159	80	2	TU 4	2	20-30	debris	1			chert					na								1.22
159	65	1	TU 1	1	7-20	flake	1	no		chert	matte finish	no evidence	fine grained	brown	1-50	0.25	3	15	18	3	3	7	0.97
159	65	2	TU 1	1	7-20	flake	1	no		chert	matte finish	no evidence	fine grained	light red	0	0.00	2	11	11	2	1	2	0.16
159	65	3	TU 1	1	7-20	flake	1	proximal		chert	matte finish	no evidence	fine grained	grey	0	0.00	3	11	10	1	1	6	0.21
159	65	4	TU 1	1	7-20	flake	1	no		quartzite	matte finish	no evidence	coarse grained	grey	0	0.00	1	17	30	2	2	13	1.81
159	65	5	TU 1	1	7-20	debris	3			chert					na								1.26
159	65	6	TU 1	1	7-20	debris	3			quartzite					na								1.56

Table C-1. Debitage Attribute Data (continued)

Trinomial (41LR...)	FS #	Extension	Provenience	Level	Depth range (cmbs)	Element	Count	Fragment	Edge modified	Raw material	Raw material finish	Raw material heated	Raw material texture	Raw material color	Cortex (%)	Cortex midpoint	Dorsal scars	Length	Width	Thickness	Platform Thickness	Platform Width	Weight (g)
159	85	1	TU 4	7	70-80	flake	1	no		claystone/siltstone/sandstone	matte finish	no evidence	coarse grained	light brown	100	1.00	0	33	20	8	6	10	6.62
159	85	2	TU 4	7	70-80	flake	1	no		quartzite	matte finish	no evidence	coarse grained	light red	51-99	0.75	1	35	17	6	3	5	3.46
159	85	3	TU 4	7	70-80	debris	1			chert					na								0.18
159	84	1	TU 4	6	60-70	flake	1	no		chert	matte finish	no evidence	fine grained	light red	51-99	0.75	4	37	20	9	2	8	5.49
159	84	2	TU 4	6	60-70	flake	1	no		quartzite	matte finish	no evidence	coarse grained	light brown	51-99	0.75	1	23	20	6	5	10	2.76
159	84	3	TU 4	6	60-70	biface thinning flake	1	no		claystone/siltstone/sandstone	matte finish	no evidence	coarse grained	light brown	0	0.00	3	19	11	2	2	7	0.5
159	84	4	TU 4	6	60-70	debris	1			chert					na								4.69
159	84	5	TU 4	6	60-70	debris	2			claystone/siltstone/sandstone					na								1.58
159	84	6	TU 4	6	60-70	debris	2			quartzite					na								5.53
159	73	1	TU 1	9	90-100	flake	1			quartzite	matte finish	no evidence	coarse grained	dark red	1-50	0.25	3	33	21	7	4	16	6.57
159	73	2	TU 1	9	90-100	flake	1			chert	matte finish	no evidence	fine grained	brown	0	0.00	2	22	14	2	2	14	0.93

Table C-1. Debitage Attribute Data (continued)

Trinomial (41LR...)	FS #	Extension	Provenience	Level	Depth range (cmbs)	Element	Count	Fragment	Edge modified	Raw material	Raw material finish	Raw material heated	Raw material texture	Raw material color	Cortex (%)	Cortex midpoint	Dorsal scars	Length	Width	Thickness	Platform Thickness	Platform Width	Weight (g)
159	73	3	TU 1	9	90-100	debris	2			quartzite					na								6.73
159	63	1	TU 2	3	30-40	debris	1			chert					na								0.51
159	63	2	TU 2	3	30-40	debris	1			quartzite					na								0.21
159	20	na	ST 77	2	20-40	debris	1			chert					na								0.82
159	19	1	ST 77	2	20-40	flake	1			chert	matte finish	no evidence	fine grained	light brown	1-50	0.25	2	13	21	3	2	5	0.94
159	19	2	ST 77	2	20-40	debris	1			chert					na								0.26
159	19	3	ST 77	2	20-40	debris	1			quartzite					na								0.32
159	59	1	ST 59	2	20-40	flake	1			quartzite	matte finish	no evidence	coarse grained	light brown	51-99	0.75	3	22	21	4	6	18	3.27
159	59	2	ST 59	2	20-40	debris	1			chert					na								0.34
159	18	na	ST 76	1	0-20	flake	1			quartzite	matte finish	evidence	coarse grained	dark red	100	1.00	0	12	13	2	3	7	0.59
159	75	1	TU 1	11	110-120	flake	1	distal		chert	matte finish	no evidence	fine grained	brown	100	1.00	0		22	8			4.12
159	75	2	TU 1	11	110-120	flake	1			quartzite	matte finish	no evidence	coarse grained	light brown	1-50	0.25	3	25	31	7	19	7	5.36
159	10	na	ST 58	1	0-20	debris	1			chert					na								0.58
159	79	na	TU 3	4	40-50	debris	1			claystone/siltstone/sandstone					na								1.68

Table C-1. Debitage Attribute Data (continued)

Trinomial (41LR...)	FS #	Extension	Provenience	Level	Depth range (cmbs)	Element	Count	Fragment	Edge modified	Raw material	Raw material finish	Raw material heated	Raw material texture	Raw material color	Cortex (%)	Cortex midpoint	Dorsal scars	Length	Width	Thickness	Platform Thickness	Platform Width	Weight (g)
159	62	1	TU 2	2	20-30	flake	1	no		chert	matte finish	no evidence	fine grained	light brown	51-99	0.75	1	15	13	4	5	11	0.97
159	62	1	TU 2	2	20-30	flake	1	no		chert	matte finish	no evidence	fine grained	dark red	1-50	0.25	2	16	10	3	2	5	0.47
159	62	1	TU 2	2	20-30	flake	1	no		chert	matte finish	no evidence	fine grained	light brown	0	0.00	1	12	17	1	2	3	0.3
159	62	1	TU 2	2	20-30	flake	1	prox		chert	matte finish	no evidence	fine grained	light brown	0	0.00	2	14	11	2	2	6	0.32
159	62	1	TU 2	2	20-30	debris	1			chert					na								0.99
159	62	1	TU 2	2	20-30	debris	1			quartzite					na								0.45
159	62	1	TU 2	2	20-30	debris	1			claystone/ siltstone/sandstone					na								0.34
159	64	1	TU 2	4	40-50	debris	3			chert					na								1.87
159	64	2	TU 2	4	40-50	debris	2			claystone/ siltstone/sandstone					na								0.37
159	81	1	TU 4	3	30-40	flake	1	no		chert	matte finish	no evidence	fine grained	dark red	100	1.00	0	19	13	3	3	9	1.14
159	81	2	TU 4	3	30-40	debris	1			quartzite					na								0.16
159	12	1	ST 59	3	40-60	flake	1	no		chert	matte finish	no evidence	fine grained	grey	1-50	0.25	3	32	33	9	4	7	8.75

Table C-1. Debitage Attribute Data (continued)

Trinomial (41LR...)	FS #	Extension	Provenience	Level	Depth range (cmbs)	Element	Count	Fragment	Edge modified	Raw material	Raw material finish	Raw material heated	Raw material texture	Raw material color	Cortex (%)	Cortex midpoint	Dorsal scars	Length	Width	Thickness	Platform Thickness	Platform Width	Weight (g)
159	12	2	ST 59	3	40-60	debris	2			chert					na								0.98
159	87	na	TU 4	9	90-100	biface	1		biface	chert	matte finish	no evidence	fine grained	light brown	1-50	0.25	na	30	22	8	na	na	5.7
159	15	na	ST 66	2	20-30	biface	1	proximal	biface	chert	matte finish	evidence	fine grained	light brown	0	0.00	na	12	26	8	na	na	4.9
159	77	na	ST 77	4	40-50	biface	1	prox/dist	biface	quartzite	matte finish	no evidence	fine grained	brown	0	0.00	na	23	15	8	na	na	3.3
159	86	na	TU 4	8	80-90	biface	1	no	biface	chert	matte finish	no evidence	fine grained	brown	0	0.00	na	27	16	7	na	na	3.8
159	68	na	TU 1	4	40-50	flake	1	distal	unifacial retouch	quartzite	matte finish	no evidence	coarse grained	light brown	1-50	0.25	na	41	22	10	na	na	7.4
159	18	na	ST 76	1	0-20	flake	1	medial	bifacial retouch	quartzite	matte finish	no evidence	coarse grained	brown	1-50	0.25	na	41	26	12	na	na	12.3
161	52	na	TU 1	7	70-80	flake	1	distal	unifacial retouch	quartzite	matte finish	no evidence	fine grained	light brown	51-99	0.75	0	37	26	14	na	na	6.3
159	63	1	TU 2	3	30-40	core	1	no	na	quartzite	matte finish	no evidence	coarse grained	light brown	51-99	0.75	0	70	65	58	na	na	257.9
161	55	4	TU 2	4	30-40	core	1	no	na	quartzite	matte finish	no evidence	fine grained	light brown	51-99	0.75	na	62	47	39	na	na	128.3
154	1	na	TST 5	1	20-40	debris	1			claystone/siltstone/sandstone													0.3

Table C-1. Debitage Attribute Data (continued)

Trinomial (41LR...)	FS #	Extension	Provenience	Level	Depth range (cmts)	Element	Count	Fragment	Edge modified	Raw material	Raw material finish	Raw material heated	Raw material texture	Raw material color	Cortex (%)	Cortex midpoint	Dorsal scars	Length	Width	Thickness	Platform Thickness	Platform Width	Weight (g)
226	40	na	TU 4	2	10-20	debris	1			chert													0.81
162	6	na	ST 20	3	40-60	debris	1			quartz													0.18
162	4	2	ST 15	2	20-40	debris	1			chert													0.42
203	43	na	TU 2	2	20-30	debris	1			quartzite													0.29
161	52	na	TU 1	7	70-80	debris	1			chert													0.21
161	55	na	TU 2	4	30-40	debris	1			quartzite													2.12
161	54	na	TU 2	3	20-30	debris	1			chert													0.54
161	57	2	TU 2	2	10-20	debris	1			chert													0.52
161	51	na	TU 1	5	50-60	debris	1			petrified wood													13.91
159	78	3	TU 3	3	30-40	debris	1			chert													0.94
159	70	3, 5	TU 1	6	60-70	debris	2			chert													0.71
159	70	4	TU 1	6	60-70	debris	1			quartzite													0.25
159	14	2	ST 63	2	20-40	debris	1			quartzite													3.64
159	67	1, 2, 5	TU 1	3	30-40	debris	3			quartzite													1.3
159	66	3, 4	TU 1	2	20-30	debris	2			quartzite													1.24

Table C-1. Debitage Attribute Data (continued)

Trinomial (41LR...)	FS #	Extension	Provenience	Level	Depth range (cmbs)	Element	Count	Fragment	Edge modified	Raw material	Raw material finish	Raw material heated	Raw material texture	Raw material color	Cortex (%)	Cortex midpoint	Dorsal scars	Length	Width	Thickness	Platform Thickness	Platform Width	Weight (g)
159	83	3	TU 4	5	50-60	debris	1			quartzite													0.24
159	69	9, 10, 11	TU 1	5	50-60	debris	3			quartzite													2.01
159	69	8, 12	TU 1	5	50-60	debris	2			chert													0.27

This page intentionally left blank.

Appendix D: Measuring Cortex Ratios at 41LR159

Introduction

The cortex ratio method is a popular method of assessing the degree to which raw materials may have been transported over the course of their use lives. It works by comparing the amount of cortex in an assemblage to an amount we would expect to be present if the entire reduction sequence happened on site. The following describes the measures used to create the cortex ratio analysis.

Measuring the Amount of Surface Area Covered by Cortex in the Assemblage

There are several parameters that need to be estimated in this methodology. First is the total surface area of the assemblage. This is done by adding together the products of length and width across all artifacts. The cortical surface area of relatively thick artifacts, like cores or other chunky nodules, is estimated using the equation for measuring the surface area of an ellipsoidal volume: $S = 4\pi(3 \cdot \text{volume}/4\pi)^{2/3}$.

Second is the amount of the observed surface area that is covered by cortex. For each flake, or core, this is estimated by multiplying its surface area, by the midpoint of the measured cortical cover. For example, if a flake was 20 mm by 30 mm, and had a cortex code of 1-50%, then the amount of cortical cover would be estimated as $(20 \times 30 \text{ mm}) \times 0.25$, or 150 mm². The result of both of the previous steps is an estimate for how much surface area there is on the chert, and quartzite artifacts, as well as an estimate of how much of that surface area is cortical.

Measuring the Total Volume of Chert and Quartzite in the Assemblage

The next value needed is an estimate of the volume of chert and quartzite present in the assemblage. To accomplish this, I identified the density of both raw materials, and used this to calculate volume, by dividing the density constant for that raw material by the weight of each piece. To measure density, I placed samples of chert and quartzite in a graduated cylinder, and measured their volume in milliliters and measured their density as grams per milliliter. These densities were then used to estimate the volume of each piece in the assemblage given their mass (weight (g)/density constant = volume). In cases where volumes were measured with a graduated cylinder, and for which we also had axial measurements, the relationship between the estimated volume based only on axial measurements, and the known

volume is linear, and very strong ($r^2=0.94$, $p \text{ value} = >.001$, $n=8$) which suggests that using the axial measurements in this assemblage to estimate the volume can provide a good estimate of the volume of any given piece.

Estimating Volume and Surface Area of Nodules Reduced at 41LR159

The next values needed are an estimate of volumes and surface areas of the nodules reduced at 41LR159. This is accomplished by either measuring naturally occurring or burnt nodules collected over the course of the project, or by measuring the largest flake of a given raw material and using that as a proxy for nodule size. The latter strategy was taken for chert, since no chert cores were recovered, or burnt chert nodules. Cores with few removals, and complete, or nearly complete (at least 60% complete) burnt quartzite were measured. Volume was measured by placing each piece in a graduated cylinder. Weight was measured to the nearest hundredth of a gram. Length, width, and thickness of these nodules was also measured with digital Mituyo calipers.

Since there were no chert cores or nodules recovered, the maximum length of a chert flake recovered from 41LR159 is treated as a proxy for the width of the largest cobble exploited at the site. To explain briefly, most knappers when they remove the largest flakes, tend to remove those flakes across the midsection of cobbles, along the second-shortest axis of the piece. Long flakes could be removed along the long axis, but unless knappers are adept at systematically producing blades (which is not the case at Camp Maxey), they will tend not to knap flakes that extend beyond the midline of a cobble along its long axis. For example, in Mousterian contexts, most of the longest flakes are only as long as the maximum width of cobbles exploited, and tend to be much shorter than the maximum length of those cobbles (Lin et al. 2015). We expect the relationship between the length of the longest flakes and cobble width to be similar at Camp Maxey.

The longest quartzite flake recovered from either assemblage was 41 mm, which falls in the lower range of the distribution of nodule widths identified across 6 measured quartzite nodules and cores (mean = 48.5 mm, $sd = 12.1$). This is also broadly reflective of the two quartzite cores recovered. One recovered from 41LR161, in TU 2, Level 4, was 62-x-47-x-39 mm, and weighed 128.3 g. Its largest flake scar is 38-x-31 mm long, somewhat smaller than the largest quartzite flake. The second core recovered from TU 2, Level 3 of 41LR159 is also an early stage core with only three removals. It measures

70-x-65-x-58 mm and weighs 257.9 g. The largest flake scar on this core is as 53-x-23 mm, marginally larger than the largest flake.

The longest chert flake recovered was only 37 mm long, which suggests that chert nodules exploited were small relative to the size of quartzite nodules recovered from the site. However, this is still larger than the maximum width of the only chert nodule identified in the assemblage, which was only 29 mm wide. This smaller nodule is likely more representative of the smaller nodules available in the area surrounding Camp Maxey. The larger flake length relative to nodule size suggests, again, that some of the exploited chert was brought in from elsewhere.

To derive an estimate of nodule size for a chert flake that is 37 mm long, the relationship between the volume of nodules at Camp Maxey, and their width was modelled. Again, as outlined above the relationship between both has been illustrated to be strong: knowing linear dimensions gives us a lot of information about the volume of a nodule. While this model was applied only to quartzite nodules, there is little reason to assume the relationship would not hold for a chert nodule. That linear model is then used to generate a prediction for the volume of a nodule assuming it had a width matching the longest chert flake recovered: 37 mm.

Estimating the Number of Nodules Reduced to Produce the 41LR159 Assemblage

Now that there are both estimates for maximum nodule size (derived from measuring nodules recovered from Camp Maxey, or by modelling the relationship between flake

size, and nodule volume), and the amount of volume in the assemblage, the next variable to calculate is the number of nodules reduced to produce the 41LR159 assemblage. This is accomplished by dividing the total assemblage volume, by the estimated original nodule sizes.

Measuring the Expected Amount of Cortex

The modelled number of nodules that would have to have been reduced to explain the amount of material in the assemblage is used to estimate the total surface area, and total amount of cortex, that would have been present on those nodules. Here, the equation for calculating the surface of a cylinder given its volume is used: $4\pi(\text{volume}/\pi)^{2/3}$.

Measuring the Cortex Ratio (Expected/Observed)

Finally, to measure the cortex ratio, the observed amount of cortex is divided by the expected amount of cortex, assuming the entire reduction sequence happened on site, and assuming the nodules sampled, and dimensions of the largest flakes are broadly representative of the kinds of cores reduced. If the ratio is around 1, then there is about the amount of cortex present in the assemblage that we would expect if the assemblage represented the whole reduction sequence. If the ratio is greater than 1, it would suggest that cortex is over-represented. This would be more consistent with a scenario in which we were sampling flakes from a site where people performed primary reduction, then transported cores with much of their cortex removed elsewhere. If the ratio is less than one, then that means that there is an under-representation of cortex. In this case, initial reduction likely happened in part elsewhere, resulting in relatively little cortical cover.

Appendix E: R Code for Monte Carlo Simulation

```
library(here)
library(ggplot2)
library(readxl)
library(dplyr)

elements<-"flake|biface thinning flake|core|Biface") # Pick only these artifact elements for measuring cortex ratio
set.seed(4213)
#### Cortex ratio following Lin et al.
Spheroid.Surface<-function(V){
  S<-4*pi*(3*V/4*pi)**(2/3)
  return(S)
}

Spheroid.Volume<-function(L){
  (4/3)*pi*(.5*L)**3
}

Ellipsoid.Surface<-function(l,w,t,p){
  a<-(.5*l)
  b<-(.5*w)
  c<-(.5*t)
  S<-4*pi*(((a*b)**p+(a*c)**p+(b*c)**p)/3)**(1/p)
  return(S)
}

Ellipsoid.Volume<-function(l,w,t){
  a<-(.5*l)
  b<-(.5*w)
  c<-(.5*t)
  V<-(4/3)*pi*a*b*c
  return(V)
}

## Test functions to make sure they work
Spheroid.Surface(10)
Spheroid.Volume(5.5)
Ellipsoid.Surface(10,10,10,1.6)
Ellipsoid.Volume(5.5,3.2,2.4)

# gather volumes of all nodules and their surface areas.
get.nodule.vols<-function(data){

  df<-as.data.frame(matrix(nrow=length(data$L), ncol=9))
```

```

    colnames(df)<-c("FS","RM","Element","True.volume","Spheroid.vol","Spheroid.Surface","Ellipsoid.vol","Ellipsoid.
    Surface")

df$FS<-data$`FS`#`
df$RM<-data$RM
df$Element<-data$element
df$True.volume<-data$vol.ml
df$Spheroid.vol<-Spheroid.Volume(data$L)
df$Spheroid.Surface<-Spheroid.Surface(Spheroid.Volume(data$L))
df$Ellipsoid.vol<-Ellipsoid.Volume(data$L,data$W,data$T)
df$Ellipsoid.Surface<-Ellipsoid.Surface(data$L,data$W,data$T,1.6)

return(df)

}

calculate.surface.area<-function(x){

indices<-grep("flake|biface thinning flake",x$element)
for(i in 1:length(indices)){
  x[indices[i],]$Estimated.surface.area<-prod(x[indices[i],]$L,x[indices[i],]$W, na.rm=TRUE)
}
indices<-grep("core|Biface",x$element)

for(i in 1:length(indices)){
  x[indices[i],]$Estimated.surface.area<-Ellipsoid.Surface(x[indices[i],]$L,
                                                            x[indices[i],]$W,
                                                            x[indices[i],]$T,
                                                            1.6)
}

x$Estimated.surface.area<-x$Estimated.surface.area/100 #convert to square cm
x$Cortical.area<-x$Estimated.surface.area*x$Cortex.midpoint

return(x)
}

# Estimate volume from mass of all elements in assemblage.
convert.mass.to.volume<-function(x,rm,density){
  x<-as.data.frame(x)
  x[grep(rm,x$RM),]$Estimated.volume<-x[grep(rm,x$RM),]$`Weight (gm)`/density
  x[grep(rm,x$`Debris type`),]$Estimated.volume<-x[grep(rm,x$`Debris type`),]$`debris weight (gm)`/density
  output<-x
  return(output)
}

measure.cortex.ratio<-function(data,nodules, max.flk.length){

```

```

df<-as.data.frame(matrix(NA,ncol=7,nrow=1))
colnames(df)<-c("Assemblage volume","Assemblage surface area","Assemblage cortical area",
               "Modelled nodule volume","Expected nodule N",
               "Expected cortex","Cortex ratio")
rm.vol<-sum(data$Estimated.volume, na.rm=TRUE)
df[,1]<-rm.vol
rm.surf<-sum(data$Estimated.surface.area, na.rm=TRUE)
df[,2]<-rm.surf
rm.surf.cort<-sum(data$Cortical.area, na.rm=TRUE)
df[,3]<-rm.surf.cort

lm<-lm(vol.ml~W,data=nodules)
new.data<-as.data.frame(max.flk.length)
colnames(new.data)<- "W"
modeled.nodule.volume<-predict(lm, newdata=new.data) # This is in cubic cm.
df[,4]<-modeled.nodule.volume

modeled.nodule.count<-sum(rm.vol, na.rm=TRUE)/modeled.nodule.volume
df[,5]<-modeled.nodule.count

expected.cortex<-(4*pi*(modeled.nodule.volume/pi)**(2/3)*modeled.nodule.count) #Find surface area of the modeled
volume, and multiply by number of nodules modeled.

df[,6]<-expected.cortex
cortex.ratio<-rm.surf.cort/expected.cortex

df[,7]<-cortex.ratio

return(df)

}

#### Read in data and clean
#### NOTE REPLACE THE WORKING DIRECTORY TO TARGET THE MAXEY DEBITAGE .CSV FILE
setwd(paste(gsub("Debitage/R analysis", "Debitage", here::here() ),sep="/"))
####
####
data<-read_excel("Maxey lithic analysis V2.xlsx")
nodules<-read_excel("Nodule volumes and densities.xlsx")
nodules<-nodules[which(nodules$Trinomial=="41LR159"),]

data[,grep("^L$|^W$|^T$|^PT$|^PW$|^Weight..gm.$|^Debris.count$|^debris.weight..gm.$", names(data))]<-sapply(data[,gr
ep("^L$|^W$|^T$|^PT$|^PW$|^Weight..gm.$|^Debris.count$|^debris.weight..gm.$",names(data))],as.numeric)

data$Estimated.volume<-NA #Initialize new column to receive the estimated volume based on raw material weight given
density

```

```
data$Estimated.surface.area<-NA # Initialize to receive estimated surface area given L* W for flakes, and the ellipsoidal
  formula for cobbles/cores
data<-data[grepl("41LR159",data$Trinomial),]
data<-data[grepl(elements, data$element),]
flakes<-data[grepl("flake",data$element),]

## Make initial calculations before calculating cortex ratio

data<-calculate.surface.area(data)

# Take our info about the density of chert and quartzite, and use it to calculate the volume given the measured weight of chert
# and quartzite.

data<-convert.mass.to.volume(data, "Chert", 2.1) #units are cm cubed.
data<-convert.mass.to.volume(data, "Quartzite", 2.5) #units are cm cubed

#Following Lin et al's code
#The goal in this section is to identify whether there is a statistically significant difference between
#Cortex ratios between quartzite and chert at a given site.
#This is a permutation test, described by Lin et al. in their 2012 paper in Journal of Archaeological Science.
#here we generate the null hypothesis distribution of some statistic (the core ratio differences between sites), by permuting
#the combined data of two compared groups (chert and quartzite artifacts from the same site).

#We are comparing the true difference in estimated cortex ratios between both raw materials, to all possible cortex ratio
  differences.
#step 1. is define the cortex ratio difference between chert and quartzite.
#step 2. Combine both chert and quartzite assemblages.
#step 3. Randomly draw a sample without replacement of a number of artifacts equal to the number of chert artifacts
#step 4. Assign the remainder of the sample to a second group equal to the number of quartzite artifacts
#step 5. measure the cortex ratios for both groups, and measure the difference in the cortex ratio between both as well.

list<-list()

sample1<-data[grepl("Chert",data$RM),]
cr1<-measure.cortex.ratio(sample1, nodules, max(sample1[grepl("flake",sample1$element),]$L, na.rm=TRUE))

sample2<-data[grepl("Quartzite",data$RM),]
cr2<-measure.cortex.ratio(sample2, nodules, max(sample2[grepl("flake",sample2$element),]$L, na.rm=TRUE))
cortex.difference<-abs(cr1$`Cortex ratio`-cr2$`Cortex ratio`)

table<-rbind(cr1, cr2)
table<-round(table,2)
table$Group<-c("Chert","Quartzite")
write.csv(table, "Cortex_ratio_summary.csv")

iterations<-10000
results<-vector(mode="numeric",length=iterations)
combined.samples<-rbind(sample1, sample2) # combine both samples to prep for permutation steps
rnames<-(row.names(combined.samples))
```

```

for (i in 1:iterations){

  indices<-sample(rnames,nrow(sample1), replace=FALSE) # prep to draw a number from the pooled sample equal to number
    of chert artifacts

  sample1_sample<-combined.samples[as.numeric(indices),] #draw samples for new group 1

  sample2_sample<-combined.samples[-as.numeric(indices),] #draw samples for new group 2.

  #Measure cortex ratio differences for these permuted samples drawn from the entire combined chert/quartzite dataset
  d<-sample1_sample

  cr1.sample<-measure.cortex.ratio(d, nodules, max(d[grepl("flake",d$element),]$L, na.rm=TRUE))$`Cortex ratio`

  d<-sample2_sample

  cr2.sample<-measure.cortex.ratio(d, nodules, max(d[grepl("flake",d$element),]$L, na.rm=TRUE))$`Cortex ratio`

  results[i]<-abs(cr1.sample-cr2.sample) # add each difference between the permuted pairs of samples to a vector. This is our
    test distribution.

}

#Proportion of randomly sampled differences in between assemblages. Or the probability that the
#observed ratio could have been drawn from this population of differences.
length(results[which(results < abs(cortex.difference))])/10000

# Make plot
cutoff<-quantile(results,.95)

hist.y <- density(results, from = 0, to = .5) %$%
data.frame(x = x, y = y) %>%
mutate(area = x >= cutoff)

setwd(here::here())
pdf("Cortex_ratio_result.pdf", width=6, height=5)
ggplot(data=hist.y,aes(x=x, ymin=0, ymax=y, fill=area))+
  geom_ribbon()+geom_line(aes(y=y))+
  geom_vline(xintercept=abs(cortex.difference), linetype="dashed", size=1.6)+
  guides(color=guide_legend(override.aes=list(fill=NA)), color=guide_legend(nrow=1), fill="none") +
  annotate(geom = 'text', x = cortex.difference, y = .75, color = 'black',

    label = paste('Observed difference \nin cortex ratio between\nchert and quartzite:',round(cortex.difference,2)), hjust =
      -0.02)+

  annotate(geom = 'text', x = .26, y = 1.25, color = 'black',
    label = paste("95th percentile of cortex ratio\n differences \nin test distribution:",round(cutoff,2)), hjust = -0.07)+
  xlab("Cortex ratio differences") +

```



```
ylab("Density") +  
  theme_bw()  
dev.off()
```

```
cortex.difference
```